Modelling of Electrically Driven Membrane Processes

Rype, Jens-Ulrik

Publication date:
2003

Document Version
Publisher's PDF, also known as Version of record

Modeling of Electrically Driven Membrane Processes

Ph.D. Thesis
by
Jens-Ulrik Rype

Department of Chemical Engineering
Technical University of Denmark

Supervisor: Ass. Prof. Gunnar Jonsson

October 2002

ISBN 87-90142-93-4.
Printed by Book Partner, Nørhaven Digital, Copenhagen, Denmark

Preface

This thesis represents the results of work done in The Membrane Group at Department of Chemical Engineering, Technical University of Denmark, during the period from August 1st1997, to October 30th 2000, supervised by Associate Professor Gunnar Jonsson.

Part of the work concerning recovery of citric acid from lime fruit waste was carried out at the Department of Food Science (ENCB) at the National Polytechnical University (IPN) in México City, under the supervision of Dr. Gustavo Gutierrez Lopez.
The work concerning browning inhibition of pear juice was carried out the same place under the supervision of Dr. Lidia Dorantes de Parada.

I would like to acknowledge all the people that in some way contributed to the completion of this work. Some of the people, I especially like to thank are listed below:

- My supervisor Gunnar Jonsson is thanked for his trust, help and assistance all the way through my study at the Membrane Group.
- My two supervisors, Dr. Lidia Dorantes and Dr. Gustavo Gutierrez at *Escuela National de Ciencias Biologicas* in México City are thanked for their assistance both within and outside the university and for letting me meet their faboulous families.
- I would like to thank my good friend and co-worker Arvid Garde for entusiatic cooperation and for sharing his inventive ideas with me.
- Rodolfo Garcia-Sámano was a valuable co-worker in assisting me with all my experimental work in México.
- Bente Lundgaard, Jens Lipnizki, Sune Jacobsen and the rest of the shifting personnel in the Membrane Group at DTU are thanked for assistance and friendship throughout the study.
- I thank Dr. Margarita Naish, University of Reading and Dr. Porsdal Poulsen from Department of Biotechnology, DTU, for setting up my stay in México financially through the ALFA programme.
- I need to thank the workshop at Department of Chemical Engineering and especially Ivan Pedersen and Henning Koldbech, who skillfully transformed our constantly changing and improving designs into real experimental equipment.
- And I would like to thank the Technical University of Denmark for my scholarship and the opportunity to perform this work and for believing in the future of the patent application.

Summary

The present work is centered on applications of electro-membrane processes mainly intended for the agricultural or food industry. The applications are divided among three areas:

- The recovery of citric acid from lime juice waste.
- Inhibition of Anjou pear juice browning.
- Recovery and production of lactic acid from a fermenter.

The recovery of citric acid encompasses a theoretical and experimental evaluation of electrodialytic separation of the citrate ion at different valences by changing pH, and the resulting impact on process parameters like current efficiency and energy consumption. These results suggested that the electrodialytic recovery of citrate at valence –2 ($HCit^{2-}$) was superior in respect to the chosen parameters. Results from *in situ* experiments on stripped lime juice containing 4% citric acid from a lime processing factory in Mexico is included. The *in situ* experiments were largely inhibited by membrane fouling from organic matter. A minor study in microfiltration and ultrafiltration of the lime juice waste is included as well as a more extensive study on concentration of citrate by nanofiltration. The intentions of applying electrodialysis as a direct measure to recover citric acid from the stripped lime juice had to be renounced because of the fouling problems involved. Extensive pretreatment of the waste has to be implemented before electrodialysis can be considered further. Nanofiltration seems a feasible alternative for concentration of the citrate-rich waste stream.

The inhibition of enzymatic browning (caused by polyphenol oxidase (PPO)) of Anjou pear juice by acidification was studied. Experiments with acidification to below pH 2.5 of juice by electrodialysis with bipolar membranes and subsequent adjustment back to the juice's original pH-level by the same method "reversed" after a short period of storage demonstrated that it was possible to inhibit and almost eliminate the enzymatic browning caused by PPO significantly.

Lengthy investigations in electro-membrane processes for lactate recovery from fermentation broth lead to a new process with a built-in anti-fouling mechanism, entitled *reverse electro-enhanced dialysis* process, which has been submitted as patent application. The membrane setup in this process resembles a Donnan dialysis setup with anion-exchange membranes, but current is added for increased flux, and the electrical migration is controlled by competitive transport between lactate and hydroxide ions at different pH-levels. Current is reversed at short intervals for destabilization of fouling build-up.

The reverse electro-enhanced dialysis process was extensively tested on both model solutions and fermentation broths, simulating continuous fermentation operation. Lactate fluxes combined with high retention of sugars, calcium, and magnesium was found to be satisfactory. Process factors like current efficiency and energy consumption was evaluated and found to be initially unsatisfying. It was estimated that optimization of equipment and of operation parameters by computer simulations could improve the economical evaluation of the process. The process was able to run for prolonged operation times when current was reversed compared to similar runs without current reversal.

The efficiency loss incorporated by the frequent current reversals in the reverse electro-enhanced dialysis process was examined by constructing a mathematical model, which was implemented into a computer program. The constructed program was subsequently able to estimate values for current efficiency, overall flux, energy consumption and necessary membrane area for a part of a reverse electro-enhanced dialysis process.

A plant able to produce 10,000 tons lactic acid (88%) annually was designed, incorporating the reverse electro-enhanced dialysis process and process parameters estimated from experiments and

simulations. The extraction of lactate from fermentation broth through the reverse electro-enhanced dialysis unit was combined with an electrodialysis with bipolar membranes, an electrodialytic desalination and an evaporator system for final purification. An economical evaluation of the designed plant was conducted. Initial investment was estimated to DKK 145.5 million. Assuming the lowest current market price of 88%-lactic acid of DKK 9.50/kg and comparing it to estimated running costs of DKK 49.2 million per year still yielded an annual profit of DKK 45.8 million and an estimated break-even time of 6.3 years.

Summary (Danish)

Denne tesis fokuserer på praktisk anvendelse af elektro-membran processer beregnet på landbrugs- eller fødevareindustri. Anvendelserne er fordelt på tre fokusområder:

- Udvinding af citronsyre fra citrusfrugt spildstrøm.
- Inhibering af enzymatisk mørkfarvning af juice fra Anjou pærer.
- Udvinding og produktion af mælkesyre.

Udvindelsen af citronsyre omfatter en teoretisk og eksperimentel undersøgelse af elektrodialytisk separation af citrat ionen ved forskellige valenstrin ved at ændre pH og den resulterende påvirkning af udvalgte procesparametre som strømeffektivitet og energiforbrug. Ud fra de udvalgte parametre fås den mest fordelagtige udvinding af citrationen ved valensen –2 ($HCit^{-2}$). Resultater fra *in situ* forsøg på spildet fra en citrusfrugtfabrik i México indeholdende 4% citronsyre er inkluderet i rapporten. *In situ* forsøgene blev i høj grad påvirket af tilsmudsning af ionbyttermembranerne fra det organiske materiale i spildet, hvilket affødte en overfladisk undersøgelse af mikro- og ultrafiltrering af spildet og en mere indgående undersøgelse af nanofiltrering af spildet. Den oprindelige intention om at anvende elektrodialyse til en direkte opkoncentrering af citrusfrugtspildet blev forkastet på grund af omfattende problemer med membrantilsmudsning. Omfattende forbehandling af spildstrømmen vil være nødvendig før elektrodialyse kan udføres på spildet. Nanofiltrering viser potentiale som et alternativ til opkoncentrering af den citronsyrerige spildstrøm.

Inhibering af enzymatisk mørkfarvning (på grund af polyphenol oxidase (PPO)) af Anjou pærejuice gennem forsuring blev undersøgt. Eksperimenter med forsuring af juicen til under pH 2.5 ved elektrodialyse med bipolære membraner og efterfølgende justering tilbage til juicens oprindelige pH-niveau med samme proces "vendt om" efter en kort opbevaringsperiode viste, at det var muligt at nedsætte og næsten eliminere den enzymatiske mørkfarvning foranlediget af PPO signifikant.

Længerevarende undersøgelser af mælkesyreekstraktion fra fermenteringsvæske med elektro-membran processer førte til udviklingen af en proces med indbygget anti-tilsmudsningsmekanisme. Processen er blevet døbt *strømvendende elektro-forstærket dialyse* og er indgivet som patentansøgning. Membranopsætningen svarer til opsætningen i en Donnan dialyse proces med anionbyttermembraner, men elektrisk strøm sendes gennem systemet for at forstærke iontransporten, der er kontrolleret af konkurrerende transport mellem laktationer og hydroxidioner ved skiftende pH-niveauer. Strømvending er inkorporeret for at destabilisere opbyggede lag af organisk tilsmudsning på membranerne.
Den strømvendende elektro-forstærkede dialyse proces blev gennemgribende testet på både model opløsninger og fermenteringsvæsker ved en opsætning, der simulerer en kontinuert fermentering. Tilfredsstillende laktatfluxe kombineret med høj tilbageholdelse af sukkerstoffer, calcium og magnesium blev konstateret. Procesfaktorer som strømeffektivitet og energiforbrug var ikke tilfredsstillende, men det blev anslået at optimering af udstyrsdesign og af operationsparametre gennem computersimulationer kunne bringe disse op i et økonomisk acceptabelt niveau. Processen var i stand til at køre uden stop over længere perioder, når der blev indført strømvending, end hvis dette blev udeladt.
Strømvendingen medfører et effektivitetstab, der blev undersøgt ved konstruktionen af en matematisk model, der blev implementeret som et computer program. Dette program var i stand til efterfølgende at producere estimater for strømeffektivitet, samlet laktatflux, energiforbrug og nødvendigt membranareal for dele af en strømvendende elektro-forstærket dialyse proces.

En produktion af 10,000 tons mælkesyre (88%) om året blev designet baseret på kontinuert fermentering og den strømvendende elektro-forstærkede dialyse proces ved at benytte procesestimater bestemt fra eksperimenter eller gennem simuleringer. Ekstraktionen af laktat fra fermenteringsvæske blev kombineret med elektrodialyse med bipolære membraner, afsaltning ved hjælp af elektrodialyse og fordampning for at opnå den ønskede renhedsgrad. En økonomisk evaluering af produktionen blev foretaget. Investeringen blev vurderet til at være kr. 145.5 millioner. Med en meget konservativ pris for 88% mælkesyre på kr. 9.50/kg og løbende, årlige omkostninger på kr. 49.2 millioner, opnås stadig en årlig profit på kr. 45.8 millioner og dermed en tilbagebetalingstid på omkring 6.3 år.

This thesis consists of a short summary and a general introduction to the background of the thesis work.
The main chapters of the thesis consist of a general theory chapter and three main problems associated with electro-membrane separation processes:

Chapter 1 – Chapter 1 contains a basic summary of electrodialysis and membrane theory to which later chapters refer.

Chapter 2 – In this chapter, the results of membrane related recovery processes is collected with the focus on recovering *citric acid* from lime fruit waste.

Chapter 3 – This chapter discloses the results from experiments, where browning of pear juice from Anjou pears is inhibited by bipolar electrodialysis technology.

Chapter 4 – This chapter conveys results obtained with different membrane related recovery processes toward the aim of discovering a feasible process for recovering *lactic acid* from fermentation broth. This chapter also includes the description of a new, patented unit operation named *reverse electro-enhanced dialysis*, which was invented during the cause of this project. It also entails a section where a numerical program is produced for computer simulations to investigate improvement of the aforementioned reverse electro-enhanced dialysis process, and the economical evaluation of a plant producing 10,000 tons of 88% lactic acid per year using this technology.

Table of content

1

1 Theory

1.1 Membrane separation technology

Membrane separation technology is met with increasing, commercial interest, since membrane processes can be tailored to fit many separation needs. In connection with the increasing global environmental awareness concerning industrial waste cleaning, recovery, and recycling, the industry have turned to membrane processes as a reliable and flexible method of improving waste treatment. Membrane processes can concentrate waste, while recovering possible valuable components for reuse. Often different membrane processes are combined to yield better results, so-called hybrid membrane processes.
Membrane processes generally involve large investment costs, but usually run at high efficiency, thus lowering operating costs.

Membranes are (not surprisingly) always the key element in membrane separation processes. The name membrane comes from the Latin: *membrana* meaning "thin skin". The IUPAC definition describes membranes as: 'structure, having lateral dimensions much greater than its thickness, through which mass transfer may occur under a variety of driving forces'. According to Dr. Mulder of the University of Twente (Mulder 1991) the definition of a membrane is "a selective barrier between two phases".

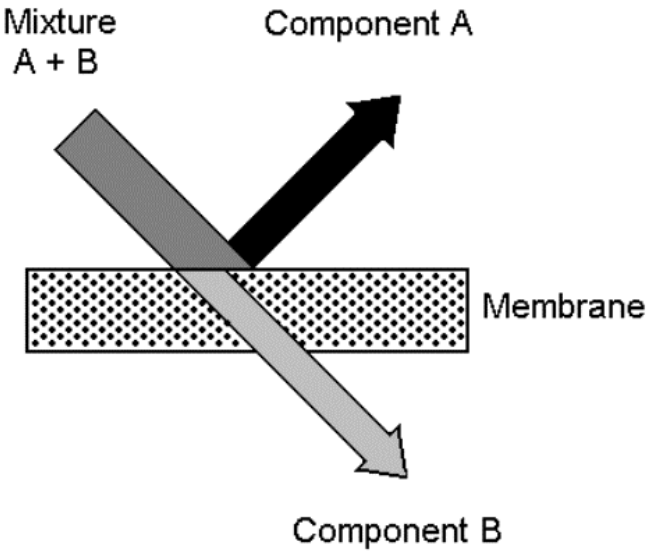

Figure 1.1 Ideal membrane separation.

Membranes come in many forms: porous or non-porous, polymeric or ceramic, natural or artificial. The selectivity that is their main advantage depends both on the size of the pores and membrane

material. Some kind of external driving force like a pressure gradient, concentration gradient or electrical field acting across the membrane is required for a separation to take place.
Table 1.1 entails a list of some typical membrane processes and their driving forces.

Membrane process	Driving force	Typical pore size
Microfiltration	Pressure	0,05 – 10 μm
Ultrafiltration	Pressure	1 – 100 nm
Nanofiltration	Pressure	0,1 – 2 nm
Reverse Osmosis	Pressure[a]	Nonporous
Gas Separation	Pressure[a]	Nonporous (or < 1 μm)
Pervaporation	Pressure[a]	Nonporous
Dialysis	Concentration gradient	1-5 nm or nonporous
Electrodialysis	Electrical field	Nonporous
Liquid Membranes	Concentration gradient	Nonporous (liquid)
Membrane Distillation	Temperature	0,2 – 1 μm

Table 1.1 Outline of different membrane processes and corresponding driving forces and typical membrane pore sizes. [a] - not directly pressure driven (Mulder 1991).

The pressure driven membrane filtrations are often categorized according to the type of membrane used, with reverse osmosis (RO), nanofiltration (NF), ultrafiltration (UF), and microfiltration (MF) as the four most common processes. This division is in fact very fuzzy because no sharp distinction can be made between adjacent membrane types where their pore size and hereby separation properties overlap. Typically, pore size or molecular weight cut-off (MWCO) is used to distinguish between MF, UF, and NF, but when it comes to differentiating NF from RO another approach is useful. Due to their dense nature, the NF/RO membranes are instead characterized in terms of salt (Na^+ and Ca^{2+}) rejection as well as organic rejection. There is no clear-cut definition between RO and NF except the relative rejection capabilities. In Figure 1.2 the effect of different pore sizes is demonstrated for the four pressure driven processes. Open membranes with large pores only reject bacteria-sized or larger particles, while very dense (nonporous) membranes reject even salts.

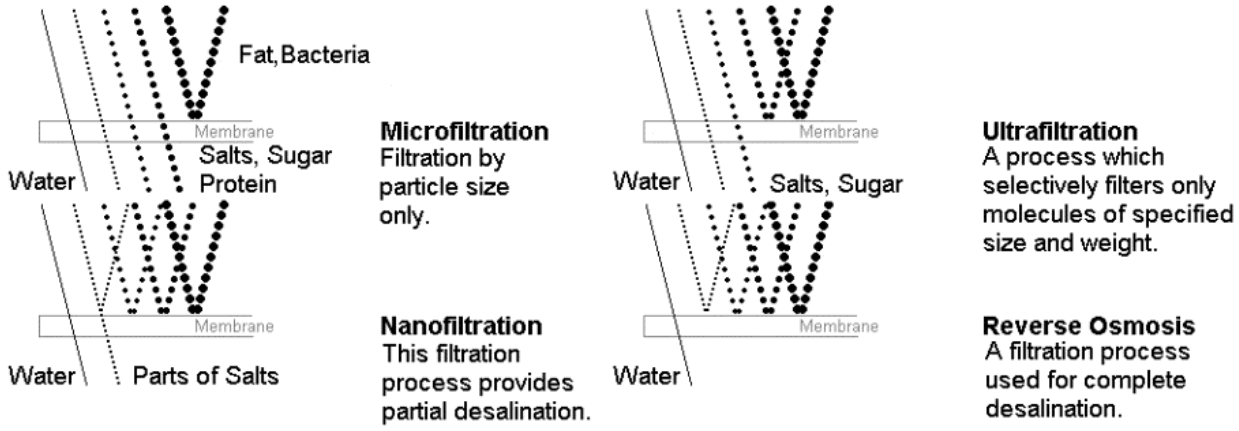

Figure 1.2 Comparison in particle rejection by membranes for four types of separation. (•••) fats, bacteria, (••) proteins, vira, (••) sugars, amino acids, (•••) salts, (—) water (Mulder 1991).

The definitions of dialysis and electrodialysis are more clear-cut even though both terms cover several sub-processes. Dialysis is a membrane process in which transport is driven by concentration differences across a separating membrane (Koros *et al.* 1996). Dialysis is probably best known from

treatment of blood in *hemodialysis* where undesired metabolites and toxic by-products such as urea and creatine are transported across a membrane between the blood and a refreshing solution under the influence of a concentration gradient. A special type of dialysis, named Donnan dialysis, ion-exchange membranes are utilized, which primarily facilitate transport of charged molecules. Electrodialysis is a membrane-based separation process in which ions are driven through an ion-selective membrane under the influence of an electric field (Koros *et al.* 1996). The principles and main theory of electrodialysis separation is elaborated on in the following.

1.2 Electrodialysis

1.2.1 Electrodialysis principle

Electrodialysis differs from the other membrane processes by utilizing electrical current as the main driving force in matter separation. This limits the possible solutes targeted for recovery separation to charged particles. The charged particles must be mobile, and the separation media must be able to transfer the electrical current with relatively low resistance. Electrodialysis is almost exclusively carried out on liquids.

The principle of electrodialysis is related to electrolysis as shown on Figure 1.3.

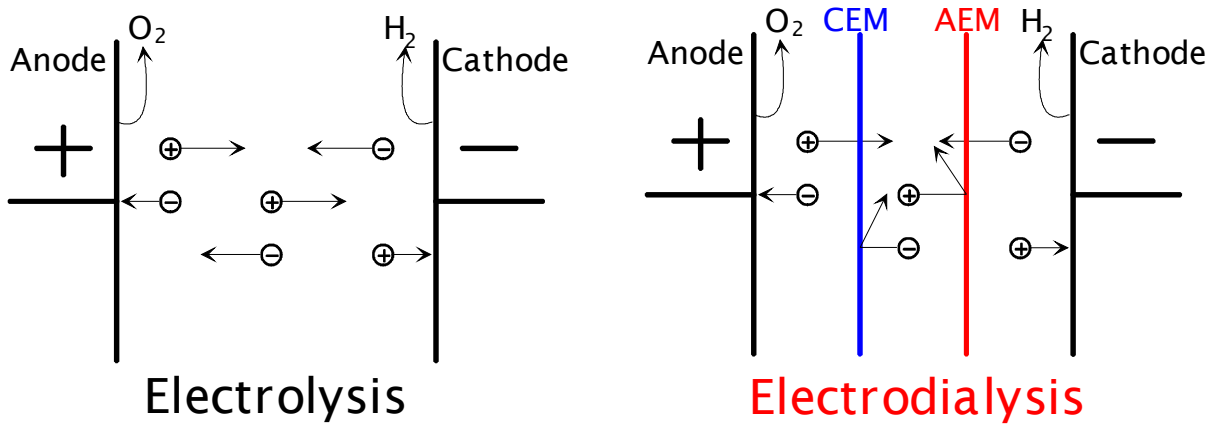

Figure 1.3 Left side demonstrates a standard electrolysis process. Right side demonstrates the same process with inserted ion-selective membranes. CEM = cation-exchange membrane. AEM = anion-exchange membrane.

The reason for inserting *ion-exchange membranes* as they are commonly referred to as is to prevent the migrating cations and anions from reaching the electrodes, where often unwanted electrode processes occur. The ion-exchange membranes can be employed to concentrate process streams, separate ionic species from non-ionic species, or recover or extract charged solutes from waste streams. One example is the removal of salts from seawater or brackish water. Some places, electrodialysis is utilized as a pre-treatment for this purpose to purify drinking water. Other places, the process concentrates seawater for a more economical production of table salt.

The standard configuration of a desalting process utilizing the electrodialysis principle is shown in Figure 1.4.

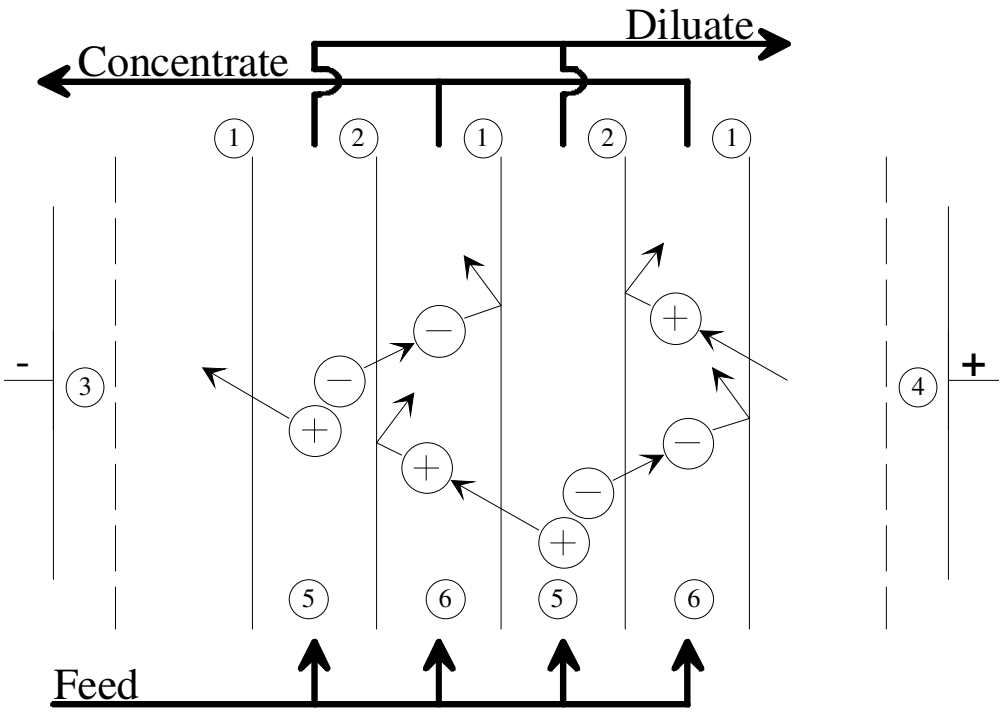

Figure 1.4 Principle of simple electrodialysis process. Diagram shows the membrane configuration with alternating cation-selective ① and anion-selective ② membranes between two electrodes (③ and ④), one at each end of the stack.

The drawing shows a membrane configuration with alternating cation-selective ① and anion-selective ② membranes. A cation-selective membrane (cation-exchange membrane) permits only positive ions to migrate through it. An anion-selective membrane (anion-exchange membrane) permits only passage to negatively charged ions. At each end of the membrane stack, electrodes (a cathode ③ and an anode ④) are placed, supplying a well distributed electrical field of direct current across the membrane stack. Between every membrane, *spacers* are placed. Spacers make sure that there is room between membranes for the liquid process streams to flow along the membrane surfaces.

A special, conductive solution is added to each electrode chamber, where electrode processes are taking place. Usually, an electrode solution that does not result in unwanted reaction products is utilized for this purpose. A sulfuric solution as "electrode rinse" splits water molecules into hydrogen gas at the cathode ③ and oxygen gas at the anode ④.

For a simple desalting process, feed is entered into the flow channels and directed into the spacers. The electrical current influences the charged ions in the feed solution, and similar to ordinary electrolysis, cations are carried towards the cathode, while anions are carried towards the anode. The cations in every second spacer ⑤ are able to migrate through the cation-selective membrane ① into the next spacers flow chamber ⑥. In these flow chambers ⑥, the cations are trapped, unable to migrate through the anion-selective membrane ②. The anions in the flow chambers ⑤ are able to migrate towards the anode through the anion-selective membrane ② and into the alternating flow chambers ⑥. In these flow chambers ⑥, the anions are trapped, unable to migrate further, since they are faced with a cation-selective membrane ①. The two electrodes are kept separated from the processed solutions.

Thus, cations and anions are migrating out of every second flow chamber ⑤ into the remaining chambers ⑥. The result is that by collecting the outlet of the flow chambers ⑤ and ⑥ separately, a depleted and an enriched solution is created. This setup is common for concentrating seawater for table salt production or as pre-treatment for desalting brackish water to create drinking water.

A repeating section of the electrodialysis stack is named a *cell pair*. In the example of Figure 1.4, the cell pair consists of one cation-exchange membrane ①, anion-exchange membrane ②, one dilution chamber ⑤, and one concentration chamber ⑥. In commercial electrodialysis stacks, many hundred cell pairs can be stacked between one set of electrodes, thus improving energy efficiency and negating the electrode effects to great extent.

1.2.2 Membrane spacers

The spacers that keep the membranes apart and allow process streams to flow between them exist in several forms and can greatly influence the separation process. In most cases, the spacers are non-conductive. Otherwise, most of the electrical current that should drive the ion transport in the process streams would go through the spacers with less resistance. In other cases, at very low electrolyte concentrations, conductive spacers have advantages since the conductivity of these process streams are to low to carry an operation. The ions are transported to the ion-exchange membranes by diffusion in these operations. The spacer's main function is to promote contact between the process stream and the membrane surface while supporting the ion-exchange membranes. Ion-exchange membranes are generally not mechanical stable and even small pressure differences from the process streams can cause a rupture in a membrane.

To promote a good mass transfer from process stream to membrane surface, turbulent flow inside the spacers between membranes is provoked by adding *nets* to the spacers or constructing channels that causes the flow to take a longer path along the membrane surface (tortuous path). Some of the spacers that have been designed and tested experimentally during the equipment construction phase of this work are presented in Figure 1.5.

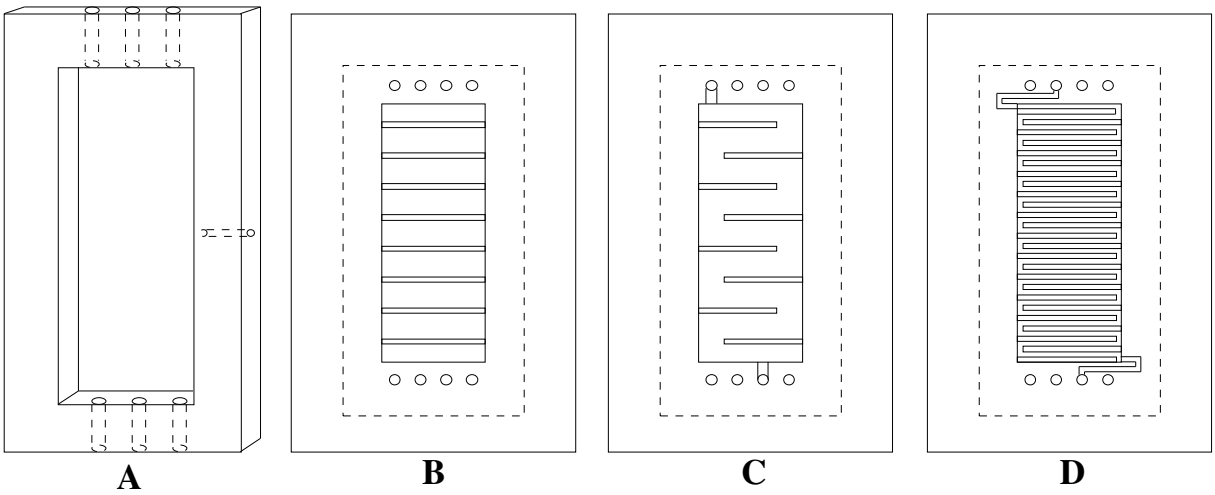

Figure 1.5 A. Sheet-flow spacer. **B.** Sheet-flow spacer with ribs. **C & D.** Tortuous path spacers.

The sheet-flow spacer **A** in Figure 1.5 is designed for difficult process streams with lots of particles and other material that hold potential for clogging up the system. By adding polymer nets to this spacer type, the flow can generally continue unobstructed and the membranes are supported. The net spacers promote turbulent flow because the flow must often change direction as demonstrated in Figure 1.6. The **B** spacer has ribs with intervals that cause a wave motion in the flow. This increases turbulence and ion transport between the membranes. The tortuous path spacer forces the process streams to follow a winding route along the membrane surface, increasing the contact period of the separation. This provides a much higher utilization of the active membrane surface, but results in increased pressure drop of the process stream being pumped through the equipment.

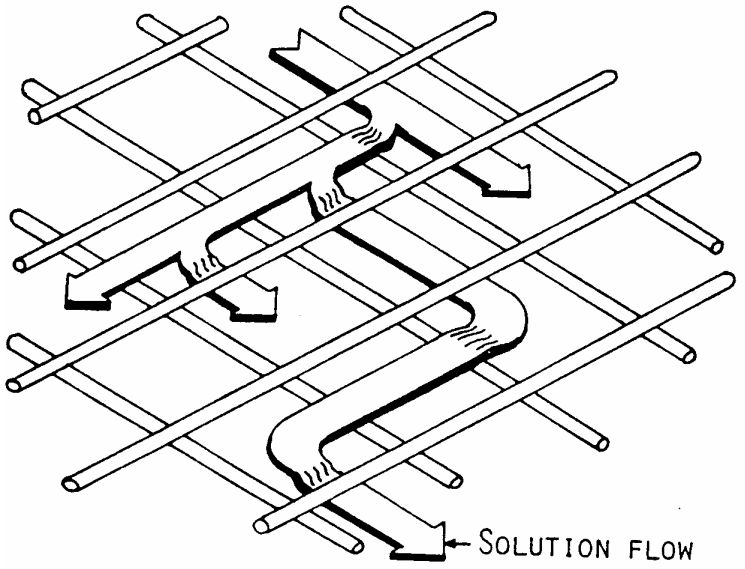

Figure 1.6 Net spacers force the flow to often change directions.

1.2.3 Ion-exchange membranes

Charged polymer membranes have been investigated for well over 100 years. Most natural and artificial membranes consist of polymers and the porous membranes investigated in the past inherently carry at least some ionizable groups (except in a few instances) and are therefore charged (Sélégny 1976). The basis of classic electrochemistry was founded around the turn of the 20th century with capacities like Ostwald, Nernst and Donnan being some of the most notable forerunners. Charged membranes have been investigated ever since, and while the results obtained in this field were mostly confusing during the 19th century, an increasing understanding of charged membranes and their basic functions has developed during the 20th century.

Commercially created ion-exchange membranes (IEM) are normally composed of crosslinked polymeric gels with fixed positive or negative charges. A fixed, immobile charge must be balanced by a dissolved mobile ion of opposite charge to preserve electroneutrality. Hence, to avoid precipitation or crystallization of the ionic groups inside an ion-exchange membrane, it is necessary to keep the membranes constantly wetted to preserve functionality. The polymers with high ion-exchange capacity have a strong tendency to swell, which is held in check by a high degree of crosslinking (Kesting 1985).

Two general different types of ion-exchange membranes exist. An ion exchange membrane with fixed positive charges allows primarily negative ions to enter and pass through the membranes internal matrix. This is then named an *anion-exchange membrane* (AEM). Typical fixed charges in anion exchange membranes are (Strathmann 1992):

$$-NH_3^+ \quad -RNH_2^+ \quad -R_3N^+ \quad =R_2N^+ \quad -R_3P^+ \quad -R_2S^+$$

Similarly, a membrane with fixed negative charges allows the free passage of cations and is hence named a *cation-exchange membrane* (CEM). Fixed charges commonly used in cation exchange membranes are:

$$-SO_3^- \quad -COO^- \quad -PO_3^{2-} \quad -HPO_2^- \quad -AsO_3^{2-} \quad -SeO_3^-$$

Normally the most strongly acidic or basic groups like the quaternary ammonium group ($-R_3N^+$) or the sulfonic group ($-SO_3^-$) are preferred in commercial membranes, since they are completely dissociated over nearly the entire pH-range.

The name "ion-exchange membrane" is perhaps a little misguiding, since ion exchange membranes work quite different from ion-exchange resins, normally employed in ion-exchange columns. In ion-exchange resins, ions of opposite charge are replaced by other ions of same general charge, while ions of the same charge as that of the resin are allowed free passage. An example on this is the demineralization of water, where calcium and magnesium ions are replaced by hydrogen or sodium ions, while anions like chloride and sulfate pass right through. In ion exchange membranes ions of opposite charge than the membranes fixed charges (counter-ions) can jump from one fixed group to the next and are hence mobile inside the membrane, while ions of same charge as the membrane (co-ions) are electrically repulsed by the fixed charges. The co-ions are still mobile inside the ion-exchange membrane, but because of the repulsion and the necessity of preserving electroneutrality, the concentration of co-ions is much lower compared to that of the counter-ions. The principle is sketched on Figure 1.7 with a polymer carrying fixed sulfonic groups.

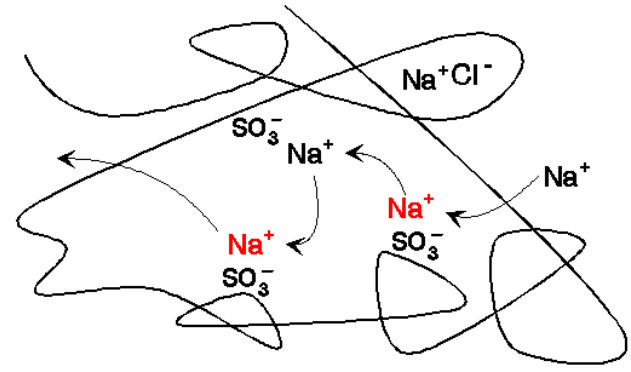

Figure 1.7 Migration of sodium ions through a cation exchange membrane.

The mobile ions are respectively sodium (counter-ions) and chloride (co-ions). The sketch shows how the sodium ions migrate through the polymer by "jumping" from one fixed sulfonic group till the next, while chloride needs to be paired with a sodium ion at all time. The mechanism of

excluding co-ions from ion exchange membranes is referred to as Donnan exclusion, which is elaborated on later in this chapter.

The Donnan exclusion and the selectivity of an ion-exchange membrane depend on different factors (Strathmann 1992). Both properties increase with:

- increasing concentration of fixed charges,
- increasing valence of the co-ions,
- decreasing valence of the counter-ions,
- decreasing electrolyte concentration in the mobile phase,
- decreasing affinity between the exchanger groups and the counter-ions.

Other important parameters for the ion-exchange membrane's properties include the density of the polymeric network, the hydrophobic and hydrophilic properties of the polymer matrix, the distribution of the charge density, and the morphology of the membrane.

To be most effective an ion-exchange membrane should possess the following properties:

- *High permselectivity*. The ion-exchange membrane should be highly permeable to counter-ions and impermeable to co-ions.
- *Low electrical resistance*. The permeability for the counter-ions driven by an electrical potential gradient should be as high as possible.
- *Good mechanical and form stability*. The membrane should be mechanically strong to withstand handling during equipment assembling/disassembling as well as minor pressure changes during operation. Also low degree of swelling or shrinking in transition from dilute to concentrated electrolyte solutions is important to preserve form and avoid equipment leakage.
- *High chemical stability*. The membrane should be inert to the electrolyte solutions and their electrolysis products. This means stability in the operating pH-range and resistance to oxidizing agents.

Optimizing properties of ion-exchange membranes often result in a compromise, because the parameters involved most often work in opposite directions. Higher degree of cross-linking improves mechanical stability, but increases the electrical resistance as well. Higher concentration of fixed charges causes lower electrical resistance, but increases swelling which lowers mechanical stability. Hence, commercial ion-exchange membranes are usually manufactured with specific properties for different tasks. Membranes with increased chemical resistance, mechanical stability, or low diffusion rates can be obtained as needed for a given process. Monovalent-selective membranes, that are permeable to monovalent counter-ions while excluding multivalent counter-ions as well as co-ions, are also commercially available. These special grade membranes are used in the table salt production, when sodium chloride is concentrated from seawater with electrodialysis, thus only concentrating the sodium and chloride ions with a minimum of the metal, sulfate, calcium, or magnesium ions normally present in seawater.

A special version of an ion-exchange membrane is the bipolar membrane. The bipolar membrane is composed of two halves: an anion-exchange film and a cation-exchange film connected by a very thin (about 1 nm thick) neutral interface junction. A bipolar membrane is sketched on Figure 1.8.

When the membrane is placed in an electrical field as shown in the figure water molecules split into hydroxide ions and protons.

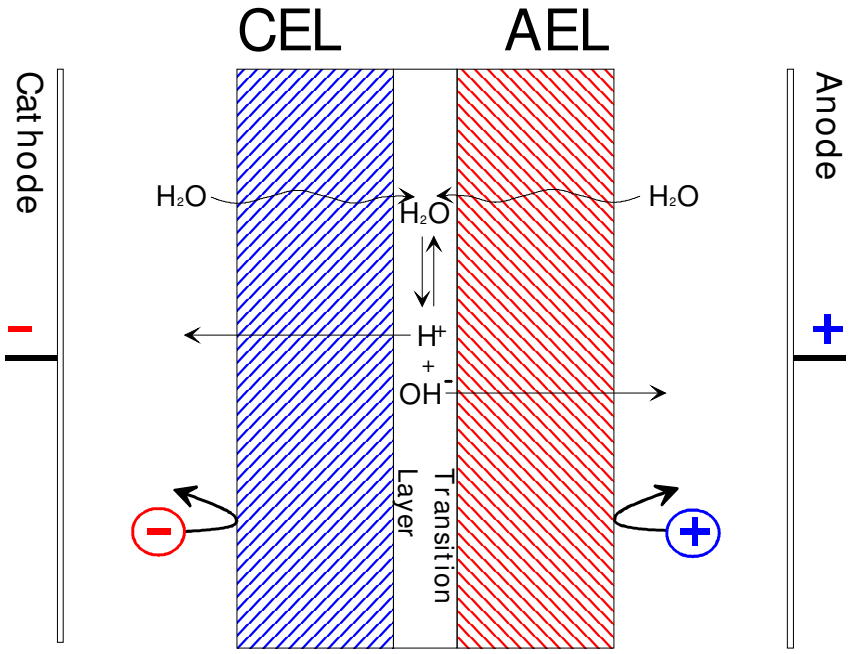

Figure 1.8 Schematics of bipolar membrane. Cations are rejected by the anion-exchange layer (AEL) and anions are rejected by the cation-exchange layer (CEL). The electrical potential drop across the transition layer catalyses dissociation of water that diffuses into the membrane.

The applications possible by this watersplitting process are many. By producing hydrogen and hydroxide ions while transferring electrical current *and* serving as an impermeable wall to both cations and anions, it is possible to regenerate acids and bases from mixed solutions.

1.2.4 Donnan exclusion

To explain the mechanisms of the ion-exchange membrane's selective behavior towards positive and negative ions, consider a cation-exchange membrane in contact with a dilute ionic solution as sketched on Figure 1.9. In this case the cations are the counter-ions and the anions are the co-ions. For the exclusion to be effective, the membrane's concentration of fixed charges (the membrane's ion-exchange capacity) must be higher than the concentration of the electrolyte. Under normal operating conditions, the concentration of mobile cations inside the membrane is much higher than in the dilute solution to preserve electroneutrality of the fixed negative groups. The concentration of mobile anions, however, is much lower (if existing) inside the membrane than in the solution.

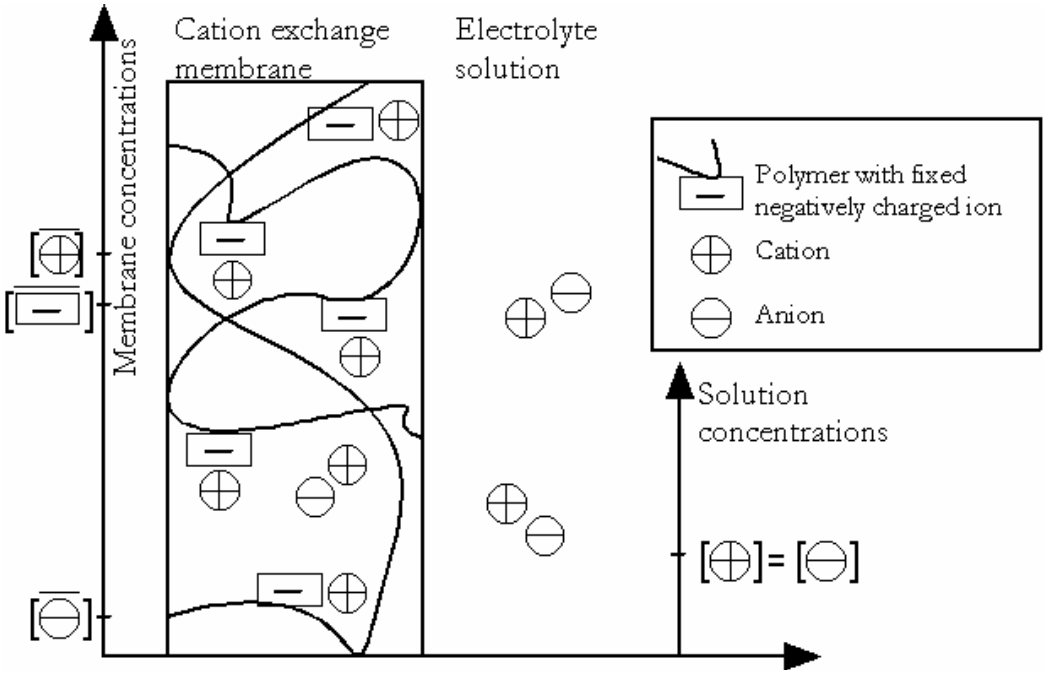

Figure 1.9 The distribution of cations and anions between a cation exchange membrane and a dilute electrolyte solution. Inside the membrane fixed negative charges are balanced by mobile counter-ions (cations). The axis gives a rough estimation of the concentration levels of the ions inside the membrane (indexed with ¯) and in the solution at equilibrium.

For neutral molecules, ordinary diffusion would take place to level out the concentration differences. The cations and anions all carry charges and attempts to balance the concentration differences are disturbing electroneutrality both inside the membrane and in the external solution. Cations diffusing out of the membrane and into the external solution create a positive surplus of charge (space charge) in the solution just outside the membrane and anions from the external solution diffusing into the membrane create a negative space charge just inside the membrane surface. This creates an electrical field across the membrane-solution interface that opposes further diffusional flow as shown in Figure 1.10.

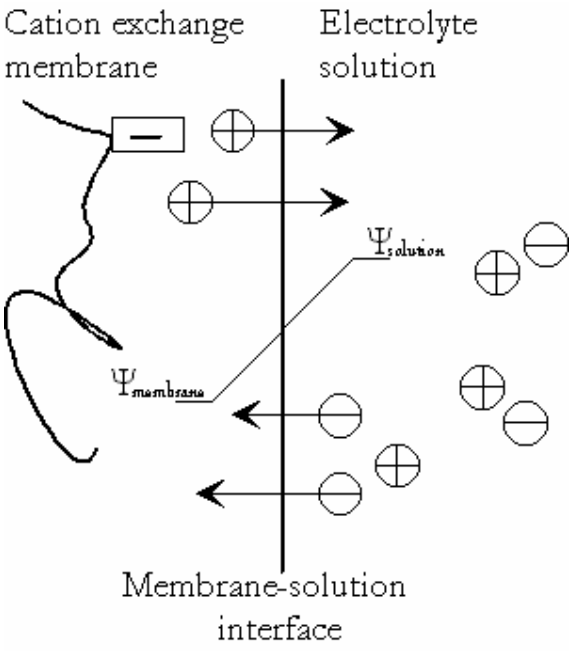

Figure 1.10 Cations diffusing out of the membrane while anions diffuse into the membrane resulting in the establishment of an electrical field $\Delta\Psi = \Psi_{membrane} - \Psi_{solution}$ that balance out the driving diffusion forces.

At electrochemical equilibrium this electrical field balances the driving diffusion forces of the ions. This potential allows the counter-ion concentration to be higher, and the co-ion concentration to be lower inside the membrane than in the external solution. Since the co-ions are repelled from the membrane, the electrolyte itself is repelled, because of the electroneutrality requirement. This exclusion of electrolyte is named *Donnan exclusion* and the electrochemical equilibrium is named *Donnan equilibrium* in honor of his pioneer work in this area (Donnan 1911).

The electrical potential $\Delta\psi$ that arises can be calculated from the electrochemical potentials μ of the mobile ions. Neglecting pressure differences between the membrane's liquid phase and the external solution, the electrochemical potential for every ionic species can be expressed:

Equation 1.1 $$\mu_j = \mu_j^{\mathrm{O}} + RT \ln a_j + z_j F \psi$$

μ° is the chemical standard potential, R is the gas constant (8.31 J/mol·K), and T the temperature (K). a and z are the activity and ionic charge, respectively. F is the Faraday number (96485 C/eq.) and ψ the electrical potential.

At steady state the chemical potential for each component is equal on both sides of the electrolyte/membrane interface. Using index m for membrane conditions and s for solution conditions, this can be expressed as:

Equation 1.2 $$\mu_j^{\mathrm{O},m} + RT \ln a_j^m + z_j F \psi^m = \mu_j^{\mathrm{O},s} + RT \ln a_j^s + z_j F \psi^s$$

At equilibrium the chemical standard potential μ_j° is equal in both phases. Hence the potential difference between membrane and solution $\Delta\psi$ that arises can be calculated by rearranging the previous equation to:

Equation 1.3 $$\Delta\psi = \psi^m - \psi^s = \frac{RT}{z_j F}\ln\frac{a_j^s}{a_j^m}$$

$\Delta\psi$ is named the *Donnan potential*, ψ_{Don}. Since the Donnan potential that arises from the distribution of the cations must be equal to the potential that arises from the anion distribution, Equation 1.3 can be changed to:

Equation 1.4 $$\frac{RT}{z_+ F}\ln\frac{a_+^s}{a_+^m} = \frac{RT}{z_- F}\ln\frac{a_-^s}{a_-^m}$$

which rearranges into:

Equation 1.5 $$\left(\frac{a_+^s}{a_+^m}\right)^{1/z_+} = \left(\frac{a_-^s}{a_-^m}\right)^{1/z_-}$$

From Equation 1.5, some general considerations concerning Donnan equilibrium is reflected on in the following examples.

Example A
For a single monovalent salt ($z_+ = 1$, $z_- = -1$) like sodium chloride in a dilute (0.01 M) solution, assuming activity contants $\gamma_\pm \approx 1$, Equation 1.5 rearranges into:

Equation 1.6 $$\frac{C_+^m}{C_+^s} = \frac{C_-^s}{C_-^m}$$

In this example, $C_+^s = C_-^s = 0.01$ M. For a cation-exchange membrane the membrane's ion-exchange capacity (concentration of fixed ionic groups) is assumed to be around 1 M, which means that the concentration of mobile cations in the membrane, C_+^m is around 1 M to balance the fixed charges. From Equation 1.6 it then follows that C_-^m must be in the region of 0.0001 M. This example of a typical electrodialysis setup, demonstrates that the membrane's concentration of mobile cations is about 10.000 times larger than the concentration of mobile anions, meaning the selectivity of cations over anions in this membrane in this solution is 99.99%.

From Equation 1.6 it is clear that the higher the counter-ions' concentration ratio between membrane and solution (C_+^m/C_+^s), the higher the ratio of the solution/membrane concentration of the co-ions (C_-^s/C_-^m). This results in higher selectivity. The opposite is also applies. The lower the counter-ion ratio becomes, the result is a lower co-ion ratio, which results in lower selectivity. Ion

exchange membranes generally perform poorly in high electrolyte concentrations. When the electrolyte concentration matches the membrane capacity, there is no effective selectivity.

For low electrolyte concentrations (100 times lower than the membrane's ion-exchange capacity) it is safe to assume that co-ion concentration is insignificant inside the membrane.

Example B
In a dilute electrolyte solution with both monovalent and divalent cations in contact with a cation-exchange membrane, Equation 1.3 still applies. Consider a mixed electrolyte solution with sodium chloride and calcium chloride and for simplicity, the charge equivalent concentrations of both cations are the same. The Donnan potential that arises at equilibrium affects both ions. Following the same routine from Equation 1.3 as before for the two types of cations and still neglecting activity coefficients, the ensuing expression is reached:

Equation 1.7 $$\left(\frac{C_{+}^{m}}{C_{+}^{s}}\right)^{2} = \frac{C_{2+}^{m}}{C_{2+}^{s}}$$

This equation shows that the ratio of the divalent cation concentration between membrane and external solution will be the square of the ratio of monovalent cation. E.g. if the sodium concentration inside the membrane rises to 10 times the sodium concentration of the external solution, the membrane's calcium concentration would be 100 times larger than the solution's concentration of calcium.

The higher the ionic charge of a counter-ion, the more readily it will enter and fill the membrane's capacity spots.

Example C
To calculate the intermembrane concentration of mobile counter- and co-ions, consider the need for electroneutrality of both phases in the system at equilibrium. For a salt in the initial solution:

Equation 1.8 $$\sum_{j} z_j C_j^s = 0$$

The same equation can be set up for the membrane's mobile phase, including the membrane's ion exchange capacity C_R:

Equation 1.9 $$\sum_{j} z_j C_j^m + z_R C_R = 0$$

Assuming a cation-exchange membrane with monovalent fixed charges ($z_R = -1$) in contact with a monovalent salt ($z_+ = +1$, $z_- = -1$), Equation 1.8 and Equation 1.9 rearranges into:

Equation 1.10 $$C_{+}^{s} = C_{-}^{s} \quad \text{and} \quad C_{+}^{m} = C_{-}^{m} + C_R$$

Combining these two equations with the Donnan exclusion condition in Equation 1.6, the membrane's co-ion concentration C_-^m can be obtained from the following expression:

Equation 1.11 $$\frac{C_-^s}{C_-^m} = \sqrt{\frac{C_R}{C_-^m} + 1}$$

For dilute solution, the ratio $C_R/C_-^m >> 1$ and Equation 1.11 can be simplified to:

Equation 1.12 $$C_-^m = \frac{\left(C_-^s\right)^2}{C_R}$$

Equation 1.12 confirms the theoretical estimation of the co-ion concentration of 0.0001 M inside a cation-exchange membrane with a capacity of 1 M in contact with a 0.01 M monovalent electrolyte as treated in example A.

For more complex electrolyte solutions, the results must be evaluated separately from case to case, and the assumption of activity coefficients at unity must be questioned. But for dilute, monovalent electrolytes Equation 1.12 yields very good estimates.

1.2.5 Ion transport

The following studies the transport of ions through ion-exchange membranes to evaluate the mechanisms involved and to assist in modelling of electrodialysis processes.

Ion transport can in most cases be broken into three possible contributions: convective transport, diffusive transport and migration. Simplified to one dimension (x), the total flux J of an ionic component j can be estimated from this equation:

Equation 1.13 $$J_j = vC_j - D_j\frac{dC_j}{dx} - \frac{z_j F C_j D_j}{RT}\cdot\frac{d\psi}{dx}$$

J_j, C_j, D_j, z_j are respectively the flux, the concentration, the diffusion coefficient and the ionic charge of component j. v is the convective flow velocity, F the Faraday number, R the Gas constant, T the temperature and ψ the electrical potential.

Ion-exchange membranes are generally nonporous; hence the convective ion transport (vC_j) can be neglected in Equation 1.13 when considering trans-membrane transport.

According to the Einstein relation, the ionic mobility of component j, u_j can be introduced into Equation 1.13 as (Atkins 1992):

Equation 1.14 $$u_j = \frac{z_j F D_j}{RT}$$

By neglecting convective transport and inserting Equation 1.14 reduces Equation 1.13 to the Nernst-Planck equation (Mulder 1991):

Equation 1.15 $$J_j = -D_j \frac{dC_j}{dx} - u_j C_j \frac{d\psi}{dx}$$

Two large applications incorporating ion-exchange membranes are *dialysis* and *electrodialysis*. In dialysis the diffusional flux is often the dominant ion transport, which then gives rise to an electrical migration flux. In electrodialysis processes an electrical field is exerted across the membranes promoting the migration transport, which often provokes a diffusional flux that works counter to the desired separation direction.

Equation 1.15 shows that non-charged molecules are only subject to diffusion through ion-exchange membranes, but solvent transport must still be considered. For aqueous solutions, three different transport mechanisms affect the desired molecules:

- *Osmosis*. In the case of electrodialysis, ions are often driven through ion-exchange membranes against their concentration gradient to create concentrated and diluted product streams. The concentration difference between the separated electrolyte solutions creates an osmotic pressure gradient that affects the solvent in an attempt by Nature to establish equilibrium.
- *Electroosmosis*. Since the dissolved ions coordinate solvent molecules to stay dissolved during transport, significant amounts of solvent are moved by electroosmosis.
- *Watersplitting*. In some instances, high polarization effects at the membrane surfaces promote the "water-splitting" effect, causing water molecules to dissociate into hydrogen and hydroxide ions.

The five different transport effects that are commonly present across ion-exchange membranes during electrodialysis operations are schematically shown on Figure 1.11.

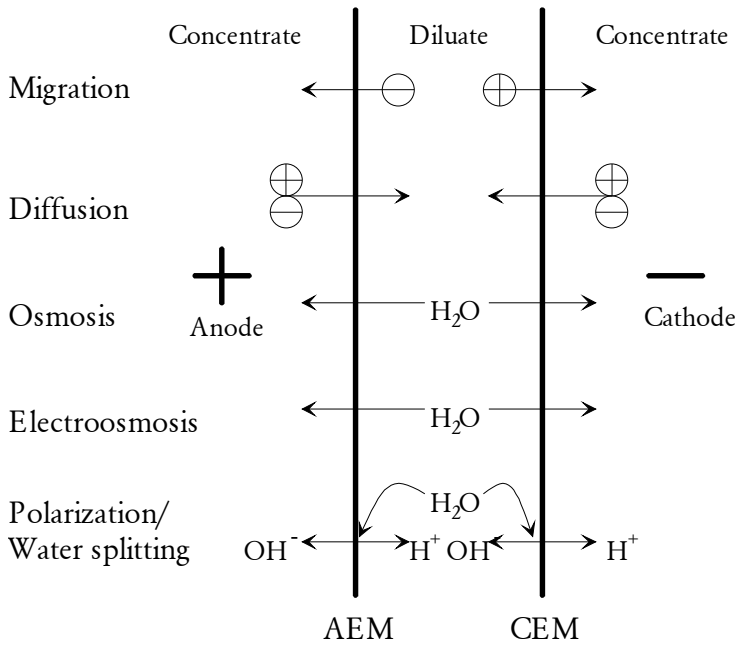

Figure 1.11 Transport mechanisms across ion-exchange membranes in electrodialysis. AEM indicates an anion exchange membrane and CEM a cation exchange membrane.

A theoretical value for the transport of a given ion species j can be expressed by a transport number *t*, which is defined as the fraction of total electrical current density ***i*** carried by the ion:

Equation 1.16 $$t_j = \frac{i_j}{i}$$

If the interaction between ions is neglected the transport number in diluted solutions can be expressed by:

Equation 1.17 $$t_j = \frac{|z_j| u_j C_j}{\sum_k |z_k| u_k C_k}$$

z is the charge, u is the mobility, and C is the concentration of the ion. The denominator is a summation of all ionic species present. For a dissolved, monovalent salt, e.g. NaCl the transport number of Na^+ and Cl^- in solution is 0.39 and 0.61, respectively, since the mobility of chloride is higher than that of sodium. For KCl the transport number of both K^+ and Cl^- is approximately 0.5, since their mobility is approximately the same in solution. However, inside e.g. the anion-exchange membrane the transport number of Cl^- would in theory approach unity, while the transport number of cations approaches zero, since Donnan exclusion causes the concentration of anions inside a anion-exchange membrane's mobile phase to be several magnitudes higher that the concentration of cations.

Similarly, the transport number inside a cation-exchange approaches unity for cations and zero for anions.

pH has a great influence on transport numbers since deviations from neutral pH yields a higher level of either hydrogen or hydroxide ions. Furthermore, the ionic mobility of both hydrogen and hydroxide ions is much higher compared to other organic or inorganic ions ($u_{H+} \approx 7 \cdot u_{Na+}$ and $u_{OH-} \approx 2.5 \cdot u_{Cl-}$) (Atkins 1992).

1.2.6 Polarization

Polarization is an essential, limiting factor in the performance of an electrodialysis process. Polarization at the surface of an ion-exchange membrane arises from the difference between the transport number of an ionic species in the membrane and in the solution. Figure 1.12 shows a simple, one-dimensional model of the concentration profiles in the boundary layer for two different current densities ($\boldsymbol{i}_1$ and $\boldsymbol{i}_2$) where cations are entering a cation-exchange membrane. The model is based on the assumption that the external solution is a turbulent stream flowing along the membrane surface (the bulkphase) and that a stagnant, boundary layer of laminar flow exists very close to the surface. At equilibrium, without electrical current or other driving forces, the bulkphase concentration is uniform throughout the external solution, including the boundary layer. As a driving force in form of electrical current is added, ions start to migrate to and through the ion-exchange membrane. Since the electrical current is carried by both cations and anions in solution, but only by one type of ions through the ion-exchange membranes, polarization occurs. Since ions are drawn into the membrane about twice as fast, as they can be carried to the membrane surface, the concentration profile through the laminar boundary layer changes. This is shown on Figure 1.12. The bulkphase is considered turbulent and perfectly stirred, and is unaffected by polarization. The development of a concentration profile across the boundary layer gives rise to a diffusional flux of ions to the membrane surface to balance the unequal migration fluxes.

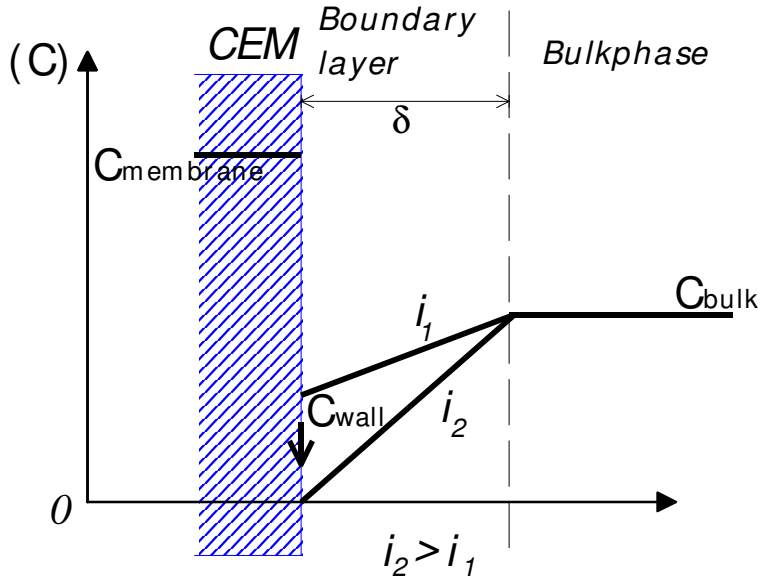

Figure 1.12 Concentration profile in the boundary layer of an ionic species entering the membrane. The two profiles are shown for different current densities where $\boldsymbol{i}_2$ is equal to the critical current density.

As the current density is increased, polarization increases and wall concentration drops until a critical (or limiting) value of the current is reached where $C_{wall} \approx 0$. This marks the limit where diffusion can no longer supply ions fast enough to keep up with the electrical migration through the membrane. At this point a further increase in the current density would result in the excess current being carried by H^+ and OH^- generated by the splitting of water molecules at the membrane surface. The highest attainable current density before watersplitting occurs depends on the bulk concentrations and hydrodynamics of the process streams, as given by the following equation (Mulder 1991):

Equation 1.18 $$i_{\lim} = \frac{z \cdot D \cdot F \cdot C_{bulk}}{(t^m - t^s) \cdot \delta}$$

z is the ionic charge, D is the diffusion coefficient, F is the Faraday number, C_{bulk} is the bulk concentration, δ is the boundary layer thickness, and t^m and t^s are the transport numbers in the membrane's mobile phase and the external solution, respectively.

Electrodialysis processes should be operated at lower than limiting current densities in order not to waste energy. Generally, processes operate at 80-90% of the limiting current density.

1.2.7 Fouling

Membrane fouling, scaling and poisoning are major problems in electrodialysis operations that must be avoided whenever possible.

Membrane fouling is used as a term to describe the adsorption of macro-particles or bio-matter like proteins on membrane surfaces. Large, charged molecules (MW > 1000) are generally retained by ion-exchange membranes because of their size, but their charges are attracted by the oppositely charged ion-exchange membranes and layers on top of the membranes often start to build (Lindstrand *et al.* 2000a;Lindstrand *et al.* 2000b). When oppositely charged proteins cling to the surface of an ion-exchange membrane, they affect the Donnan exclusion by neutralizing a number of fixed ions, and thus lowering the selectivity of the membrane. When the bio-matter fouling becomes more extensive, large surface areas are no longer effective for ion transport and electrical resistance increases. Build-up of bio-matter in electrodialysis also presents another problem by clogging up equipment and obstructing the flow. pH, bio-matter concentration and ionic strength of the fouling matter all affects how the process is influenced (Mulder 1991). In case of oppositely charged matter with dense charge concentration (approximately as large as the membrane capacity) fouling an ion-exchange membrane, a situation is created that resembles the bipolar membrane. This can cause increased water-dissociation, which results in energy loss, lower efficiency and pH-changes (Ramirez *et al.* 1992)
Membrane fouling is often reversible, and cleaning the system with alkaline and/or acidic agents often regenerates the membranes to the initial state of operation. The speed of the rebuilding of fouling layers on the membranes determines how often operation has to be interrupted for cleaning. By increasing the Reynolds number of the process streams through the membrane stack, it is possible to maintain a continuous removal of fouling matter that builds up and a steady-state of the fouling is reached.
The following process parameters can be changed to reduce fouling (Chiao *et al.* 1991):

- Increasing flow velocity.
- Utilizing spacer design with channels that promotes turbulence.
- Periodically stopping in the electrical current.
- Periodically alternating flow chambers and reversing current direction (*reverse electrodialysis*).
- Periodically cleaning the system.
- Pretreatment of fouling content (precipitation, filtration, enzyme treatment).

In some commercial membranes like the Neosepta® AMX anion-exchange membrane (Tokuyama Corp., Japan), the length and degree of crossbinding have been adjusted to allow larger molecules to pass through the membrane (Strathmann 1992). This reduces the fouling build-up of small particles.

Membrane scaling commonly occurs when the feed contains fair amounts of multivalent cations, especially calcium and magnesium. When divalent cations like calcium and magnesium passes through cation-exchange membranes into an alkaline solution, they immediately precipitate on the membrane surface as their respective hydroxide salts ($Ca(OH)_2$, $Mg(OH)_2$). This scaling affects the process fast by reducing effective membrane area, and increasing electrical resistance.

Membrane poisoning occurs when charged ions in the process streams react irreversibly with the membrane. The reaction can be a chemical reaction that changes the membrane and the membrane properties. When poisoning degrades the membranes, membrane maintenance and replacement must occur at regular intervals, which is a heavy expense. Only in exceptional cases (e.g. highly valuable products) can membrane poisoning be tolerated for lengthy operations.

1.2.8 Mass transfer

Increasing the Reynolds number does not just reduce fouling, but increases the mass transfer of the separation process as well. The mass transfer for the separation is most critical across the laminar boundary layer along the membranes' surfaces. The mass transfer coefficient k for the boundary layer can be expressed as:

Equation 1.19 $$k = \frac{D}{\delta} = \frac{Sh * D}{d_h}$$

D is the diffusion coefficient, δ is the boundary layer thickness, *Sh* is the Sherwood number, and d_h is the hydraulic diameter in the flow spacer. The Sherwood number can be related to the Reynolds number, *Re* and Schmidt number, *Sc*. For turbulent flow, which is common for electrodialysis separation, the Sherwood number can be expressed by the Dittus-Boelters relation (Jonsson and Boesen 1984):

Equation 1.20 $$Sh = 0.023 \mathrm{Re}^{0.8} Sc^{0.33}$$ (turbulent flow)

For laminar flow, the relation becomes:

Equation 1.21 $Sh = 1.86\left(\mathrm{Re}\, Sc \, {d_h}/{L} \right)^{0.33}$ (laminar flow)

L is a measure of the flow path length. By designing the flow spacers that regulates the flow along the membrane surfaces to promote high Reynolds number, the boundary layer thickness is decreased and ions are more readily transported in the solutions. Polarization is reduced as a consequence of the increased mass transfer.

For estimation of a boundary layer thickness in a designed spacer, the Sherwood number can be calculated according to Equation 1.20. From the Sherwood number, the mass transfer coefficient can be obtained and from that, the boundary layer thickness as in Equation 1.19.

1.2.9 Current efficiency

An important factor to measure in order to evaluate efficiency of an electrodialysis process is the current efficiency, η. The current efficiency is an expression of the amount of electrical energy added to the system that is being utilized for the targeted separation. The current efficiency is a combination of the selectivity of the membrane (Donnan exclusion), the pH of the feed solution, back diffusion of already transferred ions, and current leakage in the manifold system.

The selectivity of the ion-exchange membranes determines the amount of co-ion leakage. A high selectivity lowers the amount of charge carried by leakage of co-ions. Lower selectivity results in more co-ions being transported through membranes against the desired separation direction, thus causing decreased efficiency.
pH of a feed solution is important, since a large deviation from neutrality mean a significant amount of hydrogen or hydroxide ions is present. Unless these ions are among the desired targets of an electrodialytic separation, they are going to compete with the targeted ions, thus lowering the efficiency of the process.
Back diffusion does not directly cause a loss of efficiency, but then high levels of concentration occurs, backdiffusion of concentrated salts is significant, resulting in an indirect decrease of efficiency, since energy utilized for the extraction of ions that diffuse back to the diluted feed is wasted.
Another possibility to loose efficiency lies within the design of process equipment. The electrical current will travel from electrode to electrode by the route that offers lowest electrical resistance. Insulation of the equipment must be considered, as well as flow channel design. Some electrical current travel through the flow manifolds, decreasing the effective current density through the central cells.

One way to determine the current efficiency of an electrodialysis unit is given in this equation:

Equation 1.22 $\eta = -\dfrac{z \cdot F \cdot Q_F \cdot \Delta C_F}{n \cdot I} \qquad \Delta C_F = C_{F,out} - C_{F,in}$

z is the charge of the targeted ion, F is the Faraday number, Q_F is the volumetric feed flow, ΔC_F is the difference between the feed inlet and outlet concentrations from the stack, n is the number of cell pairs in the stack and I is the total electrical current through the stack.

Equation 1.22 can be interpreted as the amount of the desired target ions ($-Q_F \cdot \cdot \Delta C_F$) converted into electrical current ($\cdot z \cdot F$) divided by the actual current added (I) and nominated per cell pair (n). This equation has some flaws, when applied to actual process measurements. If other transport processes like diffusion, osmosis, or electroosmosis takes place during the separation, their added transports of ions or solvent impacts on the result either positively or negatively. Through Equation 1.22, efficiencies higher than 1 are sometimes obtained as a result of positive diffusion along with the migration. By measuring solvent transport and calculating osmotic pressures, it is possible to eliminate their influences, when assuming process interaction is insignificant.

1.2.10 Energy consumption

The energy needed for transferal of a given amount of a targeted ionic species across an ion-exchange membrane from a feed solution to a product stream is an important parameter in evaluating the suitability of an electrodialysis process. The minimal thermodynamic work, W_{min} required for separating a monovalent salt is given by the Gibbs free energy, ΔG (Strathmann 1992):

Equation 1.23 $$W_{\min} = \Delta G = 2RT(C_F - C_D)\left(\frac{\ln\frac{C_F}{C_D}}{1-\frac{C_F}{C_D}} - \frac{\ln\frac{C_F}{C_C}}{1-\frac{C_F}{C_C}}\right)$$

C_F is the feed concentration. C_D and C_C are the concentration in the diluate and concentrate, respectively. ΔG is the Gibbs free energy required for decreasing the concentration in 1 liter of solution from C_F to C_D.

The actual energy consumption required for a separation is considerable higher due to:

- Ohmic resistance in the solutions and membranes.
- Necessary cooling of system.
- Polarization effects.
- Resistance in electrode system.
- Resistance in external electrical system.
- Current efficiency is less than 1 per cell pair.
- Process streams need to be pumped.

A great deal of energy is spent to overcome the ohmic resistance of the system, which results in heating of the process streams and equipment. Since the polymers that ion-exchange membranes are based on, show speedy degradation at higher temperatures, cooling of the process streams is needed.

The ohmic resistance in the electrolytes, R_s can be calculated from:

Equation 1.24 $$R_s = \frac{1}{\kappa} \cdot \frac{l}{A_m}$$

κ is the conductivity of the electrolyte, l is the thickness of the flow chambers (distance between membranes) and A_m is the active cross-section area of the stack. The resistances in the ion-exchange membranes, R_m depend on the membrane type and the mobile ions. Typical values for the specific membrane resistance can often be found in supplier's data-sheets or measured by the difference in the conductivity across an electrolyte with and without a membrane inserted. For a bipolar membrane higher electrical resistance is encountered as a result of a minimum necessary potential drop across the interface layer, required for catalyzing watersplitting.
Polarization effects as described in the previous section can cause the specific resistance of the boundary layers R_p to differ significantly from the resistance of the bulk solutions, especially at currents near the limiting current density. The overall cell resistance can be expressed as the summation over the resistance of solutes, membranes and polarization layers:

Equation 1.25 $$R_{Stack} = \sum R_s + \sum R_m + \sum R_p$$

Resistance in the electrode system and the external electrical system is often neglected, because of the insignificant contribution to the overall resistance in a stack composed of 200-300 cell pairs. Since an electrodialysis stack typically consists of repeating cell pairs, it is customary to determine a specific resistance of a cell pair, R_{Cell}:

Equation 1.26 $$R_{Cell} = R_{Diluate} + R_{Concentrate} + R_{CEM} + R_{AEM} + R_p$$

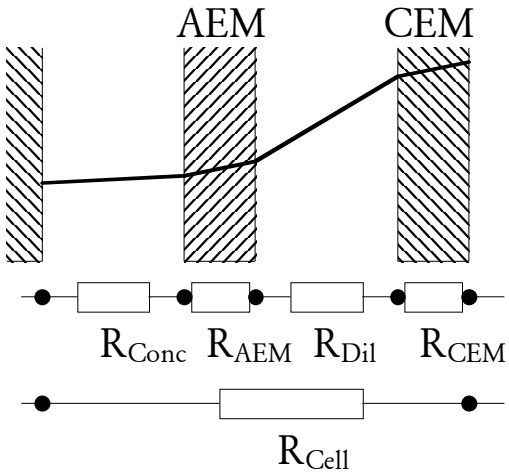

Figure 1.13 The potential drop across a cell pair. Usually, the highest resistance occurs across the dilute solution because of low conductivity.

Polarization effects are very hard to determine, since the nature of the polarization depends on the surface characteristics of the ion-exchange membranes as well as local flow conditions.

The electrical work, W (Watt) needed to run the process can be estimated from the electrical current, I added and the total resistance R_{Total} of the system:

Equation 1.27 $W = I^2 \cdot R_{Total}$; $R_{Total} = R_{Electrodes} + R_{Electrical\ System} + nR_{Cell}$

Equation 1.27 does not include energy for pumping or cooling. The energy input needed for pumping the different process streams can be estimated from:

Equation 1.28 $W_{Pumping} = \sum_j k_j Q_j \Delta p_j$

k is a constant related to the efficiency of the pump, Q is the volume flow, and Δp is the pressure difference between pump inlet and discharge.

The energy consumption E (kWh/kg product) is expressed as energy needed to extract/recover 1 kg of product:

$$E = -\frac{I^2 \cdot R_{Total} + W_{Pumping} + W_{Cooling}}{Q_F \cdot \Delta C_{F,j} \cdot MW_j}$$

Q_F is the volumetric feed flow, $\Delta C_{F,j}$ is the difference in feed concentration of *j* from outlet to inlet, MW_j is the molar weight of the product.

1.2.11 Advantages and disadvantages

Electrodialysis holds several advantages and disadvantages that must be taken into account, whenever evaluating different separation processes for a specific process.

Advantages of electrodialysis include:

- Specific extraction of charged components, where pressure driven separations mainly select according to molecular size and form.
- High energy efficiency, which reduces operating costs.
- The process is easy and fast to control, since the driving force is electrical.
- The process is robust and versatile, allowing the process to run at different speeds.
- Maintenance is simple.

Disadvantages include:

- Relatively high investment cost, since commercial ion-exchange membranes are expensive
- Bad efficiency at very low conductivity. For creating pure water, electrodialysis is often used as pretreatment to bring down concentration, then other processes like reverse osmosis and ion-exchange removes the last remaining ions.
- Ion-exchange membranes become easily *fouled* in bio-matter. Charged proteins and cells cling to the membrane surfaces, reducing effective membrane area and membrane selectivity.

1.2.12 Electrodialysis applications

Many applications of electrodialysis exist and even more are possible. As mentioned earlier, desalting sea water or brackish water are being employed different places in the world, often in remote locations not covered by larger water purification plants.

Industrially, electrodialysis is mainly utilized for recovering ionic components from waste streams in order to obey environmental legislation and recycle valuable components. Electrodialysis is also utilized in food industry for removal of salts and organic acids.

Electrodialysis is traditionally used to perform several general types of separations (Strathmann 1985):

- Removal of salts, acids and bases from aqueous solutions.
- Separation of ionic compounds from neutral molecules.
- Separation of monovalent ions from multivalent ions.
- Regeneration of acids and bases from mixed salt solutions.

Because the electrodialysis process is a very "clean" process (there are no chemicals added to perform the separation), it has received increasing interest from the food and drug industry over the past decade. There have been numerous reports on scientific work done in the field of organic acid separation and especially the electrodialysis concentration and purification of lactic acid have received a lot of attention. There are already commercially plants purifying lactic acid by electrodialysis in Denmark and Japan that this author is aware of.

New and improved ion-exchange membranes make new processes possible. Through mono-selective ion-exchange membranes (m-iem), it is possible to separate monovalent ions from multivalent ions as demonstrated in Figure 1.14.

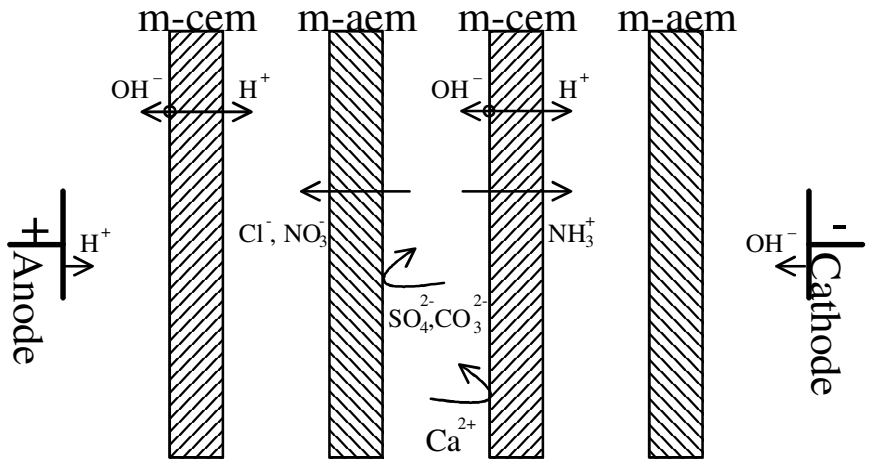

Figure 1.14 Electrodialysis setup utilizing mono-selective membranes to separate monovalent ions from multivalent ions. m-cem = mono-selective cation-exchange membrane. m-aem = mono-selective anion-exchange membrane.

By utilizing the special properties of bipolar membranes, it is possible to regenerate mixed salt solution to acids and bases as well as acidifying organic acids. Three different membrane setups are sketched for a dissociated organic or inorganic salt M^+X^- in Figure 1.15.

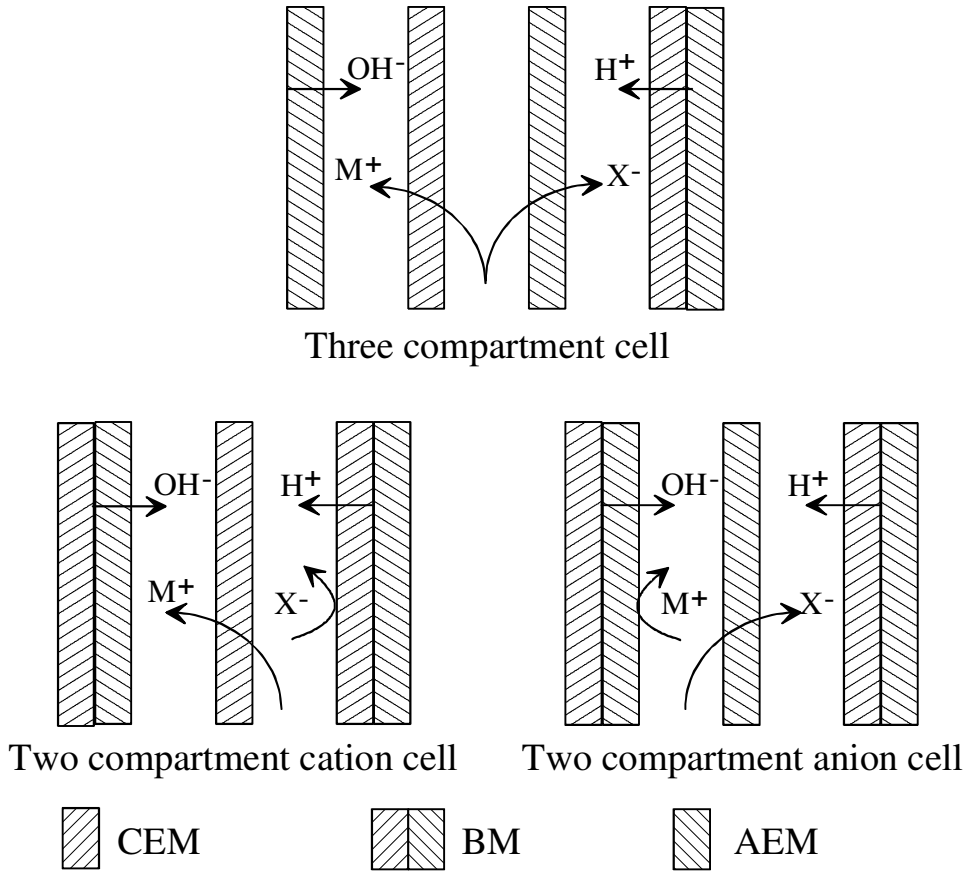

Figure 1.15 Demonstration of possible membrane setups with bipolar membranes.

The bipolar membranes utilize the water splitting abilities as mentioned in the section describing the ion-exchange membrane to deliver hydrogen and hydroxide ions for creating or regenerating acids and bases.

1.3 Nanofiltration

As a filtration process, nanofiltration (NF) lies somewhere between reverse osmosis and ultrafiltration. Nanofiltration allows higher fluxes than reverse osmosis, but still demonstrates good retention towards multivalent salts and large molecules. Nanofiltration is characterized by a high selectivity between mono- and multivalent ions such as sodium (low retention) and calcium (high retention), and the retention of salts is caused by Donnan exclusion as most NF membranes are charged. Hence, the retention of charged molecules by NF membranes is dependent of charge, while the retention of non-charged molecules is highly dependent on their molecular size and shape. Since the retention of citrate is interesting in this case, this theory section is mainly concerned with the mechanisms of polarization, and the difference between observed and true retention.

The volume flux through nanofiltration (and reverse osmosis) membranes can be described by (Mulder 1991):

Equation 1.29 $J_w = A_w(\Delta P - \sigma \cdot \Delta\pi)$

J_w is the volume flux (m/s), which is considered equal to the solvent flux. ΔP is the trans-membrane pressure (Pa) and $\Delta\pi$ is the osmotic pressure difference across the membrane (Pa). A_w can be regarded as the solvent permeability (m/s/Pa) and is composed of different solvent properties such as diffusion coefficient, solute concentration inside the membrane, and molar volume. σ is a reflection coefficient that takes the small flux of solutes into account. The reflection coefficient is a measure of the degree that the solutes are retained:

$\sigma = 1$	Ideal membrane, no solute transport
$0 < \sigma < 1$	Some solute transport
$\sigma = 0$	No selectivity, no retention of solute

A_w can be experimentally determined by measuring the pure water flux of a clean membrane ($\Delta\pi = 0$) as function of the trans-membrane pressure.

According to traditional membrane technology, the solute flux, J_s, can be described by (Mulder 1991):

Equation 1.30 $J_s = c_{\ln,s} \cdot (1-\sigma) \cdot J_w + \omega \cdot \Delta\pi$

$c_{ln,s}$ is the mean logarithmic mass concentration (g/l) and ω is the solute permeability.

The osmotic pressure for a component i, π_i, can be deduced by chemical potential calculations but is most often derived from the simplified van't Hoff equation:

Equation 1.31 $\pi_i = C_i RT = \frac{c_i}{M_i} RT$

This equation is only valid for dilute solute concentrations, though often used for approximations. By inserting Equation 1.31 into Equation 1.30, it rearranges to:

Equation 1.32 $\frac{J_s}{\Delta c} = \omega RT + (1-\sigma) \cdot J_w \cdot \frac{c_{\ln}}{\Delta c}$

Δc and c_{ln} are the concentration difference and the mean logarithmic concentration between the feed and permeate side of the membrane, respectively. By plotting experimental values of $J_s/\Delta c$ versus $J_w \cdot c_{ln}/\Delta c$, the reflection coefficient and the solute permeability can be found as shown in Figure 1.16.

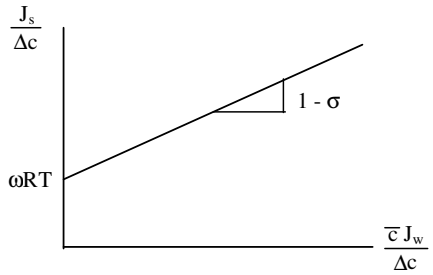

Figure 1.16 Experimental determination of σ and ω.

Unless flow rates on the feed-side of a NF membrane are very high, polarization must be considered an important factor that lowers the performance of nanofiltration separation. The polarization at the surface of a NF membrane is sketched in Figure 1.17.

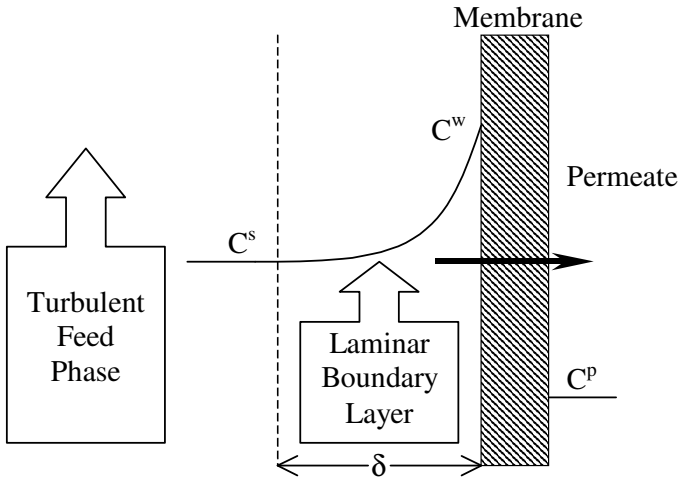

Figure 1.17 Polarization profile across laminar boundary layer at membrane surface during a pressure driven filtration process. C^s, C^w, and C^p are the solute concentrations respectively in the bulk of the feed solution, at the membrane surface, and in permeate. δ is the boundary layer thickness.

With high flow rates, turbulence mixes the feed solution sufficiently so that polarization can be neglected. Otherwise, the concentration gradient across the boundary layer must be taken into consideration.

The retention S of a solute i is defined as:

Equation 1.33 $$S_i \equiv 1 - \frac{C_i^p}{C_i^s}$$

S is called the *observed* retention, because it is calculated from the measurable concentrations of i. The *true* retention R of i by the membrane is defined as:

Equation 1.34 $$R_i \equiv 1 - \frac{C_i^p}{C_i^w}$$

The observed retention depends not only of the membrane, but also on the system's flow conditions. The true retention depends only on the membrane properties, and is a much more comparable parameter, when investigating the feasibility of a nanofiltration process. Since C^w ordinarily cannot be measured directly, an approximation is necessary to find this value.

Using the film theory, the boundary layer between the fully mixed bulk solution and the membrane surface is assumed to have constant thickness δ and stagnant laminar flow. Then the following relationship between the bulk feed concentration C^s and the membrane surface concentration C^w can be obtained (Jonsson and Boesen 1984;Mulder 1991):

Equation 1.35 $$\frac{C_i^w - C_i^p}{C_i^s - C_i^p} = \exp\left(\frac{J_w \delta}{D_i^s}\right)$$

D_i^s is the diffusion coefficient of i in the boundary layer. The ratio D_i^s/δ is a measure of the mass transfer coefficient, k_i. δ can be estimated from the Sherwood number:

Equation 1.36 $$\delta = \frac{d_h}{Sh}$$

d_h denotes the hydraulic diameter of the feed-side flow compartment. The Sherwood number can be estimated from the Schmidt and Reynolds numbers (Equation 1.20 or Equation 1.21). Using these relationships, Equation 1.35 can be written in the following form (Jonsson and Boesen 1977):

Equation 1.37 $$\frac{C_i^w - C_i^p}{C_i^s - C_i^p} = \exp\left(K \cdot \frac{J_w}{v^a}\right)$$

The constant, K, is composed of all remaining factors when substituting Equation 1.36 and either Equation 1.20 or Equation 1.21 into Equation 1.35 except for J_w and the crossflow velocity *v* that is part of the Reynolds number, and hence risen to an exponent *a*. This exponent value is either 0.33 for laminar or 0.80 for turbulent flow conditions as per Equation 1.20 and Equation 1.21. Substituting the concentration terms in Equation 1.37 with Equation 1.33 and Equation 1.34 yields:

Equation 1.38 $$\ln\left(\frac{1-S}{S}\right) = \ln\left(\frac{1-R}{R}\right) + K \cdot \frac{J_w}{v^a}$$

Thus, by plotting experimental values of ln[(1-S)/S] versus J_w/v^a, a straight line should be obtained, intersecting the ordinate axis at ln[(1-R)/R]. Hence, the true retention and C^w can be deduced. The constant K can be determined as the slope of the plotted line.

2

2 Recovery of citric acid from lime fruit waste

2.1 Project background

2.1.1 General purpose

The general purpose of this project was to assess the technical and economical feasibility of recovering citric acid from stripped lime juice by electrodialysis. If successful this process could turn a harmful waste product into a valuable byproduct.

2.1.2 Project participants

This project was carried out partly at Department of Chemical Engineering at the Technical University of Denmark (DTU) under the supervision of Associate Professor Gunnar Jonsson and partly at the Escuela Nacional de Ciencias Biologicas (Department of Food Science) at the Instituto Politecnico Nacional (National Polytechnic University) in México City under the supervision of Dr. Gustavo Fidel Gutierrez Lopez. The project was initiated by Professor Porsdal Poulsen from Department of Biotechnology (DTU). Taniart Productos S.A. de C.V., Tecomán, México provided waste samples and cooperation in on site experiments. Part of the project was sponsored by EC's ALFA program and Carlsberg Memorial Scholarship.

2.1.3 Introduction

The origin of the citric acid is a waste stream from an agro-industrial plant located in Tecomán, México. Lime fruits are pressed and the "juice" is processed to recover the essential oils by distillation. After the stripping of the oils, the residual liquid from the distillation process contains about 4 % citric acid, some sugars, soluble proteins and other organic acids as well as calcium, some insoluble dust and carbon particles. This lime-waste is discharged to a nearby brook, where it is damaging the wildlife because of high acidic content. The company desires to employ a process that recovers the citric acid in concentrated form, turning it into a commodity while reducing the burden on the local environment. Around 50 to 100 tons of stripped limejuice is produced each day in the high season of lime fruit production.

Electrodialysis has been widely investigated as a mean of recovering and purifying different organic acids, especially lactic acid (Boniardi *et al.* 1997a;Boniardi *et al.* 1997b;Czytko *et al.* 1987;Hongo *et al.* 1986;Lee *et al.* 1998). Lately, the recovery of citric acid by electrodialysis has also found some interest among researchers (Moresi and Sappino 1998a;Moresi and Sappino 1998b;Novalic *et al.* 1995;Novalic *et al.* 1996;Novalic and Kulbe 1998;Sappino *et al.* 1996). Most investigations have been focused on the acid recovery from fermentation broth.

The conventional method of recovering citric acid generates large amounts of gypsum waste. Substituting the conventional method with electrodialysis in the acid recovery process eliminates this waste. Another advantage by using electrodialysis is that when converting organic salts into acids, high acid concentrations are achievable and the evaporation step normally required can be omitted (Novalic *et al.* 1996;Novalic and Kulbe 1998).

2.1.4 The lime processing plant

Low quality lime fruits that are not sold as fruits are utilized are the source of citrus oil and pectin. In this process, the low quality lime fruits are pressed through a "snail" that peels the skin of the fruit. The peel is sold as a source of pectin. The remains consist of bad quality lime juice mixed with fruit pulp and pips. Citrus oils are stripped from the lime juice by a distillation process.

The remnant from the distillation process (stripped lime juice) is considered a waste product. Because a high content of citric acid remaining in the stripped limejuice is causing fast corrosion of sewers, the stripped limejuice cannot be let out in the sewer system. In Tecomán, México where the lime fruit production is prominent (and possible several other places) the acidic waste is mainly deposited on nearby plantation areas. The citric acid should still be considered an environmental hazard when the stripped limejuice is discarded directly to the surrounding countryside, because vegetation has very poor living condition in deposition areas (Bundgaard and Iversen 1992). Even though it is still accepted most places to deposit organic acid wastes on open fields, increasing environmental attention across the world can very likely result in the need for alternative options for the disposition of citric acid waste. The traditional method for citric acid extraction is the calcium precipitation process which creates about 2 kg of gypsum waste for every kg of monohydrated citric acid produced.

The average composition of the lime-waste after distillation of the essential oils is shown in this table:

Component	Amount
Citric acid[a]	40 g/l
Malic acid[a]	2.5 g/l
Formic, Lactic, Propionic and Acetic acid[a]	2-4 g/l
Glucose[a]	2.1 g/l
Xylose[a]	2.5 g/l
Arabinose[a]	1.3 g/l
Proteins/Amino acids[b]	0.4 – 0.65 %
Lipids[c]	340 mg/l
Calcium[d]	200 – 300 ppm
Magnesium[d]	50 – 75 ppm
Total amounts of solids	14 %

Table 2.1 The average composition of the lime-waste after distillation. [a)] Measured in the liquid phase by HPLC after microfiltration. [b)] Kjeldahl method. [c)] Soxlett method. [d)] Measured by AAS.

Since the remnant from the distillation process is a mixture of cooked fruit-remains, ash and dust-particles, a pretreatment of the remnant seems necessary before an electrodialysis process is possible.

2.1.5 The suggested waste treatment process

The suggested process that was discussed with Taniart Productos originally was drafted to entail the subprocesses as sketched in Figure 2.1.

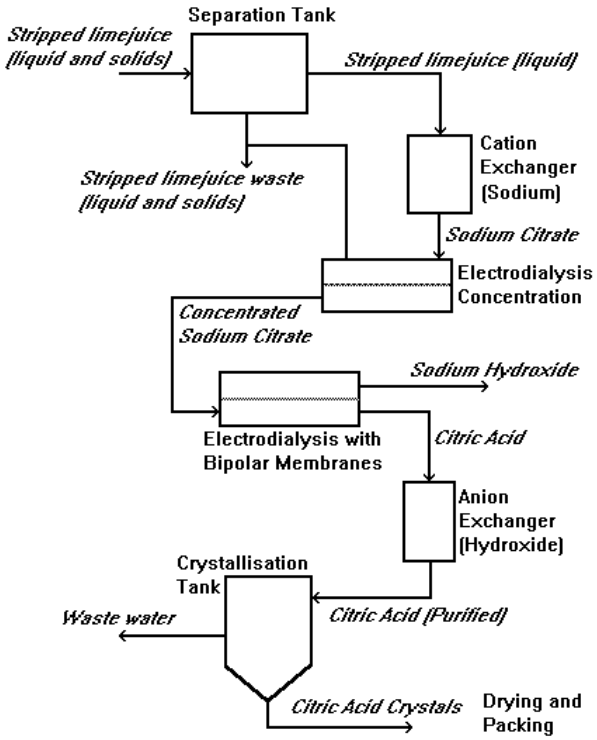

Figure 2.1 Suggested purification process for citric acid from the stripped lime juice.

The project concentrates on the two electrodialysis unit operations as these operations are the new contribution to the purification process while ion exchanging and crystallization is fairly well-known technologies. The stripped lime juice is first separated in a pure liquid and a mixed liquid/solid phase. The mixed phase is treated in a settling tank, where the solids are allowed to settle and pure liquid is decanted off the top. This liquid is mixed with the pure liquid, which has been through a cation exchanger for reduction of calcium level and adjustment of pH. Then an electrodialysis process extracts the citrate from the waste in a concentration process, from where the citrate is concentrated as citric acid in a subsequent electrodialysis with bipolar membranes. For final removal of inorganic anions, an anion exchanger is utilized, and finally pure citric acid is produced by crystallization.

This process is just a sketch for preliminary experiments to be based on. Initially, the company only desires to produce a concentrated citrate solution, if a suitable customer (possibly from the soap and detergent market) can be found.

2.1.6 Citric acid

Citric acid (2-hydroxy-1,2,3-propanetricarboxylic acid) is a natural occurring acid in animals and plants. Citric acid has been known since the 13th century and is now the most widely used organic acids in the field of foods and pharmaceuticals. Its world production in 1987 was assessed to about 300.000 tons (Jørgensen and Kjærsgaard 1987). In 1994, the world production had increased to about 620.000 tons and represented about 60% of all food acidulants that was utilized worldwide (Krishnakumar 1994). 1997 global consumption topped 736.000 ton (Lewis 1997).

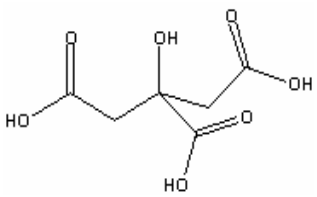

Figure 2.2 Citric acid.

Citric acid is used in food industry because of its high solubility, low pH and sour taste, and especially because it is considered safe and biodegradable. It is mainly applied to soft drinks, which account for 43% of the global market today. Citric acid is used for chemical cleaning of metal-oxides, as pH-regulator in soaps, some cosmetics, and shampoos. The soap and detergent market holds about 24% of the global market. Citric acid is used for pH regulation in jams and jellies. The acid is added as flavor to candies as well as margarine, vegetable oils etc. in low concentrations as well as diary products, fish and poultry. Frozen or canned fruits can also benefit from being exposed to citric acid. Food uses make up another 18% of the global market. The rest of the market comprises a wide array of industries from high-tech computer processor manufactures to pharmaceuticals. The global market distribution for citric acid is represented in Figure 2.3.

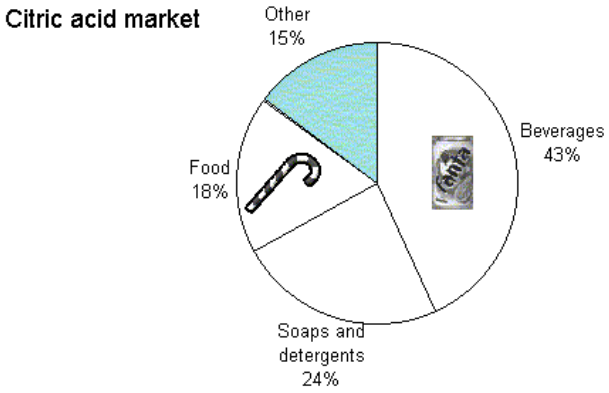

Figure 2.3 Global citric acid market (1997).

2.1.6.1 Traditional production of citric acid

Citric acid is traditionally produced by fermentation. The conventional method of recovering the acid from the broth is by precipitating citrate as calcium salt by adding calcium hydroxide. This is followed by a filtration that separate the solid calcium citrate from the rest of the organic matter.

Then citrate is redissolved by adding a surplus of sulfuric acid, and after filtering the now precipitated gypsum (calcium sulfate) from the solution, pure citric acid is produced by crystallization. This method has the significant drawback of creating huge amounts of waste products, since two kg gypsum is produced for each kg of produced citric acid.

Another more recent approach to recover citric acid from fermentation broth uses liquid-liquid extraction (LLE). This is reported to combine high yields, high selectivity and reversibility resulting in high recovery of a pure component at relatively high concentration (Baniel *et al.* 1981;Eyal *et al.* 1998b).

2.1.7 Influence of pH

The pH of the citrate solution is very important in the electrodialysis process. Generally, organic acids have lower conductivities and higher molecular weights, which reduce their mobility through membranes. Citric acid is a trivalent acid and the electrical conductivity, the transport number, the citrate flux and a number of other factors related to the electrodialysis process are dependent on the valence of the citrate ion. The dissociation steps are sketched in Figure 2.4.

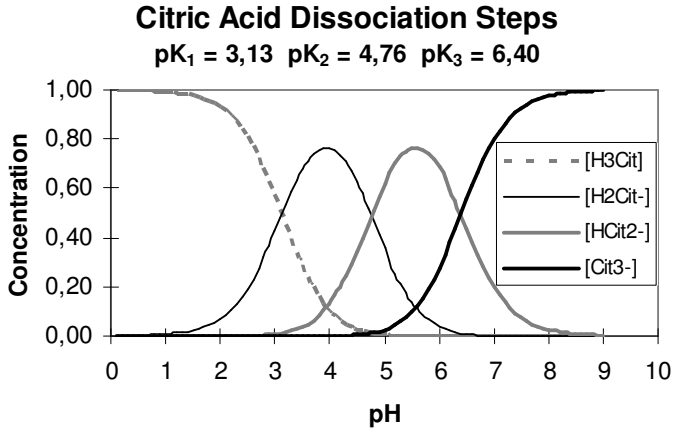

Figure 2.4 Relative concentration valence-distribution of citrate ions as function of pH.

Other investigators have concluded from model experiments that electrodialytic recovery of citric acid is preferably operated at alkaline pH-values (> 7), because this condition yields better mass transfer (Novalic *et al.* 1995). In the preliminary experiments, the influence of pH will be closer investigated, because there are several advantages by operating the recovery process at lowest feasible pH:

- In this process the acid solution is not originating from a pH-controlled fermentation, but originates directly from fruit waste at low pH (around pH 2 – 2.5). The amount of lime-waste is large and has an initial pH of around 2 – 2.5. Hence, the higher the operational pH-value, the more base must necessarily be continuously added. Even if most of the base can be regenerated during an electrodialytic purification of the citric acid with bipolar membranes, it will be of great interest for this process to find the lowest pH-value, where the process is still economical feasible.

- Water-flux is usually an unwanted flux in electrodialysis that can not be ignored. The alkaline cations, potassium and sodium, coordinate more water molecules than hydrogen ions. Higher water-fluxes through the cation-exchange membranes can thus be expected at higher pH-values from electro-osmotic water flux.
- The electrical current necessary to recover an ion is directly proportional to the ionic charge (z) divided by the current efficiency (η). And the necessary energy consumption (E) is proportional to the square of the current as expressed in Equation 2.1 (Strathmann 1992). If the change in current efficiency turns out to be small or insignificant as a function of pH, a reduction in energy consumption should be expected at lower pH-values, where the charge of citrate is lower. The lower electrical conductivity of the citrate solutions at lower pH-values works in the opposite direction, though.

Equation 2.1 $$E \propto \left(\frac{z}{\eta}\right)^2$$

Some of the disadvantages of operating the electrodialysis process at low pH are:

- Low conductivity that results in higher electrical resistance and increased heating of the solutions and equipment.
- Lower mobility through solution and membrane, resulting in decreased mass transfer.

Four pH-values have been selected for investigation of the behavior of the citrate ion at different valence forms. At pH 1.9, about 94% of the citric acid is still undissociated while some 6% is monovalent. This composition is usually employed in experiments for investigation of almost pure acid behavior in the separation processes. Some degree of citrate will always be dissociated in pure aqueous solutions of citric acid, when no stronger acid is added. At pH 3.9 76% of the total citrate is in the monovalent form, while 12% is undissociated acid and 12% is in the divalent form, hence the overall charge of citrate is –1. This doesn't prevent the small amount of divalent ions from acting chemically very different from the monovalent or undissociated ions, of course. It is expected that the experimental results reflect the overall charge, though. Analog with the previous, the overall molecular charge of citrate at pH 5.6 is –2. For the behavior of totally dissociated trivalent citrate, a pH of 7.5 or higher is chosen.

2.2 Experimental determination of influence of pH on process parameters

2.2.1 Purpose

The purpose of the preliminary model experiments was to evaluate important process parameters in electrodialysis as function of pH for this trivalent carboxylic acid. As discussed previous, there are advantages to high as well as low pH-values.

2.2.2 Experimental

2.2.2.1 Equipment

Three different kinds of spacers were designed and tested during the project. The three different spacers named JURAG-1, -2, and -3 are sketched in Figure 2.5 and the general dimensions for the three spacer setups are compared in Table 2.2.

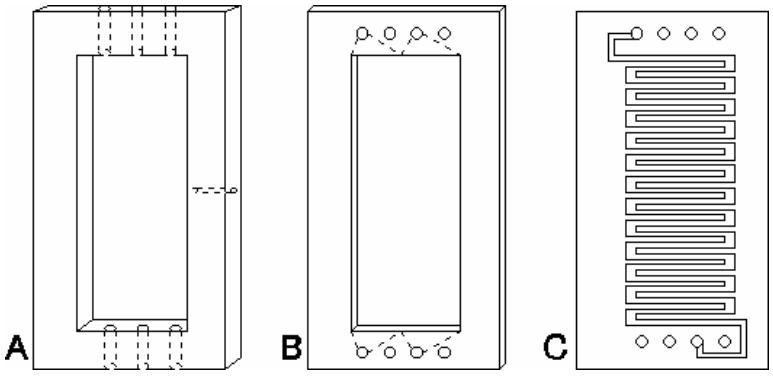

Figure 2.5 Spacer-types for the three ED setups. A) JURAG-1, B) JURAG-2 and C) JURAG-3.

Experimental Setups:	**JURAG-1**	**JURAG-2**	**JURAG-3**
# Cell Pairs	1 – 3	1 – 10	1 – 10
Spacer type	Net (Sheet flow)	Net (Sheet flow)	Tortuous path
Cross-sectional area (cm^2)	40	40	40
Effective membrane area (cm^2)	40	40	20
Spacer thickness (mm)	6	3	0.5
Spacer material	Acrylic	Teflon	Teflon

Table 2.2 Comparable data for the three setups.

As can be seen in the table, the two Teflon spacers (**B** and **C**) were thinner than the acrylic spacer (**A**), and were expected to yield lower cell resistance and energy consumption. Unfortunately, they demonstrated poor sealing abilities and developed leaking both between compartments and to the outside during experiments. Results obtained with these spacers were consequently discarded during the preliminary experiments.

The power supply for the experiments is a variable EA-PS 3032-10 Power supply from Elektro-Automatik, Germany, able to deliver 0-32 V and 0-10 A.

The ion-exchange membranes utilized were either Selemion membranes (APS-3 anion-exchange and CMV cation-exchange membranes) produced by Asahi Glass, Japan, kindly supplied by Mitsubishi International GmbH, Germany, or Neosepta membranes (BP-1 bipolar, AMX anion-exchange, and CMB cation-exchange membranes) produced by Tokuyama Corporation, Japan, and kindly supplied by Tokuyama Europe GmbH, Germany.

2.2.2.2 Methods

The experimental setup for electrodialysis experiments is sketched in Figure 2.6.

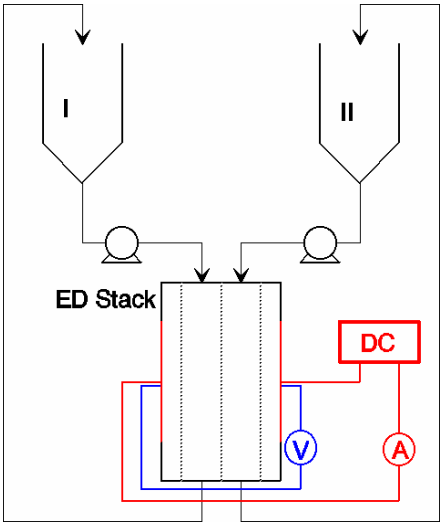

Figure 2.6 Experimental setup for batch experiments. I is feed and II is either concentrate, acid or base compartment depending on the experimental setup. In experiments with continuous electrodialysis there is no recirculation to I.

The setup for a concentration process that uses alternating anion- and cation-exchange membranes is shown in Figure 2.7.

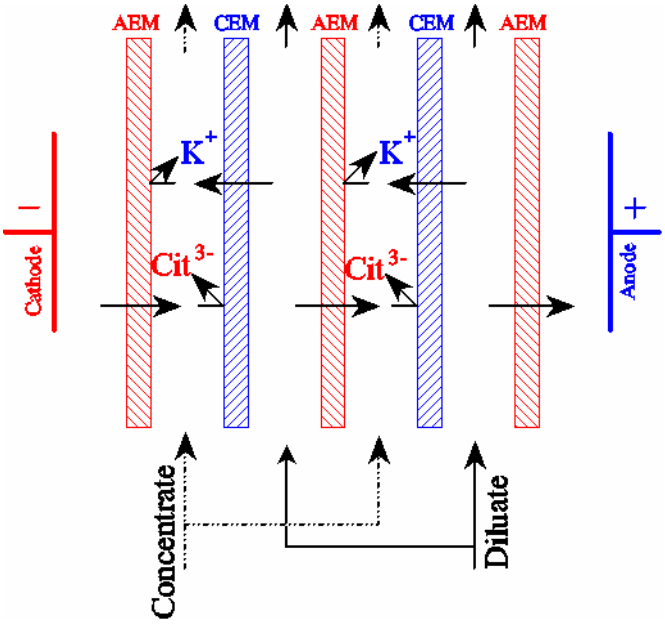

Figure 2.7 Electrodialysis concentration setup showing two cell pairs. CEM = cation-exchange membrane, AEM = anion-exchange membrane.

When determining membrane resistance in different solutions, a standard method was utilized. A single membrane was fixed between in the electrodialysis equipment between the two end prices containing the electrodes. The chosen solution was added to both sides of the membrane, and the system was left without electrical current until the membrane had obtained equilibrium with the solution. The total resistance of membrane and solution, R_{total}, was then measured with a low

voltage AC power source between two platinum plate-electrodes. By utilizing AC power, no influence from polarization arises. Afterwards, the membrane was removed, and the solution resistance, $R_{Solution}$, was measured between the electrodes.
Thus, the membrane resistance, $R_{Membrane}$, could be determined by (Lindstrand *et al.* 2000b):

$$R_{Membrane} = R_{Total} - R_{Solution}$$

2.2.2.3 Analytical techniques

The citrate concentrations were measured by HPLC. Citrate analysis was performed at 35°C on HPLC equipped with an Aminex HPX-87H column (Biorad, USA) utilizing 4 mM H_2SO_4 as eluent at a flow rate of 0.6 ml/min. The acid amounts were detected on a Waters 486 tunable absorbance detector at 210 nm and a Waters 410 Differential Refractometer. Waters Millennium Chromatography Manager software was used for quantification.

Approximately 5 ml solution was taken from both the feed tank and the base tank. pH and conductivity were measured using a pHM 201 portable pH-meter and a CDM92 Conductivity meter (both Radiometer, Denmark), respectively. After measurements, the solutions were transferred back to the system to maintain mass balance.

2.2.2.4 Membrane resistance as function of acid valence

When concentrating organic compounds with electrodialysis, the membrane resistance is usually higher. This is the case if the organic molecule is very bulky and the membranes are very tight. Since the citrate ion has to pass through an anion-exchange membrane, the electrical resistance of a Selemion APS-3 anion-exchange membrane was measured in 4% citric acid model solutions at various pH-values. The pH was adjusted with solid KOH.
A part of stripped lime juice was microfiltrated and another part ultrafiltrated. A few measurements of the membrane resistance was taken in these solutions as well and compared to the results from the model solutions. The results can be seen in Figure 2.8.

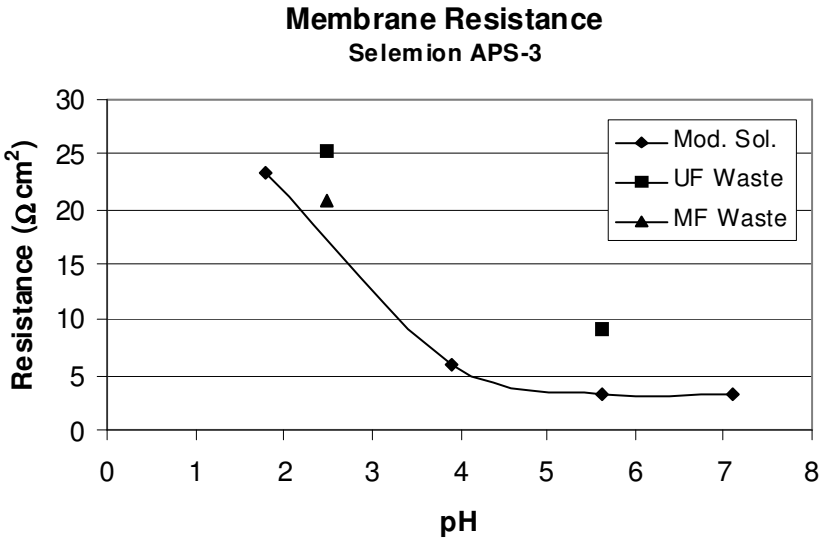

Figure 2.8 Electrical resistance across a Selemion APS-3 anion-exchange membrane in 4% potassium citrate model solution (◆) compared to membrane resistance in microfiltrated (▲) or ultrafiltrated (■) lime-waste sample at different pH-values.

As expected the electrical resistance across the membrane is greatest for the pure acid/unadjusted juice, when the major part of the acid is not dissociated and the conductivity is low. The electrical resistance of the membrane follows the resistance of the model solutions, so apparently there is no significant sterical hindrance for the citrate ion to pass through the APS-3 anion-exchange membrane. The higher resistance of juice samples compared to the model solutions must be the result of higher content of fouling material like proteins and fibers.

The membrane resistance of the APS-3 was also measured in a 0.5 M NaCl solution and found to be 1.78 $\Omega \cdot cm^2$.

2.2.2.5 Influence of pH and current density

To investigate the influence of pH and current density on electrodialysis of potassium citrate a small 3^2 factorial design was set up. Each experiment was a simple concentration experiment setup with alternating anion- and cation-exchange membranes as shown in Figure 2.7 and employing the type A spacer from Figure 2.5 since the two other spacer types demonstrated various flaws that influenced consistency in the experiments.

The pH-values for the experimental design were chosen from a consideration of the general dissociation steps of citrate. The values of current density, ***i*** and pH are listed in Table 2.3.

Factors	Low = 0	Middle = 1	High = 2
pH	3.9	5.6	8.0
***i* (mA/cm²)**	10	20	30

Table 2.3 Factor-values in the experimental design.

As discussed earlier and as can be observed from Figure 2.4, the first two pH-values are chosen so the overall valence of the citrate ions is respectively one and two. At pH 8 the citrate ions should be fully dissociated and the ion-valence should be three. At pH 3.9 more than 75 % of the citrate ions are mono-substituted, while both di-substituted and non-dissociated citrate ions are represented in about equal amounts of about 12 %. This results in an overall citrate valence in the solution is one, but it can be argued that it is first and foremost the ions of the highest valence that get transported to and through the membranes. It is the same situation at pH 5.6 with an overall citrate ion valence of two, but it is probably primarily the trivalent citrate ions that are carrying the current.

The 4% solutions were prepared from pure citric acid and pH was then adjusted by addition of solid KOH.

The other factors in the experiments that were kept constant are listed with values here:

Factor	
Experimental Setup	JURAG-1
Membranes	Selemion APS-3 and CMV
Feed flow (ml/s)	9
Concentration (g/dm^3)	39 ± 2
$V_{diluate,0}$ (ml)	350
$V_{concentrate,0}$ (ml)	300
Time (min)	60
Temperature (°C)	25 ± 1

Table 2.4 Constant factors in the experimental design.

The responses that were calculated for each experiment were solute flux (J_S), water flux (J_W), Current efficiency (η), Citrate recovery (ρ) and specific energy consumption (E) and results are shown in Figure 2.9 - Figure 2.13.

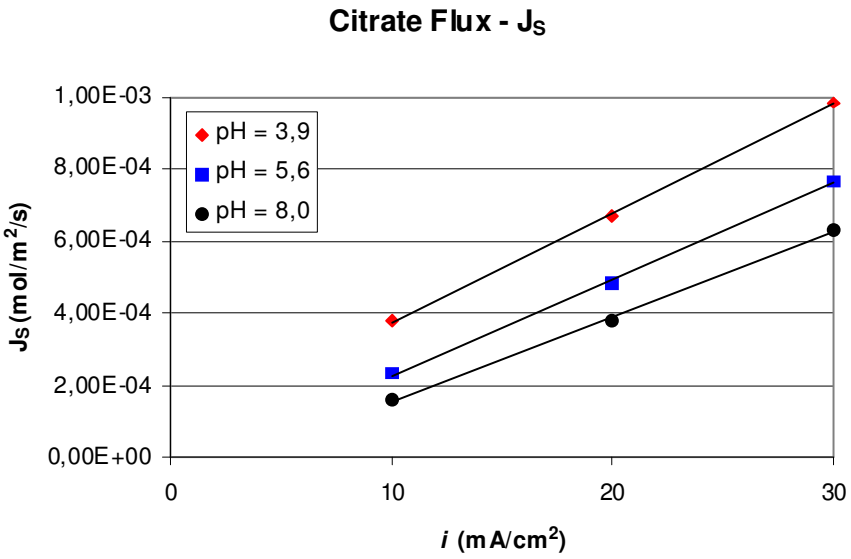

Figure 2.9 Citric acid flux through the anion-exchange membranes.

The citrate flux follows the current density as expected. J_S is highest for the lower pH-values, because the same amount of electrical current transports more citrate molecules than at higher pH-values and the current efficiency differs not very much between the pH-values as seen in Figure 2.11**.**

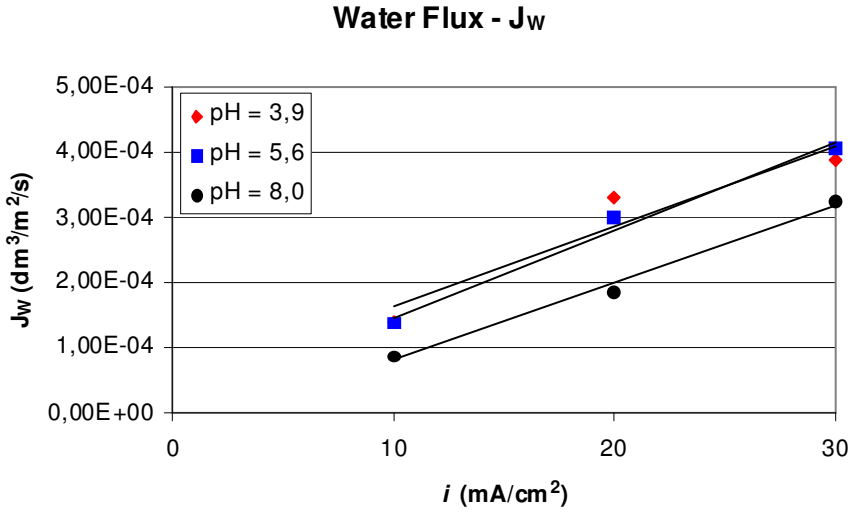

Figure 2.10 Water flux averaged on total membrane-area.

J_W follows the solute flux somewhat since the water flux is primarily caused by electro-osmosis. By dividing the solute flux by the water flux, a theoretical value of the maximum obtainable

concentrations of the potassium citrate (from a 4 % solution) can and has been estimated as shown in Table 2.5.

i (mA/cm^2)	pH = 3.9	pH = 5.6	pH = 8.0
10	26	16	18
20	20	16	20
30	24	18	19

Table 2.5 Theoretical values of maximum concentration (%) estimated by J_S/J_W.

From this table, a maximum obtainable concentration of 26 % is estimated when concentrating a 4 % solution by electrodialysis. At higher pH-values the maximum concentration decreases somewhat due to increased waterflux. The potassium ions coordinate more water-molecules than the hydrogen ions and so the electro-osmotic effect is more pronounced at higher pH-values where the potassium concentration is higher.

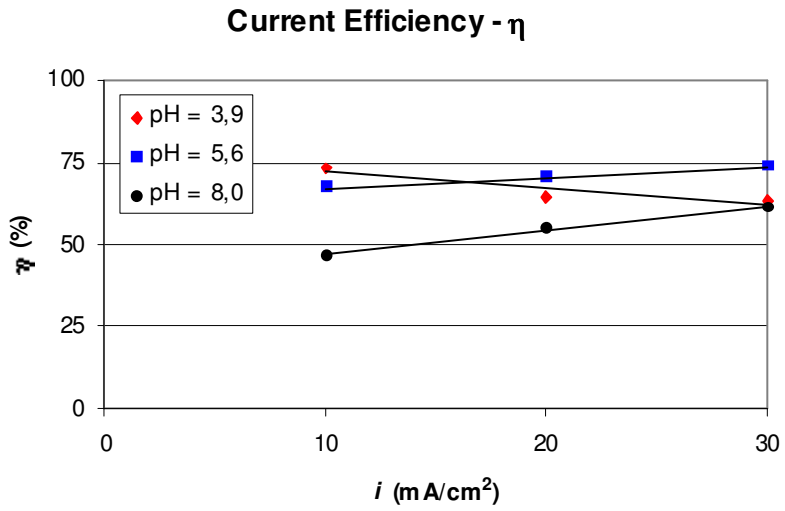

Figure 2.11 Current efficiency.

The current efficiency is shown in Figure 2.11 and no significant trend can be discerned from the current density and pH. η is usually lower when concentrating organic instead of inorganic solutions but higher general efficiency should be expected with better spacer design.

There is a definite trend in the citrate recovery as can be observed in Figure 2.12. The recovery is increasing with increasing current density and decreasing pH.

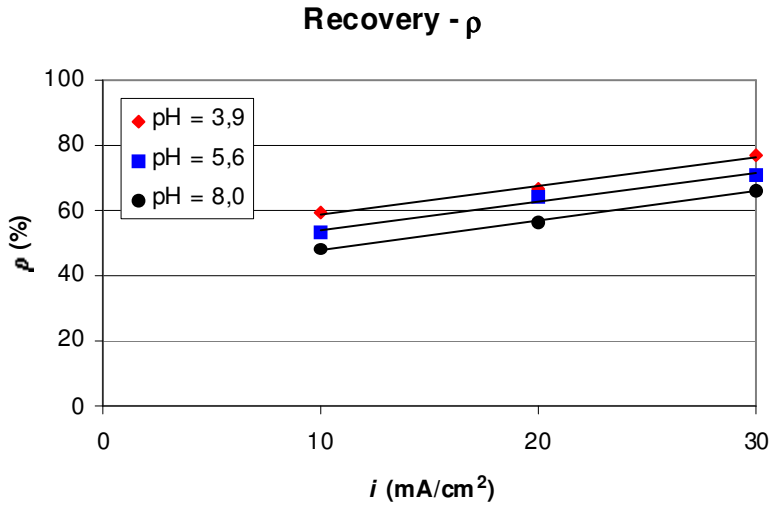

Figure 2.12 Citric acid recovery.

The specific energy consumption in Figure 2.13 shows that the higher solute fluxes at lower pH-values do not make up for the lower conductivity.

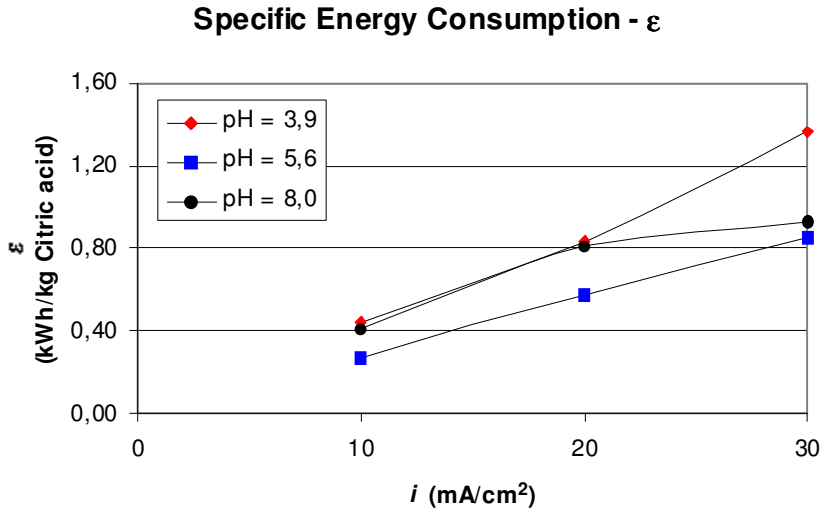

Figure 2.13 Specific energy consumption, E.

But the fact that more current is necessary to transfer the same amount of citrate molecules at higher pH can actually be observed. In these experiments the middle pH-value yields the best (lowest) energy consumption as a combination of higher conductivity than at lower pH and lower amount of necessary current for transfer because of lower valence than at pH 8.0.

Thinner spacers would lower the energy consumption of the process, which the solution of lowest conductivity would benefit most from.

2.2.2.6 Influence of base for pH-adjustment

To investigate the influence of the base used for pH-adjustment, two other bases were chosen for comparison: sodium hydroxide and ammonium hydroxide. Since the electro-osmotic waterflux is highly depending on the water dragged by the cation migration, some differences should be noted. Potassium and sodium ions ordinarily behave very similar in electrodialysis processes, except potassium's mobility is about 50% higher than sodium's. Ammonium's mobility is about the same as potassium's, but coordinate fewer water molecules.

A tortuous path spacer as depicted in Figure 2.14 was utilized for these experiments for verify that the energy consumption is lower with thinner spacers. These Teflon spacers are 2 mm thick compared to the 6 mm acrylic spacers from the previous experiments.

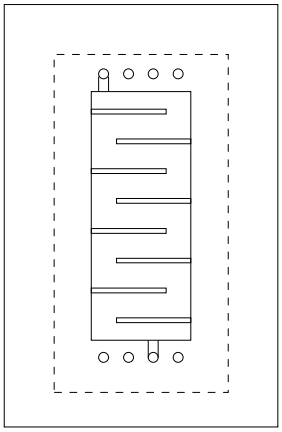

Figure 2.14 Tortuous path spacer used for the experiments comparing different bases.

The three bases were tested at three different pH-values, and each experiment was duplicated. Again, the Teflon spacers demonstrated bad sealing abilities, even when using Teflon tape for sealing the edges. The water fluxes were too inconsistent to verify any trends with certainty.

Water flux (l/m²/s)	pH = 3.9	pH = 5.6	pH = 7.5
Sodium	$3.48 \cdot 10^{-4}$	$3.91 \cdot 10^{-4}$	$3.91 \cdot 10^{-4}$
Ammonium	$3.37 \cdot 10^{-4}$	$3.67 \cdot 10^{-4}$	$3.11 \cdot 10^{-4}$
Potassium	$3.24 \cdot 10^{-4}$	$3.56 \cdot 10^{-4}$	$3.72 \cdot 10^{-4}$

Table 2.6 Average water fluxes.

Energy Consumption (kWh/kg)	pH = 3.9	pH = 5.6	pH = 7.5
Sodium	4.93	2.97	2.60
Ammonium	4.08	3.02	2.28
Potassium	3.85	2.59	2.06

Table 2.7 Average energy consumption.

The citrate flux is shown in Figure 2.15 and suggests a slightly lower flux with ammonium than with potassium or sodium hydroxide. The inconsistency of the results is reflected in the very large error bars.

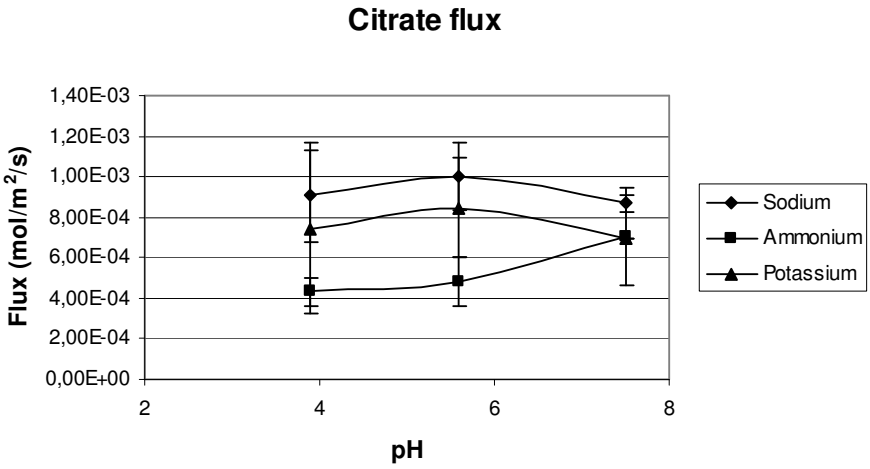

Figure 2.15 Citrate flux as function of pH, when adjusted by three different hydroxide bases.

The average energy consumption was found to be higher than in the previous experiments as shown in Figure 2.16, which is in opposition to the expected reduction due to thinner spacers.

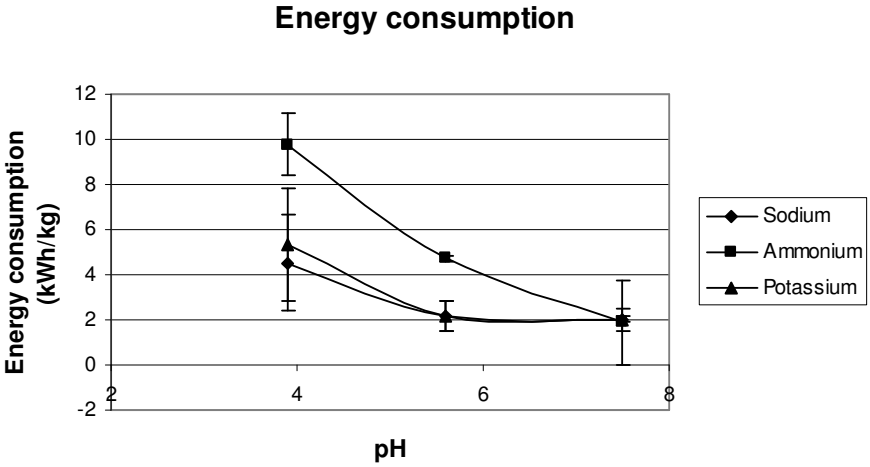

Figure 2.16 Energy consumption for transferring citrate as function of pH, adjusted by three different bases.

The conclusion on the comparison between bases for pH-adjustment has to be that the results were not conclusive enough to reveal any significant difference. The divergence in results between the spacer types is much more evident. The spacer design still has to be revised.

2.3 In situ experiments

2.3.1 Purpose

The purpose with performing *in situ* experiments was to verify whether the citrate rich waste stream from the lime processing factory could be directly extracted on concentrated by electrodialysis. Two weeks off a three month stay as a guest researcher at IPN, México City, was relocated to the factory located at Tecomán in the State of Colima, México. During these two weeks, experiments were performed on the fresh lime juice at the local laboratory/kitchen facility.

For evaluation of optimal process parameters, stripped lime juice at different pH-values should be attempted concentrated.

2.3.2 Experimental

2.3.2.1 Methods and equipment (IPN)

Some model experiments were performed at IPN, México City, to test the electrodialysis equipment. Some of the equipment brought from Denmark had to be supplemented by local utilities due to local power conditions (the power grid yielded 110 V as opposed to 220 V).

The primary equipment necessary for the electrodialysis experiments was designed by the Membrane Group and constructed at the workshop at the Department of Chemical Engineering at DTU. It consists of an electrodialysis stack with 6 acrylic flow-spacers (6 mm), that can be arranges as the experiments requires, and two endpieces holding platinum electrodes.
The ion-exchange membranes are kindly supplied by Tokuyama Europe GmbH (Neosepta CMB, AMX and BP-1 membranes) and by Mitsubishi International GmbH, Germany, (Selemion APS-3 and CMV, Asahi Glass, Japan).

Pumps (EHEIM 1048 09 993, EHEIM, Germany) were easily obtained locally. Unfortunately, the acquired DC power supply did not function for as long as it took to complete an experiment, and spend most time in the repair shop than. For replacement, the DC power supply for a laptop computer (AC Adapter (Input 100-240V~, 1.10-0.55A, 50-60Hz, Output 16-10V=, 2.2-3.2A)) was utilized as a last resort. This power supply could regrettably not be adjusted. Conductivity was measured by a Conductronic CL8 (Conductronic S.A., Puebla, México). Voltage and current density was initially measured by a FLUKE 83 III Multimeter (John Fluke Mfg. Co., Inc., Everett, Washington), and later by a LCD Auto Range Digital Multimeter 22-163 (Radio Shack®).

The citrate concentration was detected in model solution by measuring the Brix index (on a Refractometer No. 16171, ERMA Optical Works, LTD., Tokyo, Japan) and comparing with standard curves.

The membrane setup was similar to the setup sketched in Figure 2.7.

2.3.2.2 Influence of pH and flow velocity

Some model solution tests with 4% sodium citrate solutions were performed at the University. Some of the possible parameters to adjust were the initial feed pH and flow velocity. For the purpose of demonstrating the equipment for local researchers, a new research plan was sketched:

	pH = 1.2	pH = 3.9	pH = 8.3
FV = 1 g/s	*Exp. M3.8*	*Exp. M3.4*	*Exp. M3.5*
FV = 5 g/s	*Exp. M3.6*	*Exp. M3.7*	*Exp. M3.9*
FV = 10 g/s	*Exp. M3.1*	*Exp. M3.3*	*Exp. M3.2*

Table 2.8 Experimental plan for comparing responses as function of sodium citrate feed pH and flow velocity (FV).

Due to several incidences, not previously encountered by the author in Scandinavian research work[1], the research plan was not completed.

Some responses as result of the completed experiments are presented in appendix 7.1.1. The less accurate measurements of citrate concentration by Brix index than standard HPLC are evident from these results and must be taken at most as relative measurements. The only clear trend in the results is increasing energy consumption with increasing feed pH.

2.3.2.3 Methods and equipment (Tecomán)

The electrodialysis equipment and pumps were similar to the equipment utilized at IPN. The DC power supply was still the laptop power supply. Current density was measured by the LCD Auto Range Digital Multimeter 22-163 (Radio Shack®) and voltage by a HC-213 voltmeter (Hung Chang, P.R. of China). Brix index was measured by a handheld refractometer (II Index Instruments, Ramsey, Cambs.). A VIKING Digital Thermometer 1000 (Frode Pedersen & Co. AS, Allerød, Denmark) was utilized for measuring temperature, and pH was measured by an IMPO type 13.50 pH-meter (IMPO Electronic a/s).

For rough filtration, Cadelite 4187 was utilized. A filter made of a paper napkin was filled by the kieselguhr and lime juice waste was poured through it. The permeated solution was then filtered again by a new paper filter to remove kieselguhr remains.

For calcium removal, a cation-exchange resin, Puralite C100, was obtained. The resin was first charged with hydrogen ions in hydrochloric acid (200g resin to 500 ml demonized water and 12 ml conc. HCl for 15 minutes). Then the acid was removed, and the resin dried. Then the resin was mixed with lime juice (200g resin to 1 liter juice) for 20 minutes or until pH was stable in the mixture.

A Centra GP8 centrifuge (IEC - Int. Eq. Com., MA, U.S.A.) assisted in the pretreatment of the juice with kind assistance from Danisco Ingreedients, Tecomán, México. The samples were treated at 2000 RPM for 5 minutes.

The local Danisco Ingreedients laboratory also kindly measured the clarity of the juice at 650 nm by a Spectronic 20D (Milton Roy Company, U.S.A.).

Experimental samples was intended to be collected and measured by HPLC upon return to IPN or DTU for more accurate measurements of citrate and other organic matter content. Regrettably, the samples were lost by the courier upon return to the IPN.

[1] Including among other things a bomb scare, a gas contamination alert and an earthquake.

2.3.2.4 Experiments with stripped lime juice

It was very quickly established that pretreatment of the stripped lime juice was necessary. Initial experiments with decanted juice demonstrated fouling to a degree that ended every experiment after 15 minutes due to excessive electrical resistance.

By filtering the lime juice through kieselguhr, the juice became a lighter color but was still cloudy. It was thought that the dust particles from the kieselguhr were responsible, and repeated paper filtrations of the juice seemed to clarify it.

This clarified juice solution was tested in the first experiment that lasted longer than 15 minutes, and is summarized below:

Operation mode:	Batch ED, 3 cell pairs, constant voltage
Driving Force:	16.0 V (cv)
Feed:	Stripped lime juice, kieselguhr-filtrated (500 ml)
Concentration side:	same as feed solution (500 ml)
Electrode rinse:	0.1M Na_2SO_4 (1000 ml)
Membranes:	Tokuyama CMB and AMX
pH:	2.4

Since the concentration samples were lost, the Brix index during the experiment can be regarded as an expression of the concentration of biological matter. Since the amount of citric acid is very high compared to other acids and sugars remain relatively unaffected, Figure 2.17 suggests the concentration is possible though slow at the low pH.

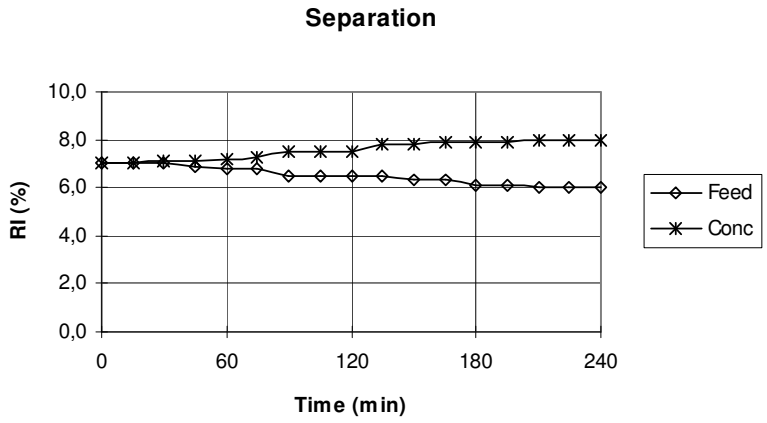

Figure 2.17 Brix index measurements during a concentration experiment on kieselguhr-filtrated lime juice.

Figure 2.18 shows the electrical current changes during the experiment. Since the power supply fixes the voltage at approximately 16V, the figure shows a steady increase in electrical resistance. This is due to a combination of reduced conductivity in the dilution circuit and the built-up of fouling.

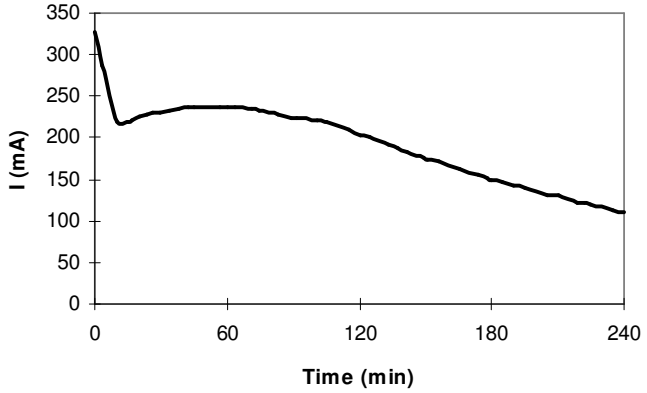

Figure 2.18 Electrical current (I) during experiment.

After the initial experiment, more stripped lime juice was filtered and clarified. According to the first experiment, 1 liter juice was used for each experiment with 500 ml initially in dilution and concentration circuit, respectively. This time, the juices were pH-adjusted by adding concentrated sodium hydroxide. The juices became darker upon pH-adjustment, transforming the color of the initial orange-yellow liquid to a darker red color.
The experiments that had the same basic process parameters as in the previous experiments, expects as noted below:

I - Decanted stripped lime juice, kieselguhr-filtrated, adjusted by NaOH to pH 7.2.
II - Decanted stripped lime juice, kieselguhr-filtrated, adjusted by NaOH to pH 9.5.
III - Decanted stripped lime juice, kieselguhr-filtrated, ion-exchanged, adjusted by KOH to pH 8.5.
IV - Decanted stripped lime juice, kieselguhr-filtrated, ion-exchanged, adjusted by KOH to pH 5.9, added 10g sodium bisulfite.

The results are all very similar as demonstrated in Figure 2.19.

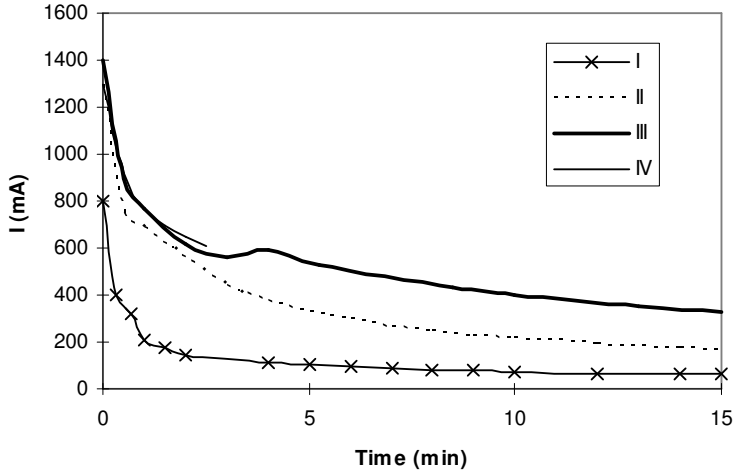

Figure 2.19 Electrical current during initial minutes of experimental concentrations of pH-adjusted, kieselguhr-filtered lime juice.

The electrical resistance increased manifold during the first couple of minutes which indicates strong fouling. It seems that the pH-adjustment catalyses a precipitation of some protein in the juice, which could possibly be either pectin or lignin.

By centrifugation of the lime juice the clarity of the juice was measured to change from 17.6 to 88.6. pH-adjustment of the juice separated from the solid phase after centrifugation still showed precipitations.

The pH of the stripped lime juice was raised and caused the now familiar precipitation. This clouded solution was kieselguhr-filtrated two times and then paper filtered several times to reasonably clarity, but still demonstrated fouling.

In *reverse electrodialysis* operations (RED), a normal ED membrane setup is utilized (Figure 2.7). But with intervals, the manifold system is switched so feed enters the spacers previously occupied by concentrate and concentration stream enters the spacers previously supporting the feed stream. The direction of the current is also switched, and a new period is initiated. This way, the fouling built up on the membrane surfaces in the feed compartments is now located in the concentration compartments. Since the current direction is reversed, the fouling layer is often washed away in the first minute after reversal, and by discarding this first amount of concentrate emerging from the stack, the membrane fouling can be disposed of. A new fouling layer starts to built up in the new feed compartments until a critical level of electrical resistance is reached, where the reversal is again instigated. Since the juice had a high degree of visible fouling, RED operations was tested.

Operation mode:	Batch RED, 3 cell pairs, constant voltage
Driving Force:	15.0V (cv)
Feed:	Twice kieselguhr-filtrated, ion-exchanged, stripped lime juice (400ml)
Concentration side:	same as feed solution (350 ml)
Electrode rinse:	0.1M Na_2SO_4 (1000 ml)
Membranes:	Selemion APS-3 and CMV

pH:	7.5 (adjusted by solid pellets of NaOH)
ρ_{Juice}:	1.044 g/ml
Flow feed:	10.5 ml/s (11.0 g/s)
Flow conc:	11.1 ml/s (11.6 g/s)

The reversals were only performed every 60 minutes, due to the relatively large loss in citrate recovery by every reversal. Since the equipment still contains relatively large amounts of liquid compared to the total amounts of feed and concentrate held by the external tanks, the high citrate amount in spacers and manifold is transferred back to the feed solution when the manifolds are switched. Likewise, the concentrated citrate solution is diluted by the citrate depleted feed solution still contained inside the spacers after reversal.

This is evident from Figure 2.20 and Figure 2.21 that demonstrates the Brix index and pH-changes of feed and concentrate during two RED experiments.

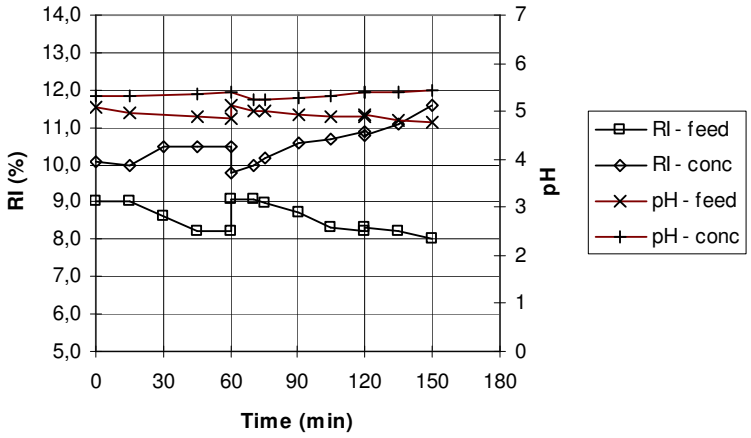

Figure 2.20 Brix index and pH-changes in feed stream and concentrate during a RED operation with pretreated lime juice.

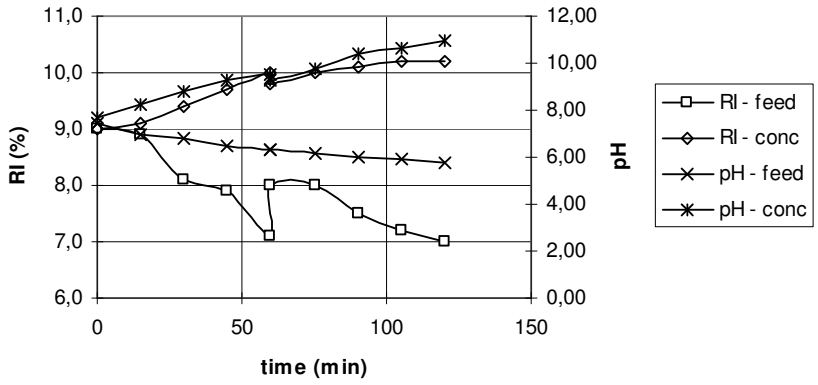

Figure 2.21 Brix index and pH-changes in feed stream and concentrate during a RED operation with pretreated lime juice.

The two experiments demonstrate that it is possible to run for extended periods through this operation mode. The fouling built-up between reversals is evident from Figure 2.22 that shows the reduction of electrical current between reversals (compare with Figure 2.20).

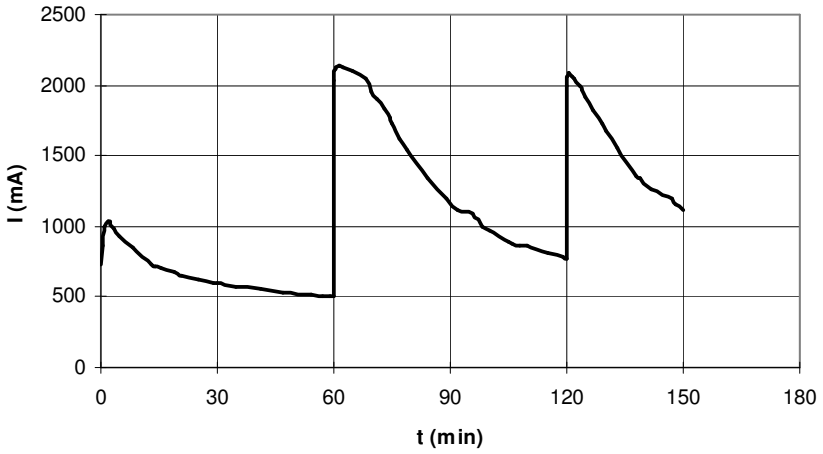

Figure 2.22 The loss of electrical current during each reversal period, demonstrating the fouling built-up.

The results shown in Figure 2.20 and Figure 2.22 originate from an experiment, where the first reversal was a simple manifold switch, which demonstrated a great step back in the separation (when considering the Brix index an indication of acid concentration). The second reversal after 120 minutes included an attempt to empty the equipment for a much liquid as possible, before switching the manifolds. As can be observed in Figure 2.20, the second reversal had only insignificant effect on the concentration.

2.3.2.5 Conclusion on in situ experiments

The conclusion on the *in situ* experiments demonstrated the need for further knowledge of the fouling content of the stripped lime juice, and indicated the need for an effective pretreatment. The concentration process is possible at lowest pH, but the conductivity is very low, and thus, the citrate flux is low and the energy consumption high. For an economical feasible process, model experiments indicate that a medium range feed pH is most optimal, but the stripped lime juice has revealed a heavy fouling caused by precipitating bio-matter when the pH is raised, even after intensive pretreatments including kieselguhr-filtration, ion-exchange and centrifugation. Operations with *reverse electrodialysis* demonstrated potential, but the experiments were carried out in batch mode, meaning that new fouling material was *not* added during operation. In the real application, fresh lime juice would be continuously added to the process, resulting in increasing fouling. Whether the RED operation can handle this fouling in real application remains to be seen.

2.4 Pretreatment experiments

2.4.1 Purpose

During the *in* situ experiments with the stripped lime juice, it became clear that a clarification of the stripped lime juice was necessary before an electrodialysis process was possible. Even after a clarification with kieselguhr- or microfiltration, the lime-waste samples were fouling the ion-exchange membranes and no electrodialytic concentration of the organic acid could take place. The fouling occurred after the lime-waste was adjusted with potassium hydroxide to raise the pH. The pH-adjustment caused a precipitation that was suspected to be caused by some of the remaining proteins in the lime-waste. This precipitation was found to foul membranes rapidly, thus raising the electrical resistance and blocking the solute transport.

The stripped limejuice is available from the distillation units and therefore leaves with a temperature around 120-140°C. To secure longer lifetimes for the ion-exchange membranes in the electrodialysis equipment the lime juice probably has to be pretreated by cooling, filtration and calcium removal. To prevent precipitation at higher pH-values the amount of proteins in the juice should be reduced. The cooling should be accomplished by heat-exchanging the outgoing stripped limejuice with the cold juice entering the distillation units.

The filtration must clarify the juice and remove the sand and carbon particles as well as most of the proteins to avoid precipitations later on in the purification process. A sand filter or a microfiltration (MF) should be able to remove the particles and thereby clarify the juice. An ultrafiltration (UF) is possibly the best solution for removing proteins, which are suspected of causing the fouling.

A cationic ion-exchange should lower the calcium content to a negligible level to secure longer lifetime of the bipolar membranes.

2.4.2 Clarification

The pretreatment that was most investigated was the clarification of the juice. The stripped lime juice holds a lot of dirt from the fruits and carbon-particles from the distillation process. A micro- or kieselguhr-filtration could easily remove these particles.

When filtering the lime-waste through a Durapore membrane (poresize 0.22 µm), the MF-membrane was covered by a layer of dust and particles, which lowered the volume flux considerably with time as shown in Figure 2.23.

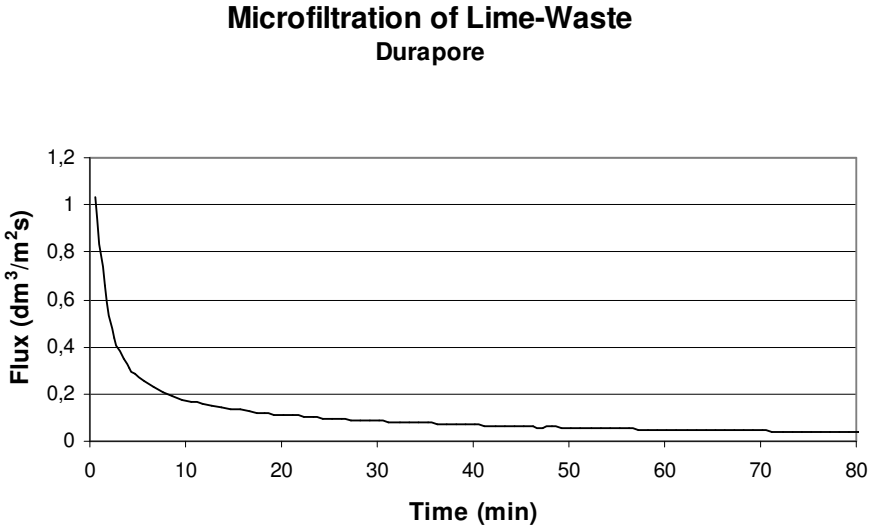

Figure 2.23 Microfiltration volume-flux through a Durapore membrane in a batch MF experiment with stripped lime juice.

Using the method proposed by Bowen et al. (Bowen *et al.* 1995) on repeated MF-experiments suggested that the membrane blocking largely is the result of the formation of a cake layer with some degree of intermediate blocking. It seems that even though the solution is very dirty and fouls the membranes, it is a reversible fouling that is easily washed of.
Also filtration with Kieselguhr has been tested and seems like a reasonable alternative for a clarification process.

2.4.3 Ultrafiltration

To avoid severe precipitation in the lime-waste as a result of pH-adjustment, ultrafiltration was investigated. It was found that the amount of precipitation was smaller when the pH-adjustment followed an ultrafiltration with cut-off values less than MW 50,000 and totally removed at MW 20,000.
Two different membranes GR61PP and CA600PP from Dow Denmark A/S both with Cut-Off values of MW 20,000 were investigated and some of the results are compared in Figure 2.24.

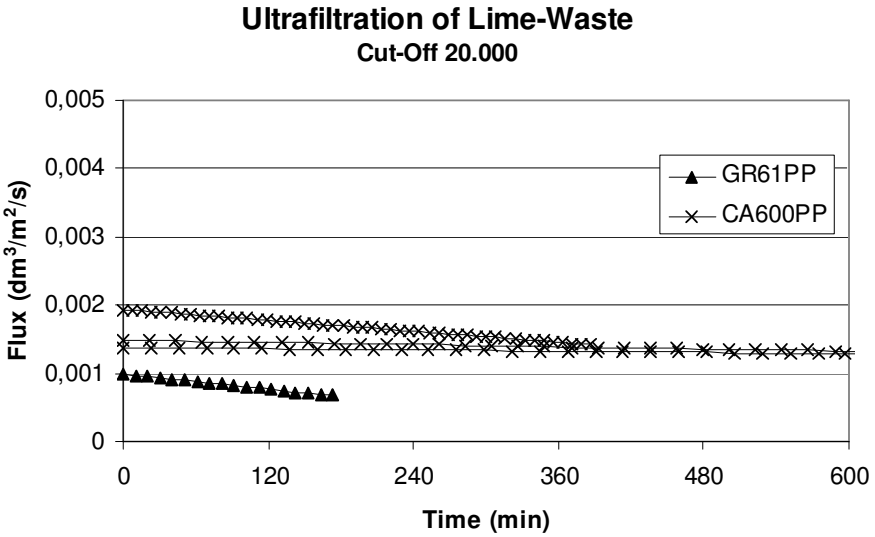

Figure 2.24 Comparison of volume-fluxes at 5 bar TMP through UF-membranes GR61PP and CA600PP, Dow Denmark A/S.

It was found that the volume-flux through the cellulose-acetate membrane (CA600PP) is almost twice as large as the volume-flux through the polysulfone membrane (GR61PP) and it has less tendency to become fouled. The CA600PP-membrane was also found to have a smaller retention of citrate than the GR61PP.

Following filtration by microfiltration *and* ultrafiltration, the precipitations in the stripped lime juice seemed much less pronounced when pH was subsequently adjusted.

2.4.4 Removal of calcium and magnesium

Other investigated pretreatments include ion-exchange (IX) and nanofiltration (NF). The large calcium and magnesium content in the stripped lime juice (Table 2.1) has to be removed before electrodialysis with bipolar membranes is possible to prevent membrane scaling.
To remove the divalent cations, NF was investigated as an alternative to IX and found to retain calcium and magnesium to a high degree, but the rentention of citric acid is around 90 % and so NF has so far been abandoned in favor of IX. But NF could be considered for a preliminary concentration of citate if membrane fouling is not too bad.
Using cation-exchange resin Puralite C100 regenerated by 1 M HCl the Calcium and Magnesium content of microfiltrated lime-waste dropped below 1 ppm, which is the recommendable limit for electrodialysis with bipolar membranes.

2.5 Electrodialytical citrate concentration

2.5.1 Purpose

In this section, the electrodialytic concentration of citrate from stripped lime juice when including several pretreatments steps is demonstrated to verify that the indications of citrate concentration by Brix index is valid.

2.5.2 Experimental

2.5.2.1 Methods and equipment

The equipment and methods are the same as mentioned in paragraphs 2.2.2.1 to 2.2.2.3.

The lime-waste was first microfiltrated using Durapore membranes (poresize 0.22 μm), then ultrafiltrated through a CA600PP membranes (Cut-Off value MW 20,000 from Dow Denmark A/S), passed through a column equipped with cation-exchange resin Puralite C100, and finally adjusted to pH 3.9 with solid KOH before the electrodialysis.

2.5.2.2 Concentration of pretreated stripped lime juice

A batch ED experiment on stripped lime juice that was stepwise microfiltrated, ultrafiltrated and ion-exchanged, was carried out to verify the recovery of citrate from the juice. The pH of the juice was not adjusted to avoid fouling and the experiment was performed on juice at pH 2.3.

Operation mode:	Batch ED, constant current
Cell pairs:	3
Driving Force:	800-200mA (cc)
Feed:	MF, UF, IX lime juice (340 ml)
Concentration side:	4% H_3Cit model solution (310 ml)
Electrode rinse:	0.1M K_2SO_4 (500 ml)
Ion-exchange membranes:	Selemion APS-3 and CMV
pH:	2.3
Volume flow (feed):	11.7 g/s
Volume flow (Conc.):	12.2 g/s
MF-filtration membrane:	Durapore
UF-filtration membrane:	CA600PP
Ion-exchange resin:	Puralite C100

The result of the citrate concentration is shown in Figure 2.25.

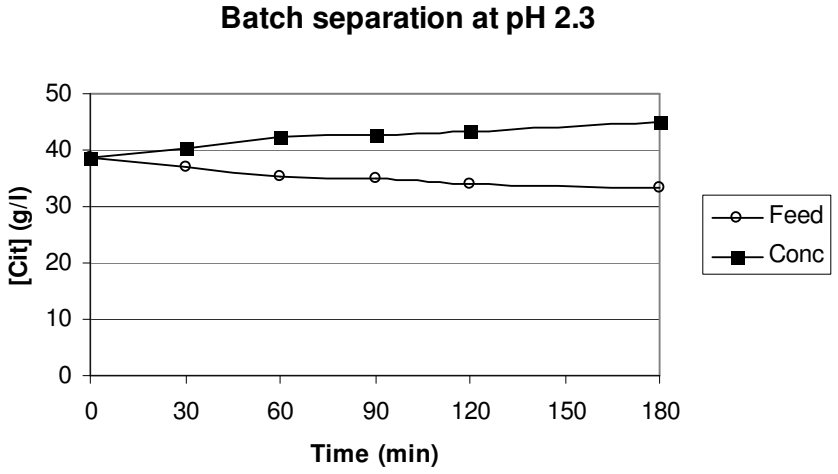

Figure 2.25 Citrate concentration and depletion on stripped lime juice.

The flux is disappointingly low when compared to model experiments. Even after extensive pretreatment of the lime juice and no pH-adjustment, fouling occurs as can be seen in Figure 2.26 that shows the changes in voltage and current density during the experiment. It was necessary to lower the current density stepwise three times to accommodate the increasing electrical resistance.

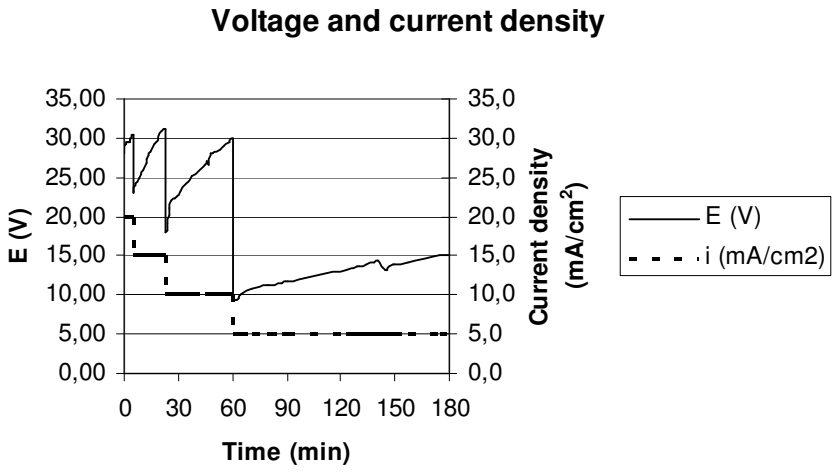

Figure 2.26 Changes in voltage and current density during the batch ED experiment.

The experiment was repeated with pretreated lime juice adjusted by sodium hydroxide to pH 8.

Operation mode:	Batch ED, constant current
Cell pairs:	3
Driving Force:	800-200mA (cc)
Feed:	MF, UF, IX lime juice (370 ml)
Concentration side:	4% Na_3Cit model solution (360 ml)
Electrode rinse:	0.1M Na_2SO_4 (500 ml)
Ion-exchange membranes:	Selemion APS-3 and CMV
pH:	8
Volume flow (feed):	10.8 g/s
Volume flow (Conc.):	12.7 g/s
MF-filtration membrane:	Durapore
UF-filtration membrane:	CA600PP
Ion-exchange resin:	Puralite C100

This yielded a much higher flux and a faster concentration as shown in Figure 2.27.

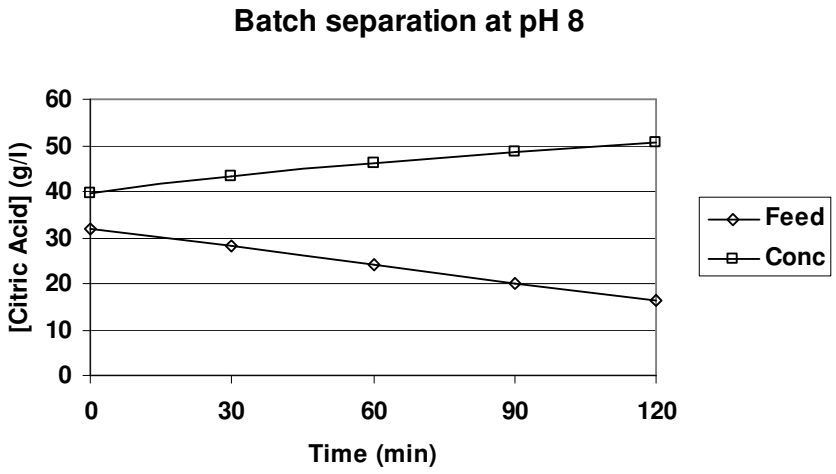

Figure 2.27 Citrate concentration and depletion on stripped lime juice.

This experiment did not demonstrate the fouling tendency experienced earlier, and the precipitations were less pronounced when the juice was ultrafiltrated. This is a positive

2.5.2.3 Organic acid flux

Some competitive transport is expected from other anions. Since the only other anion present in significant amount is malic acid, the flux of citrate and malic acid was compared in similar ED experiments on model solutions (4 % citric acid, 0.25 % malic acid, and 0.25 % glucose, adjusted to pH 3.9 by solid KOH), microfiltrated lime juice (4% citric acid, adjusted to pH 3.9 by solid KOH), and lime juice that was both microfiltrated, ultrafiltrated and ion-exchanged (3.6% citric acid, adjusted to pH 3.9 by solid KOH).

The fluxes measured during the first hour of a concentration experiment are compared in Table 2.9.

	Model Solution	Lime juice (MF)	Lime juice (MF+UF+IX)
$J_{Citrate,1\ hr}$ (mol/m^2·s)	$5{,}63 \cdot 10^{-4}$	$1{,}31 \cdot 10^{-4}$	$1{,}30 \cdot 10^{-4}$
$J_{Malic,1\ hr}$ (mol/m^2·s)	$5{,}82 \cdot 10^{-5}$	$2{,}14 \cdot 10^{-5}$	$3{,}53 \cdot 10^{-5}$
$J_{Sugars,\ 1\ hr}$	~ 0	~ 0	~ 0

Table 2.9 Fluxes measured after 1 hour of batch ED concentration experiments on model solution or pretreated lime waste at pH 3.9.

The citrate content of the model solution and the microfiltrated lime juice is about 4%, but some citrate is lost during ultrafiltration and ion-exchange steps, resulting in 3.6% citrate content. Still, the fluxes from the lime juice are comparably, and much lower than in model solution.

The sugars are retained sufficiently during the first hour of concentration that they are not detected in the concentrate solution.

2.5.3 Conclusion of electrodialytical concentration of citrate

When extensive pretreatment of the stripped lime juice is applied, the experiments verify that electrodialytical concentration is possible. The scope of the project was to discover whether electrodialysis could be applied to recover citric acid from the stripped lime juice for a simple recovery process, and to this point, the results are not too positive.

So far, it seems necessary to employ a combination of cooling, rough filtration (microfiltration or sandfiltration), ultrafiltration, and ion-exchange. The ion-exchange step is only necessary, is the citrate must be acidified to citric acid through electrodialysis with bipolar membranes. Without ion-exchange, the ED process is estimated to be able to produce 15-20% concentrated sodium or potassium citrate. The energy consumption seems high, because of lower citrate fluxes in the pretreated lime juice than in model solutions, which is probably caused by the presence of various biological substances. It has been suggested by Taniart Productos that an enzymatic treatment the stripped lime juice would be considered, but no results have been presented.

2.6 Nanofiltration

2.6.1 Purpose

A major drawback by electrodialysis with bipolar membranes is that any significant presence of divalent cations like calcium and magnesium has a tendency to destroy operations through membrane scaling by precipitating as hydroxide salts. Some of the proven technologies for removal of divalent ions are ion-exchange (IX) or nanofiltration (NF). Ion-exchange is a simple process, but demanding in terms of raw materials and creates an amount of wastewater whenever the ion-exchange resin must be regenerated. Hence, nanofiltration was investigated with model solutions containing calcium and magnesium ions and citric acid. In experiments, retention of calcium and magnesium higher than 90% was found, thus making this a feasible process to get rid of the earth-alkali ions and at the same time remove the bio-matter, which apparently presents a fouling hazard in electrodialysis operations. However, since retention of citric acid is also higher than 90%, it is not a very feasible separation process as pretreatment for an electrodialysis concentration.

For reverse osmosis membranes, it has been reported that retention of organic acids depends on pH. This is explained by assuming undissociated acid permeates freely through the membranes while the dissociated acid-ion is rejected (Timmer *et al.* 1993). Nanofiltration could possible be an alternative to electrodialysis in concentration of the citric acid. In this part, nanofiltration experiments on model citrate solutions at different pH-values are investigated.

2.6.2 Nanofiltration experiments

2.6.2.1 Equipment and material

Two kinds of nanofiltration equipments were used in this investigation. Preliminary experiments were performed using a batch cell, and then a crossflow filtration unit was employed. Both equipments were designed and manufactured in cooperation between the Membrane Group and the workshop at the Department of Chemical Engineering, DTU. The batch cell is depicted in Figure 2.28. The feed container volume is 750 ml and made of stainless steel. The membrane area available for separation is 140 cm^2. Pressure in the feed tank is controlled by Nitrogen gas through a valve.

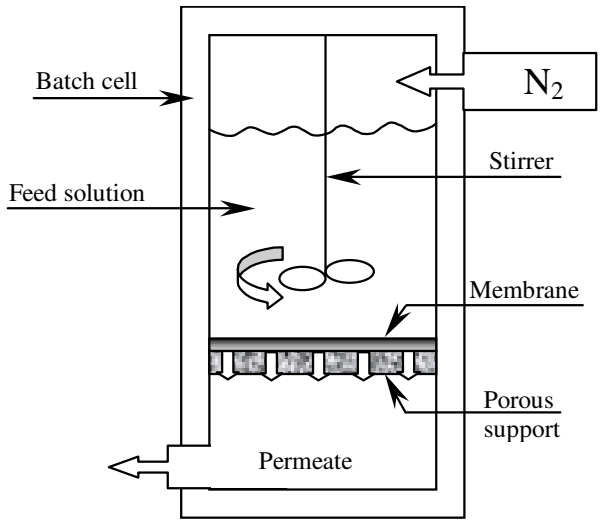

Figure 2.28 Batch-cell for filtration experiments.

Setup for the crossflow operation is shown in Figure 2.29. Feed solution is held at constant temperature by a thermostatic bath. The crossflow cell is made of stainless steel with an effective membrane area of 37 cm^2.

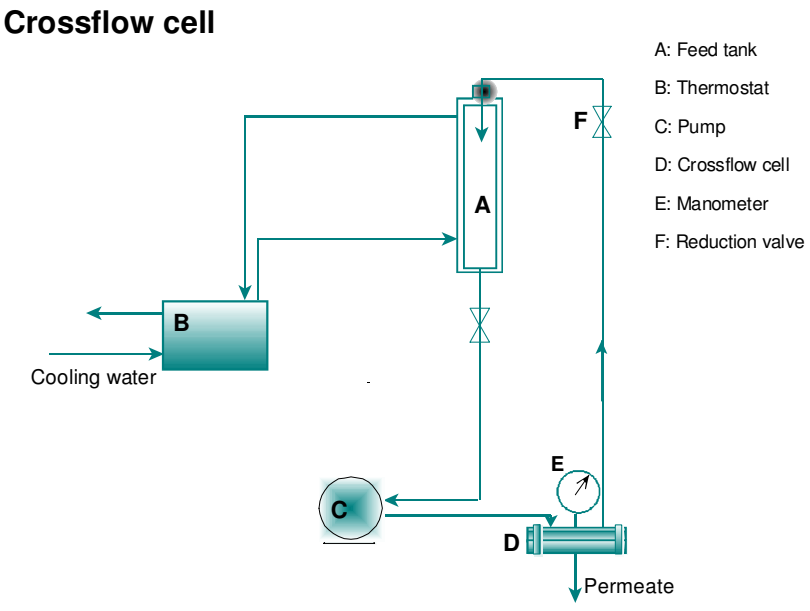

Figure 2.29 Crossflow filtration setup.

A nanofiltration membrane NF45 (DSS, Nakskov, Denmark) was chosen for all the experiments.

Citrate concentrations were measured by RI using an Animex HPX-87H column (Biorad Lab., Richmond, U.S.A.).

2.6.2.2 Batch-cell experiments

4% citrate solutions, adjusted to the desired pH-value with potassium hydroxide, were prepared. Chosen pH-values are 1.9 (no potassium hydroxide added), 3.9, 5.6, and 7.5. These values are chosen to reflect the four valences of citrate (0, -1, -2, and -3) as discussed previously.

A flat-sheet membrane (NF45) with a surface area of 0.014 m^2 is fixed in the bottom of the batch-cell and 750 ml feed solution is then placed in the stirred dead-end filtration batch-cell. The feed cell is pressurized by nitrogen. Two transmembrane pressure levels are investigated: 30 atm. and 50 atm. Permeate is collected at intervals, weighed for flux measurements, and sampled to determine citrate content. All experiments take place at room temperature (20°C). The pure water flux of the membranes is measured before and after every experiment.

The experiments are stopped when the membrane flux drops below 1 kg/m^2h or the feed volume is less than 150 ml.

These experiments give an impression on the concentration levels that could theoretically be achieved.

2.6.2.3 Crossflow experiments

4% citrate solutions are prepared like in the batch-cell experiments. 3.5 liter of this feed solution is transferred to the system and pumped through the equipment. Temperature is kept at 25°C. Pressure is added to the feed side of the crossflow cell by a reduction valve. When a stable flux is obtained, permeate is collected and the flux is measured. pH in the permeate is measured and samples to determine citrate concentration is taken from permeate and feed. The flux and citrate concentrations are determined for seven different values of the feed-side pressure between 5 and 50 atm.

2.6.2.4 Nanofiltration results

In the batch cell, a stirrer controls the flow conditions, and the boundary layer thickness, which is changing with distance from the stirred center, is not easily estimated by experimental data. In these experiments, only the observed retention of citrate is calculated as defined in Equation 1.33. The true retention should be higher than the observed retention. The observed retentions of citrate as function of the membrane flux in the batch cell are shown in

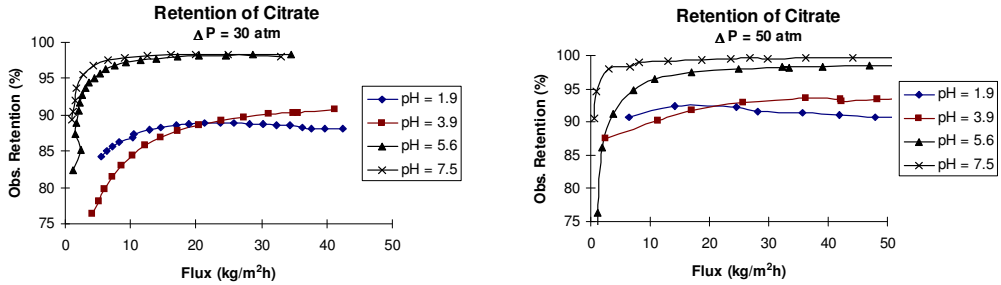

Figure 2.30 Observed retention of citrate at varying pH-values in the batch cell experiments. The left and right figure show the retention with transmembrane pressure of 30 and 50 atm., respectively.

The results of the batch experiments are as expected for nanofiltration. The higher the charge of the citrate ion, the higher is the retention. The difference in retention is especially noticeable when the citrate goes from monovalent to divalent form. The retention is still high for the uncharged citric acid, probably due to the size of the molecule.

During the batch experiments, the citrate concentration in the feed cell rose due to the high retention, while the overall flux dropped. The steady increase in feed concentration causes a rise in osmotic pressure across the membrane, thus lowering the flux according to Equation 1.29 and Equation 1.31. Figure 2.31 shows the relationship between the membrane flux and the citrate concentration in the retained feed phase.

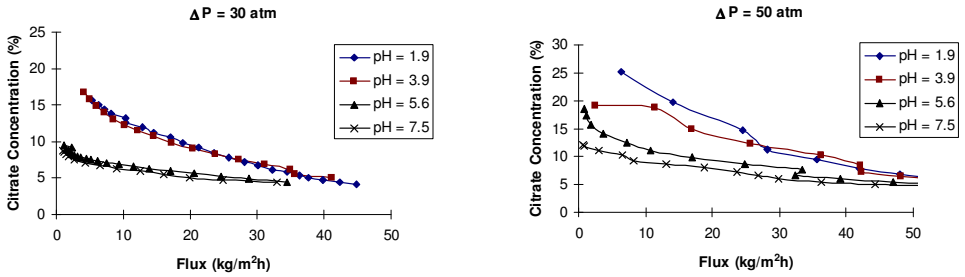

Figure 2.31 Relation between membrane flux and retained citrate concentration.

While the retention is clearly higher for the polyvalent forms of citrate, the highest citrate concentrations can be obtained for the monovalent or undissociated citrate form in these dead-end filtrations. At the very high retention levels, the citrate concentration in the permeate is very low, thus a very large concentration gradient exists across the membrane. This leads to a higher osmotic counterpressure, resulting in faster flux decrease. However, the recovery of citrate is much lower at lower pH-values, because of much higher permeate concentration. For practical applications of concentrating citrate by nanofiltration, the pH-value must be chosen by highest priority: high recovery or high product concentration.

By plotting the concentration difference between the feed and permeate on a logarithmic scale versus the flux, the limiting concentration difference between feed and permeate concentration can be found by linear regression at zero flux. This corresponds to the transmembrane concentration

difference, ΔC, where the osmotic pressure exactly counters the transmembrane pressure, ΔP. The results are plotted in Figure 2.32. At zero flux, there is no solute polarization ($C^w = C^s$), and the concentration difference measured and shown here, is the actual concentration difference across the membrane.

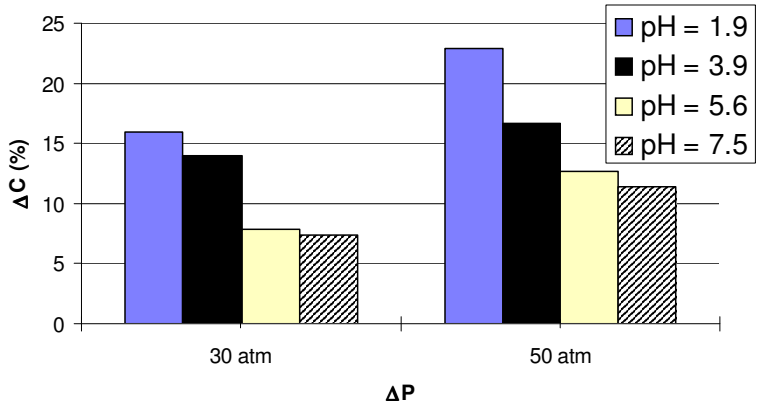

Figure 2.32 Limiting citrate concentration difference across NF45 membrane at four different pH-values and two different transmembrane pressures.

As can be observed from the figure, the highest possible concentration difference, which corresponds to the lowest retention, can be found at the lowest pH-values. This corresponds very well with theory, since the citrate ion has the highest valences at pH 5.6 and 7.5 (respectively –2 and –3) and thus, the highest retention can be observed at these values. At pH 1.9, where the citrate ions are nearly all undissociated, and at pH 3.9, where the ionic charge is around –1, the retentions are much lower.

The reflection coefficients, σ, which reflect the degree of retention, have been found as explained in the nanofiltration theory part in Figure 1.16. The values are collected in Table 2.10 along with the corresponding osmotic pressure differences.

	ΔP = 30 atm		ΔP = 50 atm	
	σ	Δπ (atm.)	**σ**	Δπ (atm.)
pH = 1.9	0.72	41	0.74	67
pH = 3.9	0.80	37	0.84	60
pH = 5.6	0.95	32	0.96	52
pH = 7.5	0.95	31	0.98	51

Table 2.10 Reflection coefficients and their corresponding osmotic pressure differences.

From the values in Table 2.10, the high retentions of citrate at pH 5.6 and 7.5 are evident. Here the citrate ions are almost completely retained (σ close to 1) and the corresponding osmotic pressure cancels the volume flux at nearly the same value as the transmembrane pressure.

For calculations of the true retentions of the citrate ions, the crossflow cell setup was utilized. This module has a stable boundary layer, which's thickness can be estimated from the Sherwood relations (Equation 1.20 and Equation 1.21) by the Reynolds and Schmidt numbers. The calculations are added to appendix 7.1.2. By a feed flow rate of 6.5 dm^3/min., the flow is turbulent (Re > 5000) and the boundary layer thickness is estimated to 0.05 cm.

By measuring solvent flux and citrate concentrations in the permeate as function of transmembrane pressure, the true retention can be calculated from Equation 1.33, Equation 1.34 and Equation 1.35 by using the obtained value for the boundary layer thickness. The solvent fluxes are presented in Figure 2.33.

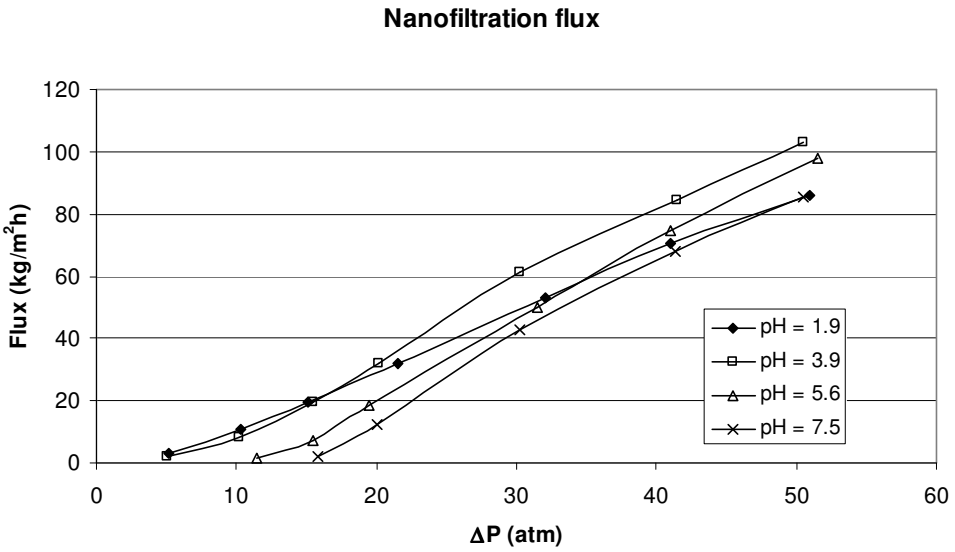

Figure 2.33 The solvent flux as function of transmembrane pressure with a NF45 membrane at different pH-values of 4% potassium citrate.

Figure 2.34 shows the observed retention of citrate at different pH-levels in the crossflow cell as function of the solvent flux.

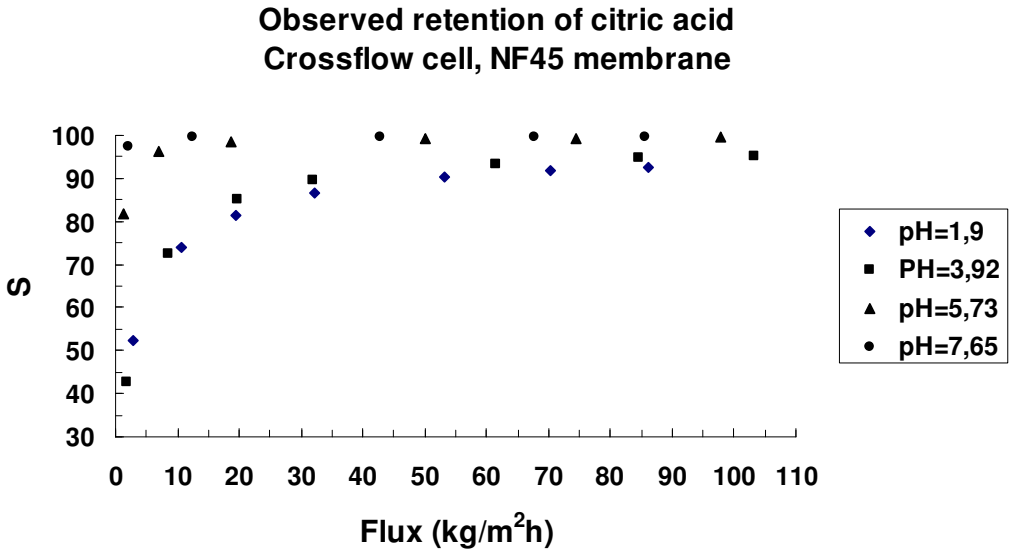

Figure 2.34 Observed retention of citric acid at different pH-values as function of the solvent flux.

The true retention is not depending on solvent flux, but solely on the molecule and the membrane. As described in the theory section 1.3 about nanofiltration, the true retention, R, can be obtained by depicting ln[(1-S)/S] as function of $J_w/v^{0.8}$ (turbulent flow) and by interpolation, ln[(1-R)/R] can be found where the line crosses the ordinate axis. The technique is demonstrated in appendix 7.1.2. The results are presented in Table 2.11.

Citrate feed pH:	True retention, R (%)
1.9	80
3.9	83
5.7	98
7.6	100

Table 2.11 True retention of the citrate ion at various pH-values.

2.6.3 Conclusion on nanofiltration experiments

The nanofiltration experiments revealed that NF is a feasible process for concentration of a citric acid solution. Almost total retention of the citrate ions can be obtained by increasing pH to 5-7. By keeping pH at 1.9, concentrations as high as 25% was reached in the retained solution, but this included a higher loss of citrate through the permeate.

Whether the nanofiltration process can be implemented directly to decanted, stripped lime juice was not investigated due to lack of juice samples, but some rough filtration step is probably necessary to remove large particles.

3

3 Inhibition of enzymatic browning in pear juice by electrodialysis

3.1 Project background

3.1.1 Purpose

The overall purpose of this project was to investigate the possibility to inhibit the enzymatic browning of fruit juice by utilizing electrodialysis technology. This could be an interesting alternative to thermal processes, since the electrodialysis process runs at room temperature and thus, preserves flavor molecules that are otherwise boiled off at higher temperature, and furthermore, no foreign substances are added to the juice.

First part of the experiment was to investigate if lowering the pH of the pear juice would inhibit the browning process, and if successful, investigate how low in pH the juice needed to go to reach an acceptable inhibition.

3.1.2 Project participants

This project was sponsored by the EC's ALFA program. The project was co-supervised by Dr. Gustavo Gutierrez Lopez and Dr. Lidia Dorantes de Parada at the Escuela Nacional de Ciencias Biologicas (Department of Food Science) at the Instituto Politecnico Nacional (IPN), México City, and carried out in cooperation with Ph.D.-student Rodolfo Garcia-Sámano.

3.1.3 Introduction

The application of electrodialysis technology with bipolar membranes in food industry has been tested by Canadian researchers (Tronc *et al.* 1997;Tronc *et al.* 1998). This research team investigated the effect on cloudy apple juice. It was decided to investigate whether these results could be reproduced with other types of fruit juice. For this project, Anjou Pears were chosen, since they contain large quantities of polyphenols and polyphenol oxidase (PPO).

It has been proved that temporary decrease of the pH of cloudy apple juice by addition of hydrochloric acid, irreversible inhibits the enzymatic activity of polyphenol oxidase (PPO) (Zemel *et al.* 1990). The lowering of pH changes the tertiary structure of the PPO. Even after the juice is readjusted to the original pH of the apple juice by an alkaline substance like sodium hydroxide, the PPO activity is strongly inhibited, and thus, reducing the browning effect. There is no commercial value of this process as the added acid and base will produce a salt making the juice flavor unacceptable.

By using electrodialysis with bipolar membranes (EDBM), it is possible to substitute the potassium ions in a fruit juice with hydrogen ions at room temperature, without further additions or changes in the juice composition. After temporarily storing the juice at the resulting low pH-value, the EDBM process can be reversed, substituting the same potassium ions back into the juice for the hydrogen ions, until the original pH and juice composition is attained (Bazinet *et al.* 1998;Tronc *et al.* 1997).

3.1.3.1 Anjou pears

The average composition of a pear is portrayed in Figure 3.1 and detailed in Table 3.1. The pears are shown in Figure 3.2.

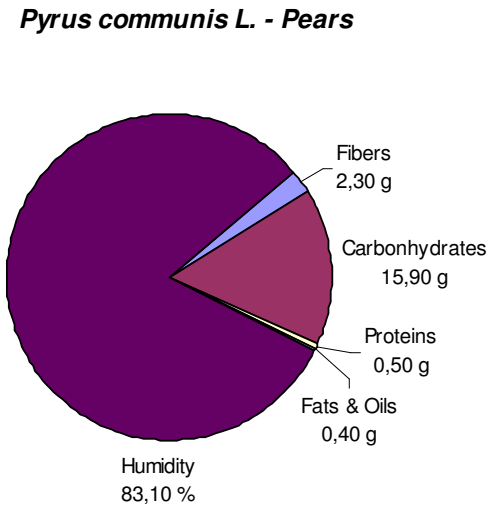

Figure 3.1 Average pear composition Energy: 61.00 kcal. Edible part: 81.00%.

Lipids		Minerals		Vitamins	
Total fats g	0.40	Calcium mg	9.00	Vitamin A mcg	1.00
Cholesterol g	0.00	Phosphor mg	11.00	Ascorbic acid mg	4.00
Total saturated g	0.02	Iron mg	0.20	Vitamin B1 mg	0.02
Monounsaturated g	0.08	Magnesium mg	6.00	Riboflavin mg	0.04
Polyunsaturated g	0.09	Sodium mg	0.00	Niacin mg	0.10
		Potassium mg	125.00	Piridoxin mg	0.02
		Zinc mg	0.12	Folic acid mcg	7.00
				Cobalamin mcg	0.00

Table 3.1 100 g net weight of raw fruit (Muñoz de Chávez *et al.* 1996).

Figure 3.2 Anjou pears used in the experiment.

3.2 Experimental

3.2.1 Methods and equipment

Equipment

A spectrophotometer (UV-1201, Shimadzu, Japan) was used to measure enzymatic activity. A COLORMATE was used to measure lightness and redness index of solutions.

The primary equipment necessary for the electrodialysis experiments was designed by the Membrane Group and constructed at the workshop at the Department of Chemical Engineering at DTU. It consists of an electrodialysis stack with 6 acrylic flow-chambers that can be arranged as required and two end-pieces with platinum electrodes.
The ion exchange membranes were kindly supplied by Tokuyama Europe GmbH (Neosepta CMB and BP-1 membranes).

The power supply to be utilized in experiments broke down. Hence, the AC adapter for a laptop PC capable of supplying 19V and 3.2A DC supplies the electrical power for electrodialysis experiments. Other necessary equipment includes two multi-meters, LCD Auto Range Digital Multimeter 22-163 (Radio Shack®).

The membrane setup is shown in Figure 3.3.

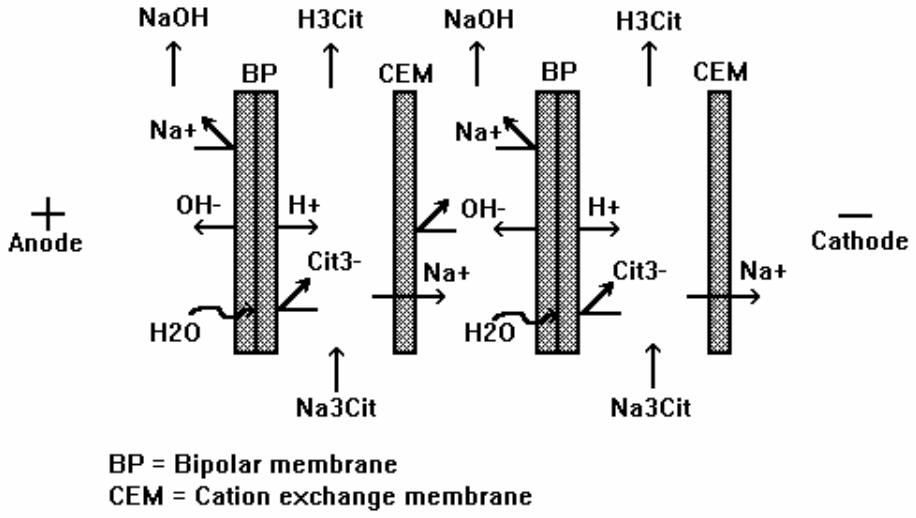

Figure 3.3 Electrodialysis with bipolar membranes.

The figure shows a sodium citrate solution entering the membrane unit. Inside the unit, the sodium ions are transported out of the feed solution and hydrogen ions are introduced to substitute the sodium ions, hence, preserving the electroneutrality of the feed solution. This is a well-known process for transforming an organic acid salt into the pure acid. A direct electrical current of about 10 to 250 mA/cm^2 is the driving force that makes positively charged ions (cations) migrate towards the cathode and negatively charged ions (anions) migrate towards the anode. The selective cation-exchange membranes (CEM) allow sodium to be removed from the feed and collected in an alkaline stream. The bipolar membrane (BP) effectively rejects both sodium ions and citrate ions, which creates a strong electrical potential across the bipolar membranes. This localized field catalyzes deionization of water molecules, which diffuse into the bipolar membrane and leaves as hydrogen and hydroxide ions.

Juice samples

Juice samples were prepared by mixed pear fruit without the peel and core by equal amount of water in a blender. Then the mixture was filtered through a cloth 2-3 times to remove remnants from the fruit, but the filtered juice still hold the proteins and enzymes that makes it cloudy.

Enzymatic activity

The enzymatic activity is a measure of the potential browning that will occur over time. The enzymatic activity is "triggered" by addition of Catechol and if the PPO is active, the samples changes color quickly.

The enzymatic activity was measured by the following method:

- 1 ml of pear juice was mixed with 2.5 ml of a Catechol solution. The Catechol solution was prepared in a 0.5M phosphate buffer that made sure all measurements were done at pH 6.5±0.2, and so that the Catechol concentration in the mixture was 10mM±0.25mM every time.
- The mixture was shaken and immediately transferred to the spectrophotometer. The absorbency was noted every 5 seconds for 90 seconds at 395nm wavelength. The initial

slope was calculated (using Microsoft Excel's trendline function) to be the speed of the *enzymatic activity*.

- Each measurement of enzymatic activity was repeated three times.

3.2.2 Results and Discussion

3.2.2.1 Inhibition of enzymatic browning

To investigate how low in pH it was necessary to go for obtaining an acceptable inhibition of PPO, a series of experiments were conducted. Pear juice was produced by stirring equal amounts of pear (without peel and core) and aqueous acid solution. The acid was either citric acid or hydrochloric acid to eliminate the possibility that it was either of these acids, which produced the inhibition effect instead of simply the lowering of pH. Then, the mixture was filtered through a cloth filter to obtain a cloudy pear juice solution.

After some storage period at the lower pH-value (ranging from 2.0-4.6), the pH of the juice samples was readjusted with sodium hydroxide to the original level around 4.2-4.6. The enzymatic activity was measured for the readjusted juice, and over a longer period of time, the lightness and redness index of the cloudy juice was tracked by Colormate measurements.

The lightness and redness index for a few samples are shown in Figure 3.4.

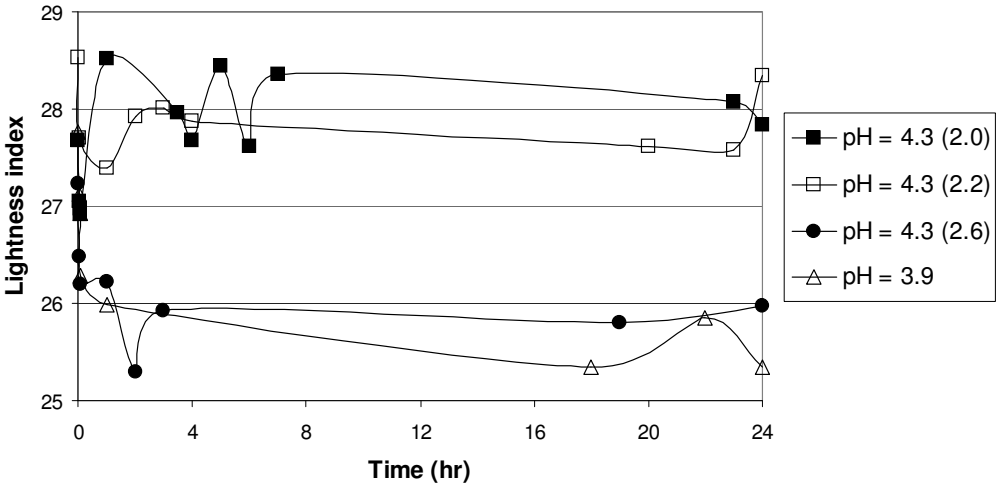

Figure 3.4 Lightness index during a 24 hour period for 4 pear juice samples after preliminary pH-adjustment to respectively 2.0, 2.2, 2.6 or 3.9, followed by readjustment to original pH except the last sample.

The lightness index of the juice samples showed that the juice adjusted below pH 2.5 was much lighter in color than other juice samples. There was a development of redness in the darker samples too, which is also a typical indicator of browning.
Failure to utilize the Colormate properly, failed to show a significant development in colorization, though it was obvious when looking at the samples visually as shown in Figure 3.5.

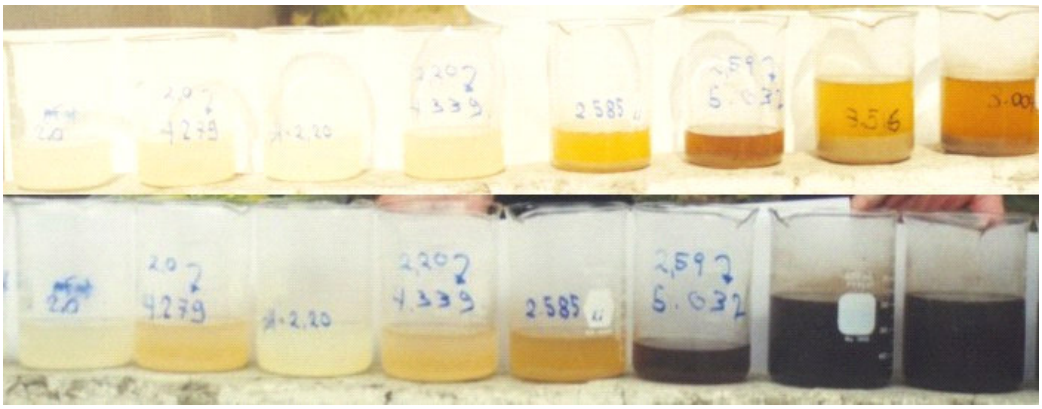

(a) (b) (c) (d) (e) (f) (g) (h)

Figure 3.5 Development of browning in pear juice samples. The top half of the figure shows the juices shortly after readjustment, the lower half shows the browning 24 hours later. (a) and (b) were initially adjusted to pH 2.0, and (b) was readjusted to pH 4.3. (c) and (d) were initially adjusted to pH 2.2, and (d) was readjusted to pH 4.3. (e) and (f) were initially adjusted to pH 2.6, and (f) was readjusted to pH 5.0. (g) and (h) were adjusted to respectively 3.6 and 3.0. (a), (c), (e), (g), and (h) were not readjusted.

In the picture, it can be observed that the readjusted juices (b), (d), and (f) are darker in color than their respective counterparts (a), (c), and (e), which means that the PPO activity had not been fully eliminated, before the readjustment. Still, the juices adjusted to pH 2.0 and 2.2 before readjustment clearly shows inhibition of browning, compared to the other juice samples. The juice colors are compared in the scheme in Figure 3.6.

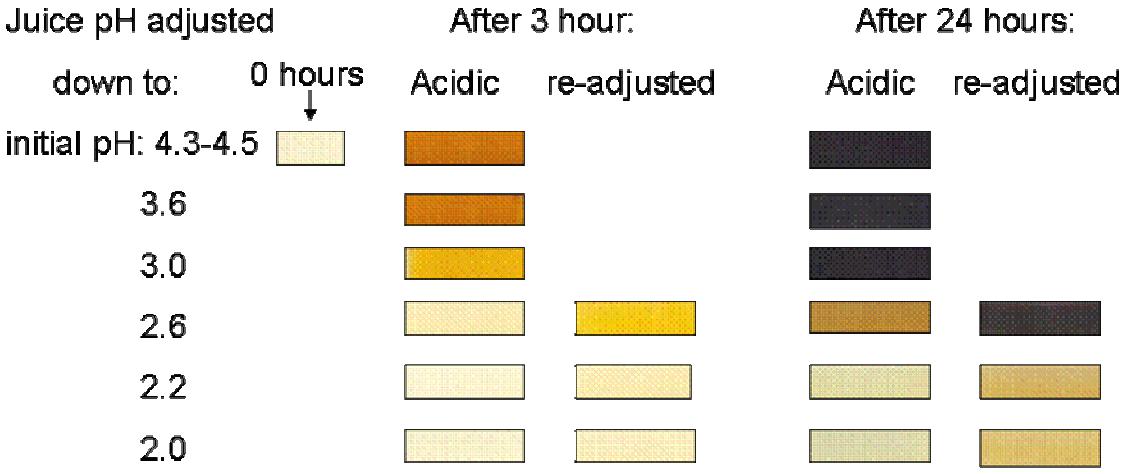

Figure 3.6 Overview of the juice colors as a result of storage at various pH-values.

Figure 3.7 illustrates the results of the pH-adjustment in juice samples, where the PPO activity is shown as function of the initial pH-value that the juice was lowered to, before being readjusted to pH 4.6.

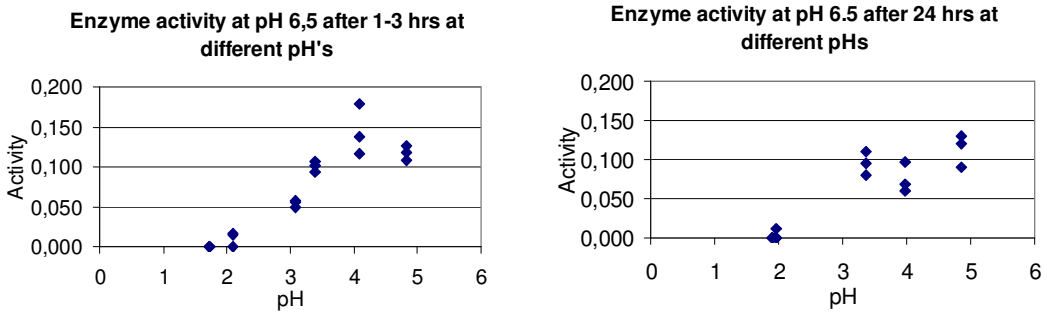

Figure 3.7 Enzymatic activity of pear juice after having spend 1-3 hours (left) or 24 hours (right) at a lower pH-value before being readjusted to original pH-level.

The left sheet in Figure 3.7 shows the readjusted juice's activity after a few hours of storage at room temperature at low pH, while the juice in the right sheet has been stored cold (5°C) at low pH for 24 hours, before being readjusted. The activity of juice stored at pH-values greater than 2.5 show a decrease in PPO activity that is still unacceptable high. No significant difference in PPO activity could be observed resulting from extended storage time, when the juice was adjusted to pH 2.5 or lower. This is contrary to observations done by other researchers.

It was concluded that the pear juice had to be adjusted below pH 2.5 for the PPO to be effectively inhibited. No significant differences were observed between juice samples adjusted by hydrochloric acid or citric acid.

3.2.2.2 The browning process

To expand the knowledge of the browning process in juices, the Michaelis-Menten constant, K_M, and maximum reaction rate V_{Max} of the browning process was investigated for Anjou pear juice and Mango juice. Different analytical methods to measure these constants were tried and yielded different results, as shown in Table 3.2 and Table 3.3.

Method	K_M (mM)	V_{Max} (Abs/s)	R^2
Lineweaver and Burk	23.21	0.00151	0.8515
Augustinsson	**13.85**	**0.00115**	0.9121
Eadie and Hofstee	9.89	0.001	0.3138

Table 3.2 Anjou pear enzyme.

Method	K_M (mM)	V_{Max} (Abs/s)	R^2
Lineweaver and Burk	22.13	0.00034	0.6484
Augustinsson	**12.54**	**0.00027**	0.7783
Eadie and Hofstee	3.15	0.00021	0.0248

Table 3.3 Mango enzyme.

The R^2-values is a measure of the degree of linear fit of the different methods. It was found that the Augustinsson method yielded the best fitting of the data and that the Eadie and Hofstee method yielded the worst fit.

3.2.2.3 Electrodialysis experiments

The electrodialysis experiments were unfortunately constantly disrupted by a faulty power supply, but a few successful experiments supplied some promising results with the DC power supply for a laptop computer.

700 g raw Anjou Pear is pressed and mixed with 700 ml of water; then filtered through a cloth to retain the fruit pulp. 500 ml of the mixture goes into the ED equipment for acidification; the rest is saved for control tests.
500 ml potassium chloride (0.25M) is prepared for the alkaline solution. For electrode rinse, 2 liters of potassium sulfate (0.1M) is circulated in the electrode compartments.

The Equipment was set up in a two-compartment EDBM-configuration with three cell pairs of alternating bipolar and cation-exchange membranes as shown in Figure 3.3.

The solutions were put in circulation with pear juice entering the setup in the same compartments as the sodium citrate in Figure 3.3, and potassium chloride in the remaining compartments. After some time to obtain equilibrium, the experiment was started. The voltage was kept constant around 20V across the entire stack and the current rose from about 400mA to 1A (from 10 to 25 mA/cm^2) during the process. By EDBM, the potassium ions of the juice were extracted to the potassium chloride solution and substituted by hydrogen ions. The potassium ions were contained in the alkaline solution. The pH in the juice compartment and in the alkaline compartment was monitored, as shown in Figure 3.8.

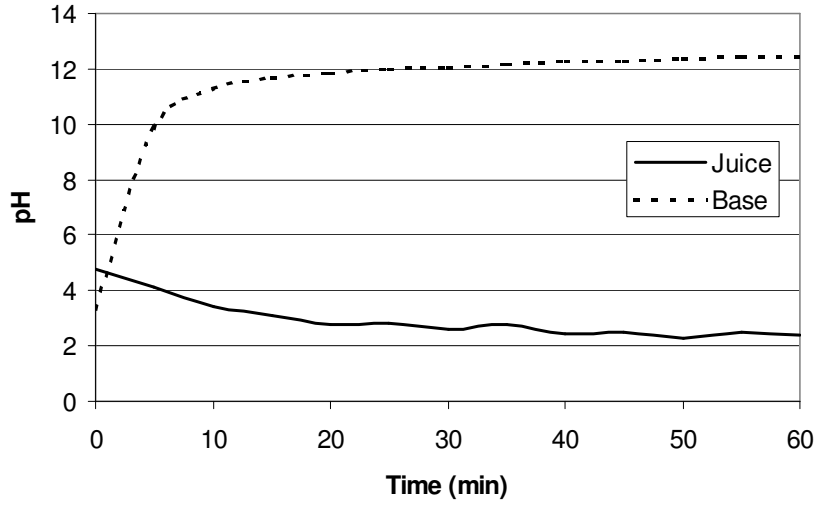

Figure 3.8 pH-changes during EDBM experiment.

After 30 min., the pH in the cloudy juice had fallen from 4.8 to 2.6, and after another 30 minutes, pH 2.4 was reached. The enzymatic activity of the juice was measured 25 and 50 minutes into the experiment and compared to the enzymatic activity of the control juice. After 50 minutes, the enzymatic activity of the adjusted juice had fallen significantly when compared with the control juice, and it was decided to end the experiment after 60 minutes. No ions from the potassium chloride solution entered the juice during the run. The pH was lowered by replacing potassium by hydrogen ions, created from water splitting.

The adjusted juice and the control juice were stored for 24 hours at 5°C. The alkaline solution was also stored. After 24 hours, the enzymatic activity was almost eliminated.

Then the adjusted juice was readjusted by reversing the EDBM process. This time, the juice was circulated in the compartments previously occupied by the potassium chloride, and the stored, alkaline potassium chloride solution was circulated through the acid compartments. The juice was thus readjusted to pH 4.8 by neutralizing the hydrogen ions by hydroxide ions while returning the potassium ions to the juice, and again the juice's enzymatic activity was compared with the control juice.

The enzymatic activity of the juice sample compared with the control juice during different stages of the process is shown in Figure 3.9.

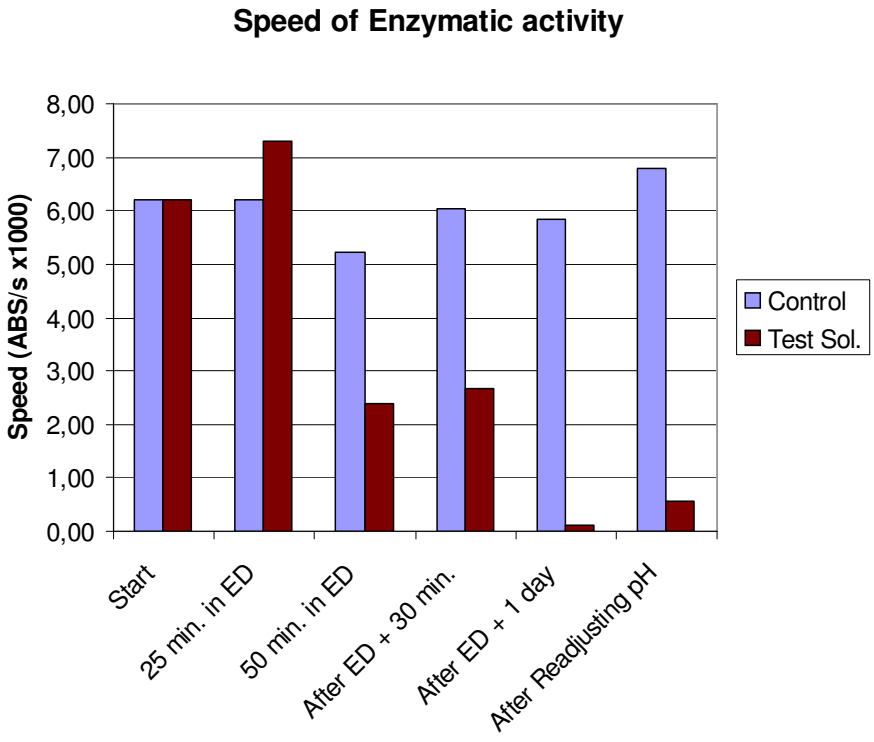

Figure 3.9 Comparison between enzymatic activity of test juice and control juice during the pH-adjustment process.

A small increase in enzymatic activity can be seen, when the juice was readjusted, meaning that some of the PPO had been able to regain their tertiary structure from their denatured state and hence, their functionality. Still, a considerable inhibition could be observed when compared to the control samples.

3.3 Conclusion on browning experiments

This investigation successfully confirmed that the browning of cloudy fruit juice can irreversible be inhibited by temporarily lowering the pH. It was also confirmed that the EDBM process is a feasible process for this task.

It was shown in this project that cloudy juice from Anjou pears is receptive to this treatment. Since the process is performed at room temperature and no foreign substances are added to the juice, this process seems very good for preserving the original flavor of fruit juice. Potassium ions from the juice are temporarily extracted and only hydrogen ions and later hydroxide ions are added, making the juice slightly more diluted. Whether the electrical field passed through the juice creates some chemical changes in the composition is probably something that should be investigated, if this process is to be commercialized, but to the author's knowledge, this is not the case.

4

4 Recovery of lactic acid from fermentation broth

4.1 Background

4.1.1 Introduction

Conversion of agricultural crop residues and agro-industrial waste streams into lactic acid is a process with dual beneficial effects. On one hand agricultural waste poses an environmental threat and on the other hand represents an abundant renewable raw material for several value-added products e.g. bio-gas, ethanol, fibers and different organic acids such as lactic acid. Lactic acid is an important chemical used in a variety of industrial and food applications, but its main potential is as precursor for manufacture of the biodegradable polymer, poly(lactic acid) (PLA). PLA is a bio-based and biodegradable polyester that can replace traditional plastics synthesized from fossil hydrocarbon resources in many industrial applications including packaging of foods, and hence, solve many waste problems related to packaging materials.

The art of producing lactic acid by fermentation has received much attention in the past decade and judging by the number of resent patents and scientific articles research has been especially tense in the past 3-5 years. There are several vital factors affecting large scale fermentative production of lactic acid. The choice of substrate, lactic acid bacteria species, operating conditions and separation processes are a few main factors of importance for commercial production.

Following fermentation, lactic acid must be recovered and purified. One major hurdle in fermentative production of lactic acid from agricultural waste is finding an economical competitive recovery process that honors the demand for high product purity.

4.1.2 Lactic acid

2-hydroxypropanoic acid better known as lactic acid is a chiral molecule with the two optically active forms, L(+)-lactic acid and D(-)-lactic acid, as shown in Figure 4.1. Lactic acid is the simplest and most widely occurring hydroxyl-carboxylic acid and is found in most living organisms from anaerobic prokaryotes to humans (Datta and Glassner 1990).

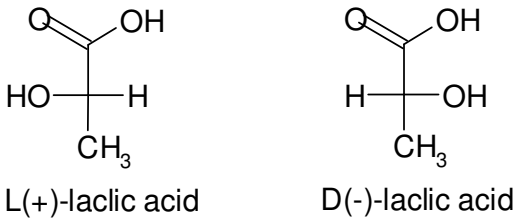

Figure 4.1 The two optically active forms of lactic acid.

In pure anhydrous form lactic acid is a white crystalline solid with a melting point of 52.7-52.8°C for either pure isomer and 17-33°C for a racemic mixture. The pure form is quite difficult to obtain and for industrial purposes, lactic acid is handled in concentrated aqueous solutions. The consistence is syrupy and depending on how it is produced, it can be colorless or slightly yellow. Lactic acid is a mono-carboxylic acid with a pK_a-value of 3.88 at 25°C, resulting in a dissociation curve as shown on Figure 4.2, where the degree of dissociation is plotted as function of pH. It can be seen that below pH 2 virtually all of the acid is undissociated and above pH 6, lactic acid is almost totally dissociated.

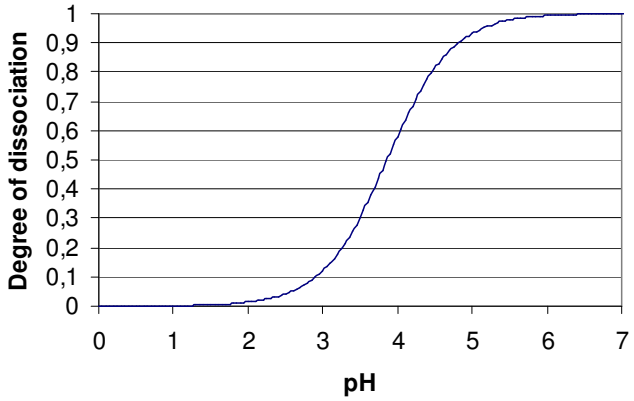

Figure 4.2 Degree of dissociation of lactic acid as function of pH.

As a bulk chemical lactic acid is available in technical, food and pharmaceutical grade at concentrations of typically 50, 80 or 88%. Pharmaceutical grade lactic acid satisfies United States Pharmacopoeia (USP) or European Pharmacopoeia (Ph. Eur.), which dictate the strictest requirements regarding the purity. The food grade must live up to the requirements of the E270 number in Europe, but no particular restrictions apply to technical grade lactic acid, other than those set by buyers.

4.1.3 Lactic acid fermentation

There are two main routes for producing lactic acid; *synthetically*, by the hydrolysis of lactonitrile or through *fermentation* of carbohydrates by action of lactic acid bacteria (LAB). The predominant part of the lactic acid production is achieved by carbohydrate fermentation, which is also the preferred technology when it comes to meeting future demands for lactic acid.

The conventional method for producing lactic acid by fermentation consists of 4-6 days batch fermentation with pH-control by addition of calcium carbonate. Lactic acid concentration reaches around 10 wt% (Datta and Glassner 1990). The broth is then filtered to remove biomass, treated in carbon columns, evaporated and acidified using sulfuric acid to convert the calcium lactate to lactic acid and insoluble calcium sulfate (gypsum). There are several drawbacks to this conventional process. In the carbon columns waste are generated and active carbon must frequently be replaced. More importantly, every ton of lactic acid produced also generates one ton of gypsum is as waste. This gypsum holds high levels of organic residues from the fermentation and has no commercial

value. Furthermore, the batch process can be subject to both strong product and substrate inhibition that limits performance.

The above mentioned shortcomings can be circumvented by working with a continuous system (Ohashi *et al.* 1999;Tejayadi and Cheryan 1995;Zayed and Winter 1995) providing means for continuous removal of lactic acid and recycling or immobilization of cells, hereby increasing productivity.

4.1.4 Organic acid extraction and purification

Extracting and purifying lactic acid from fermentation broth include separating the acid from the LAB cells, the many proteins and amino acids, the inorganic ions, the residual, unconverted carbohydrates (sugars) and other organic acids produced during the fermentation. Several other research groups worldwide have studied this field since Hongo (Hongo *et al.* 1986) in 1986 was among the first to suggest electrodialysis as a possibility for a continuous recovery of organic acids from fermentation broth. Numerous problems associated with this recovery method have been pointed out during the last couple of decades, and numerous solutions have been suggested to overcome these problems.

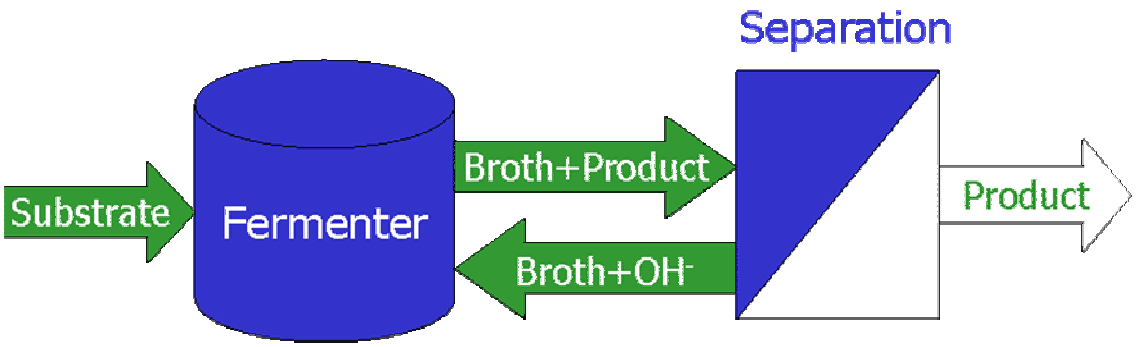

Figure 4.3 Principle design of continuous fermentation with constant organic acid (product) removal and pH-control.

One of the most significant obstacles when trying to extract organic acids directly from a fermentation broth through electrodialysis is membrane fouling. The biological material from the fermentation broth tends to adsorb on to ion-exchange membranes since most of the biological proteins and cells have some kind of locational charged groups, by which they are attracted to the surface of oppositely charged membranes.

Another problem that arises when purifying organic acids through electrodialysis with bipolar membranes is *scaling*. Divalent cations like calcium and magnesium that passes through cation-exchange membranes into an alkaline solution, immediately precipitates on the membrane surface as hydroxide salts ($Ca(OH)_2$, $Mg(OH)_2$). This scaling affects the process fast by reducing effective membrane area, and increasing electrical resistance.

Several pretreatments to extraction of organic acids from fermentation broth have been suggested, investigated and patented:
Microfiltration is commonly used for filtration of fermentation broth (Borgardts *et al.* 1998b;Boyaval *et al.* 1996;Kulozik 1998). Microfiltration retains cells but allows proteins to

permeate through the membrane along with the organic acids, which presents a fouling problem for a subsequent electrodialysis processing.
Ultrafiltration have received much attention because this process retain most fouling bio-matter, including cells and proteins, allowing only small molecules like inorganic salts, organic acids, peptides and amino acids to pass. Ultrafiltration is also subject to fouling, but module designs employing back-flushing or back-shock techniques or where the flow creates high surface shear reduce the impact of bio-matter build-up considerably. Ultrafiltration of fermentation broth is well known (Van Nispen et al. 1991) and reduces bio-matter content sufficiently for subsequent electrodialysis processing. Unfortunately, ultrafiltration allows inorganic cations like calcium and magnesium to pass, and these ions present severe risk for membrane scaling in later steps involving electrodialysis.
Nanofiltration and *reverse osmosis* has received attention as this filtration method is able to retain most calcium and magnesium. Shortcomings of nanofiltration include fouling and low fluxes for this operation.
The type of unit operations needed for further purification strongly dependents on which kind of impurities the initial feedstock contains, but many processes including *electrodialysis* (Boniardi *et al.* 1996;Boniardi *et al.* 1997a;Boniardi *et al.* 1997b;Borgardts *et al.* 1998a;Borgardts *et al.* 1998b;Czytko *et al.* 1987;de Raucourt *et al.* 1989;Hongo *et al.* 1986;Lee *et al.* 1998;Mani and Hadden 1998;Miao 1997;Nomura *et al.* 1987;Van Nispen et al. 1991;Vonktaveesuk *et al.* 1994) and reverse osmosis (Liew *et al.* 1995;Timmer *et al.* 1993;Timmer *et al.* 1994), nanofiltration (Jeantet *et al.* 1996;Mani and Hadden 1998;Miao 1997;Timmer *et al.* 1993;Timmer *et al.* 1994), *diffusion dialysis* (Portner and Markl 2001), *Donnan dialysis* (Zheleznov *et al.* 1998), *ion exchange* (Beschkov *et al.* 1995;Mani and Hadden 1998;Miao 1997;Rincon *et al.* 1997), *carbon adsorption*, *extraction* (Kleerebezem *et al.* 2000;Scholler *et al.* 1993;Siebold *et al.* 1995), *evaporation* and recently *esterification* combined with pervaporation/distillation and hydrolysis of the ester (Eyal *et al.* 1998a) has been suggested.

A common factor for the separation processes mentioned above is the fact that no single process is able to meet all the demands listed previously. By combining several of the processes, it is possible to meet requirements but each additional process adds to the operation costs. For commercial production of lactic acid as food additive or poly(lactic acid), it is necessary to keep production costs at a competitive level. This can only be achieved by keeping the separation steps at a minimum, and each necessary step must be operated at high efficiency.

Several process combinations have been patented (Borgardts *et al.* 1998a;Cockrem and Johnson Pride 1993;Datta and Glassner 1990;Datta and Tsai 1998;Eyal *et al.* 1998a;Soine 1998) and a few have been tested commercially, but none have reached a commercial break-through yet.

4.2 Reverse Electro-Enhanced Dialysis

4.2.1 Process development

The efforts that eventually led to a patented recovery process are founded in years of work employing electrodialysis technology for recovering lactic acid from different fermentation media.

Extracting organic acids from fermentation broth through ion-exchange membrane accomplishes many advantageous separations in one step. Only small (MW < 1000) organic molecules are extracted and of these, predominantly charged ions like inorganic ions and organic acids. Retained

in the depleted broth is most bio-matter, including cells and proteins, as well as unconverted substrate sugars. The feed stream can be recycled to the fermentation for further substrate utilization with reduced inhibition of cell growth. If only anion-exchange membranes are utilized, scaling problems are avoided and only inorganic anions and negatively charged organic acids and amino acids are extracted.
To preserve electroneutrality of this separation process, the extracted anions can preferably be substituted by hydroxide ions. This makes the depleted fermentation broth alkaline, and the recycled stream assists or replaces the pH-control of the fermentation.

This principle is solved by a Donnan dialysis process as shown in Figure 4.4. It was suggested and patented by Dr. Böddeker and others in 1998 (Böddeker *et al.* 1997). The feed stream, which is rich in organic acid and other bio-matter, is pumped directly from a fermenter into every second chamber in a membrane stack. The low pH (around 5-6) of the feed compared to an alkaline solution in every other second flow chamber generates a concentration difference for hydroxide ions across the anion-exchange membranes. This causes hydroxide ions to diffuse through the membranes, producing a positive potential difference across the membranes. This potential drives anions like lactate out of the feed solution in the opposite direction of the hydroxide ions. This way lactate is extracted from the feed into the alkaline solution while it passes through the Donnan dialysis stack.

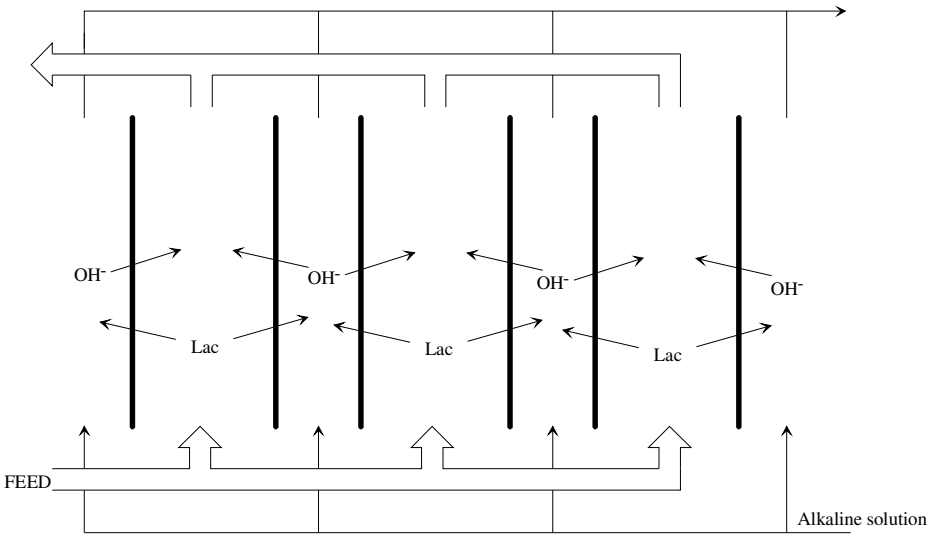

Figure 4.4 Extraction of lactate ions (Lac) in Donnan dialysis with just anion-exchange membranes ▌.

Dr. Böddeker addresses the fouling issues by commenting that the high flow velocity keeps the fouling build-up at a minimum, because of high surface shear. Also the constant flux of hydroxide ions into the feed stream is assumed to continuously remove or destabilize any fouling build-up. Furthermore, the process demonstrates the advantages of high selectivity towards the organic acids as suggested above. The main disadvantage of the Donnan dialysis process is a slow flux of organic acids out of the feed, increasing demands for large membrane areas.

Previous experiments with reverse electrodialysis have demonstrated good anti-fouling results in process streams from fermentation broth (Garde and Rype 1997). Experiments with short pulses of reversed electrical current in order to destabilize a fouling layer gave no conclusive results (Garde *et al.* 2002). The scope of the continuous development process was to investigate whether it would be beneficial to enhance the lactate extraction flux utilizing electrical current while maintaining the efficient setup of the Donnan dialysis process as demonstrated in Figure 4.4.

A problem that must be addressed when adding electrical current to a Donnan dialysis setup is competitive ion transport. The competitive transport is demonstrated in Figure 4.5. When adding electrical current to the dialysis setup, the anions are the only ions allowed to travel through the stack. And lactate and hydroxide ions are both going to compete against each other for transferring the current.

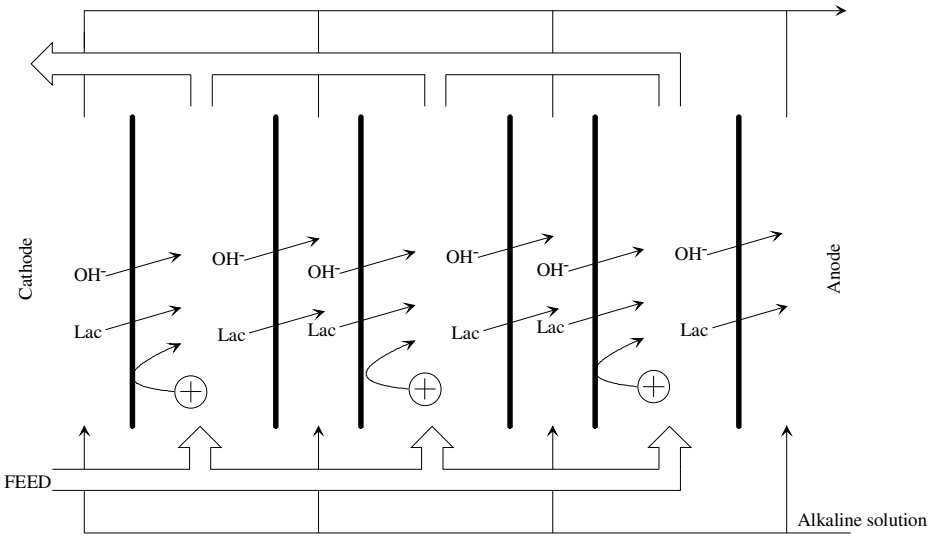

Figure 4.5 Competitive transport between lactate and hydroxide ions. ▌= anion-exchange membranes.

When trying to enhance the lactate flux from feed to alkaline solution, the electrical current must enhance the lactate flux in the feed chambers while *not* enhancing hydroxide flux. When the lactate ions enter the alkaline stream, they should remain there and not continue toward the anode through the second membrane and thus return to the feed. Thus, in the alkaline process stream, the electrical current should preferably be transported by the hydroxide ions.

To ascertain the possibilities for a selective flux enhancement of lactate rather than hydroxide ions in the feed stream and of hydroxide rather than lactate ions in the alkaline stream, the transport numbers for both ions are compared as function of the pH.

In the following, it is assumed for the sake of simplicity that only one organic acid anion (lactate) exists in the feed from a fermenter and that the only one other anion involved is hydroxide. To balance the anions, hydrogen ions and another inorganic cation (sodium) are added to the equation. It is assumed that pH is higher than 6, so that lactic acid can be considered totally dissociated (ionic) as described in paragraph 4.1.2.

The ions must constantly maintain electroneutrality:

Equation 4.1 $$\sum_j z_j C_j = 0$$

and the standard water dissociation constant K_W applies:

Equation 4.2 $$C_{H^+} \cdot C_{OH^-} = K_W = 10^{-14}$$

The transport numbers for all ions in a solution can be calculated as described in Equation 1.17. Ionic mobilities for all four ions are taken or calculated from data (Atkins 1992).

Assuming a lactate concentration of 0.2 M, the transport numbers of hydroxide and lactate ions are depicted in Figure 4.6 as function of pH. The transport numbers of the cations indicate how much electrical current they transport between membranes, but since they are not able to penetrate the anion-exchange membranes significantly, their contribution is of no real consequence.

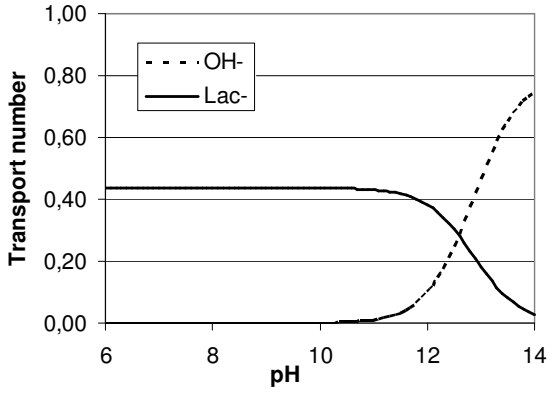

Figure 4.6 Transport numbers for hydroxide and lactate ions as function of pH in a solution with 0.2 M lactate.

It is obvious from this simple model that below pH 11, lactate is almost exclusively carrying electrical charges in relation to the hydroxide ions. Above pH 12.5, hydroxide ions carry an increasing amount of the current at the expense of lactate. This simple model predicts that adding electrical current to a Donnan dialysis setup as described above, should increase lactate flux from a feed stream at pH below 11, and increase hydroxide flux from an alkaline solution at pH above 13 while not returning too much lactate to the feed as sketched in Figure 4.7.

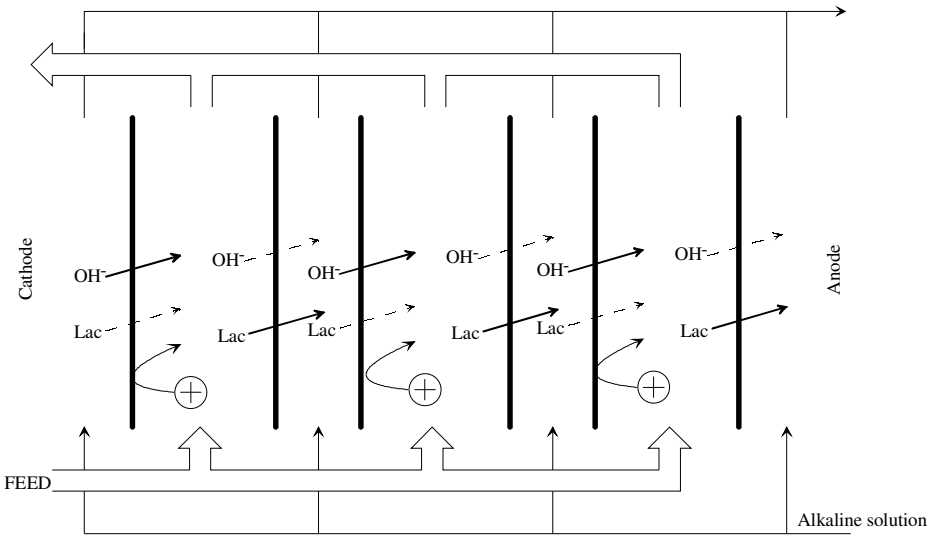

Figure 4.7 Theoretical result of electro-enhancement of the dialysis setup with anion-exchange membranes [1].

To compare the transport numbers of lactate and hydroxide ions at different lactate concentrations, the relation between the transport numbers are shown as a function of pH for different lactate concentrations in Figure 4.8. The relations are shown on a logarithmic scale.

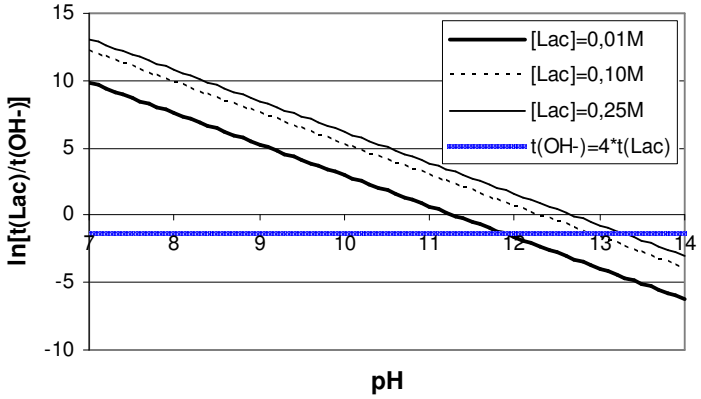

Figure 4.8 The relation between the transport numbers of lactate and hydroxide as function of pH at different lactate concentrations on a logarithmic scale. $t(OH^-)=4 \cdot t(Lac)$ responds to the relation where 80% of the transported anions are hydroxide.

From Figure 4.8, the critical pH where the transport number of lactate equals the transport number of hydroxide can be found where the lines cross 0. Assuming feed solutions are going to stay at pH-values below 10, the competition between lactate and hydroxide heavily favors lactate being extracted from the feed. For the alkaline solution, the situation where equal amounts of lactate and hydroxide are transported back to the feed is much too inefficient to consider a turning point. The figure also shows a line ($t(OH^-)=4 \cdot t(Lac)$) where 80% of the anions returned to the feed are hydroxide ions. From the intersection between this line and the transport number relation curves, it

can be observed that the more lactate is collected in the alkaline solution, the higher the pH-value needs to be. If the alkaline solution only needs to sustain a 0.01 M lactate concentration, pH 12 is sufficient, while higher lactate levels demands higher pH-values. Otherwise, a severe reduction in efficiency is the outcome. Higher pH demands more of the equipment and lowers the membrane lifetime, which is why the alkaline pH-level has to be considered.

By adding electrical current to the process the ion fluxes can be increased by several orders of magnitude compared to diffusion fluxes. But this also increases the speed of fouling material building up at the membrane surfaces. Especially bio-matter that is charged will respond to the electrical current and cling to the membranes. As can be observed from Figure 4.7, hydroxide ions enter one side of the feed chambers, constantly destabilizing fouling build-up. On the other side of the feed chamber, the fouling builds up. Exploiting the symmetrical setup of the dialysis unit it is possible to reverse the electrical current without need to change manifolds and chamber designation. By changing the direction of the electrical current, the flux of hydroxide ions into the feed chambers changes side as well. This results in destabilization and removal of the fouling layer that has been building up while a new fouling layer starts building up on the opposite side of the feed chamber as demonstrated in Figure 4.9.

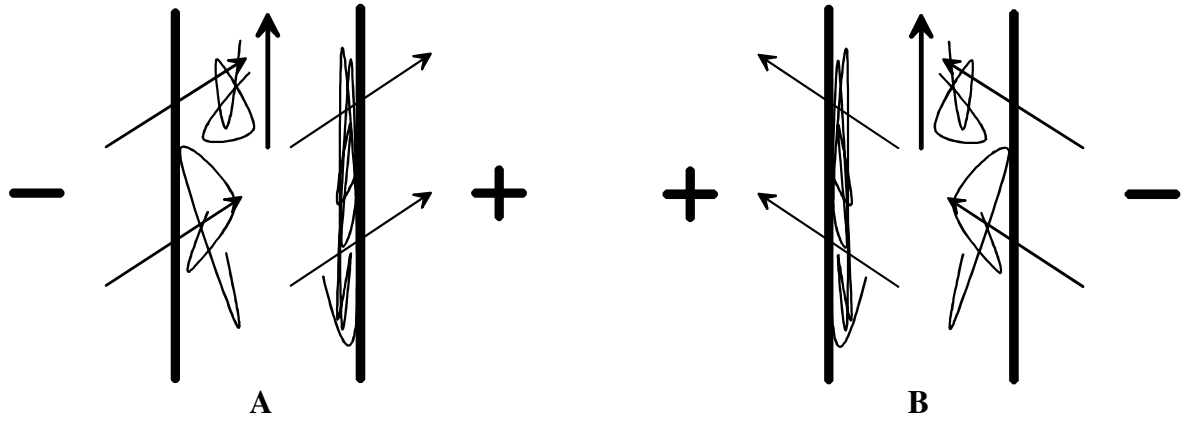

Figure 4.9 Build-up of fouling bio-matter on one side of feed compartments, while the opposite side is "cleaned". When the electrical current is reversed, the cleaning process is shifted to the other side of the feed compartments.

As shown in the following paragraphs, preliminary results with this setup gave results that supported the theoretical speculations above. The process setup as shown in Figure 4.7 with reversing direction of the electrical current at frequent intervals was named *Reverse Electro-Enhanced Dialysis* (REED).

4.2.2 Reverse electro-enhanced dialysis initial experiments

Numerous experiments with reverse electro-enhanced dialysis were carried out to evaluate the performance of this novel extraction process. Preliminary experiments were performed to investigate different parameters of the equipment and process. Experiments with both model solutions and fermented brown juice as the feed solution have been performed.

4.2.2.1 Materials and methods

Membranes

Tokuyama Corporation, Tokyo, Japan, kindly supplied the three different kinds of ion-exchange membranes used in the experiments; Neosepta® AMX anion-exchange membranes, Neosepta® ACS anion-exchange membranes, and Neosepta® CMH cation-exchange membranes. The AMX membranes are standard grade membranes, CMH and ACS are special grade membranes. CMH membranes have high chemical resistance and high mechanical strength and ACS are mono-anion permselective membranes.

Membranes with high chemical resistance were chosen because they are exposed to highly alkaline (pH > 12) solutions.

Experimental equipment

The equipment consisted of own design and was constructed at the workshop at Department of Chemical Engineering (DTU, Lyngby, Denmark) from transparent acrylic plates. The stack was assembled with four anion exchange membranes (AEM) and two cation exchange membranes (CEM), forming two feed compartments, three base compartments, and two electrode chambers as shown in Figure 4.10.

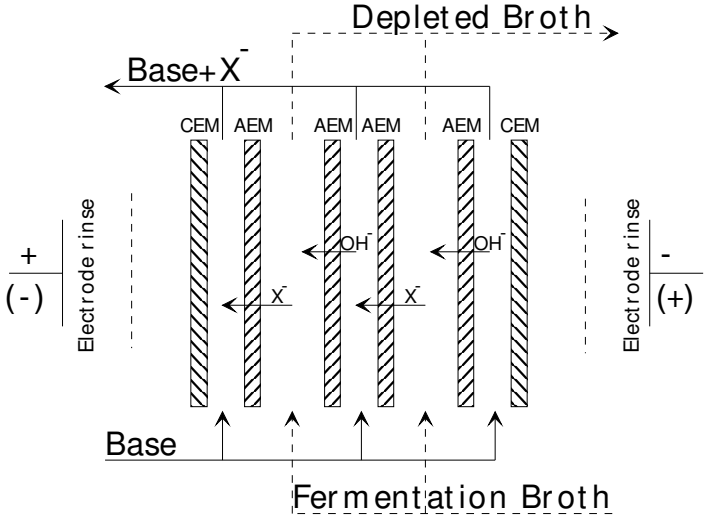

Figure 4.10 Membrane configuration of the reverse electro-enhanced dialysis stack in laboratory experiments. CEM = cation-exchange membrane. AEM = anion-exchange membrane.

Each membrane had an active area of 40 cm^2. The thickness of the feed compartments, where fermentation broth enters, was 12 mm. Net spacers were omitted to minimize the risk of plugging of the flow path. The thickness of the base compartments was 6 mm and net spacers were introduced to promote turbulent flow in these compartments. The two outermost chambers had one platinum electrode each (with an electrode area of 31.5 cm^2), separated from the rest of the compartments by a set of cation-exchange membranes. Solutions (feed and alkaline) were circulated from feed tank and base tank through the stack by means of two gear pumps (Micropump® F5734, Concord CA, USA). The mass flow through each gear pump was 9 g/s. The electrode solution was circulated separately using a centrifugal pump (Type no. 1250 21 9, EHEIM, Germany). A power supply (EA-PS 3032-10 (0-32V/0-10A), Elektro-Automatik, Germany), which delivered direct current at constant current density to the stack, was connected to a multimeter (Radio Shack LCD Digital

Multimeter, Tandy Corp., US) for accurate readings of the current density. A computer-controlled relay (10A) reversed the direction of the current at regular intervals. In the feed chambers, Ag/AgCl electrodes were placed so the voltage drop across a cell pair could be continuously measured and data collected by an IBM PC through a scopemeter (Fluke 123 – Industrial Scopemeter, Fluke Corporation, USA). A titration device (TTT 80 Titrator, Radiometer, Denmark) that added lactic acid/fermentation broth to the feed tank, was employed in some experiments and controlled by the pH of the feed tank. The entire experimental setup is shown in Figure 4.11.

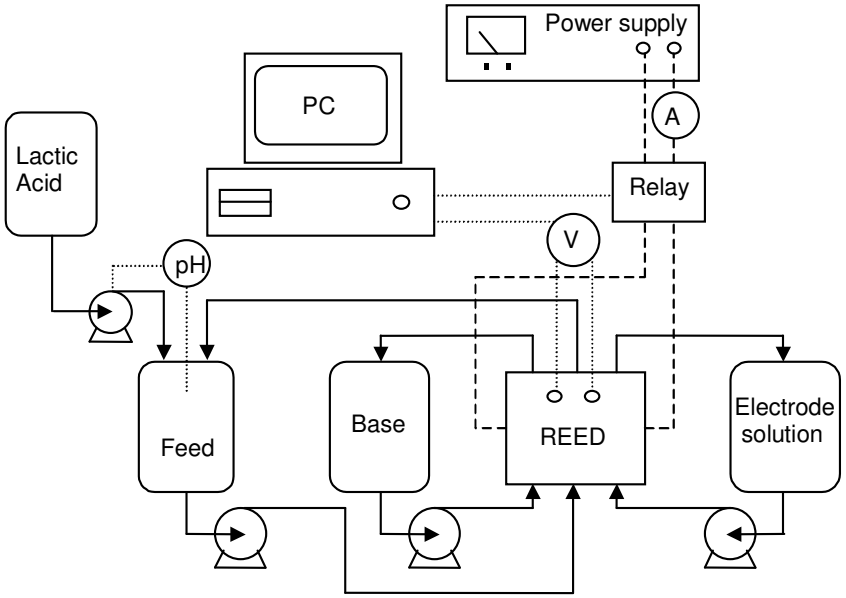

Figure 4.11 Setup for reverse electro-enhanced dialysis (REED) experiments.

All the tanks were equipped with heating/cooling jackets connected to a water bath.

4.2.2.2 Experimental routines

The equipment for setting up a direct extraction from a real fermentation was not available for the preliminary experiments. The fermentation process was simulated by using model solutions of pre-fermented broth as feed solution, and constantly adding more organic acid to the feed during experiments.

The conditions of each experiment varied, but the general routine was to enter a feed solution into the feed tank and an alkaline solution into the base tank. The feed solution was either a specially mixed model solution containing lactic acid or fermented brown juice. The feed solution was titrated with dry sodium hydroxide pellets to pH 5.5. In some experiments, calcium and magnesium hydroxide were added, for investigation of the calcium and magnesium retention. The alkaline solution consisted of either 0.1 M or 0.5 M sodium hydroxide or potassium hydroxide. An aqueous solution of 0.1 M Na_2SO_4 was passed through the electrode compartments. The temperature of the process streams was kept constant at 40°C during experiments.

Experiments began by filling the stack with the process fluids and starting the pumps. When the solutions were running through the stack, the experiment was started by turning on the electrical

current. The computer-controlled relay reversed the electrical current at set intervals, which lay between 10 to 60 seconds in preliminary experiments.

Samples were taken from the feed and base tanks at regular intervals. pH, conductivity, and lactic acid concentration were measured in the collected samples. The voltage drop across the middle cell pair was continuously logged by computer.

4.2.2.3 Analytical techniques

The lactate and sugar concentrations were measured by HPLC. 1 ml solution was taken from both the feed and the base tank and acidified using concentrated sulfuric acid (96%). Lactate analysis was performed at 35°C on HPLC equipped with an Aminex HPX-87H column (Biorad, USA) utilizing 4 mM H_2SO_4 as eluent at a flow rate of 0.6 ml/min. The lactic acid amounts were detected on a Waters 486 tunable absorbance detector at 210 nm. Sugars were detected on a Waters 410 Differential Refractometer. Waters Millennium Chromatography Manager software was used for quantification.

Approximately 5 ml solution was taken from both the feed tank and the base tank. pH and conductivity were measured using a pHM 201 portable pH-meter and a CDM92 Conductivity meter (both Radiometer, Denmark), respectively. After measurements, the solutions were transferred back to the system to maintain mass balance.

Calcium and magnesium were measured by Atom Absorbance Spectroscopy (AAS).

4.2.2.4 Initial experiments résumé

Initial experiments on reverse electro-enhanced dialysis were performed using model solutions of lactic acid. To investigate fouling behavior, the model solutions were later replaced by fermented brown juice.
In the following, a number of experimental parameters are investigated. The titration device was not operating in these experiments.

4.2.2.5 REED experiment 1: Initial testing

For feed, 250 ml 7% lactic acid solution, adjusted to pH 5.5, was prepared. 1800 ml 0.1 M NaOH were prepared for the alkaline solution. The stack was equipped with Neosepta ASC mono-selective anion-exchange membranes and Neosepta CMH cation-exchange membranes.

A constant current of 1A (250 A/m^2) was applied across the stack. The direction of the current was reversed every 60 seconds.

The changes in lactate concentration are shown in Figure 4.12.

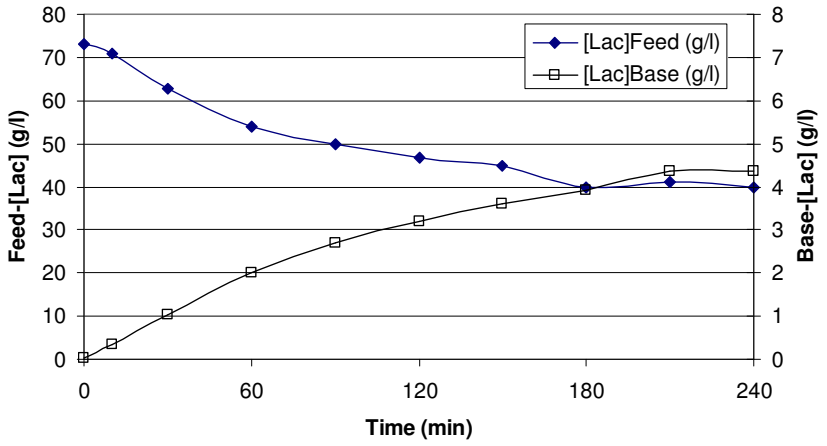

Figure 4.12 Lactate concentration changes in feed and alkaline solution. Feed concentration noted on left side, base concentration noted on right side.

The lactate concentration in the 250 ml feed decreased from around 70 g/l to 40 g/l, while the lactate concentration in the 1800 ml alkaline solution increased to 4-4.5 g/l. The lactate that was extracted from the feed was replaced by hydroxide ions.
It was observed how the pH in the feed solution rose, especially during the first hour, due to the replacement of lactate by hydroxide. The pH of the alkaline solution dropped accordingly, as shown in Figure 4.13

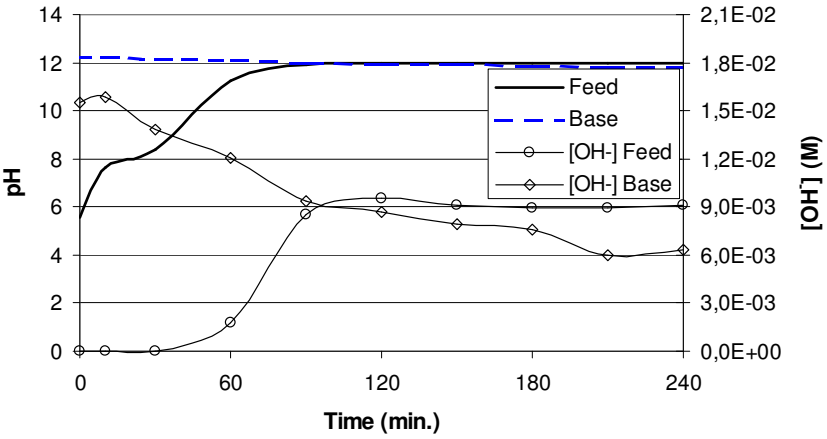

Figure 4.13 pH and corresponding hydroxide concentrations of feed and alkaline solutions during REED experiment.

The figure shows the pH-values as well as their corresponding hydroxide concentrations. When the pH-value of the feed reached the same level as in the base, the flux of hydroxide ions receded significantly. Still, the continued flux of lactate as well as some hydrogen ion leakage from the electrode rinsing solution lowers the pH in the base.

The impact of the pH in the feed stream on the lactate extraction is evident in Figure 4.14, where the lactate flux and the power consumed to extract 1 kg lactate during the experiment is compared to the feed pH.

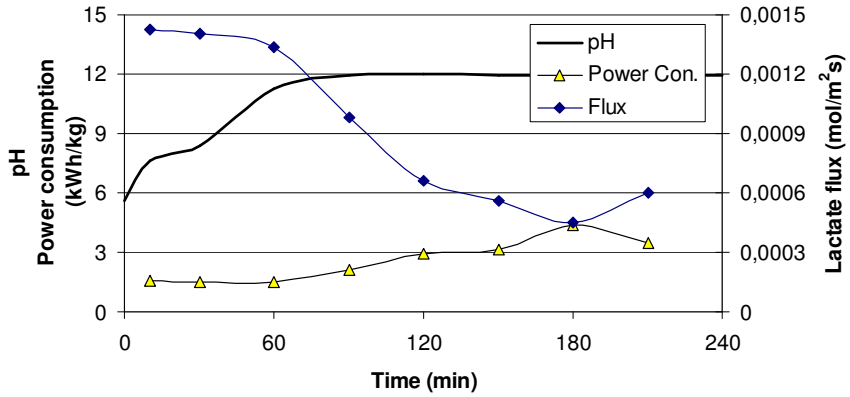

Figure 4.14 Lactate flux and power consumption during the experiment compared with the pH of the feed.

When the pH rises in the feed, the competition between electrical migration of lactate and hydroxide starts to favor the hydroxide ions. Thus, the efficiency of the process decreases significantly. This increases the energy consumption necessary to extract 1 kg of lactate, because a lesser part of the current is used for lactate transport. The lactate flux and the current efficiency are depicted in Figure 4.15 at different stages in the process as function of the feed solution's pH.

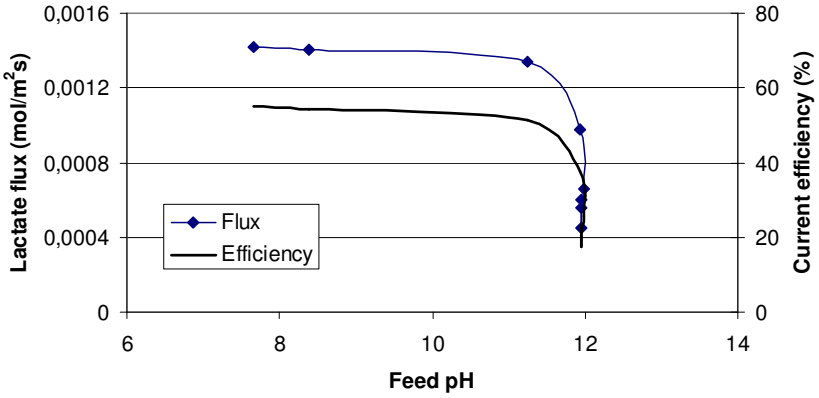

Figure 4.15 Lactate flux and current efficiency at different feed pH-values.

In this figure, the drop in extraction efficiency is very evident. The extraction must take place at pH-values lower than the drop-off value, which is around pH 11.5 in this case.

From this experiment, we concluded that the process was able to continuously extract lactate ions from the feed solution, while the current was reversed at regular intervals. The efficiency was acceptable, when the feed pH was below 11.5. In accordance with theory, the competitive transport

of hydroxide ions is less pronounced at lower pH-values, resulting in better current efficiency and lower power consumption.

4.2.2.6 REED experiment 2: Comparison between reverse electro-enhanced dialysis and Donnan dialysis

To investigate the effect of the enhanced fluxes by adding electrical current to a Donnan dialysis setup, the two processes were compared.

Using the exact same setup and solution compositions as in the previous experiment, the experiment was repeated but without electrical current. As before, lactate ions were extracted, and the feed alkalized, but at significantly slower rate. Feed pH rose at a lower rate and has less influence on the dialysis flux.

The fluxes in this Donnan dialysis experiment are compared to the fluxes of the reverse electro-enhanced dialysis experiment (REED experiment 1) in Figure 4.16.

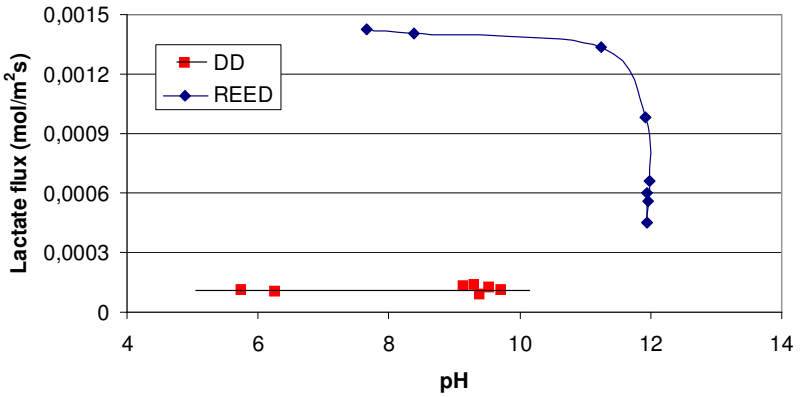

Figure 4.16 Flux comparisons between conventional Donnan dialysis (DD) and reverse electro-enhanced dialysis (REED).

This experiment demonstrates that by electro-enhancing the dialysis setup, the extraction flux increases by a factor of 10 when staying well below critical pH-values.

4.2.2.7 REED experiment 3: The effect of current reversal

To investigate the expected loss of efficiency that is an effect of reversing the current, an experiment was performed that was similar to REED experiment 1 described previously in this section. The only difference was that the electrical current was not reversed in this particular experiment.

The current efficiencies in the two similar experiments are compared in Figure 4.17.

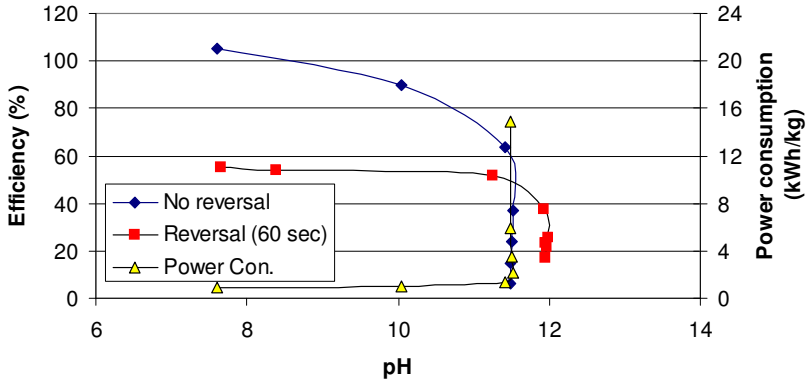

Figure 4.17 Current efficiency with and without current reversal. Power consumption without current reversal. Discrepancies in the pH break-off value are caused by slight changes in feed and base volumes.

The current was much better utilized without current reversal, because of a buffer effect in the ion-exchange membranes. This buffer-effect is addressed more extensively later in this chapter in the modeling section. When the process is reversed at regular intervals, a new steady-state has to be established, resulting in the process running less time at fully developed membrane profiles. The resulting power consumption was lower in this experiment.
The current efficiency in Figure 4.17 for the experiment without current reversal started out with a value above 100%. This is because it has been calculated from the combined fluxes of lactate migration and diffusion, which together exceeds the optimal migration flux.

This experiment demonstrates that a weakness of reversing the electrical current during a reverse electro-enhanced dialysis process is a decrease in current efficiency. Since the current reversal is only adding to the operation as an anti-fouling measure, and a non-fouling model solution is utilized in the initial experiments, the reversal effect is still worth further investigation.

4.2.2.8 REED experiment 4: Calcium retention

Important for the further purification of the extracted lactate, is the reverse electro-enhanced dialysis module possibility for a coupling with a *bipolar electrodialysis* (EDBM) unit, where the lactate can be concentrated and acidified and the alkaline solution regenerated. But divalent cations like calcium and magnesium have a serious scaling effect on the bipolar membranes, and it is important that the anion-exchange membranes retain enough of these ions, so the alkaline solution with the extracted lactate contain less than 2 ppm calcium and magnesium.

The initial experiment (REED experiment 1) was repeated with a feed solution of 7% lactic acid adjusted to pH 5.5 after 100 ppm calcium hydroxide was added. Samples were taken from the feed and base during the 4 hour experiment, and measured by Atom Absorbance Spectroscopy (AAS).

No traces of calcium were found in the base or the electrode rinsing solution in any of the samples. This shows that the ACS membrane is sufficiently selective to fulfill the requirement of retaining calcium. And it can be assumed that the ACS membranes have a similar effect on magnesium.

4.2.2.9 REED experiment 5: Comparing anion-exchange membrane effects

The first experiment (REED experiment 1) was repeated with similar conditions, but this time with the standard Neosepta AMX anion-exchange membranes replacing the special grade ACS membranes. The feed concentration was 7.5% lactate.

The lactate flux and current efficiency values were very similar to the values found with the special grade anion-exchange membrane. The calcium retention was also comparable high. The only significant difference was observed in the power consumption as shown in Figure 4.18.

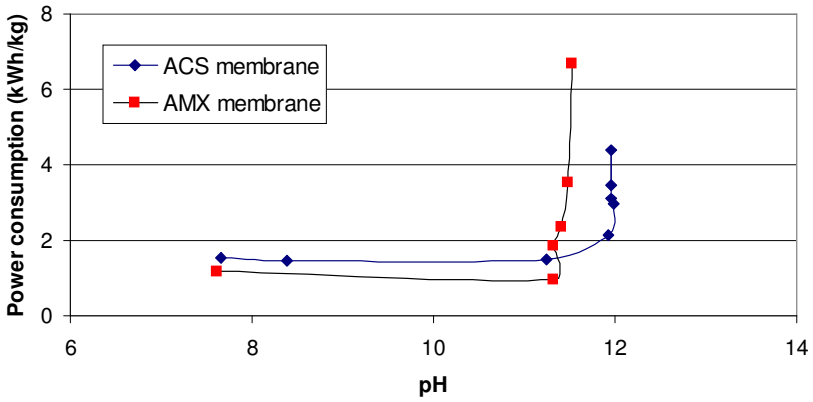

Figure 4.18 Difference in power consumption with regard to the chosen anion-exchange membrane.

The lower electrical resistance of the AMX membrane compared to the ACS membrane lowers the overall cell resistance and thus, the power consumption necessary to extract 1 kg lactate.
The difference in drop-off pH-value is due to the difference in starting lactate concentrations in the feed, not because of the membranes.

The AMX membrane allows multivalent anions to pass as well as monovalent anions. In a feed solution with a high content of divalent ions, the competitive transport from these ions would lower the current efficiency with the AMX membrane compared with the ACS membrane. The mono-selective ACS membrane rejects these multivalent ions and the only competition to lactate extraction arises from other monovalent anions.

4.2.2.10 REED experiment 6: The anti-fouling mechanism

REED experiments 1 and 3 were repeated, but this time the feed solutions consisted of fermented brown juice from food pellet production. The brown juice was adjusted to contain 7 % lactic acid content and solid sodium hydroxide was added to reach pH 5.5 in the broth.

The first part of this experiment included a run including reversal of the electrical current, and the second part repeated the first run, but the electrical current was not reversed during the second run.

The different lactate fluxes at the changing pH-values of the feed are compared in Figure 4.19 for the two runs of this experiment. The lactate flux in these experiments with brown juice were lower than when using model solutions, but even with current reversal, the lactate flux from brown juice

was still 5 times larger than in the Donnan dialysis experiment (REED experiment 2) using model solutions.

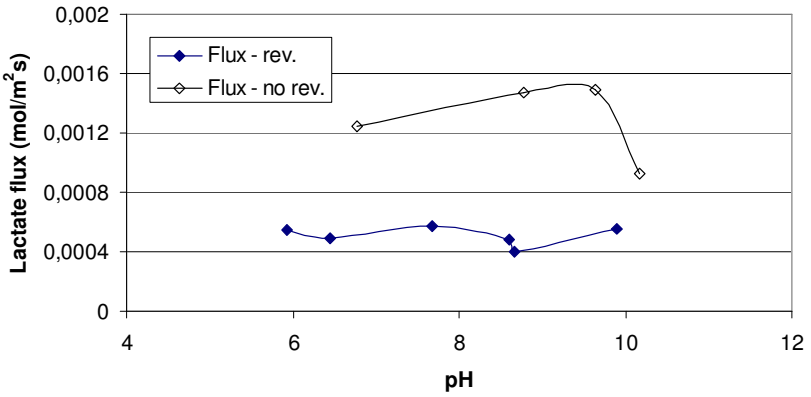

Figure 4.19 Lactate flux compared with and without current reversal.

As demonstrated earlier with model solutions, the lower current efficiency experienced when utilizing current reversal is reflected in the lactate fluxes shown in Figure 4.19. The voltage drop across a cell pair, E_{Cell} is compared in Figure 4.20 for experiments with and without current reversal.

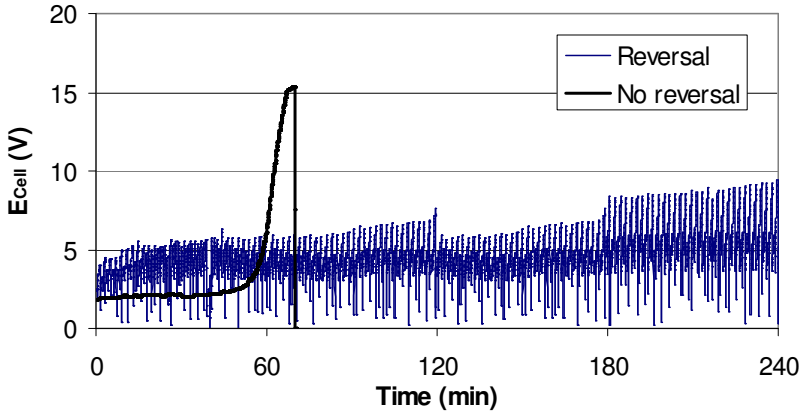

Figure 4.20 Numerical values of the voltage drop across a cell pair during REED experiments on fermented brown juice with and without reversal of the current. The "noise" on the potential curve for the reversal run is caused by the frequent reversal of current. The voltage drop changes between positive and negative values every time the current is reversed, but in this case, for reason of comparison, only the numerical value is shown.

The cell voltage drop reflects the electrical resistance to ionic migration through a cell pair since the electrical current density is kept stable at 250 A/m^2.The average cell voltage drop is observed to be lower when current reversal is *not* employed during the first 50 minutes of this experiment. After 50 minutes, the cell voltage drop increases dramatically, which shortly after leads the termination of the experiment due to extreme resistance. Whether this result was due to build-up of fouling on the membrane surfaces or caused by plugging of a flow tube in the equipment from bio-matter could

not be determined. The relatively sudden increase in cell voltage drop suggests that tube plugging is the main cause in this experiment.

Why the average cell voltage drop (and thus, the average electrical resistance) was lower when current reversal was *not* employed is not clear since the electrical conductivities of the solutions in the compared experiments were comparable. The increased resistance must be affected by the ion-exchange membranes that already demonstrate an efficiency-reducing buffer effect in connection with current reversal.

The result of this experiment suggests that current reversal should only be employed when the build-up of fouling has a sufficient impact on resistance increase, which was not observed by the fermented brown juice in these experiments. Apparently, the shear stress from the feed flow on the membrane surfaces was ample means to keep the fouling build-up from amounting to a serious impediment of the extraction process. An increased period between the current reversals may well reduce the negative impact on resistance and efficiency, which each reversal seems to cause.

When current was reversed at regular interval (60 seconds), the experiment was seen to continuously extract lactate for a four hour period. The average cell resistance increased during this period as shown numerically on Figure 4.20.

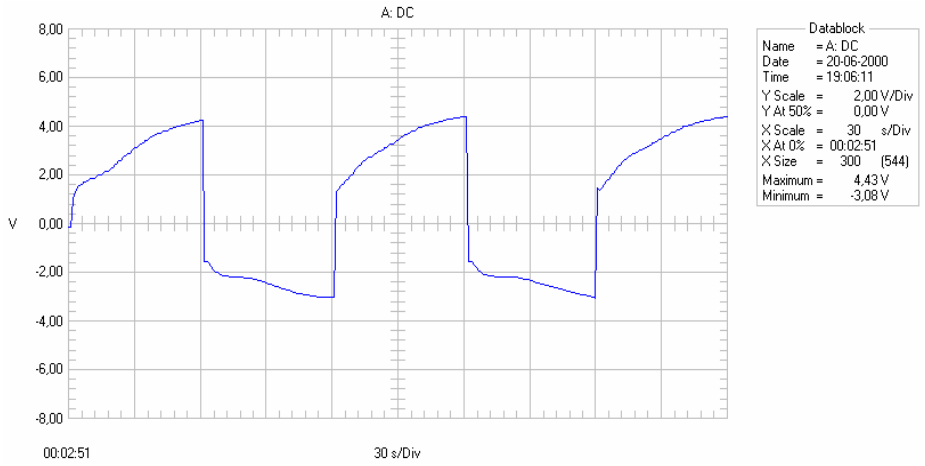

Figure 4.21 Extract of the voltage drop across the cell pair with current reversal every 60 seconds.

Figure 4.21 shows in detail how every reversal was followed by a steady increase in resistance because of fouling build-up. However, every reversal of current was followed by a regain of the cell resistance to the original level. This shows that most of the fouling buildup was reversibly removed by reversing current direction.

4.2.2.11 Conclusion on initial experiments

From initial experiments, it was concluded that the reverse electro-enhanced dialysis (REED) process acted according to theory and was worth investigating further. The self-cleaning mechanisms of reversing the electrical current were not superior to experiments where current was not reversed, when the feed contained biological material, which was surprising. Most references conclude that ion-exchange membranes are not suitable for separation and extraction directly from

fermentation broth because of significant fouling, but in the initial experiments, the impact of fouling has been less severe than expected. The wide spacers and manifolds compared with the low number of spacers in the lab equipment must contribute to a better flow distribution and higher shear at the membrane surfaces, which reduces the fouling impact.
In these experiments a small batch of pre-fermented feed was used, which means that the potential fouling content is fixed and non-living. In direct coupling with a fermentation process, the fouling content is both living and growing in amount, and in this case, the current reversal should demonstrate a more significant advantage in comparison to not reversing the current.

The initial experiments demonstrated that the feed pH should be kept below the observed drop-off values. The pH-value of the drop-off in efficiency and flux is slightly different from experiment to experiment, but it is mostly depending on the initial lactate content. The size and construction of the equipment made it close to impossible to empty the entire equipment of residual water pockets left from cleaning procedures between experiments. Thus, the original feed pH and lactate level differs a little from experiment to experiment depending on the amount of residual water in the equipment.

The conclusion of the initial REED testing showed that it was possible to combine the self-cleaning mechanism with increased lactate flux. Whether the REED process is economical superior to a dialysis process or when leaving out current reversal for higher efficiency and shorter operation times could not be determined from the few initial experiments.

4.2.3 Experiments simulating continuous extraction of lactate from fermentation broth

To start simulating the conditions when lactate is extracting in conjunction with a continuous fermentation, the titration device was added to the setup as shown on Figure 4.11 to simulate the continuous addition of fresh broth to the stack. A pH-sensor was introduced in the feed tank, and the titration device was programmed to maintain the pH of the feed at 5.5 by adding additional fermentation broth to the feed. Since the initial feed solution was not removed in these experiments, added broth was concentrated in respect to lactic acid (80 g/l) and had a pH of 2.1. Thus, it was only necessary to add a small volume to the feed to preserve to pH while also adding small amounts of bio-matter. The membrane setup was not changed and the methods and equipments utilized are also identical to what was used in previous experiments.

When lactate is continuously removed from a fermenter, a low lactate concentration with some unconverted sugar is more realistic than the 7% lactate concentrations utilized in initial experiments. The feed solutions in the following experiments all contained 2% lactic acid adjusted to pH 5.5 by potassium hydroxide. Since the pH of the feed solution is preserved, the alkaline concentration in the base was increased from 0.1 M to 0.5 M. This gives the alkaline solution a much higher capacity for extracted lactate. Sodium hydroxide was replaced by potassium hydroxide, since agricultural waste is more probable to contain free potassium ions and these ions are almost identical in behavior under the present circumstances.

4.2.3.1 REED experiment 7: Retention of calcium

Since retention of “hard” ions like calcium is crucial to subsequent purification steps, the calcium retention was investigated again following the changes in procedure for the experiments.

Two experimental runs tested the retention of calcium: one using the special grade ACS membrane and one using the standard AMX membrane.

The feed solution was 500 ml 2% potassium lactate at pH 5.5 in both cases, and the alkaline solution 500 ml 0.5 M KOH. About 200 ppm calcium hydroxide was added to the feed.
The current was reversed every 30 seconds in these experiments.

The extraction experiments lasted for four hours each. Pure lactic acid was added to the feed tanks through titration, keeping the feed pH at 5.5. The results of one of the experiments (utilizing AMX membranes) are depicted in Figure 4.22.

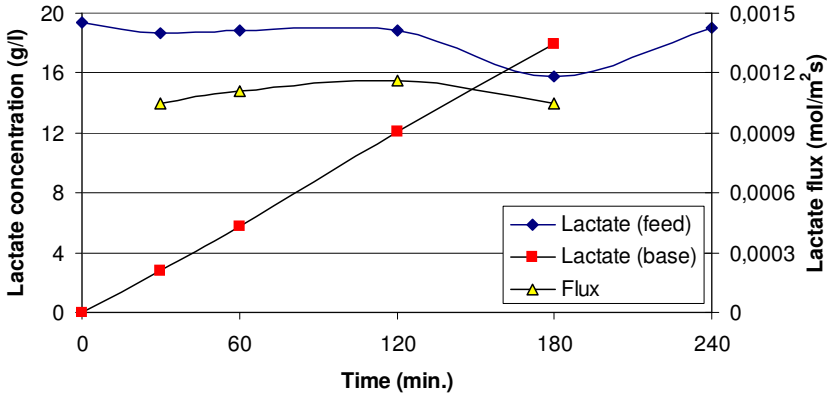

Figure 4.22 Lactate concentrations in feed and base and the lactate flux during the experimental run utilizing AMX membranes.

This figure demonstrates how the lactate concentration is maintained in the feed tank through the constant titration, which maintains a stable lactate flux and thus, the lactate is easily extracted to the alkaline solution. Much higher lactate content can be sustained in the alkaline solution without significant transport of lactate back to the feed due to the increased base concentration of 0.5 M. The results of the two experimental runs were almost identical.

The calcium retentions of both membranes are both sufficiently high to accommodate the restrictions set for bipolar membranes, as can be seen from results in Table 4.1.

	Neosepta AMX			Neosepta ACS		
Time (min)	$[Ca^{2+}]_{Feed}$	$[Ca^{2+}]_{Base}$	$[Ca^{2+}]_{Elec}$	$[Ca^{2+}]_{Feed}$	$[Ca^{2+}]_{Base}$	$[Ca^{2+}]_{Elec}$
0	179	0.08	0.52	170	0.07	
30	182	0.22		172	0.12	
60	186	0.27		173	0.18	0.35
120	183	0.46	0.49	176	0.41	
180	180	0.67		185	0.47	
240	181		0.59	197	0.64	0.20

Table 4.1 Calcium concentrations in ppm in feed and base tank and electrode rinse during two experiments with different anion-exchange membranes.

No significant difference in calcium retention could be observed for the two membrane types. The build-up of calcium in the base is insignificant and will not be of consequence in a continuous process.

4.2.3.2 REED experiment 8: Retention of unconverted sugars, calcium, and magnesium in brown juice

To make sure, calcium and magnesium would not enter a complex compound in a feed containing bio-matter that was able to penetrate the anion-exchange membranes, the previous experiment was repeated with brown juice as feed solution. The brown juice contained 700 ppm calcium and 400 ppm magnesium. This experiment was also an investigation of the diffusion flux of unconverted sugars from the feed to the base. Since most of the feed solution from a fermentation broth is recycled back to the fermenter, it is important to retain the unconverted sugars, too, so the conversion efficiency of the fermenter is preserved. The stack was equipped with ACS membranes.

During a 2 hour period, only very small amount of divalent cations was detected in the base and electrode rinse as indicated in Table 4.2.

Time (min)	$[Ca^{2+}]_{Feed}$	$[Ca^{2+}]_{Base}$	$[Ca^{2+}]_{Elec}$	$[Mg^{2+}]_{Feed}$	$[Mg^{2+}]_{Base}$	$[Mg^{2+}]_{Elec}$
0	667	0.15	x	394	0.01	x
60	737	0.09	x	425	0.01	x
120	705	0.13	0.19	403	0.02	0.05

Table 4.2 Calcium and magnesium concentrations in ppm in feed, base, and electrode rinse during REED experiment 8. (x) marks samples where no traces could be detected.

The leakage of divalent cations is even smaller than in the previous experiments even though the added concentrations are much higher. Unlike, in the model solutions where calcium and magnesium were free ions, the majority of the cations were probably bonded to the biological material in the brown juice and thus more easily retained by the membranes.

The unconverted sugars in the brown juice were all sufficiently retained. Only insignificant amounts of sugars were detected in the base. Some diffusion of sugars is to be expected, but commercial anion-exchange membranes with excellent retention of sugars are easy to come by.

4.2.3.3 REED experiment 9: Shorter frequency of reversal during long time operation

The last experiment with the reverse electro-enhanced dialysis setup that is disclosed in this chapter is a fouling experiment that lasted for 7 hours. The electrical current was reversed every 10 seconds in this experiment, to investigate whether the shorter intervals would result in lower overall cell resistance, and consequently lower power consumption.

The feed consisted of 250 ml brown juice with 2% lactic acid. Brown juice with high lactic acid content was titrated to maintain the pH-value of the feed. The alkaline solution was 250 ml 0.5 M KOH.

After four hours, the alkaline solution was replaced with a fresh solution to continue operations without saturating the base with lactate.

The nature of the voltage drop across the central cell pair changed during the experiment as shown on Figure 4.23.

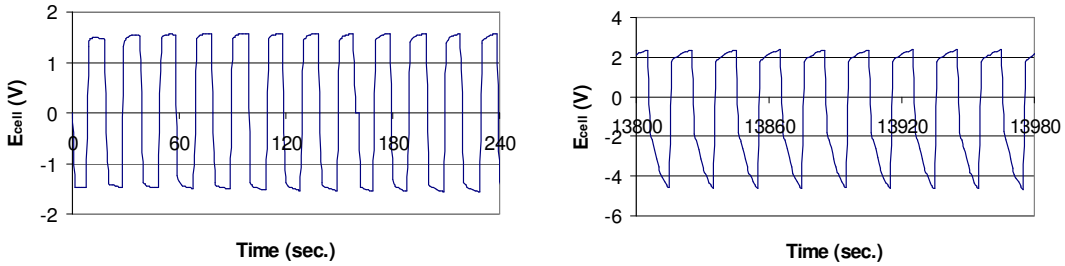

Figure 4.23 Comparison between the voltage drop across the cell pair in the beginning and in the middle of REED experiment 9.

Between each current reversal, the familiar build-up of resistance was obvious as demonstrated in the two graphs in Figure 4.23. The increase in cell resistance between reversals was much more pronounced later in the experiment than in the beginning. It also seems that one membrane surface was more receptive to the fouling than the opposite surface in the feed chamber, giving the graph an asymmetrical look. This could possibly be contributed to uneven flow distribution in the spacers.

The overall voltage drop of the cell increased from 1.5 V in the beginning of the experiment to 1.9 V near the end. Between reversals, the 1.9 V increased to 2.8 V or 8 V, respectively, depending on the current's direction.

The lactate concentration in the feed was kept relatively constant due to the constant titration as shown in Figure 4.24. The figure also shows the lactate concentration in the two batches of base.

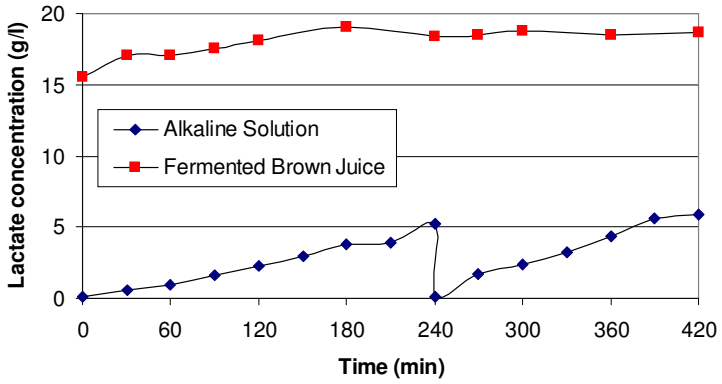

Figure 4.24 Lactate concentration in feed (fermented brown juice) and base (alkaline solution).

The flux of lactate was lower than expected from earlier experiments. Moreover, the current efficiency was found to be 3%, which is unacceptable. The low efficiency and fluxes were later

discovered to be the result of the short intervals between current reversal. As will be demonstrated in the subsequent modeling section later in this chapter, it is necessary for the membrane profiles inside the membranes to shift before acceptable current efficiencies can be reached, which takes some time. During this buffer time, only low efficiencies can be obtained as seen in this case.

The self-cleaning mechanism allowed the process to run for the full 7 hours of operation.

4.2.4 Conclusion on the reverse electro-enhanced dialysis process

The reverse electro-enhanced dialysis has shown promise with regards to minimizing the harmful effects of fouling. The basic electrical resistance of a cell pair is partially regained after each current reversal, which makes longer operation times possible between otherwise necessary cleaning interruptions. A slow build-up of fouling over time has been observed and the necessity of regular membrane cleaning can probably not completely eliminated.

The anion exchange membranes exhibit satisfactory retention of calcium and magnesium, which enables subsequent bipolar electrodialysis. Only very limited amounts of sugars are lost through the anion-exchange membranes to the base compartments making high substrate utilization possible.

The feed to the reverse electro-enhanced dialysis becomes alkaline from the replacement of lactate with hydroxide ions, which makes it ideal for pH-control of a fermenter.

A disadvantage is the low current efficiency, which must be improved through optimization of the time intervals between current reversals.

The process works as hypothesized, but the current efficiency needs to be significantly improved for the process to gain any commercial interest.

The advantages and disadvantages of the REED process as they are so far discovered are compiled below:

Advantages	Disadvantages
• Continuous extraction of organic anions from fermentation broth at high flux • Retention of Ca^{2+}, Mg^{2+} • Retention of unconverted sugars • Continuous membrane cleaning • pH-control of fermenter	• Low current efficiency • Co-extraction of inorganic anions • High alkaline resistant membranes needed

4.3 Modeling of reverse electro-enhanced dialysis

4.3.1 Introduction

Further analysis of the effect of current reversal on the ion-exchange membranes' concentration profiles in REED is important to evaluate the possibilities for optimization of the process' efficiency. In this chapter, a mathematical model attempts to describe the changing concentration profile of the mobile phase inside an anion-exchange membrane located in a reverse electro-enhanced dialysis stack.

The mobile ions inside the membrane are subject to periodical reversal of electrical current and react accordingly. With the model, it is possible to describe how the ions react to the changing driving forces, especially electrical migration and concentration diffusion. A computer simulation can give estimates that help to develop and optimize the reverse electro-enhanced dialysis process.

The mathematical model was solved by a numerical method using Fortran programming. The first version of the program only simulates separation of model aqueous solutions of lactate at various pH-values. The simulation takes polarization at the membrane surfaces into account, since polarization has significant influence on boundary conditions.

4.3.2 Model creation

To model the changing concentration profile across an ion-exchange membrane after each reversal of electrical current, consider an elemental part of the membrane with the dimensions $\Delta x \Delta y \Delta z$ as shown in Figure 4.25.

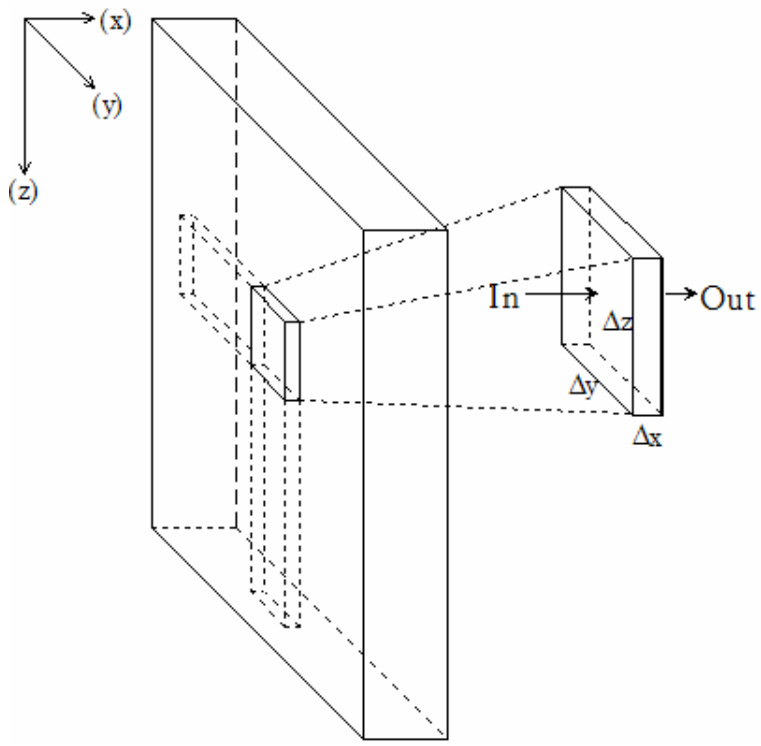

Figure 4.25 Membrane element as basis for modeling.

For this modeling of the changing membrane profiles, some assumptions are included.

- Only unidirectional ion-transport is considered. Ions are considered to move only along the direction of the x-axis. This assumption usually yields very satisfactory results for electrodialysis processes based on plate-and-frame modules.

- The ion-exchange membrane is assumed to be perfectly homogeneous with evenly dispersed ion-exchange groups. This assumption is probably wrong for most membranes. In polymer membranes, the ion-exchange groups are more hydrophilic than the rest of the polymeric network, and tend to collect in hydrophilic regions. Thus, the membranes tend to consist of regions with high ion-exchange capacity and thus higher degree of ion-transport and other regions with low ion-exchange capacity and corresponding lower ion-transport. However, assuming a homogeneous ion-exchange capacity, the unidirectional model results in a homogeneous ion flux through the membrane, which should reflect the average membrane flux.
- It is assumed that ions are only transported by electrical migration and diffusion. Usually, convective ion transport is driven by a pressure difference and is insignificant in electrodialysis processes with nonporous membranes (Mulder 1991). Electro-convective transport and osmotic and electro-osmotic effects are also neglected. Electro-convective transport is not significant at the relatively low current densities, at which the process is operated. Osmotic and electro-osmotic transport mainly influences the solvent transport, which is not investigated in this model.

First objective is constructing an amount (mol) balance for the membrane element:

Equation 4.3 $IN = OUT + ACCUMULATED$

The IN part of the equation, is considered the number of moles entering the element through the element-surface of dimension $\Delta y \Delta z$ at the distance x from the membrane surface in the transport direction during a small time period described as Δt. The OUT part is similar to the IN part, except the mole-flux through the surface at $x+\Delta x$ is considered.

$$IN = J_i(x,t) \cdot \Delta y \Delta z \Delta t$$

Equation 4.4

$$OUT = J_i(x+\Delta x,t) \cdot \Delta y \Delta z \Delta t$$

As expression for the flux J_i of component i, the Nernst-Planck equation (Equation 1.15) might be utilized. Since constant electrical current is applied, another approach is taken in this case.

The electrical migration is defined as the part, t_i^m, of the total current density, i_d (A/m^2), that is carried by component i. t_i^m is the transport number of component i as defined in Equation 1.17.
The flux composed of migration and diffusion can now be expressed by:

$$J_i(x,t) = -\frac{i_d}{z_i F} t_i^m(x,t) - D_i \frac{dC_i(x,t)}{dx},$$

Equation 4.5

$$where \quad t_i^m = \frac{|z_i| u_i^m C_i(x,t)}{\sum_k |z_k| u_k^m C_k(x,t)}$$

The ACCUMULATION part of Equation 4.3 is the molar change inside the elemental volume $\Delta x \Delta y \Delta z$ during the time from t to $t+\Delta t$.

Equation 4.3 can be expressed as follows:

Equation 4.6

$$\left(-\frac{i_d}{z_i F} t_i^m(x,t) - D_i \frac{dC_i(x,t)}{dx}\right) \cdot \Delta y \Delta z \Delta t =$$
$$\left(-\frac{i_d}{z_i F} t_i^m(x+\Delta x,t) - D_i \frac{dC_i(x+\Delta x,t)}{dx}\right) \cdot \Delta y \Delta z \Delta t +$$
$$\left(C_i(x,t+\Delta t) - C_i(x,t)\right) \cdot \Delta x \Delta y \Delta z$$

Dividing the equation with $\Delta x \Delta y \Delta z \Delta t$ and assuming that the increments Δx and Δt are able to approach 0, Equation 4.6 is written as a differential equation:

Equation 4.7

$$-\frac{i_d}{z_i F} \frac{\partial t_i^m(x,t)}{\partial x} - D_i \frac{\partial^2 C_i(x,t)}{\partial x^2} + \frac{\partial C_i(x,t)}{\partial t} = 0$$

Knowledge of the concentration of all ion species is needed to calculate the transport number, making it necessary to solve Equation 4.7 simultaneously for all involved ion species. To simplify this problem, another assumption has been added.

- Only two ion species are considered significant enough to be included in the anion-exchange membrane's mobile phase: the hydroxide ions and the target acid ions, which is lactate in this instance. This assumption includes the assumption that the co-ion concentration in the ion-exchange membrane is insignificant. According to the Donnan exclusion theory; when having external solute concentrations lower than a tenth of the membrane's ion-exchange capacity, the co-ion concentration consists of less than one percent of the membrane's total mobile ions.

Hence, the sum of the concentrations of hydroxide and lactate must correspond to the ion-exchange capacity of the membrane, C_R:

Equation 4.8

$$C_{Lac}(x,t) + C_{OH}(x,t) = C_R$$

The membrane's ion-exchange capacity C_R is constant throughout the membrane following the assumption of a homogenous membrane. By Equation 4.8 the transport number can be simplified to:

Equation 4.9

$$t^m_{Lac}(x,t) = \frac{u^m_{Lac} C_{Lac}(x,t)}{u^m_{Lac} C_{Lac}(x,t) + u^m_{OH}\left(C_R - C_{Lac}(x,t)\right)} = \frac{C_{Lac}(x,t)}{(1-\mu)C_{Lac}(x,t) + \mu C_R}; \qquad \mu = \frac{u^m_{OH}}{u^m_{Lac}}$$

Introducing μ as the dimensionless relation between the mobility of hydroxide and lactate ions, reduces Equation 4.9. Differentiating Equation 4.9 yields:

Equation 4.10

$$\frac{\partial t^m_{Lac}(x,t)}{\partial x} = \frac{\mu C_R}{\left((1-\mu)C_{Lac}(x,t) + \mu C_R\right)^2} \frac{\partial C_{Lac}(x,t)}{\partial x}$$

$C_{Lac}(x,t)$ is then substituted by U(x,t), defined as:

Equation 4.11

$$U(x,t) = (1-\mu)C_{Lac}(x,t) + \mu C_R$$

Inserting the evolved expression of Equation 4.10 into Equation 4.7 and using the substitution in Equation 4.11, the following expression for lactate is reached:

$$-D_{Lac} U(x,t)^2 \frac{d^2U(x,t)}{dx^2} + \alpha \frac{dU(x,t)}{dx} + U(x,t)^2 \frac{dU(x,t)}{dt} = 0$$

Equation 4.12

$$\textit{where} \qquad U(x,t) = (1-\mu)C_{Lac}(x,t) + \mu C_R$$

$$\alpha = \frac{i_d}{F}\mu C_R \qquad \mu = \frac{u^m_{OH}}{u^m_{Lac}}$$

The hydroxide membrane concentration is obtained from Equation 4.8 after solving Equation 4.12 for lactate.

4.3.3 Determination of boundary values

4.3.3.1 Physical conditions

To decide on border values for solving Equation 4.12, consider the following:

- For this modeling, the development of concentration profile is considered for regions of continuous separation of two aqueous streams (I and II) as suggested in Figure 4.26. It is assumed that the compositions of the two solutions do not change within these regions.
- The thickness of the membrane, L, limits the development of concentration profiles to an interval, where $x \in [0, L]$

Polarization at the membrane surface has great influence on the membrane concentrations, since the wall concentrations are in Donnan equilibrium with the membrane concentrations just inside the membrane.

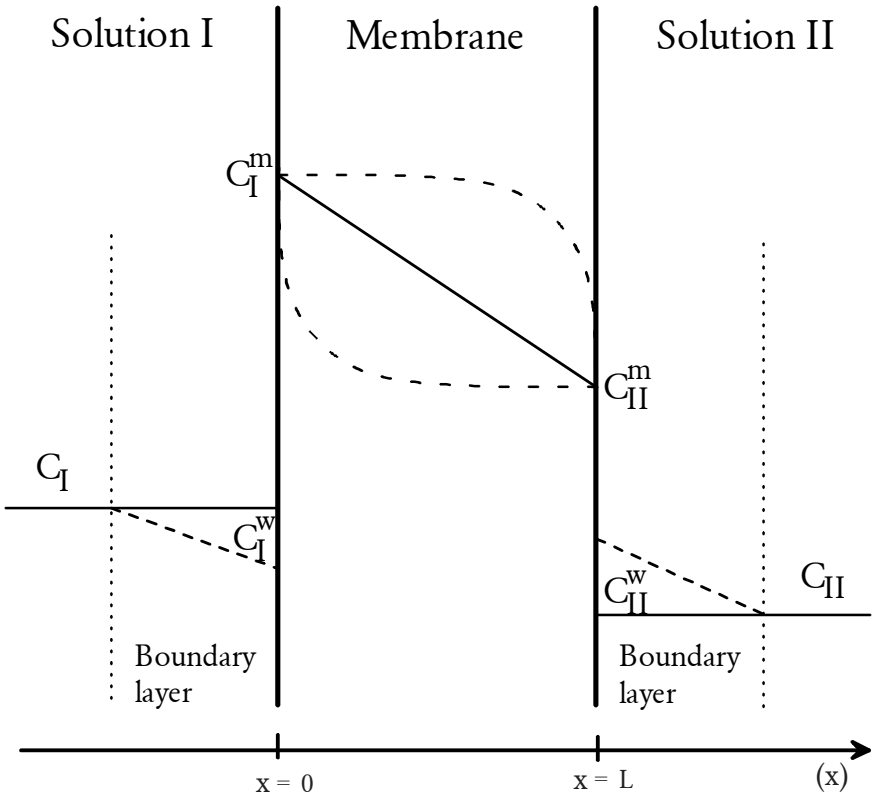

Figure 4.26 Assumed starting concentration profile of lactate (—), and assumed profile development (---).

Boundary conditions at x = 0:

- After polarization is stabilized outside the membrane at x = 0, the surface flux into the membrane is stable and the membrane concentration at x = 0 is constant from that time on. For simplicity, this assumption has been extended to assuming a constant membrane concentration at x = 0 at all times. The constant membrane concentration is calculated as the steady-state concentration in Donnan equilibrium with the membrane wall concentration just at the membrane surface.

Boundary conditions at x = L:

- Determination of the membrane concentration at x = L is more complex than at x = 0. As a new profile is established, the membrane concentration at x = L also changes. For this model, the membrane concentration is calculated by setting up two equations.
    1. The flux through the last membrane layer at x = L must equal the flux through the boundary layer just outside the membrane.
    2. The wall concentration and the membrane concentration at x = L are connected through the Donnan equilibrium condition.

  This means, that this boundary condition must be evaluated simultaneously with the profile.

Boundary conditions at t = 0:

- As a starting profile (t = 0), the correct choice would be to insert the final values of the concentration profile from a previous simulation, so the new profile can realistically evolve when current is reversed. However, this profile has to be available before it is accessible. Thus, a diffusion profile has been chosen for a model starting profile. The diffusion profile is assumed to be a linear profile between the membrane concentrations at the membrane surfaces as decided by Donnan equilibrium. This profile is shown in Figure 4.26.

4.3.3.2 Solving the Donnan equilibrium condition

The two boundary conditions for Equation 4.12 both depend on the Donnan equilibrium. Since only hydroxide and lactate ions are considered, the membrane concentrations can be easily determined. From Equation 1.3 the following equation must be satisfied:

Equation 4.13 $$\psi_{Don} = \frac{RT}{-1 \cdot F} \ln \frac{a^s_{Lac}}{a^m_{Lac}} = \frac{RT}{-1 \cdot F} \ln \frac{a^s_{OH}}{a^m_{OH}} \Rightarrow \frac{C^m_{Lac}}{C^w_{Lac}} = \frac{C^m_{OH}}{C^w_{OH}}$$

Electroneutrality inside the membrane must be satisfied as well:

Equation 4.14 $$C^m_{Lac} + C^m_{OH} = C_R$$

Combining these two equations, the membrane concentration can be calculated by this very simplified version of the Donnan equilibrium, if the lactate concentration and hydroxide concentration (or pH) of the external solution at the membrane surface (wall) is known:

Equation 4.15 $$C^m_{Lac} = \frac{C^w_{Lac}}{C^w_{Lac} + C^w_{OH}} \cdot C_R$$

4.3.3.3 Solving the polarization condition

Though polarization at the membrane surfaces follow similar conditions, the approach to calculating the membrane wall concentrations were slightly different from the side where electrical current enters the membrane to the side where the electrical current exits the membrane.
At the membrane surface (I), where the anions enter the membrane, the polarization is negative, meaning that this surface risks depletion of ions. If this happens, watersplitting can occur.
At the surface (II) where anions exit, the polarization is most commonly positive, thus, watersplitting is not likely to occur. On the other hand, an equilibrium polarization is not assumed to arise immediately on this surface, as it is the case at the other surface.

Polarization at the surface (I) where anions enter the membrane

To calculate the wall concentrations C^w of lactate and hydroxide, it is necessary to consider the hydrodynamic flow-condition of the external solutions. Using a boundary-layer model, a boundary layer thickness δ must be chosen or calculated from Sherwood relations. From the boundary layer

thickness, a boundary layer mass transfer coefficient k_i of each component i can be calculated from the relation:

Equation 4.16 $k_i = D_i / \delta$

The wall concentration of component i is determined by:

Equation 4.17 $C_i^w = C_i^s - \frac{i_d (t_i^m - t_i^s)}{z_i F k_i}$

t^s is the transport number of i in the solution. While t^m only includes the two mobile ions in the membrane, t^s includes all mobile ions in the solution.

With the assumption of no co-ions entering the membrane ($t_{co\text{-}ion}{}^m$ = 0), Equation 4.17 can be expressed for a mono-valenced co-ion (like Sodium):

Equation 4.18 $C_{Na}^w = C_{Na}^s + \frac{i_d \cdot t_{Na}^s}{F \cdot k_{Na}}$

Calling upon the law of electroneutrality, the wall concentrations must obey the following relation:

Equation 4.19 $C_{Na}^w + C_H^w = C_{Lac}^w + C_{OH}^w$

Normally the hydrogen concentration can be related to the hydroxide concentration by the water dissociation equilibrium:

Equation 4.20 $C_H \cdot C_{OH} = K_W \qquad K_W \approx 10^{-14}$

Provoked watersplitting deviates from ordinary water dissociation equilibrium and in the case of higher than critical current densities, Equation 4.20 cannot be utilized. This case is treated later in this section.

In the case of no watersplitting, the wall concentration can be determined by inserting the simplified Donnan relation in Equation 4.15 in the expression of the transport number (Equation 4.9), which yields a quadratic equation:

Equation 4.21

$$\left(C_{Lac}^{w}\right)^2+\left(\left(\frac{i_d}{F\cdot k_{Lac}}\right)\cdot\left(1-t_{Lac}^{s}\right)-C_{Lac}^{s}-\mu C_{OH}^{w}\right)\cdot C_{Lac}^{w}$$
$$+\mu\frac{i_d\cdot t_{Lac}^{s}}{F\cdot k_{Lac}}C_{OH}^{w}+\mu C_{Lac}^{s}C_{OH}^{w} \quad = \quad 0$$

To solve Equation 4.21, it is necessary to deduct the wall concentration of hydroxide. It can be derived from Equation 4.18, Equation 4.19, and Equation 4.20, ending in another quadratic equation:

Equation 4.22 $\left(C_{OH}^{w}\right)^2+\left(C_{Lac}^{w}-C_{Na}^{w}\right)\cdot C_{OH}^{w}-K_W=0$

For hydroxide values higher than 10^{-5} M (pH > 9), Equation 4.22 can be reduced to:

Equation 4.23 $\underline{C_{OH}^{w}>10^{-5}M:}\qquad C_{OH}^{w}=C_{Na}^{w}-C_{Lac}^{w}$

Combining Equation 4.21 and Equation 4.23 yields:

Equation 4.24

$$(1-\mu)\left(C_{Lac}^{w}\right)^2+\left(\mu C_{Na}^{w}-(1-\mu)C_{Lac}^{s}+\frac{i_d}{F\cdot k_{Lac}}\left(t_{Lac}^{s}(1-\mu)-1\right)\right)C_{Lac}^{w}$$
$$+\left(\frac{i_d}{F\cdot k_{Lac}}\cdot t_{Lac}^{s}-C_{Lac}^{s}\right)\cdot\mu C_{Na}^{w} \quad = \quad 0 \qquad (pH>9)$$

With lower hydroxide concentrations, an iteration method can be employed between Equation 4.21 and Equation 4.22.

From the wall concentrations of lactate and hydroxide, the corresponding concentrations just inside the membrane can then be calculated from the simplified Donnan expression.

In the case of occurrence of watersplitting, a different approach has to be taken. Since lactate ions are drawn into the membrane as fast as they are transported to the membrane surface, the surface concentration of lactate is close to zero, although lactate is still transferred. In that case, another method is employed to determine the membrane concentration. First, the limiting flux is determined as the sum of the limited migration flux and the diffusion flux across the boundary layer. The limited migration flux can be calculated as $i_{d,lim}/(z_iF)$ from Equation 4.17, setting the wall concentration of lactate to zero. The diffusion flux in this case is $k_{Lac}\cdot C_{Lac}^{s}$. The membrane concentration is then assumed to have the value that satisfies the steady-state migration flux inside the membrane, which must equal the aforementioned boundary layer flux.

Since watersplitting is best avoided, these equations are not very interesting for this model. They are included in the modeling program, though, since the program is to be further developed along

with the Reverse Electro-Enhanced Dialysis pilot module. More details of the watersplitting calculations can be found in appendix 7.2.1.

Polarization at the surface (II) where anions exit the membrane

As mentioned earlier, the approach is slightly different at the other surface. Since the membrane profile changes with time, the surface conditions change accordingly.

- The assumption is that the lactate and hydroxide fluxes through the last membrane "layer" must equal the corresponding fluxes through the diffusion layer.
- Another assumption is that the membrane concentration C^m is in constant equilibrium with the wall concentration C^w according to the simplified Donnan equilibrium (Equation 4.15).
- For simplicity, the hydrogen ions are omitted. It is assumed that all cations are sodium ions. Otherwise, the following fourth order equations will be of the fifth order. When pH is 4 or greater, as is always the case for the simulation of the reverse electro-enhanced dialysis module in this thesis, and the corresponding lactate concentration is close to 0.1 M, the resulting error should be less than 1%.

The assumptions are described graphically in Figure 4.27.

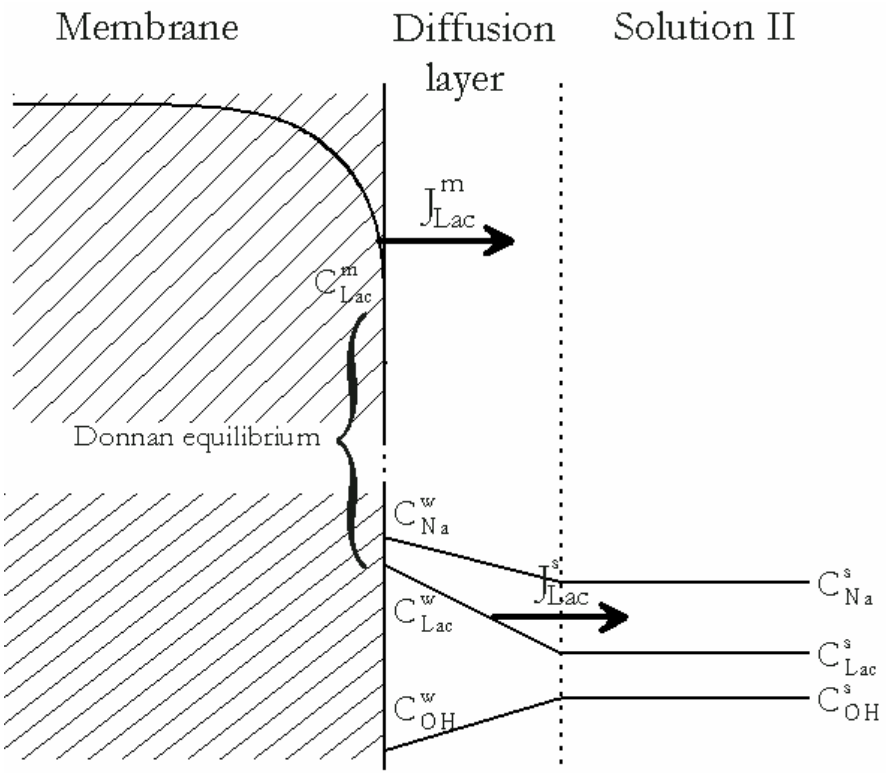

Figure 4.27 This is a graphic description of the expected concentration profiles through the diffusion layer during the process. The lactate fluxes (J^m and J^s) that are assumed uniform are shown. The corresponding fluxes for the hydroxide ions are also assumed uniform. Finally, the surface concentrations of lactate and hydroxide are assumed to maintain Donnan equilibrium with the ions just inside the membrane.

The equations that must be satisfied and solved for each timestep of the membrane profile are:

$$J^s_{Lac} = -k^s_{Lac}(C^s_{Lac} - C^w_{Lac}) + \frac{i_d}{z_{Lac}F}\cdot t^w_{Lac}$$

$$J^m_{Lac} = -k^m_{Lac}(C^{m-1}_{Lac} - C^m_{Lac}) + \frac{i_d}{z_{Lac}F}\cdot t^m_{Lac}$$

$$J^s_{OH} = -k^s_{OH}(C^s_{OH} - C^w_{OH}) + \frac{i_d}{z_{OH}F}\cdot t^w_{OH}$$

$$J^m_{OH} = -k^m_{OH}(C^{m-1}_{OH} - C^m_{OH}) + \frac{i_d}{z_{OH}F}\cdot t^m_{OH}$$

$$C^m_i = \frac{C^w_i}{C^w_{Lac} + C^w_{OH}}\cdot C_R$$

C^{m-1} is the membrane concentration one steplength (Δx) back inside the membrane, $C_{Lac}(L-\Delta x,t)$, and C^m is $C_{Lac}(L,t)$. The index of the mass transfer coefficients k_i and of the transport numbers t_i refers to the composition that is used in calculating the transport number at the wall (w) or inside the membrane at x=L (m).

By setting J^m equal to J^s for both the lactate and hydroxide ions, two fourth order equations are the result.

The wall concentration of lactate can be found by solving:

Equation 4.25 $$A_0\cdot(C^w_{Lac})^4 + A_1\cdot(C^w_{Lac})^3 + A_2\cdot(C^w_{Lac})^2 + A_3\cdot C^w_{Lac} + A_4 = 0$$

where

$$A_0 = k^s_{Lac}(\mu_{Lac} + \mu_{Na})$$

$$A_1 = k^s_{Lac}(((1+\mu)(\mu_{Lac} + \mu_{Na}) + \mu_{OH} + \mu_{Na})C^w_{OH} - (\mu_{Lac} + \mu_{Na})C^s_{Lac}) + k^m_{Lac}(\mu_{Lac} + \mu_{Na})(C_R - C^{m-1}_{Lac}) + \mu_{Na}\frac{i_d}{F}$$

$$A_2 = (k^s_{Lac}(\mu(\mu_{Lac} + \mu_{OH} + 2\mu_{Na})\cdot C^w_{OH} - (1+\mu)(\mu_{Lac} + \mu_{Na})C^s_{Lac}) + k^m_{Lac}((\mu(\mu_{Lac} + \mu_{Na}) + \mu_{OH} + \mu_{Na})C_R - (\mu_{OH} + \mu_{Na} + (1+\mu)(\mu_{Lac} + \mu_{Na}))C^{m-1}_{Lac} + 2(\mu_{OH} + \mu_{Na})\frac{i_d}{F})\cdot C^w_{OH}$$

$$A_3 = (\mu(\mu_{OH} + \mu_{Na})(k^s_{Lac}C^w_{OH} + k^m_{Lac}C_R) - (\mu(\mu_{Lac} + \mu_{Na}) + (1+\mu)(\mu_{OH} + \mu_{Na}))\cdot (k^s_{Lac}C^s_{Lac} + k^m_{Lac}C^{m-1}_{Lac}) + (\mu_{OH} + \mu_{Na} - \mu_{Lac})\frac{i_d}{F})\cdot\left(C^w_{OH}\right)^2$$

$$A_4 = -(k^s_{Lac}C^s_{Lac} + k^m_{Lac}C^{m-1}_{Lac})\mu(\mu_{OH} + \mu_{Na})\cdot\left(C^w_{OH}\right)^3$$

and the wall concentration of hydroxide can likewise be found by:

Equation 4.26 $A_0 \cdot (C_{OH}^w)^4 + A_1 \cdot (C_{OH}^w)^3 + A_2 \cdot (C_{OH}^w)^2 + A_3 \cdot C_{OH}^w + A_4 = 0$

where

$$A_0 = k_{OH}^s \mu(\mu_{OH} + \mu_{Na})$$

$$A_1 = k_{OH}^s((1+\mu)(\mu_{OH} + \mu_{Na}) + \mu(\mu_{Lac} + \mu_{Na}))C_{Lac}^w + \mu(\mu_{OH} + \mu_{Na})(k_{OH}^m C_{Lac}^{m-1} - k_H^s C_{OH}^s) + \mu\mu_{Na}\frac{i_d}{F}$$

$$A_2 = (k_{OH}^s((1+\mu)(\mu_{Lac} + \mu_{Na}) + \mu_{OH} + \mu_{Na})C_{Lac}^w - k_{OH}^m \mu(\mu_{OH} + \mu_{Na})C_R + ((1+\mu)(\mu_{OH} + \mu_{Na}) + \mu(\mu_{Lac} + \mu_{Na}))(k_{OH}^m C_{Lac}^{m-1} - k_{OH}^s C_{OH}^s) + 2\mu\mu_{Na}\frac{i_d}{F}) \cdot C_{Lac}^w$$

$$A_3 = (k_{OH}^s(\mu_{Lac} + \mu_{Na})C_{Lac}^w - k_{OH}^m(\mu(\mu_{Lac} + \mu_{Na}) + \mu_{OH} + \mu_{Na})C_R + ((1+\mu)(\mu_{Lac} + \mu_{Na}) + \mu_{OH} + \mu_{Na})(k_{OH}^m C_{Lac}^{m-1} - k_{OH}^s C_{OH}^s) + \mu\mu_{Na}\frac{i_d}{F}) \cdot (C_{Lac}^w)^2$$

$$A_4 = (\mu_{Lac} + \mu_{Na})(k_{OH}^m(C_L^{m-1} - C_R) - k_{OH}^s C_{OH}^s) \cdot (C_{Lac}^w)^3$$

recalling that μ_i is the ionic mobility of component i in solution, while μ is the dimensionless relation between the ionic motilities of hydroxide and lactate inside the membrane.

As can be noted from Equation 4.25 and Equation 4.26, the wall concentrations of lactate and hydroxide are linked together. In the numerical program a simple iteration method has been employed for solving these coupled equations. The wall concentration of hydroxide is calculated using the previous value of the wall concentration of lactate. The new value of hydroxide is used to calculate a new value for lactate, which again is used for a better calculation of the wall concentration of hydroxide. This continues until the difference between recalculated wall concentrations of lactate is sufficiently low.

When the wall concentration of lactate is established, the internal membrane concentration at the surface $C_{Lac}(L,t)$ is determined from the Donnan equilibrium (Equation 4.15).

4.3.4 Numerical solution

Because of the complexity of Equation 4.12, it was evaluated numerically. A program was written in FORTRAN using the Plato 2 compilation software from Salford Software Ltd., United Kingdom.

For modeling purpose, the membrane is divided into a number, *n*, of slices of equal thickness, Δx. Membrane concentrations are established at each interface between slices, and it is assumed that the thickness of the slices is sufficiently small that concentration profile can be considered linear within every slice. Furthermore, membrane profiles that are calculated from x = 0 to x = L, are spaced with regular time intervals, Δt. Figure 4.28 demonstrates the numerical interpretation of the model within the membrane.

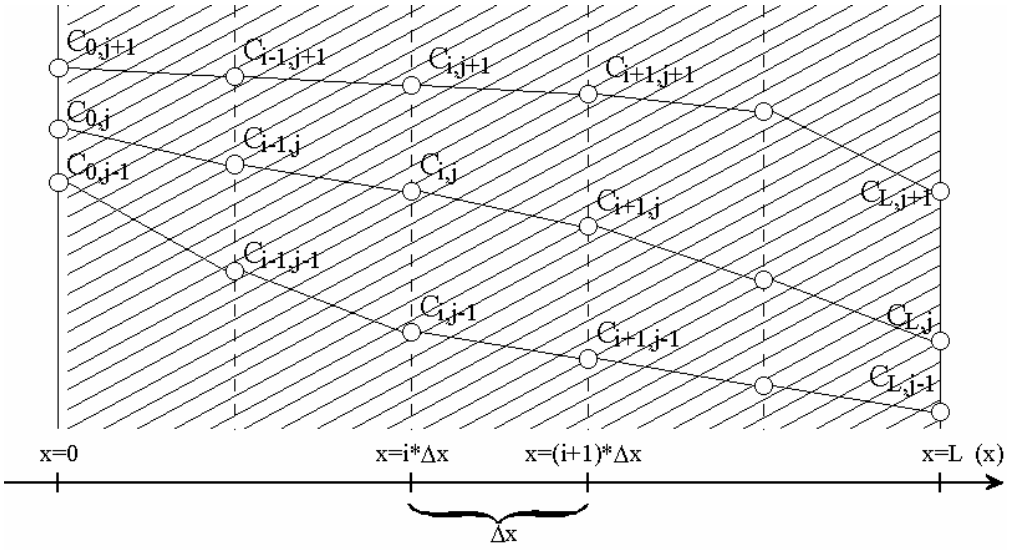

Figure 4.28 A graphical representation of how the numerical program perceives the membrane concentrations.

The substitution variable U(*x,t*), defined in Equation 4.11, is replaced by a grid point value $U_{i,j}$, where the index i stands for membrane thickness, and index j is for the time development. The membrane thickness, *L*, limits the interval of i to belong within [0, n]. The exact position in the membrane can be determined by i·Δx, where the length between each calculated point, Δx, is calculated as *L/n*. The time index, j, starts at 0, and continues to increase until a steady profile is reached, indicating that equilibrium has been obtained. The exact time since simulation start (current reversal) can be found by j·Δt.

The substitutions that are made for U as well as the first and second derivative of U:

Equation 4.27 $$U(x,t) = U_{i,j}$$

Equation 4.28 $$\frac{dU(x,t)}{dx} = \frac{U_{i,j} - U_{i-1,j}}{\Delta x}$$

Equation 4.29 $$\frac{dU(x,t)}{dt} = \frac{U_{i,j} - U_{i,j-1}}{\Delta t}$$

Equation 4.30 $$\frac{d^2U(x,t)}{dx^2} = \frac{U_{i+1,j} + U_{i-1,j} - 2U_{i,j}}{(\Delta x)^2}$$

From Equation 4.11 and the four equations above, it follows that:

Equation 4.31 $$C^m_{Lac}(x,t) = C_{i,j} = \frac{U_{i,j} - \mu C_R}{1-\mu}$$

Inserting these substitutions in Equation 4.12 yields a third order equation for $U_{i,j}$:

Equation 4.32
$$\begin{aligned}(2D^m_{Lac}\Delta t + \Delta x^2)\cdot U^3_{i,j} \;&-\; (D^m_{Lac}\Delta t(U_{i+1,j} + U_{i-1,j}) + \Delta x^2 U_{i,j-1})\cdot U^2_{i,j} \\ +\; \alpha\Delta x\Delta t\cdot U_{i,j} \;&-\; \alpha\Delta x\Delta t U_{i-1,j} \;=\; 0\end{aligned}$$

D^m is the membrane diffusion coefficient. Δt and Δx are the simulation step sizes of respectively time and length axis. α is previously defined in Equation 4.12.

By solving Equation 4.32 for $U_{i,j}$, the concentration profile can be obtained through the relation given in Equation 4.31. However, to calculate $U_{i,j}$, knowledge of $U_{i-1,j}$, $U_{i+1,j}$, and $U_{i,j-1}$ are necessary. By calculating a membrane profile across the membrane from 0 to *L*, for every time step, the simulation possesses the knowledge of $U_{i,j-1}$, since the index j-1 relates to the previous time step. A simultaneous solution for the entire profile seems necessary, but is problematic due the polynomial nature of Equation 4.32. For simplicity, we have chosen an iterative solution model. For every new step in time, the new profile is assigned initial values across the membrane. The initial profile is equal to the previous profiles final form.

The first point, $U_{0,j}$, of the profile is given from boundary conditions. The rest of the points from i = 1 to i = n-1 are calculated in turn. Simultaneously, the points are calculated backwards from i = n-1 to i = 1 to better smooth out the iteration errors. Then the last point, $U_{n,j}$, is calculated from the new values to fulfill the border condition at x = *L*. The process is then repeated until the profile changes between each iteration step are insignificant. When a new membrane profile has been thus established, the values are recorded in a computer-file. The new profile is compared with the previous profile to establish whether steady-state is reached. If not, the time index increases by one step, and a new profile is calculated.

The order in which the profiles are calculated is given as follows:

1. Input of data. The basic compositions of the solutions on both sides of the membrane (I and II) are written into the simulation manually by the user. The user determines the size of the time step, Δt, too. The program already holds standard information concerning the membrane's properties.
2. Initial values of all parameters are set or calculated.
3. Border values at the membrane's surfaces are calculated.
4. An initial diffusion profile between the two border values is established.
5. The time index is increased by one.
6. Initial guess for new profile.
7. Calculation of new profile based on previous values.
8. Establishment of final border-condition.
9. Check whether iteration error of new profile is insignificant. If iteration error is still significant, program returns to point 7. Otherwise, program proceeds to point 10.

10. Check whether the newly determined membrane concentration profile is significantly changed in comparison with the profile from the last time step. If not, steady-state is obtained and the program continues to point 11. Otherwise, the program returns to point 5 and starts to calculate the next profile.
11. The program shows the final output, which is the time from current reversal to steady-state. The user is offered the opportunity to save all data (concentration profiles at every time step, membrane surface concentrations, and membrane fluxes) into a data-file for later analysis.
12. The user is offered the opportunity to continue the simulation by reversing the electrical current. If the user declines, the simulation ends. If the user accepts, the final steady-state profile of the simulation is reversed. The composition of the two solutions is switched. The simulation is then repeated from point 2 except that the final steady-state solution replaces the diffusion profile in point 4.

The FORTRAN-program is recorded in appendix 7.2.2.

Another version of the simulation program was later developed. In this second version, the current is reversed at regular interval whether the membrane profile has reached a steady-state or not. The current efficiency and energy consumption is calculated. The current efficiency is calculated for each time step:

$$\eta_t = \frac{z_{Lac} F (J^{out}_{Lac,t} - J^{in}_{Lac,t})}{i_d}$$

where J^{out} and J^{in} represents the fluxes of lactate out of the feed solution and into the feed solution, respectively. The index t represents the time step number. Since the fluxes and the current density, id, have opposite directions, the lactate charge, z_{Lac} = -1, makes the current efficiency positive, when more lactate ions are leaving the feed than entering. The current efficiency calculated for each time step demonstrates the changes during the period until the next current reversal. The current efficiency is expected to increase until a stable membrane profile is reached, which will also stabilize the current efficiency.
The accumulated efficiency, which is the overall current efficiency calculated from the time of the last current reversal and up to the last calculated time step:

$$\eta_{overall,t} = \frac{z_{Lac} F \sum_{j=0}^{t} (J^{out}_{Lac,j} - J^{in}_{Lac,j}) \Delta t}{i_d \cdot t \cdot \Delta t}$$

The limiting value for the overall current efficiency must be the current efficiency at steady-state, which would be reached at infinite time intervals between current reversals. This indicates that the reversal of the electrical current during the process lowers the overall efficiency of the process. Thus, without a reversible buildup of fouling, the reverse electro-enhanced dialysis process is a bad solution.

The energy consumption is calculated from the electrical resistance originating from a cell pair and an emulated fouling buildup. The resulting area-specific electrical resistance [Ωm^2] is comprised of the following parts:

$$R_{Cell} = R_{SolutionI} + R_{SolutionII} + 2R_{Membrane} + R_{Polarization} + R_{Fouling}$$

The membrane resistance is taken from the manufactures information for a Neosepta AMX membrane that was the chosen membrane in most laboratory experiments (Tokoyama 1997). The polarization resistance is the resistance across the four diffusion layers at each surface of the two membranes in a cell pair. The resistances of the solutions I and II are the bulk solution resistances:

$$R_{Solution} = \frac{l}{F\sum_i |z_i| \mu_i C_i^s}$$

l is the thickness of the spacer across which the resistance is calculated. The polarization resistances are calculated by integration of the same formula across the diffusion layers.

The electrical resistance from the buildup of fouling is assumed to follow a curve that has been estimated from experimental results. The fouling curve is composed of linear and logarithmic elements.

The energy consumption, E, is calculated as the necessary energy [kWh] needed for transferring one kg of lactate ions:

$$E = \frac{i_d{}^2 R_{Total}}{(J_{Lac}^{out} - J_{Lac}^{in}) MW_{Lac}}$$

Like the current efficiency, both the actual energy consumption at each time step and the overall energy consumption are calculated.

The energy consumption relates to the production cost of the process. The energy consumption is only calculated in respect to the electrical energy used in the extraction. The lower the current density of the process becomes, the lower the energy consumption. And this improves the current efficiency until the current density reaches zero where the process emulates a pure dialysis process. The flux of lactate ions is then carried by diffusion entirely, and no electrical current is necessary. This also means that much larger membrane area is necessary, and the investment cost for the process would be much higher. Since the current efficiency is not sufficiently for estimating optimal production conditions, another parameter must be considered to evaluate all the economical aspects.

A specific membrane area, A_{Mem}, based on a lactate extraction rate is chosen to represent the equipment investment cost. From the economical evaluation of a 10,000 tons lactic acid plant (later in this chapter), the reverse electro-enhanced dialysis unit is calculated to extract 1145 kg lactate per hour, which is about 300 g lactate per second. The membrane area needed for a Specific Extraction Rate (SER) of 300 g lactate per second is found by:

$$A_{Mem} = \frac{SER}{J_{Lac}^{Total} \cdot MW_{Lac}}$$

Thus, three related factors are returned as the result of the simulation:

- Current efficiency
- Energy consumption
- Specific membrane area

All factors correspond to a very small part of the module within which the given parameters not change significantly.

4.3.5 Results

This section entails some results to demonstrate the program. A response surface is produced by the second version of the program to demonstrate the possibilities to use computer simulations for process optimization.

4.3.5.1 Parameters

Some parameters are known or can be assessed from experimental results. These include membrane properties and hydrodynamic conditions.

The ionic mobilities, μ_i, of the components (lactate ions, hydroxide ions, and sodium ions) are taken from literature (Atkins 1992). The aqueous diffusion coefficients are calculated from these mobilities. The membrane diffusion coefficients of the components are estimated from a rule of thumb that states:

Equation 4.33 $$D_i^m = \left(\frac{SW}{2 - SW} \right)^2 \cdot D_i^s$$

SW is the membrane swelling degree. D^m and D^s are the diffusion coefficients inside the membrane and in solution, respectively.

Membrane properties have been chosen to resemble a Neosepta AMX membrane (Krol 1997;Tokoyama 1997), since this type was used in some experiments.

- Membrane thickness, L = 200 μm
- Swelling, SW = 0.30
- Membrane's ion-exchange capacity, C_R = 2000 mol/m^3
- Membrane's area-specific resistance, $R_{AMX} = 3.0 \cdot 10^{-4}$ Ωm^2

From the hydrodynamic conditions of the experiments, plausible thicknesses of diffusion layers at the two membrane surfaces have been determined. At each surface, it was decided to use the same diffusion layer thickness, is δ= 59 μm as determined from previous experiments[2].

The remaining parameters that can be varied in the program simulation include:

- Lactate concentration in solution I.

[2] DTU-course no. 3922: Advanced exercises in chemical process engineering.

- Lactate concentration in solution II.
- pH of solution I.
- pH of solution II.
- Current density, i_d.

The calculation of membrane profiles continues until steady-state is reached or 100 time steps have passed. The length of each time step, Δt, is also variable.

For an evaluation of the reverse electro-enhanced dialysis process, the different stream compositions have been estimated.

4.3.5.2 Case example

A simulation is performed for a case example. A small section of the reverse electro-enhanced dialysis module is considered; or more specifically, the part of the module where the feed enters the module.

Entering the unit is a hypothetical feed stream from the fermenter carrying 200 mol/m^3 (0.2 M) lactate solution at pH 4.5. After pass, the feed stream contains 50 mol/m^3 (0.05 M) lactate. The alkaline stream passes on the opposite side of the membranes in a countercurrent setup, meaning that the alkaline solution exits the module at the same end as the fermentation stream enters as depicted in Figure 4.29.

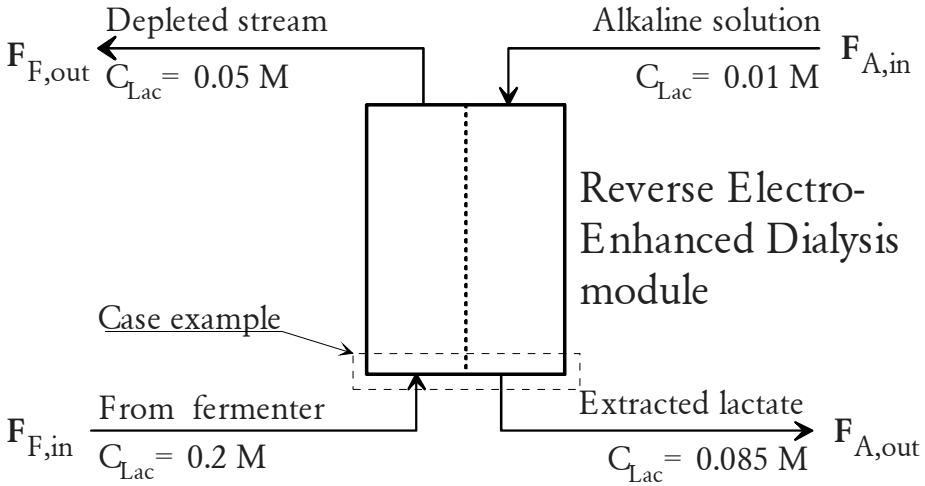

Figure 4.29 The hypothetical streams entering and exiting the reverse electro-enhanced dialysis module. The mass flow F_A is assumed twice as large as F_F.

When assuming that the alkaline stream $F_{A,in}$ enters the module with a little lactate (0.01 M) at twice the mass flow of the feed stream ($F_A = 2 \cdot F_F$), the resulting lactate concentration in the exiting alkaline solution should be approximately 0.085 M. Assuming the alkaline stream is pH 13 when entering the module, and each lactate ion collected has replaced a hydroxide ion, the exiting alkaline solution is roughly pH 12.4.

The case example examined is the first membrane segment of the module, where the feed stream enters the membrane module. Within this simulation, the feed and base concentrations through the segment are considered constant. The current is reversed at long intervals, letting a steady-state membrane profile develop every time, before current is reversed again.

The results found are presented in Figure 4.30 and Figure 4.31. These figures simulate the development of lactate concentration profiles through the anion-exchange membranes from the time of the current reversal, until the steady-state is reached.

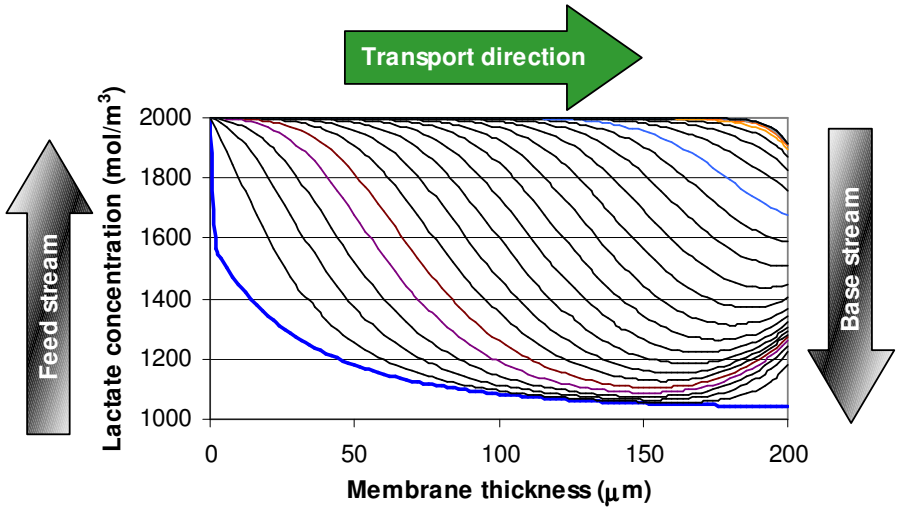

Figure 4.30 Membrane profiles of lactate concentration across the anion-exchange membranes, where lactate is extracted from feed to base. Profiles are presented at 5 seconds intervals. The fat line represents the starting membrane profile. Time from reversal to steady-state: 125 seconds.

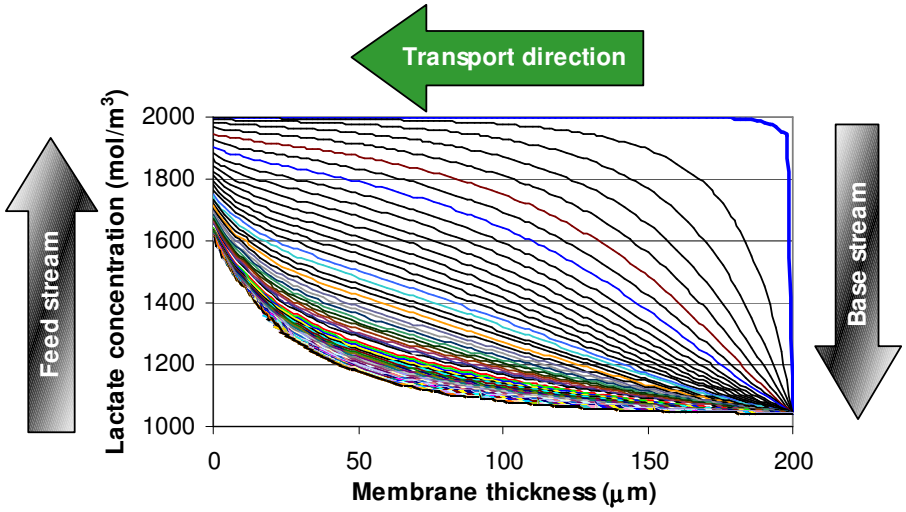

Figure 4.31 Membrane profiles of lactate concentration across the anion-exchange membranes, where hydroxide is driven into feed from base. Profiles are presented at 5 seconds intervals. The fat line represents the starting membrane profile. Time from reversal to steady-state: 385 seconds.

The membrane capacity is 2000 mol/m^3. At every point through the membrane, the sum of lactate and hydroxide ions responds to this capacity. The corresponding hydroxide concentration profiles can be found by subtracting the lactate profiles from the membrane capacity.

The two figures can be regarded in two ways. In the first manner, the figures represent the same membrane cross-section, where lactate ions fill up the membrane from the feed, when the electrical current is from right to left (meaning the negative ions are transported from left to right) as shown in Figure 4.30. After current reversal, the same lactate ions are driven out by hydroxide ions from the base, when the current is from left to right (negative ions migrate from right to left) as shown in Figure 4.31.

It is evident that the concentration profile for lactate is more quickly established when lactate ions are filling up the membrane, than when they are "pushed" by the more mobile hydroxide ions.

Another way to consider the two figures is that Figure 4.30 represents every second membrane in the stack where lactate flows from feed to base, while Figure 4.31 represents the alternate membranes, where hydroxide is transported from base to feed. Thus, by calculating the simultaneous fluxes of lactate from feed to base and from base to feed, an overall lactate flux and efficiency can be calculated.

The more time that has passed from current reversal, the higher the lactate flux from feed to base, and the lower the lactate flux from base to feed. Thus, the overall flux and efficiency of the reverse electro-enhanced dialysis process improves until steady-states are reached across all membranes. The momentary current efficiency (the efficiency in an exact moment) and the overall current efficiency (accumulated from the beginning of the reversal period) are both depicted in Figure 4.32.

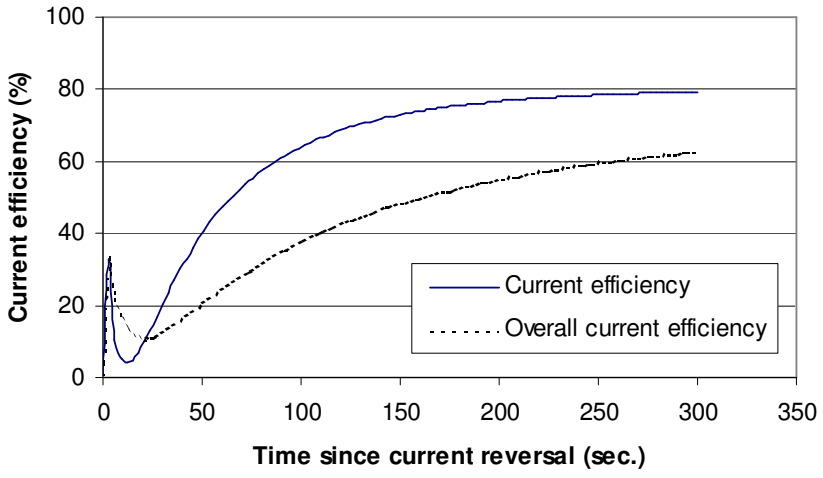

Figure 4.32 Momentary and overall current efficiency as function of time since last current reversal for the Reverse Electro-Enhanced Dialysis process.

A small peak in current efficiency arises just after the reversal when the polarization layers are breaking down, followed by a drop where polarization is rebuilt. As profiles are forming, the

current efficiency slowly grows. When steady-state is reached, the current efficiency has reached a plateau that corresponds to the maximum obtainable overall current efficiency.

4.3.5.3 Experimental plan

The parameters, which will be regarded in the response surface, are:

- Lactate concentration in feed stream. Range: 50 – 200 mol/m^3
- pH of feed stream. Range: 4 – 12
- Current density. Range: 250 – 1000 A/m^2
- Time between current reversals. Range: 60 – 600 seconds

Two subsequent parameters are set according to the values of these parameters:

- It is assumed that 90% of the lactate is extracted from the feed during a pass, and that the mass flow of the alkaline stream is twice that of the feed stream. Thus, the effluent is assumed to have a lactate concentration of 22.5 – 90 mM. This ignores the possibility that the alkaline solution holds some lactate before entering.
- The pH of the exiting alkaline solution is calculated by assuming that every lactate ion in the base stream is replacing a hydroxide ion.

The responses that are evaluated from these parameters are:

- Current efficiency (%). The amount of lactate transported during a period between two reversals in regard to the added electrical current.
- Energy consumption (kWh/kg lactate extracted). The overall energy used in regard to the amount of lactate transported during a period between two current reversals.
- Specific membrane area (m^2). This area is calculated based on the necessary membrane area needed to extract 1145 kg lactate per hour using the current parameters. This specific lactate flux was chosen to reflect the 10,000 t annual capacity of a lactic acid plant as evaluated in the following section of this chapter.

An experimental plan for a full-factor experiment with three levels of each factor has been created using the statistical software program Modde. Since the simulation program yields identical solutions with the same parameters, re-runs are pointless. The run order of the simulations is also irrelevant. The experimental plan with all factors and responses are located in appendix 7.2.3.

4.3.5.4 Contour plots

Since the numerical values created by the simulation are only illustrative for a specific point along the separation process, and the optimization tools used in the statistical program, Modde, are based on simple, linear models the resulting values can only be representative and are at the time of this report not cabable of calculating precise optimization parameters.

One of the most interesting responses from an industrial viewpoint is the separation process' energy consumption. A contour plot of the energy consumption as function of current density and current reversal time is shown in Figure 4.33.

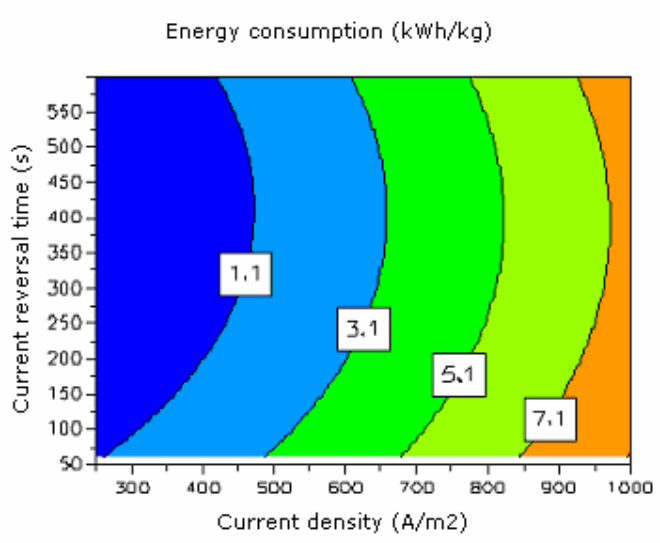

Figure 4.33 Contour plot of energy consumption. Feed pH = 8, $C_{Lactate,\ Feed}$ = 125 mol/m^3.

The plot suggests that low current density and current reversal time of 300-500 seconds are preferable for obtaining low energy consumption. The plot is produced for the central values of feed pH and lactate concentration. The corresponding plots at lower and higher feed pH are shown in Figure 4.34 and Figure 4.35.

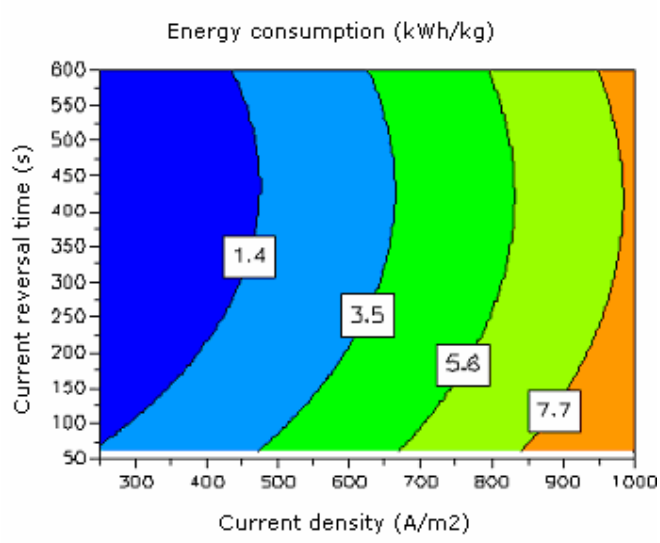

Figure 4.34 Contour plot of energy consumption. Feed pH = 4, $C_{Lactate,\ Feed}$ = 125 mol/m^3.

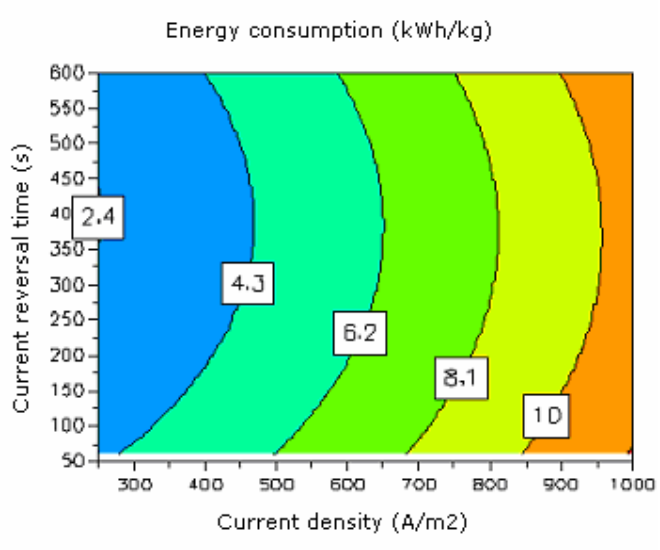

Figure 4.35 Contour plot of energy consumption. Feed pH = 12, $C_{Lactate,\ Feed}$ = 125 mol/m^3.

While these two plots show similar behavior, they also suggest an optimum within the feed pH. Only small changes can be observed by increasing the feed pH from 4 to 8, but at higher pH-values, the energy consumption increases significantly. The trend of lower energy consumption at lower current density is still evident.

The contour plots in Figure 4.36 and Figure 4.37 show the effect of lower and higher feed concentration around the central pH-value, respectively.

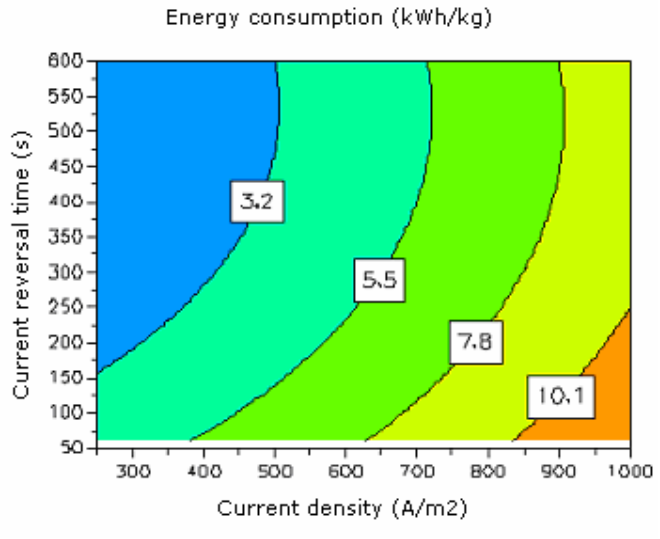

Figure 4.36 Contour plot of energy consumption. Feed pH = 8, $C_{Lactate,\ Feed}$ = 50 mol/m^3.

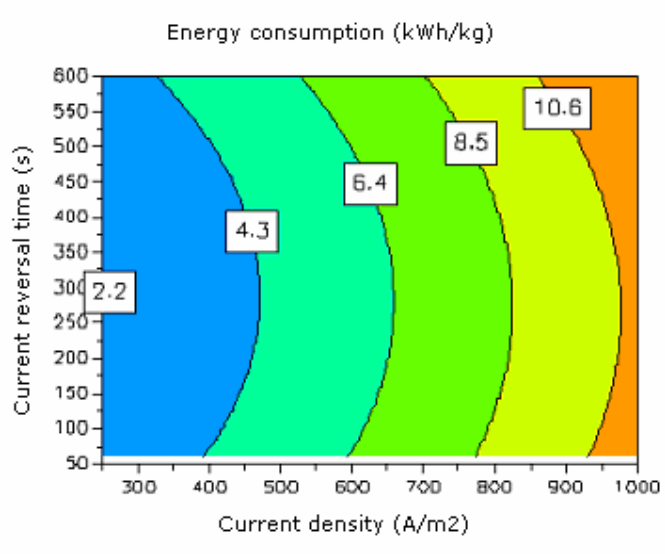

Figure 4.37 Contour plot of energy consumption. Feed pH = 8, $C_{Lactate,\ Feed}$ = 200 mol/m^3.

Comparison of the five plots suggests that some optimal region for lowest energy consumption exists within the pH-interval 4 – 12, and within the range of feed concentrations from 50 – 200 mol/m^3.

A new contour plot with the energy consumption as function of pH and feed concentration is shown in Figure 4.38 for central values of current density and reversal time.

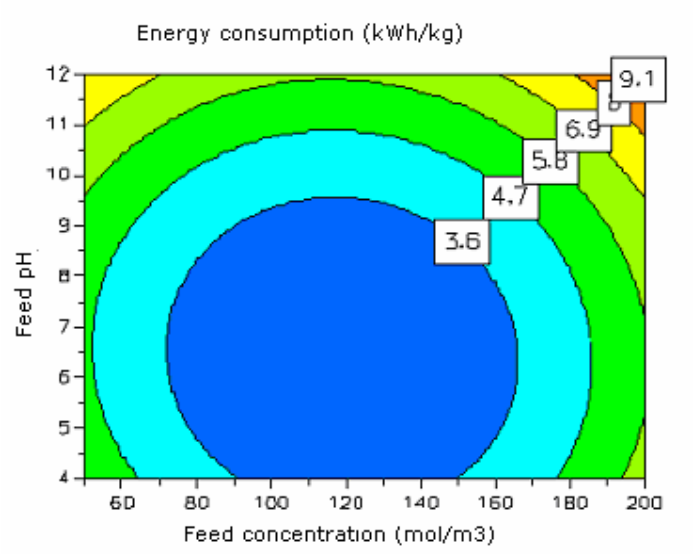

Figure 4.38 Contour plot of energy consumption. Current density = 625 A/m^2, reversal time = 330 seconds.

This plot confirms the previous hypothesis that the lowest energy consumption probably can be found within the chosen intervals of feed pH and concentration. From the first contour plots, the lowest energy consumption is possibly found at lower current density and reversal times of 300 –

500 seconds. The estimated contour plot with lowest current density 250 A/m^2 and central time reversal 330 seconds is depicted in Figure 4.39.

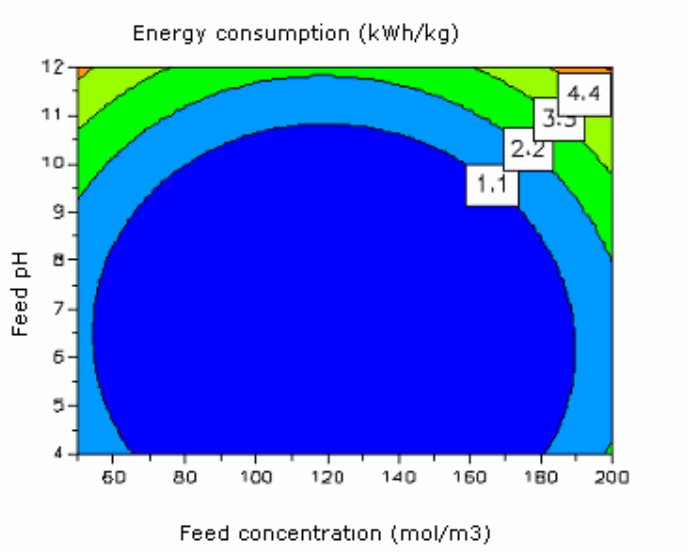

Figure 4.39 Contour plot of energy consumption. Current density = 250 A/m^2, reversal time = 330 seconds.

The statistical program estimates a large region of low energy consumption for feed concentration and feed pH at low current density. At these conditions, relatively larger variations with feed pH and concentration are possible, and seems like optimal process conditions. Lowering the current density obviously lowers the energy consumption, but also lowers the lactate extraction flux. The result is increased membrane area necessary to extract the lactate.

Calculating the specific membrane area and subjecting the results to the same level of optimization reveals a different optimal area as expected. Since the membrane area represents part of the capital investment in a new plant, the optimal membrane area is as small as possible.

The contour plots are shown in Figure 4.40 and Figure 4.41. The optimal membrane area is found at the higher current densities, though the low pH and medium to high current reversal times are still close to the previously found optimum.

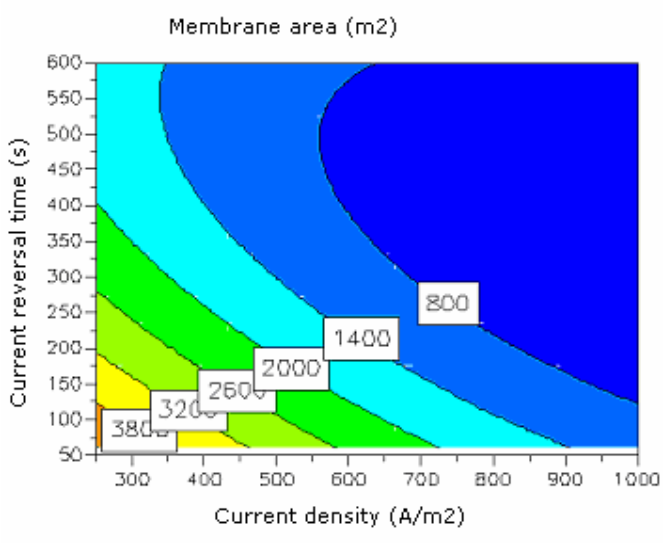

Figure 4.40 Contour plot of calculated specific membrane area. Feed pH = 4, $C_{Lactate,\ Feed}$ = 125 mol/m^3.

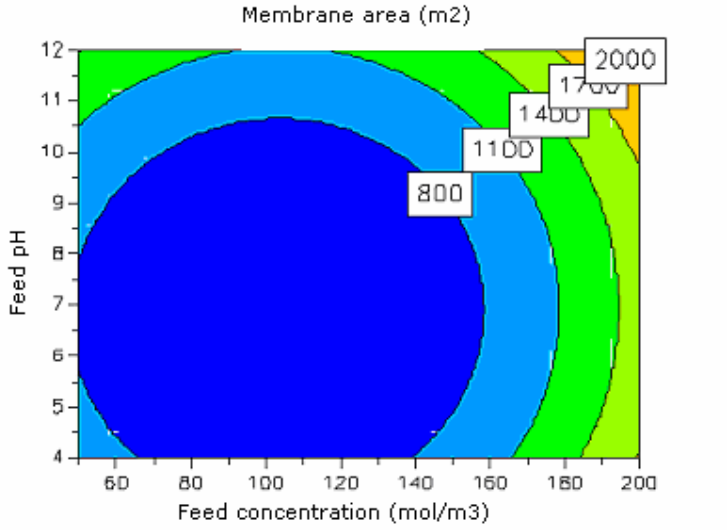

Figure 4.41 Contour plot of calculated specific membrane area. Current density = 1000 A/m^2, reversal time = 600 seconds.

The value of low feed pH was expected since this is part of the theoretical basis of the operation.

The difference between parameter values for optimal energy consumption and optimal specific membrane area lies with the current density. This was expected as the current density is closely linked to the flux.

The current efficiency increases as the current density decreases as shown when comparing the contour plots in Figure 4.42 (250 A/m^2) and Figure 4.43 (1000 A/m^2), because a higher fraction of the lactate is carried by power-free diffusion flux at lower current densities.

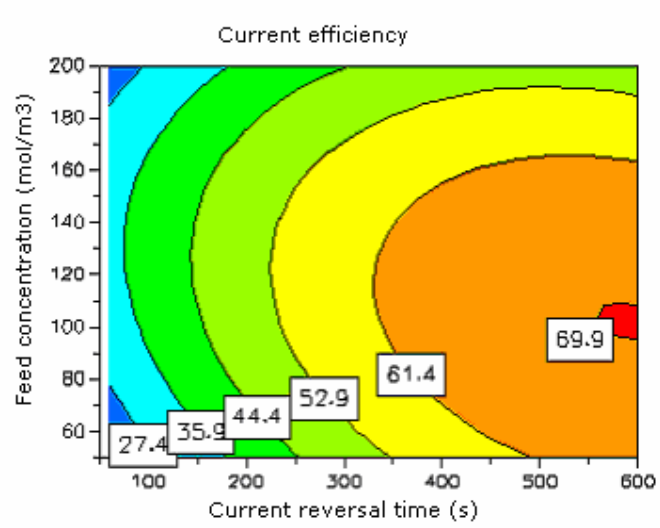

Figure 4.42 Contour plot of current efficiency. Feed pH = 4.5, current density = 250 A/m^2.

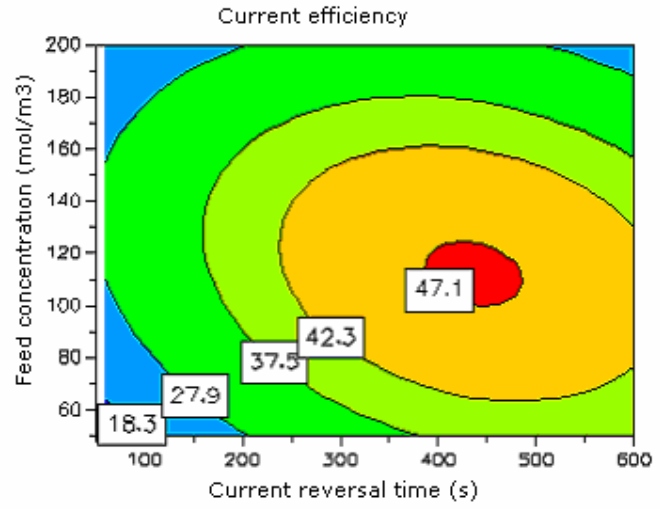

Figure 4.43 Contour plot of current efficiency. Feed pH = 4.5, current density = 1000 A/m^2.

To discern the optimum value for an industrial application, a new response, based on both energy consumption and necessary membrane area, must be calculated. For this a very simplified Net Present Value (NPV) is utilized. The NPV includes both the investment of the equipment (related to specific membrane area), and the running costs (related to the energy consumption), but this modified NPV does not include income from production sales. In electrodialysis applications, the investment can be assumed to be close to the total membrane area required, and the running costs close to the electrical energy consumption of the process. By assigning general membrane and power cost, a NPV for equipment ready to produce 10,000 t lactic acid per year can be calculated:

Membrane cost (installed):	3450 DKK/m^2
Power cost:	0.34 DKK/kWh

The NPV is calculated as Equation 4.36, which is later explained in details, setting a desired rate of return to 10% and a plant lifetime of 15 years.

Figure 4.44 and Figure 4.45 show the contour plots of the optimal regions for process operation using central parameter settings.

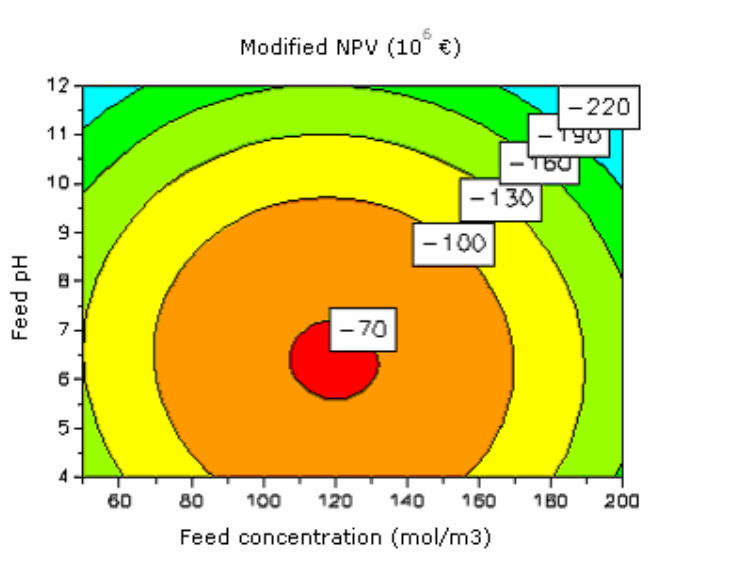

Figure 4.44 Contour plot of Net Present Value (NPV) in 10^6 € for a REED equipment producing 10,000 t lactic acid per year.

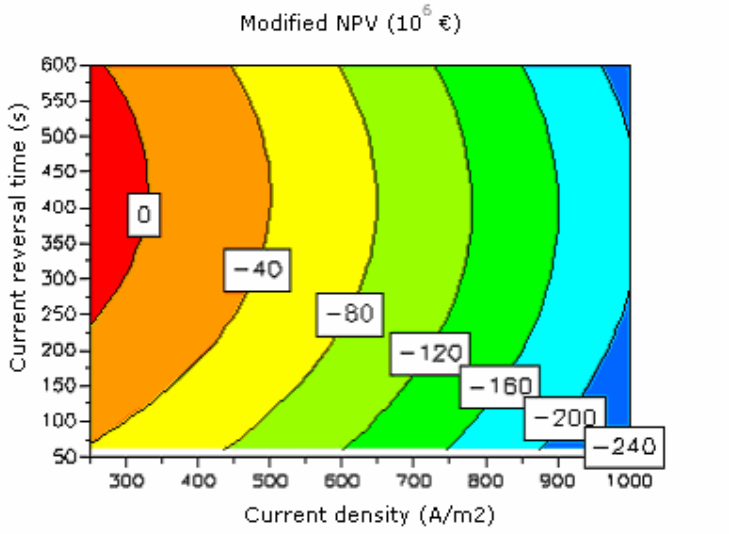

Figure 4.45 Contour plots of Net Present Value (NPV) in 10^6 € for a REED equipment producing 10,000 t lactic acid per year.

Since no production income is included in this simplified NPV, the results are all negative.

As expected from earlier findings the feed pH and concentration are not crucial parameters in optimization. There is room for some variation in current reversal time, but the running cost of energy consumption weighs more heavily on the influence of the current density on NPV than does the membrane investment. The great pH-variations in the equipment cause the assumption of an equipment lifetime of 15 years to be very optimistic. Shorter membrane lifetime of 3-8 years is more realistic, and this would shift the weight towards higher current density.

4.3.6 Conclusion

The simulation results shown here represents a very simplistic case study for a reverse electro-enhanced dialysis operation included in a designed plant producing 10,000 t lactic acid per year, as will be closely evaluated last in this chapter.

The simulation successfully accomplished the initial goals of simulating and establishing steady-state concentration profiles of lactate ions by a simple mathematical, two-component model. To accommodate membrane surface polarization a simple diffusion model was subsequently included to observe the significant influence from this effect. Watersplitting can greatly influence the steady-state system, when operating close to optimal conditions. By calculating overall lactate fluxes and reworking the program to handle the current reversal of concentration profiles, whether in steady-state or in transition, produced estimations of current efficiency as function of current reversal times. These results were compared to experimentally determined values and found to be very comparative. The program was expanded to include other parameters and continuous evaluation of energy consumption and specific membrane area, which have been demonstrated.

The results produced by the simulation program were comparable to experimental results produced in tests runs with model solutions. The most important prediction of the simulations is the time for concentration profiles inside the anion-exchange membranes to reach steady-state. As clearly confirmed in Figure 4.32, the current efficiency is heavily depending on the time between current reversals and this period should be increased as much as possible weighed against the fouling build-up.

The simulation program is still lacking in practical applicability as a process optimization tool as it can only predict a binary membrane profile through the membrane, which is adequate for the lactate/hydroxide system, when other anions are only present in insignificant amounts. For more complicated feed streams, a more complex solution must be employed for solving the coupled equations.
Further expansion of the program is currently planned to include mass balance segments along the membrane surface in the feed chamber to evaluate the change in lactate extraction from the point of entry to an optimal point of exit from the REED.

4.4 Electrodialysis with bipolar membranes

4.4.1 Introduction

Having established a possible extraction process (REED), the subsequent purification of the extracted lactate in alkaline solution, is considered in this section. The possible symbiosis between a reverse electro-enhanced dialysis (REED) process and an electrodialysis process with bipolar membranes (EDBM) is investigated for this purpose.

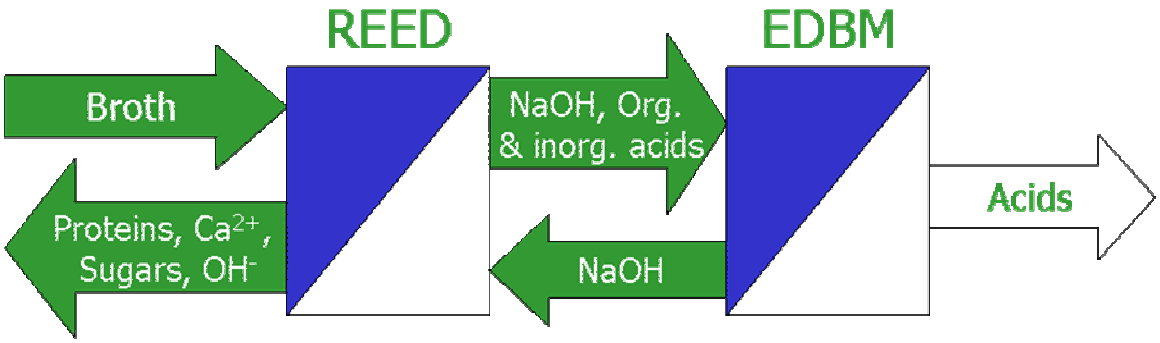

Figure 4.46 Extraction of organic acids from fermentation broth in a reverse electro-enhanced dialysis (REED) unit and continuous acid recovery and regeneration of the alkaline solution in an electrodialysis unit with bipolar membranes (EDBM).

As demonstrated in Figure 4.46, the EDBM process recovers the organic and inorganic anions from the alkaline solution, while regenerating the alkaline base for continuous operation.

4.4.2 Electrodialysis experiments with bipolar membranes

Experiments with three-compartment EDBM were carried out to evaluate the performance during removal of lactate from an alkaline feed solution. The properties of the feed are made to resemble those that would be experienced if the EDBM was connected to a reverse electro-enhanced dialysis unit.

4.4.2.1 Materials and methods

Membranes

Tokuyama Corporation, Tokyo, Japan, kindly supplied the three different kinds of ion-exchange membranes used for the experiments; Neosepta® AMX anion-exchange membranes, Neosepta® CMH cation-exchange membranes, and BP-1 bipolar membranes. The AMX is a standard grade membrane, whereas the CMH is special grade membrane with high chemical resistance and high mechanical strength.

Experimental equipment

The equipment was of own design and was constructed at the workshop at Department of Chemical Engineering (DTU, Lyngby, Denmark) from transparent acrylic plates. The stack was assembled as shown in Figure 4.47 with three bipolar membranes, two anion exchange membranes, and two

cation exchange membranes, forming two feed compartments, two acid compartments, two base compartments, and two electrode chambers. This setup is specially designed for simulating a much larger, single-pass EDBM process. The focus of these experiments is the extraction of lactate and alkaline cations from the feed. Every time the feed passes through the stack, more potassium and lactate ions are removed, lowering the feed conductivity and raising cell resistance.

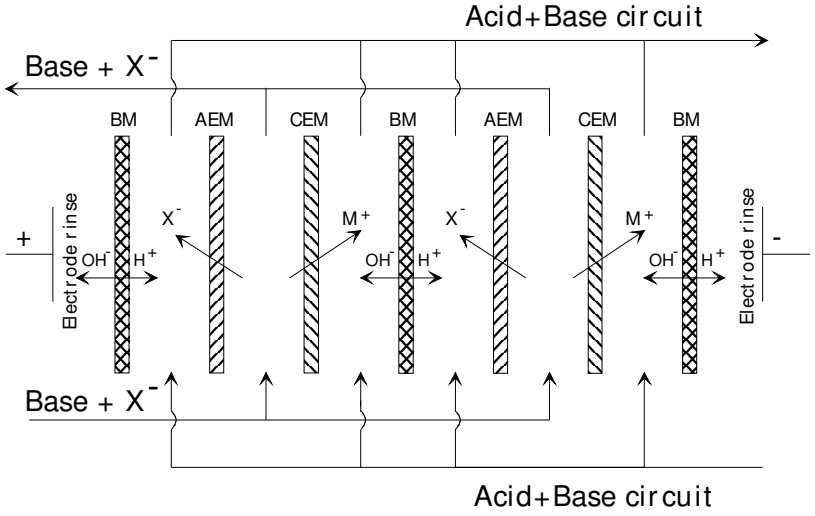

Figure 4.47 Membrane configuration in the EDBM-stack.

Each membrane had an active area of 40 cm^2. The thickness of the chambers between the membranes was six mm and net spacers were introduced to promote turbulent flow. In the two outermost chambers between the platinum electrodes (each 31.5 cm^2) and a set of bipolar membrane, electrode-rinsing solution was passed consisting of an aqueous solution of 0.1 M K_2SO_4. Feed solution was circulated from the feed tank through the feed chambers between the anion- and cation-exchange membranes by means of a gear pump (Micropump F5734, Concord CA, USA) as shown on the experimental setup in Figure 4.48. The same type of pump was used to circulate the combined acid and base stream through the acid chambers between the bipolar membranes and anion-exchange membranes and through the base chambers between the bipolar membranes and cation-exchange membranes. The mass flow through each gear pump was 3.3 g/s. The electrode solution was circulated using a centrifugal pump (Type no. 1250 21 9, EHEIM, Germany). The power supply (EA-PS 3032-10 (0..32V/0..10A), EA–Elektro-Automatik, Germany) for direct current to the stack was connected to a multimeter (Radio Shack LCD Auto Range Digital Multimeter, Tandy Corp., US) for accurate readings of the current. In the feed chambers, silver/silver chloride electrodes were placed to continuously measure the voltage drop across a cell pair and collect the data. (Fluke 123 – Industrial Scopemeter, Fluke Corporation, USA).

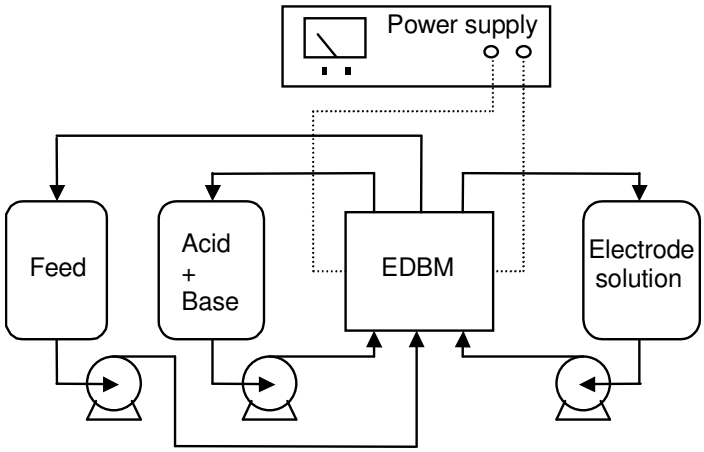

Figure 4.48 Experimental setup for the EDBM experiments.

All the tanks were equipped with heating/cooling jackets connected to a water bath and the temperature was kept at 40°C during experiments. Samples were taken from the feed tank and the combined acid/base tank every 15 minutes the first hour and then every 30 minutes until the experiments were terminated after 3 hours. pH, conductivity and lactic acid concentration were measured in the samples.

4.4.2.2 Analytical techniques

1 ml solution was taken from both the feed tank and the combined acid and base tank and acidified using concentrated sulfuric acid (72%). Lactate content was analyzed at 35°C with HPLC equipped with an Aminex HPX-87H column (Biorad, USA) using 4 mM H_2SO_4 as eluent at a flow rate of 0.6 ml/min. The acid was detected on a Waters 486 tunable absorbance detector at 210 nm. Waters Millennium Chromatography Manager software was used for quantification.

Approximately 5 ml solution was taken from both the feed tank and the combined acid/base tank. The pH and conductivity were measured using a pHM 201 portable pH meter and a CDM92 Conductivity meter (both Radiometer, Denmark), respectively. After measurements the samples were transferred back to the system.

4.4.2.3 Lactate recovery experiments

Two experiments were carried out to investigate the influence of the lactate concentration on the current efficiency and power consumption. In the first experiment 500 ml feed solution containing 0.5 M KOH and 0.2 M lactic acid was used and in the second experiment the lactic acid concentration was increased from 0.2 to 0.4 M. In both experiments 1000 ml of a 0.1 M KOH solution was circulated in the acid/base circuit. The experiments were started at a current of 1500 mA, corresponding to a current density of 375 A/m^2.

The conductivity of the feed dropped during both experiments as the lactate was extracted. Since the electrical resistance increased following the continuous feed depletion, the current was kept constant until the voltage drop across a single cell pair exceeded 11 V. The current density was then

decreased to 188 A/m^2 and further down to 94 A/m^2 and finally 50 A/m^2 whenever the 11 V limit was reached.

4.4.2.4 Experimental EDBM results and discussion

In the first experiment the migration of lactate from the feed chamber to the acid chamber was quite slow to begin with. Figure 4.49 shows only small changes in lactate concentrations during the first 60 minutes with a decrease in the feed concentration from 17.9 to 14.2 g/l.

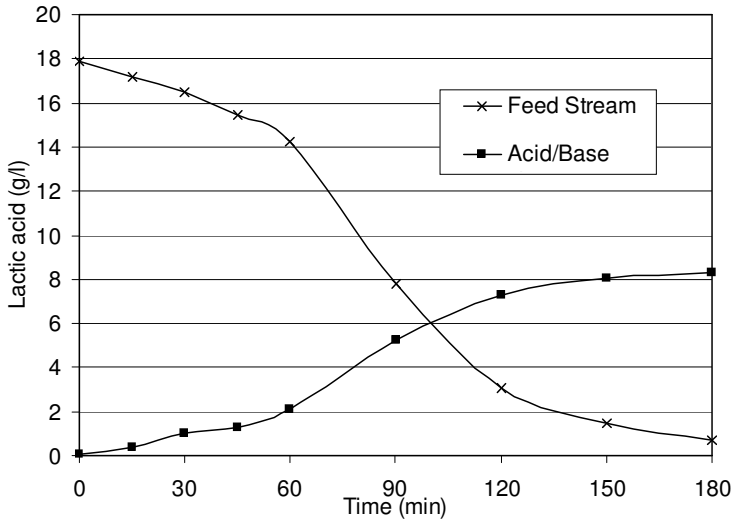

Figure 4.49 Concentration of lactate in the feed tank and acid/base tank during the first experiment.

The feed concentration changed more quickly, from 14.2 to 3.1 g/l, during the second 60 minutes period, after which the process slowed down again, resulting in a concentration of 0.7 g/l in the feed at the end of the experiment.

The slow removal of lactate from the feed stream in the beginning of the experiment is due to the presence of high amounts of hydroxide ions that transports most of the current. The initial concentration of hydroxide is roughly estimated to 0.3 M since 0.2 M of the original 0.5 M potassium hydroxide solution is assumed neutralized by the added lactate concentration of 0.2 M. Assuming that the steric factor affecting ion mobility inside the anion-exchange membrane affects the mobilities of lactate and hydroxide proportionally:

$$u_j^{Membrane} = \alpha \cdot u_j^{Solution}$$

the lactate transport number through the anion-exchange membrane should be theoretically comparable to the measured current efficiency, excluding hydrogen leakage and current leakage through manifolds.

$$t_{Lac}^{m} = \frac{\left|z_{Lac}^{m}\right| u_{Lac}^{m} C_{Lac}^{m}}{\sum_{j} \left|z_{j}^{m}\right| u_{j}^{m} C_{j}^{m}} = \frac{\alpha u_{Lac} C_{Lac}^{m}}{\alpha u_{Lac} C_{Lac}^{m} + \alpha u_{OH^-} C_{OH^-}^{m}} = \frac{C_{Lac}^{m}}{C_{Lac}^{m} + \left(u_{OH^-} / u_{Lac} \right) C_{Lac}^{m}} \approx \frac{0.2}{0.2 + 5 \cdot 0.3} = 0.12$$

The transport number is calculated from Equation 1.17 and the relative mobility of hydroxide to lactate is approximately 5.

Roughly 12% of the current should be carried by lactate in the beginning of the experiment, which is in good agreement with the current efficiency obtained from the experimental data as shown in Figure 4.50. The current efficiency, when based totally on lactate removal, is 15% in the first 30 minutes. It increases to an average of 77% between 90 and 120 minutes due to depletion of hydroxide (see the large drop in pH). By the end of the experiment the efficiency decreases again as the lactate concentration in the feed approaches zero and the effect of back-diffusion of lactate increases. The overall current efficiency is 43%, which corresponds well with roughly 2/5 of all extracted anions being lactate.

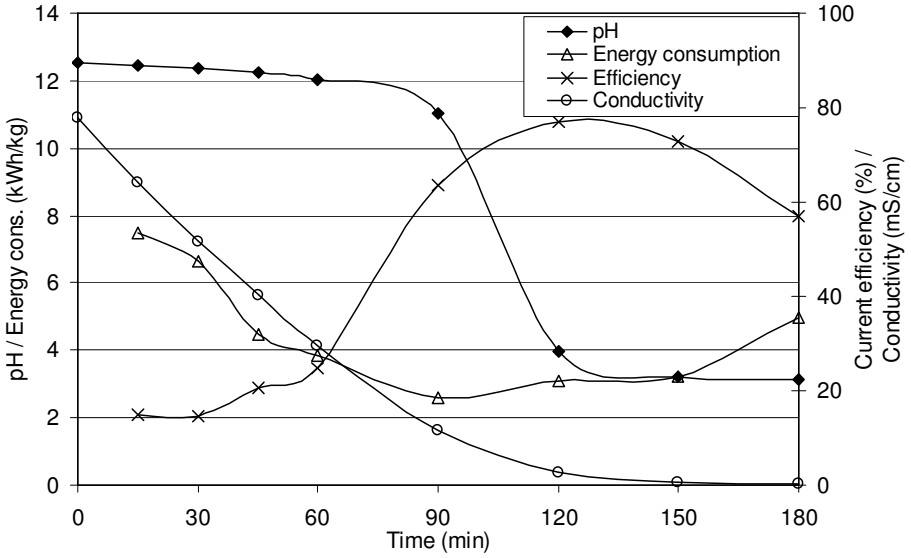

Figure 4.50 The graph shows pH, energy consumption, current efficiency and conductivity during bipolar electrodialysis of a feed stream consisting of 0.2 M lactic acid in 0.5 M KOH. The energy consumptions and current efficiencies at a given time are calculated as an average value in the time interval from the previous point up to the given point and are based only on lactate removal.

The energy needed to remove one kilo of lactate (energy consumption) is high in the beginning of the experiment due to a low current efficiency and high again in the end mainly because of a low conductivity as included in Figure 4.50. The energy consumption in the first 15 minutes and the last 30 minutes is 7.5 and 5.0 kWh/kg, respectively. The lowest energy consumption value (2.6 kWh/kg) is observed in the interval between 60 and 90 minutes and the overall consumption for the entire experiment is 3.7 kWh/kg. The energy consumption is an important factor that relates to the operating costs of the EDBM unit and is directly proportional to the ohmic resistance of the cell. Figure 4.51 shows the resistance and the voltage drop across a single cell pair, the steep drops indicating where the current density is decreased.

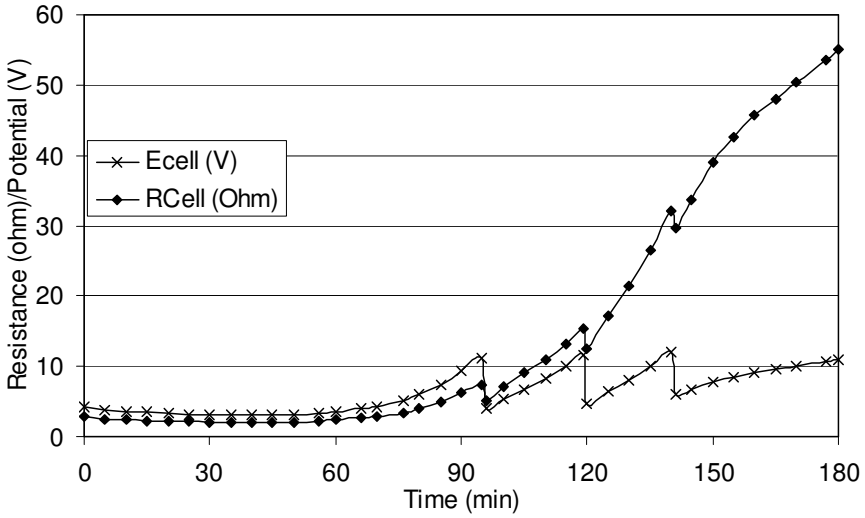

Figure 4.51 The voltage drop E_{Cell} and calculated electrical resistance R_{Cell} across a single cell pair during bipolar electrodialysis of a feed stream with 0.2 M lactic acid in 0.5 M KOH. Current density was lowered three times to account for the increasing cell resistance.

In an industrial membrane stack the thickness of the flow spacers can be considerable smaller and the hydrodynamics optimized for a high mass-transfer coefficient at the membrane surface. This would result in lower electrical resistance across a cell pair and thus reduce the energy consumption. Disregarding effects from improved hydrodynamics, an industrial cell with a typical spacer thickness of 1 mm would reduce the energy consumption for the above separation from 3.5 kWh/kg to about 2.3 kWh/kg.

In the subsequent experiment the lactate concentration was increased to 0.4 M in the alkaline feed solution. Figure 4.52 shows the concentration of lactate in the feed and acid/base tanks, which changes at a high rate already from the beginning of the experiment. The lactic acid concentration in the feed drops from 35.1 to 8.2 g/l during the first 90 minutes and further down to 0.8 g/l in the next 90 minutes.

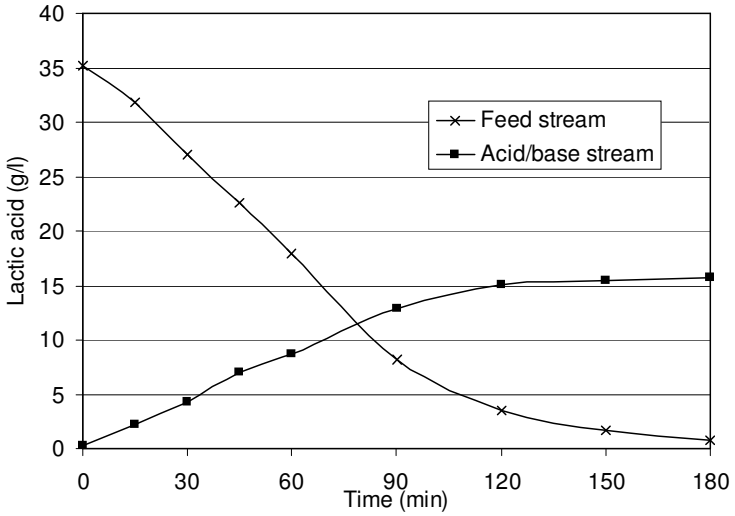

Figure 4.52 Concentration of lactate in the feed tank and acid/base tank during the second experiment with 0.4 M lactic acid in 0.5 M KOH.

The lactate removal efficiency at the start of the experiment can be estimated as in the previous experiment, comparing an initial concentration of 0.1 M hydroxide remaining after adding 0.4 M lactic acid to the 0.5 M potassium hydroxide solution:

$$t_{Lac}^{m} = \frac{C_{Lac}^{m}}{C_{Lac}^{m} + \left(u_{OH^-} / u_{Lac} \right) C_{Lac}^{m}} \approx \frac{0.4}{0.4 + 5 \cdot 0.1} = 0.44$$

By theory, the current efficiency should start at 44%. Figure 4.53 shows the experimental value of the average current efficiency during the first 15 minutes of 67%, which suggests a steep increase in the beginning of the process as the concentration of hydroxide ions diminishes. A high average current efficiency of 94% is obtained in the interval between 15 and 90 minutes and the overall current efficiency for the entire separation is 88% or approximately twice the value that was obtained in the previous experiment.

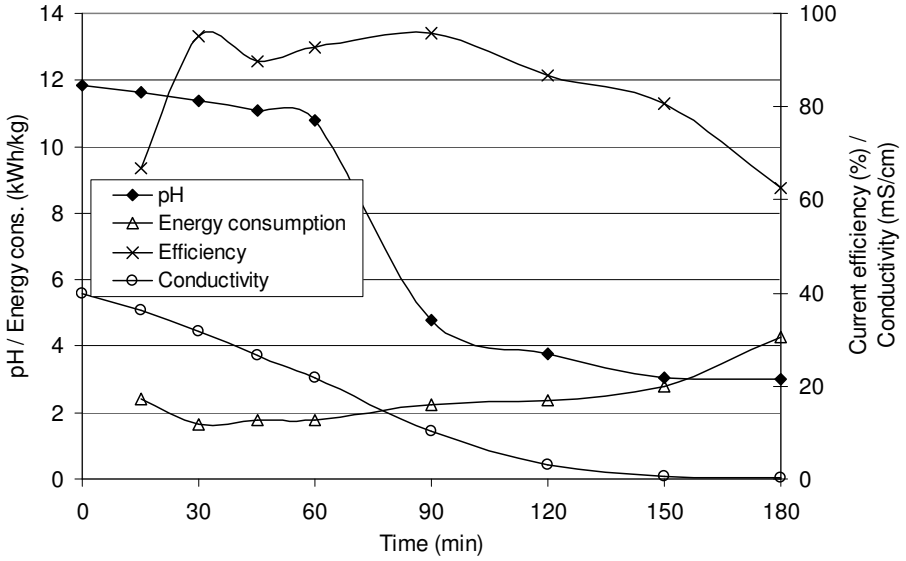

Figure 4.53 The graph shows pH, energy consumption, current efficiency and conductivity during bipolar electrodialysis of a feed stream consisting of 0.4 M lactic acid in 0.5 M KOH. The energy consumptions and current efficiencies at a given time are calculated as an average value in the time interval from the previous point up to the given point and are based only on lactate removal.

The energy consumption is quite stable throughout the experiment with an average value of 2.15 kWh/kg lactate recovered. However, in the last 30 minutes only 0.85 g/l lactate is removed at an energy expenditure of 4.28 kWh/kg. If an industrial membrane stack utilized a spacer thickness of 1 mm the energy consumption could comparably be as low as 1.48 kWh/kg.

The electrical resistance and potential drop across a single cell-pair are shown in Figure 4.54. The resistance in the first 60 minutes is roughly 60-70% higher compared to that was observed in the previous experiment shown in Figure 4.51.

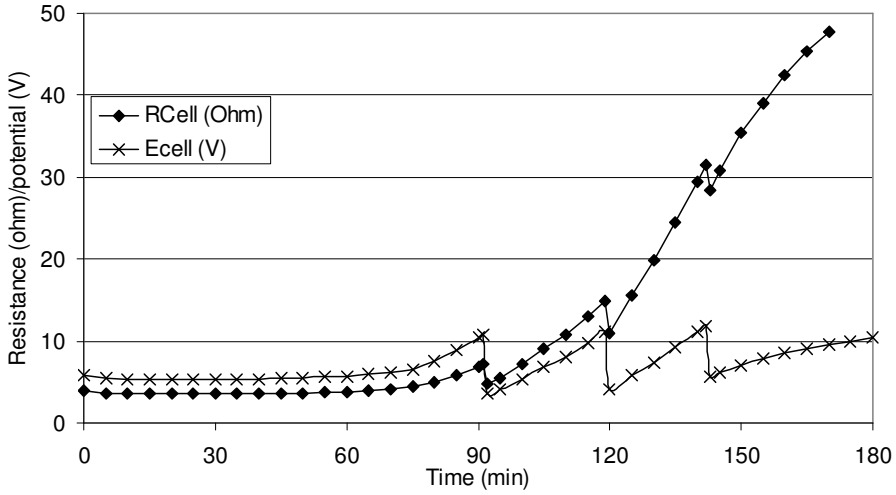

Figure 4.54 The voltage drop E_{Cell} and calculated electrical resistance R_{Cell} across a single cell pair during bipolar electrodialysis of a feed stream with 0.4 M lactic acid in 0.5 M KOH. Current density was lowered three times to account for the increasing cell resistance.

Considering the large ratio of lactate to hydroxide in the second experiment, the higher resistance is due to the mobility of lactate being 5 times lower than the mobility of hydroxide. However, the overall energy consumption is lower in the second experiment because of the much better current efficiency.

4.4.3 Conclusion on the electrodialysis with bipolar membranes

The experiments are in agreement to earlier research (Garde and Rype 1997) demonstrating the potential of EDBM for recovering lactate from an alkaline stream. Because of the capacity of the laboratory equipment, the degree to which lactate could be concentrated as lactic acid was not documented in these few experiments, but own research and other researchers (Borgardts *et al.* 1998a;Borgardts *et al.* 1998b) have documented that high levels of acid concentration are obtainable.

The concentration of lactate and the ratio between lactate and hydroxide in the feed solution is of major importance for the energy consumption. At the higher lactate concentration (0.4 M) an overall current efficiency of 88% was obtained and an average energy consumption of 2.15 kWh/kg was necessary for decreasing the lactate concentration from 35.1 to 0.8 g/l. When the lactate concentration in the feed was 0.2 M the overall current efficiency was 43% and an average energy consumption of 3.48 kWh/kg was needed to reduce the lactate concentration from 17.9 to 0.7 g/l. Most of the hydroxide ions have to be removed before the lactate starts to be extracted, yielding a low efficiency until lactate starts to dominate the migration compared to hydroxide. Since the relation between the mobilities of hydroxide to lactate is about 5, the lactate concentration has to be around 5 times the hydroxide concentration for just an even migration.

The experiments showed that the last remains of lactate was expensive to remove, not just in terms of increasing energy consumption as a result of the speedy increase in electrical resistance, but also because of a very low flux. At the end of the experiments the current density was 7.5 times smaller

than to begin with, which for a constant current efficiency imply a necessary membrane area that is 7.5 times larger for transference of a given amount of lactate.

Since the feed circuit of the bipolar electrodialysis unit is supposed to be a closed circuit connected to the reverse electro-enhanced dialysis unit, a total depletion of lactate is not essential. The level of lactate in the stream returned to the reverse electro-enhanced dialysis must depend on an optimization where the current efficiency and energy consumption of both units are taking into account. Keeping a relatively high amount of lactate in the alkaline stream that circulates between the REED and the EDBM results in higher energy efficiency and lower energy consumption in the EDBM process. But higher lactate concentration in the alkaline stream also results in lower performance of the REED process.

The energy consumption calculated in section only servers as guidelines and comparative values, and a very depending on operation parameters as well as equipment. For industrial scale equipment and optimized process parameters, lower energy consumption is anticipated.

The system layout would be different from the one utilized as shown in Figure 4.47. Taking into account that the alkaline feed stream to the EDBM unit have to be depleted of most hydroxide ions before lactate starts to be extracted, and hydroxide levels then have to be regenerated before the alkaline stream returns to the REED unit, a three compartment setup has been suggested. The three-compartment EDBM setup is sketched in Figure 4.55.

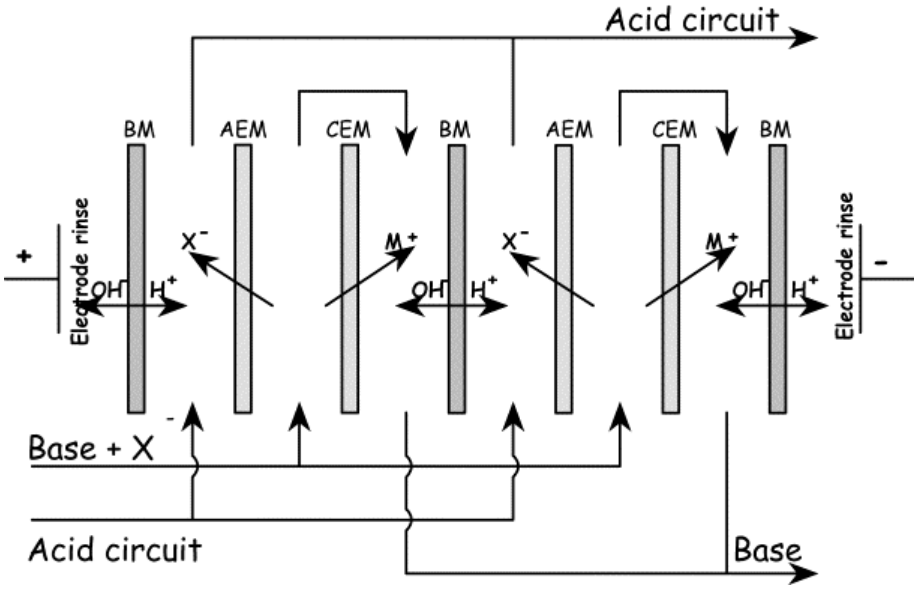

Figure 4.55 Membrane setup for the suggested EDBM process. Base holding lactate (X^-) enters the central compartments between an AEM and a CEM. The stream is depleted of ions during the pass, and returned for a second pass between the CEM and a BM, where alkaline levels are restored and the base returned to the REED. The lactate is extracted and acidified in the acid circuit together with other anions from the alkaline feed stream. AEM = anion-exchange membrane, CEM = cation-exchange membrane, BM = bipolar membrane.

This setup suggests that the alkaline stream with extracted lactate and other anions passes through the stack twice. The first pass between a cation-exchange membrane and anion-exchange membrane depletes the stream from ions until the conductivity is very low. Then the stream passes between the

cation-exchange membrane and a bipolar membrane regenerates the alkaline stream by adding the previously removed cations and fresh hydroxide ions from watersplitting in the bipolar membrane. The lactate is meanwhile extracted across the anion-exchange membranes along with most other organic and inorganic anions and acidified by the hydrogen ions produced by the bipolar membrane on the other side. It has been estimated that lactic acid can be concentration to 20-25% by EDBM (Garde 1997;Garde and Rype 1997)

To investigate the feasibility of this setup, much larger active membrane area is needed. It is crucial that a single pass removes enough hydroxide ions from the feed to also start extracting lactate, before it is possible to assess the process factors. In stead, the long single pass was simulated by passing the feed through the module several times as shown in the experiments.

4.5 Evaluation of a 10,000 tons lactic acid production plant

4.5.1 Introduction

The commercial potential in lactic acid production from renewable resources is assessed through an economical evaluation carried out for a plant capable of an annual production of 10,000 tons 88%-w/w lactic acid. The evaluation is based on a plant that utilizes the REED and EDBM technology for separation and purification previously described. The process combines different electro-membrane unit operations in a unique way that makes it fairly independent of feedstock purity. Hence, evaluation can be carried out without impact from the choice of feedstock other than the variable unit price of carbohydrates, e.g. varying amounts of Ca^{2+} and Mg^{2+} in the raw material will not change the characteristics of the separation process. Costs are assumed for a facility located in Denmark.

4.5.2 Process description and suggested flowsheet

The following unit operations are considered necessary for the lactic acid production process.

1. Recycle fermentation

From an upflow anaerobic sludge blanket (UASB) reactor with a recycle loop for product removal and pH control, a part of the bulk solution is continuously transferred to a reverse electro-enhanced dialysis unit from where the stream is recycled with cells, unconverted carbohydrates and most other bio-matter. But the inhibiting organic acids have been removed resulting in much higher possible yields. The recycled stream is also alkaline, which assists in controlling the pH of the fermenter.

2. Reverse electro-enhanced dialysis

In the REED process the product (organic acid) is extracted from the fermentation broth together with other organic and inorganic anions of low molecular weight into an alkaline process stream.

3. Electrodialysis with bipolar membranes

The EDBM concentrates and acidifies the organic and inorganic anions in a separate tank, while regenerating the alkaline stream that is recycled to the REED.

4. Electrodialysis

After acidifying the organic acids, they are mainly undissociated and no longer charged molecules. A weak electrodialysis process is suggested for removal of remaining inorganic ions.

5. Evaporation

Previous assessments have estimated that is possible to achieve a lactic acid concentration about 20-25%. Still further concentration of the acid is needed for a final product level of 88%, and this is traditionally done by evaporation. The total flowsheet is sketched in Figure 4.56.

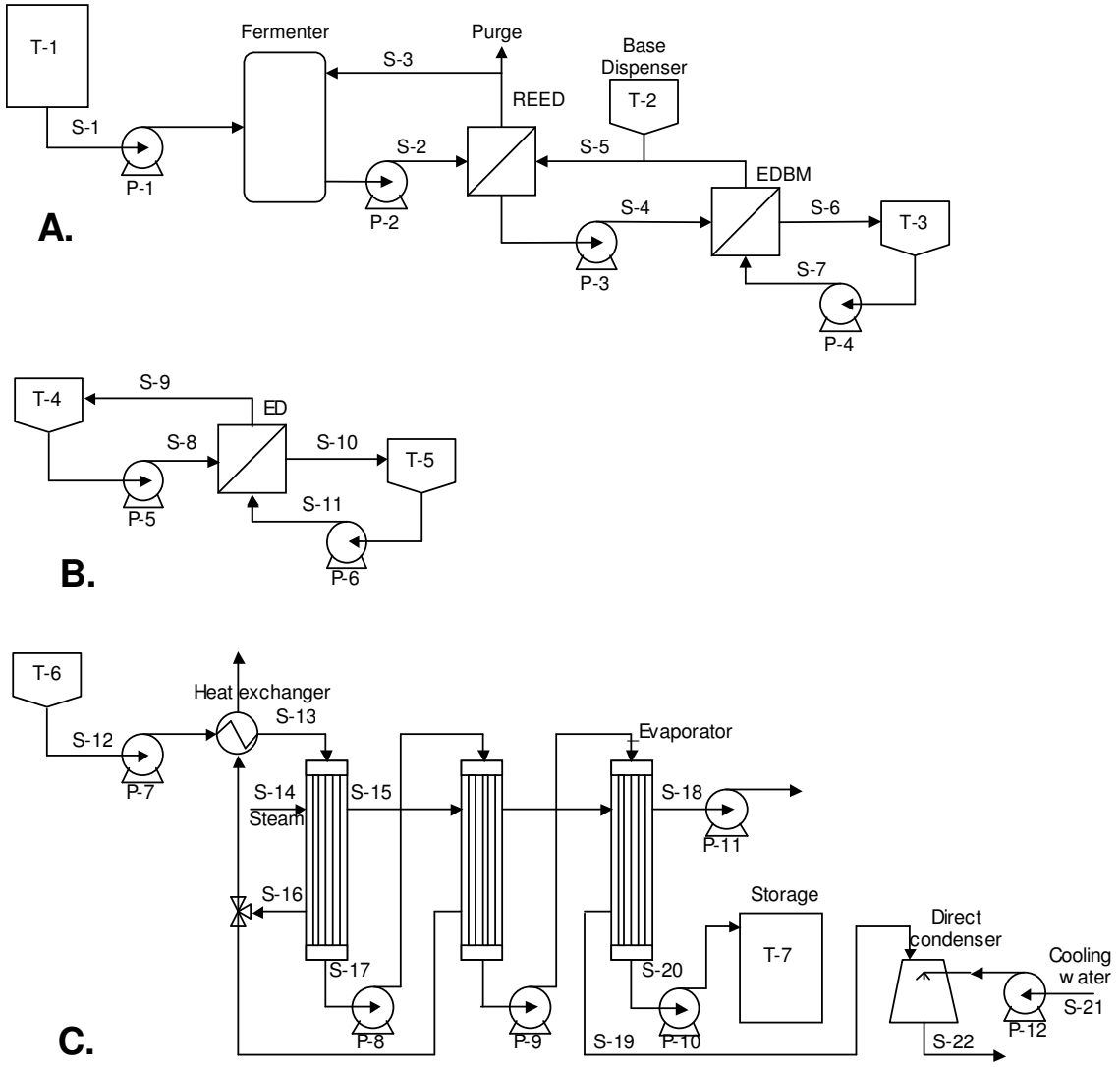

Figure 4.56 Suggested flowsheet for lactic acid production. **A**. From a continuous fermenter, lactate is extracted through a REED unit in cooperation with a EDBM unit that concentrates and acidifies the lactic acid in T-3. **B**. The acidified lactic acid is further purified by ED, where inorganic ions are removed. **C**. Finally, the lactic acid is concentrated to final product level through evaporation.

Sub-process A

From the feed tank (T-1) substrate is pumped to the recycle fermenter where sugars are fermented to yield lactic acid. A stream (S-2) is taken out and pumped to the reverse electro-enhanced dialysis (REED) unit. Lactate ions are replaced with hydroxide ions before the stream is recycled to the fermenter for pH control and higher substrate utilization. As very little water is transferred across the ion-exchange membranes in the REED, a stream corresponding to the substrate flow (S-1) is purged after the REED to preserve fermenter volume. The alkaline stream (S-4) containing lactate is pumped to the bipolar electrodialysis (EDBM) unit where lactate and any inorganic anions are concentrated and acidified in a tank (T-3). The base is regenerated and returned to the REED after make-up of the base from an alkaline storage tank (T-2). When the concentration of lactic acid in

the product tank (T-3) has reached a certain level (~20%), the acid solution is transferred to sub-process B for further purification.

Sub-process B
The acidic liquid from the EDBM process is fed to an electrodialysis (ED) unit operated as a batch process. In the ED process inorganic ions are removed from the lactic acid in T-4 and concentrated in a tank (T-5). Afterwards, the purified acid in the first tank (T-4) is connected to sub-process C.

Sub-process C
The purified lactic acid is concentrated to 88% in a series of three falling film evaporators. The acid is preheated with the pooled condensate from the first two effects before it is feed to the first effect. External steam (S-14) is supplied to the first effect, resulting in evaporation of water (S-15) which is used to drive the subsequent effect. The concentrated lactic acid leaves the bottom (S-17) to be fed to the next effect. From the last effect 88% product (S-20) is pumped to a storage tank (T-7) and the partly condensed stream (S-19) is taken to a direct condenser.

This process has been submitted and is pending patent approval (DK01/00810-PCT). The patent application is attached as appendix 7.3.

4.5.3 Unit operations specification

The sizing of each unit operation is based on some overall process assumptions combined with design parameters attained through experiments or modeling.

Overall process assumptions:

- Produces 10,000 tons 88 w-% lactic acid per year.
- Operation time of 8000 h/yr.
- Substrate is brown juice from grass pellet production.

Operation time is based on continuous production including equipment-cleaning rotation, but excluding plant downtime.

4.5.3.1 Recycle fermenters

The fermentation is done in upflow anaerobic sludge blanket (UASB) reactors with a recycle loop for product removal and pH control. The lactic acid bacteria (LAB) are immobilized on granules inside the fermenters, which minimizes the amount of biomass in the stream leaving the top of the fermenters.

Specifications

- Six separate upflow anaerobic sludge blanket bioreactors.
- Dilution rate, D, set to 0.1 h^{-1}.
- 8% sugar in the feed solution.
- Yield, Y_{SP} = 95%.
- pH 4.5.
- Recycle rate, R = 6 times the feed flow rate.
- Degree of filling, Θ = 80%.

- Production of other organic acids than the targeted acid is insignificant.
- Temperature kept at 40°C.

The relatively large number of parallel operating fermenters has been chosen to minimize the impact on the continuous production from harmful effects like cell contamination or equipment breakdown. The dilution rate is relatively low due to the complex composition of sugars in the substrate. A 95% yield is assumed based on experiments performed by this research group (Garde *et al.* 2002). The fermentation is performed under non-sterile conditions and to diminish the risk of contamination, pH is kept below 4.5. A relatively low recycle rate is chosen to prevent flushing the bacteria granules out of the fermenters. The filling degree is the utilized fermenter volume.

The Lactobacillus bacteria chosen for the fermentation produce mainly lactate, but minor amounts of other organic acids are present in the substrate. Fermentation temperature is close to the optimum growth conditions of the bacteria, and no heat-exchange is necessary, since heat is generated in the reverse electro-enhanced dialysis modules, coupled to the fermenters.

Fermenter sizing
Calculation of feed flow rate:

$$Q_F = \frac{Q_P}{Y_{SP} \cdot \theta_{REED} \cdot \theta_{EDBM} \cdot \theta_{ED} \cdot \theta_{EVAP} \cdot C_S \cdot \rho}$$

Q_P (tons/yr) is the annual production rate of lactic acid, Y_{SP} is the "Substrate to Product" yield, C_S (wt-%) is the concentration of sugar in the feed, ρ is the mass density (tons/m^3) and θ is the recovery of lactic acid in each unit operation. Using the process assumptions and inserting values for the different unit operations, Q_F is calculated:

$$Q_F = \frac{10000 t/yr \cdot 0.88}{0.95 \cdot 0.98 \cdot 1.00 \cdot 0.98 \cdot 0.98 \cdot 0.08 \cdot 1.0 t/m^3} = 123{,}024 m^3/yr = 15.4 \, m^3/h$$

An operation time of 8000 hours per year is assumed in this calculation.

To design each fermenter, the volume of each of the six fermenters can be estimated from Q_F and the dilution rate, and taking the filling degree (Θ) into account:

$$V_{Fermenter} = \frac{Q_F}{D \cdot \Theta \cdot N_{Fermenters}} = \frac{15.4 \, m^3/h}{0.1 h^{-1} \cdot 0.8 \cdot 6} = 32 m^3$$

4.5.3.2 Reverse electro-enhanced dialysis (REED)

Specifications

- Neosepta AMX and CMB ion-exchange membranes utilized.
- Purge, P = Q_F.
- Recovery of lactate, θ_{REED} = 98%.
- Current density, i_d = 250 A/m^2.
- Average current efficiency, $\eta_{Current}$ = 0.2

- Shadow effects from sheetflow spacers are insignificant.
- Cleaning cycles, 1 hour cleaning every 10 hours.
- Module stacks are composed of 200 cell-pairs.

Anion-exchange membranes with high alkaline resistance (e.g. AMH) are desired but are also too costly compared to the improvement that is obtained with such membranes. Thus, standard AMX membranes have been chosen and shorter membrane lifetimes must be expected. A new commercial anion-exchange membrane AXE-1 with supposedly improved properties could later replace the AMX membrane.
CMB are only installed to separate the process fluids from the electrode rinsing solutions. Thus, only two CMB membranes are necessary in each module stack.
Since mass balance across the fermenters must be maintained, the mass flow of the purge stream from S-3 must equal the mass flow of substrate (S-1) to the fermenters.
Since lactate not recovered in the reverse electro-enhanced dialysis modules is either purged or returned to the fermenter, a high degree of lactate recovery is presumed, which also stresses the need for a low output concentration in S-3 from the REED.
An average current density for this step is chosen to avoid watersplitting. A relatively low current efficiency is conservatively chosen, based on a combination of results from laboratory experiments on brown juice and computer modeling. It is presumed that higher efficiencies are possible.
Expecting sheetflow with open netspacers, shadowing of membrane area from spacers is assumed to be insignificant. The extra membrane area needed for fixation along the rim of the membranes is not included as prices are obtained for installed square meters of membrane.
Laboratory experiments show that operation times of more than 12 hours are possible without cleaning, but the energy consumption rises during the operation due to some minor degree of fouling that is not reversibly removed during reversal. Hence, the modules are cleaned two to three times a day in rotation.
Usually, membrane stacks are composed of 200-600 cell-pairs. The feed flow spacers are designed to allow passage of particular matter and are therefore a bit thicker than ordinary spacers. This causes a higher resistance over a single cell-pair and to keep the total voltage drop within a reasonable level, 200 cell-pairs are chosen for the REED modules.

<u>REED sizing</u>
The amount of lactate that is removed in the REED can be calculated from the amount of lactate produced in the fermenters, as:

$$m_{Lac} = Q_F \cdot \rho \cdot C_S \cdot Y_{SP} \cdot \theta_{REED} = 15.4\,m^3/h \cdot 1000\,kg/m^3 \cdot 0.08 \cdot 0.95 \cdot 0.98 = 1145\,kg/h$$

From the amount of lactate that is transferred, the corresponding active membrane area can be found, taking into account the current efficiency and current density:

$$A_{Active} = \frac{m_{Lac}}{MW_{Lac}} \cdot \frac{|z_{Lac}|F}{i_d \cdot \eta_{Current}} = \frac{1145\,kg/h}{90.08 \cdot 10^{-3}\,kg/mol} \cdot \frac{1h}{3600s} \cdot \frac{|-1| \cdot 96487\,As/mol}{250\,A/m^2 \cdot 0.2} = 6814m^2$$

Since each cell pair is made up of two anion-exchange membranes, twice the calculated active membrane area is required. Shadow effects from the spacers are considered insignificant, making the necessary actual membrane area:

$$A_{REED,needed} = 2 \cdot A_{Active} = 13{,}627 m^2$$

For cleaning purposes, it is assumed that some of the REED modules are going through cleaning cycles. Some of the membrane area is unavailable for production during cleaning, making the total anion-exchange membrane area an estimated 10% larger:

$$A_{REED,AMX} = 1.1 \cdot A_{REED,needed} = 14{,}990 m^2$$

Since two CMB membranes are necessary for every 400 AMX membranes, the required CMB membrane area is:

$$A_{REED,CMB} = A_{REED,AMX} \cdot \frac{2}{400} = 75 m^2$$

4.5.3.3 Bipolar electrodialysis (EDBM)

Specifications

- BP-1, AMH, CMB ion-exchange membranes utilized.
- 100% recovery of lactate.
- Current density, i_d = 1000 A/m^2.
- Current efficiency, $\eta_{Current}$ = 0.72
- Shadow effects from sheetflow spacers are insignificant.

Anion-exchange membranes with high resistance to alkaline conditions are required in the three-compartment setup used in the EDBM.
Though lactate is not extracted totally during the EDBM pass, lactate is recycled between the REED and the EDBM modules. Thus, all lactate is eventually recovered as lactic acid into the acid storage tank (T-3).
Current density and current efficiency is based on results from laboratory experiments.

EDBM sizing

The amount of lactate that must be transferred in the EDBM is equal to the amount, transferred in the REED. The active membrane area needed for this operation can be calculated by:

$$A_{Active} = \frac{m_{Lac}}{MW_{Lac}} \cdot \frac{|z_{Lac}|F}{i_d \cdot \eta_{Current}} = \frac{1145\,kg/h}{90.08 \cdot 10^{-3}\,kg/mol} \cdot \frac{1h}{3600s} \cdot \frac{|-1| \cdot 96487\,As/mol}{1000\,A/m^2 \cdot 0.72} = 473 m^2$$

Each cell pair consists of an AMH anion-exchange membrane, a CMH cation-exchange membrane and a BP-1 bipolar membrane. Since lactate is only transferred across the anion-exchange membrane, the necessary membrane area for each membrane type equals the active membrane area.

4.5.3.4 Electrodialysis (ED)

Specifications

- AMX and CMH ion-exchange membranes utilized.
- 98% recovery of lactate.

- Current density, i_d = 250 A/m^2.
- Current efficiency = 0.98.
- Inorganic ions content corresponding to 10% of lactic acid concentration.
- Shadow effects from sheetflow spacers are insignificant.

Due to the acidic conditions in this separation, membranes with high chemical resistance are preferred. The new AXE-1 membrane would properly be a better choice than AMX, but prices have not been available for this membrane.
Even though lactic acid is not charged at this stage it is assumed that around 2% diffuses through to the concentration loop and is lost in the purification.
The amount of inorganic ions to be removed is depending on the initial concentration in the substrate, but approximately 10% compared to the lactic acid content is considered realistic.

ED sizing
The membrane area needed for the ED-stack can be calculated from:

$$A_{Active} = \frac{m_{Lac}}{MW_{Lac}} \cdot 0.1 \cdot \frac{|z_{Lac}|F}{i_d \cdot \eta_{Current}}$$
$$= \frac{1145\,kg/h}{90.08 \cdot 10^{-3}\,kg/mol} \cdot 0.1 \cdot \frac{1h}{3600s} \cdot \frac{|-1| \cdot 96487\,As/mol}{250\,A/m^2 \cdot 0.98} = 140m^2$$

The active membrane area equals the amount of both anions-exchange membrane and cation-exchange membrane needed.

4.5.3.5 Evaporator

Multiple-effect vertical long tube (VLT) falling film evaporation was evaluated for concentration of the lactic acid solution leaving the ED-unit. A simulation program developed at DTU (Nordkvist and Grotkjær 2000) was applied for performed the calculations. The simulation program uses a modified Raoult's Law and UNIFAC 2 parametric model for the bubble point calculations.

Specifications
- 98% recovery of lactate.
- 18% lactic acid in the solution entering the first effect.
- 88% lactic acid is leaving the last effect.
- Solution entering the first effect is at the boiling point.
- The evaporator consists of six effects.

Even though no loss of lactic acid in the vapor fraction from each effect is assumed to ease the simulation, a recovery of 98% is assumed afterwards for a more realistic evaluation. The feed to the evaporator is heated to the boiling point in a heat exchanger before entering the first effect.
From a NPV (Net Present Value) analysis, the optimal number of effects is found to11, but according to APV Anhydro A/S, 6 effects are a more feasible number (Nordkvist and Grotkjær 2000). As shown in Figure 4.57 no significant increase in NPV is obtained by installing 11 instead of 6 effects, so 6 effects are chosen.

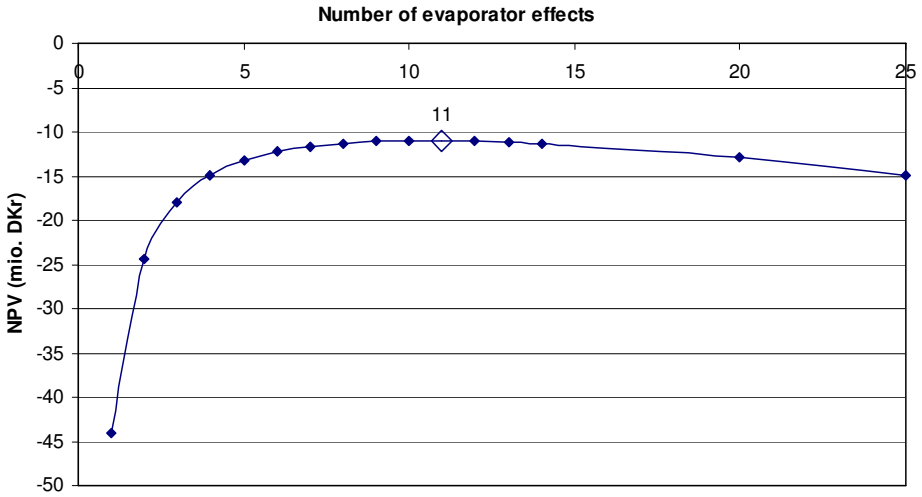

Figure 4.57 Net present value of evaporator operation vs. number of installed effects.

Evaporator sizing

Simulation of the evaporation process using six evaporator effects yields the result given in Table 4.3.

Effect	**1**	**2**	**3**	**4**	**5**	**6**
Temperature (K)	378	373	366	359	349	318
Pressure (mmHg)	858	706	558	413	265	33
BPE (K)	1,16	1,31	1,53	1,94	2,94	14,35
Liquid inflow (kg/h)	7086	6284	5427	4516	3555	2546
Liquid outflow (kg/h)	6284	5427	4516	3555	2546	1449
Vapor outflow (kg/h)	802	857	910	961	1010	1096
Lactic acid in feed (w-%)	18,0	20,3	23,5	28,2	35,9	50,1
Lactic acid in effluent (w-%)	20,3	23,5	28,2	35,9	50,1	88,0
U (W/m^2K)	2313	2185	2019	1787	1404	424
Heat transfer area (m^2)	55,0	55,0	55,0	55,0	55,0	55,0

Table 4.3 Performance of evaporator effects. Output from visual basic simulation program (Nordkvist and Grotkjær 2000).

Each effect is 55 m^2, which adds up to a total heat exchange area of 330 m^2.

4.5.4 Cost estimations

Equipment prices are estimates from data, primarily obtained through vendor quotations, books or journals or from a design project on lactic acid production completed at the Department of Chemical Engineering in 2000 (Nordkvist and Grotkjær 2000). Estimates on fermenter and evaporator costs are obtained from appropriate industrial contacts and have been scaled to match the present requirements using the following exponential scaling expression (Sinnott 1993):

Equation 4.34 $$New \quad \cos t = Original \quad \cos t \cdot \left(New \quad size \Big/ Original \quad size \right)^{n}$$

Where *n* is a specific equipment index according to Table 4.4. Prices for storage and process tanks can be estimated through the following expression:

Equation 4.35 $$Ce = C \cdot S^{n}$$

Ce is the equipment cost, C is a cost constant and, S is a size parameter given in Table 4.4. The calculated cost is a base cost for equipment made of carbon steel, which must be adjusted if other materials are chosen. If stainless steel or monel is utilized, the base cost is multiplied with 2.5 or 3.4, respectively (Sinnott 1993).

Equipment	Size range	Cost constant	Index
Process tanks	10-100m^3	1500	0.60
Storage tanks	50-8000m^3	1200	0.55
Evaporator	-	-	0.52

Table 4.4 Purchase cost factors for use in equation (Sinnott 1993).

The equipment cost for the electro-membrane processes are based on the price given in Table 4.5 below:

Membrane area	AMX[a]	AMH[b]	CMB[a]	CMH[b]	BP-1[a]
< 50 m^2	232	529	417	951	2,000
51-100 m^2	185	422	370	844	1,800
101-300 m^2	167	381	334	762	1,530
> 301 m^2	157	358	306	698	1,350

Table 4.5 Price in DM/m^2 for Neosepta ion-exchange membranes including module and utilities. The prices for the standard membranes ([a]) are provided by Tokuyama Europe GmbH, Düsseldorf, Germany (1999). Prices for special grade membranes ([b]) are found by multiplying the prices for standard membranes with a factor of 2.28, information provided by Eurodia, Wissous, France (2000).

Equipment prices are updated to 2001 prices using the "Chemical engineering plant cost index" in Table 4.6. The equipment cost for electro-membrane processes have not been adjusted to 2001 prices using Table 4.6, as this type of equipment belongs to a fairly young category of processes, where development of better technology and growing utilization tends to lower prices. This is supported by the appearance of new and cheaper membranes with better performance, e.g. AXE-1 from Tokuyama.

Year	Price index
1992	358,2
1996	381,7
1997	386,5

1998	389,5
1999	390,6
2000	392,0
2001	394,5

Table 4.6 Chemical engineering plant cost index (Hermia 1982;Schmidt and Ahring 1996). The index for 2001 was extrapolated from earlier date.

The exchange rates used for conversion of currencies into Danish Kroner (DKK) are given in Table 4.7.

Currency	Exchange rate
British Pound	12.20
US Dollars	8.66
German Marks	3.81

Table 4.7 Exchange rate for various currencies to DKK.

4.5.4.1 Fermenters

The equipment cost for the fermenters are based on a recent estimate (2000) from Aage Christensen A/S who suggested AISI 304 stainless steel tanks delivered from a local supplier (Nordkvist and Grotkjær 2000). The price for six fermenters with a volume of 11 m^3, including instrumentation and control was estimated to DKK 2,500,000. Inserting this estimate, the calculated fermenter volume and using the exponent from Table 4.4 "Process tanks" in Equation 4.34 yields:

$$C_2 = 2{,}500{,}000 \cdot \left(32/11\right)^{0.60} = 4{,}745{,}000 \quad DKK$$

Taking the changes in the plant cost index from 2000 to 2001 into account only changes the price insignificantly.

4.5.4.2 REED

The cost of the REED equipment is found by multiplying the calculated membrane area with the prices supplied for AMX and CMB in Table 4.5:

$(14{,}990 m^2 \cdot 157\ DM/m^2 + 75 m^2 \cdot 306\ DM/m^2) \cdot 3.81\ DKK/DM = 9{,}054{,}000\ DKK$

4.5.4.3 EDBM

The cost of the EDBM equipment is found by multiplying the calculated membrane area with the prices supplied for AMH, CMB and BP-1 in Table 4.5:

$473 m^2 \cdot (358\ DM/m^2 + 306\ DM/m^2 + 1{,}350\ DM/m^2) \cdot 3.81\ DKK/DM = 3{,}629{,}000\ DKK$

4.5.4.4 ED

The cost of the ED equipment is found by multiplying the calculated membrane area with the prices supplied for AMX and CMH in Table 4.5:

$$140\text{m}^2 \cdot (167\ \text{DM/m}^2 + 762\ \text{DM/m}^2) \cdot 3.81\ \text{DKK/DM} = 496{,}000$$

4.5.4.5 Evaporators

The equipment cost for the evaporator unit is based on a resent estimate performed at APV Anhydro A/S for concentration of 30,000 kg/h 4%-w/w lactic solution in an evaporator with 5 effects and a total heat transfer area of 1470 m^2 (Nordkvist and Grotkjær 2000). The price for this arrangement is 8.8 million DKK. Inserting values of the estimate and the calculated heat transfer area, equipment cost for the evaporator can be calculated from Equation 4.34:

$$C_2 = 8{,}800{,}000 \cdot \left(330/1470\right)^{0.52} = 4{,}047{,}000 \quad DKK$$

The price includes pumps for recirculation, vacuum pump and condenser for the last effect and PCL/PC control.
The optimal area of the installed heat exchanger was found from a NPV analysis utilizing the evaporator simulation program to calculate the decreasing steam requirement as function of increasing heat exchange area and literature (Sinnott 1993) to estimate the equipment price. An optimal heat exchange area of 35 m^2 for the pre-heating the feed to the evaporator resulted is an equipment price of 220,000 DKK. The total price of the last concentration step then becomes 4,267,000 DKK.

4.5.4.6 Tanks

The cost of tanks are evaluated from Equation 4.35 and summarized in Table 4.8.

Tank	Material	Volume	Price (1000 DKK)
T1 (storage)	Carbon steel	2587	1,214
T2	AISI 304	5	110
T3	AISI 316	68	634
T4	AISI 316	68	634
T5	Plastic*	7	100
T6	AISI 316	68	634
T7 (storage)	AISI 316	104	706
Total			2819

Table 4.8 Cost of tanks in 2001 prices. *Fiberglass reinforced plastic – price of tank obtained from internet source: http://www.matche.com/EquipCost/Tank.htm.

The feed storage tank, T1 is designed to hold substrate for 1 week's production and the product storage tank can hold three days production of 88% lactic acid.

4.5.4.7 Pumps

No high performance pumps are used in the plant due to the absence of filtration processes. The price for pumps suitable for this process ranges from 12,000-18,000 DKK, which is very limited compared to the other equipment pieces. An estimate for the approximately 30 pumps used in the plant is based on data supplied by Grundfoss A/S and reaches a value of 450,000 DKK.

4.5.5 Total capital investment

The total capital investment required for the lactic acid plant is summarized in Table 4.9. Estimation of the total direct and indirect plant costs is based on the factor method described by Peters and Timmerhaus, where the cost of each item is found by multiplying the total equipment cost with a specific multiplication factor applicable for a fluid-processing chemical plant (Sinnott 1993).

Item	Investment (1,000 DKK)	Multiplication factor
Fermenter	4,745	
REED	9,054	
EDBM	3,629	
ED	496	
Evaporator	4,267	
Tanks	2,819	
Pumps	450	
Total equipment cost	25,460	
Installation	11,966	0.47[1]
Instrumentation and controls	7,638	0.30[1]
Piping	16,804	0.66[1]
Electrical work	2,801	0.11[1]
Buildings	4,583	0.18[1]
Yard improvement	2,546	0.05[1]
Service facilities	17,822	0.70[1]
Land	1,528	0.06[1]
Total direct plant cost	91,147	
Engineering and supervision	8,402	0.33[1]
Construction expenses	10,439	0.41[1]
Total direct and indirect plant cost	109,987	
Contractors fee	5,499	0.05[2]
Contingency	10,999	0.10[2]
Fixed capital investment	126,485	
Working capital	18,973	0.15[3]
Total capital investment	**145,458**	

Table 4.9 Budget for total capital investment. The multiplication factor refers to: [1] = Total equipment cost, [2] = total direct and indirect plant cost, [3] = fixed capital investment.

Contractor's fee and contingency are found by applying a multiplication factor to the total direct and indirect plant cost and the sum of these three numbers gives the fixed capital investment. Adding the working capital to the fixed capital investment gives the total capital investment for the project.

4.5.6 Total production cost

The total production cost is composed of the direct production cost, the indirect production cost, fixed charges and general expenses. The method is adapted from Peters and Timmerhaus (Sinnott 1993), but the division entries follow the procedures suggested in Danish accounting (adapted from (Nordkvist and Grotkjær 2000). The total production costs are summarized in Table 4.10 and the specific items are described in details in subsequent paragraphs.

Item	(1000 DKK)
Raw materials	370
Power and utilities	18,078
Maintenance	12,649
Operating labor	4,500
Operating supplies	1,897
Total direct production cost	37,494
Laboratory charges	675
Supervisory labor	1,250
Plant overhead	5,271
Total indirect production cost	7,196
Real estate taxes	122
Insurance	1,265
Fixed charges	1,387
Administration	1,125
Distribution and marketing	1,967
General expenses	3,092
Total production cost	**49,169**

Table 4.10 Total production cost calculation scheme.

4.5.6.1 Direct production costs

Raw materials

The use of raw materials is summarized in Table 4.11. As a point of reference the price of substrate has been set to zero, which is true if, for instance, brown juice or whey permeate is utilized as

feedstock. (The green crop drying industry has expenses amounting to approx. 20 DKK/ton for brown juice disposal.) If, on the other hand, molasses or hemicellulose from wheat straw were utilized the price of substrate would be around 1.30 DKK or 2.00 DKK per kg lactic acid produced, respectively.

Item	Amount	Unit	DKK/unit	Annual cost (1000 DKK)
Substrate	9,842	ton	0/(1300-2000)	0/(12,795-17,600)
Sodium hydroxide	40	ton	3000	120
Bacteria	-	-	-	250
Total				370/(13,165-17,970)

Table 4.11 Annual cost of raw materials.

In the alkaline process stream that is circulated between the REED and the EDBM an estimated amount of 40,000 kg sodium hydroxide is added to makeup for loss, giving an annual cost of 120,000 DKK. An estimated annual price for bacteria is 250,000 DKK by contacts in fermentation industry.

Power and utilities

The requirements for power and utilities are summarized in Table 4.12. The energy consumption in the three membrane processes is calculated based on experimental data and scaled to fit parameters of large-scale equipment. The simulation program that is also used for evaporator sizing, calculates steam and cooling water requirements in the evaporator. The effluent treatment cost is taken from (Nordkvist and Grotkjær 2000).

Item	Amount	Unit	DKK/unit	Annual cost (1000 DKK)
REED	21,033	MWh	340	7,151
EDBM	22,595	MWh	340	7,682
ED	208	MWh	340	71
Pumping	1,022	MWh	340	347
Steam (Evap.)	8,569	tons	125	1,071
Cooling water (Evap.)	876,631	m^3	0,18	158
Effluent treatment	123,024	m^3	13	1,599
Total				18,078

Table 4.12 Annual cost of power and utilities.

Maintenance

Peters and Timmerhaus (Sinnott 1993) suggests that the annual maintenance cost is found as a percentage of the fixed capital investment, ranging from 2-6% for simple chemical processes and 7-11% for complicated processes with extensive instrumentation or corrosive conditions. The present process is not especially corrosive nor is extensive instrumentation required, but membranes have to be replaced after approximately 1-5 years. The average annual maintenance cost is estimated to be 10% of the fixed capital investment with 4% on labor and 6% on materials giving a total of 12,649,000 DKK.

Operating labor

It is considered likely that the plant can be operated by 3 operators in 8 hours shifts. Since the number of production hours are 8000 and one man-year is approximately 1680 hours 15 operators needs to be employed. The annual wages are 300,000 DKK per operator. Hence, the cost of operating labor is estimated to 4,500,000 DKK.

Operating supplies

Operating supplies covers many miscellaneous supplies needed to keep the process functioning efficiently. Peters and Timmerhaus (Sinnott 1993) suggest a value of 15% of the annual maintenance cost for operating supplies, which yields the amount of 1,897,000 DKK annually.

4.5.6.2 Indirect production costs

It is considered likely that the product is sold from the factory in truck loads and thus shipping and packing are neglected is this evaluation.

Laboratory charges

The cost of laboratory work for control of operations and for product-quality control is often taken as 10-20% of the operating labor (Sinnott 1993). In the present evaluation 15% is used, giving a total of 675,000 DKK /year.

Supervisory labor

It is estimated that 2 general foremen and a works engineer are required with an annual salary 400,000 DKK and 450,000 DKK, respectively. Thus, the annual cost of supervisory labor is 1,250,000 DKK.

Plant overhead

The plant overhead is taken as 60% of the total expenses for operating, supervisory and maintenance labor, resulting in an annual cost of 5,271,000 DKK. (Peters and Timmerhaus suggests 50-70%).

4.5.6.3 Fixed charges

Real estate taxes

Real estate taxes are taken to be 2% of the cost of land and buildings resulting in an annual cost of 122,000 DKK.

Insurance

The annual cost of insurances are normally 1% of the fixed capital investment (Sinnott 1993) giving an annual cost of 1,265,000 DKK.

4.5.6.4 General expenses

Administration

Administration costs correspond to 20-30% of the annual cost of operating labor. A value of 25% is used here yielding an annual cost of 1,125,000 DKK.

Distribution and marketing

Distribution and marketing costs vary widely for different chemical plants ranging from 2-20% of the total production cost. The higher figure usually applies for new products sold in small quantities and the low figure applies to large-volume products, such as bulk chemicals (Sinnott 1993). A value of 4% have been used in this evaluation as lactic acid is a bulk chemical, but new suppliers have to operate in a market where competition is considered to be hard (Nordkvist and Grotkjær 2000).

4.5.7 Annual balance

Even though the demand has increased, the price of lactic acid has been falling over the past 5-6 years due to toughened competition (Mirasol 1999). The current price (Dec. 2000) in U.S. for 88% food grade is 70-80 cent/lbs. In Europe the prices are generally lower than the U.S. level, which is due to cheap Chinese products entering the European market. Prices on 88% material have been as low as 50 or 60 cent/lbs and the 80% Chinese-grade sells at roughly 52 cents/lbs in Europe (Mirasol 1999). The market price range for lactic acid is given in Table 4.13.

Market	Price interval US$/lb	Price interval DKK/kg
US	0.70 – 0.80	13.30 – 15.20
European	0.50 – 0.60	9.50 – 11.40

Table 4.13 Price for 88 w-% food grade (Mirasol 1999). The large difference between US and European prices is caused by Chinese 80% lactic acid that sells at about 0.52 US$/lb in Europe.

Despite insertion of the lowest lactic acid price from Table 4.13 into the balance calculation, a profit close to 50% of the turnover can still be expected as seen from Table 4.14. The numbers obtained in Table 4.14 are considered as the base case.

Item	1000 DKK
Sale of lactic acid	95,000
Total production cost	49,169
Annual profit	**45,831**

Table 4.14 Annual income, total production cost and profit.

In order to evaluate the project from an investor's point of view the total capital investment must be taken into account.

4.5.8 Plant evaluation

The economic evaluation of this project is based on an interest rate of 10%, which represent the minimum acceptable rate of return. Furthermore, the expected lifetime is estimated to 15 years after which the scrap value is set to zero. An estimate of the lifetime is not determined easily as this would require insight into the current and future technologies of competitors. The lifetime depends on the applied technology and is not limited by equipment as this is easily replaced.

For calculating the economic indicators the following expression is applied for calculation of the Net Present Value:

Equation 4.36 $$NPV = -I + P\frac{(1+i)^T - 1}{i(1+i)^T}$$

NPV is the net present value of the project, P is the annual profit, *i* is the interest rate, T is the plant lifetime and I is the capital investment. In the base case where the annual profit is 45,831,000 DKK, the net present value is calculated to 203 million DKK. In Figure 4.58 NPV is plotted as function of lactic acid sales price for a substrate price of 0 and 1.30 DKK/kg lactic acid produced, respectively.

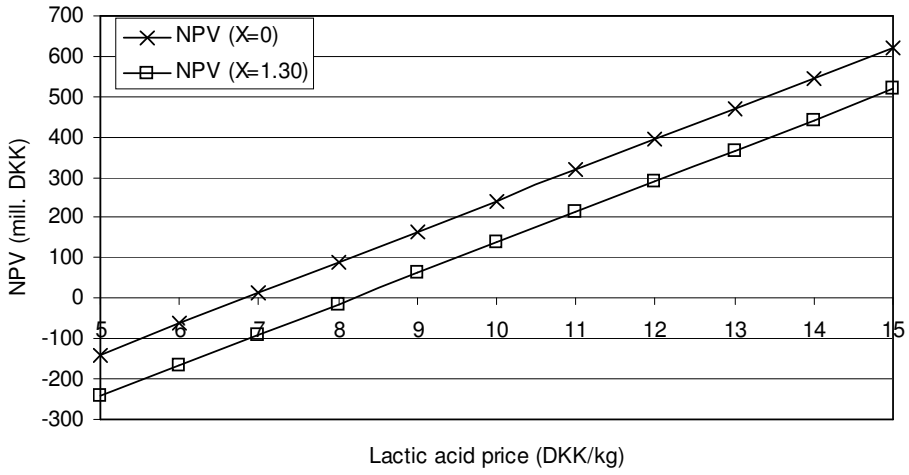

Figure 4.58 Net present value (NPV) of the 145 million DKK investment as a function of lactic acid sales price. X corresponds to the cost of substrate per kg produced lactic acid.

The internal rate of return (IRR) and break even time (BET) are in Figure 4.59 used to illustrate the sensitivity of the investment to different lactic acid sales prices between 7 and 15 DKK/kg. The internal rate of return can be found from Equation 4.36 by setting NPV equal to zero and solving for the interest rate *i*. Break even time is the minimum period before the total capital investment is paid back and can be determined in the same way by solving for the lifetime T.

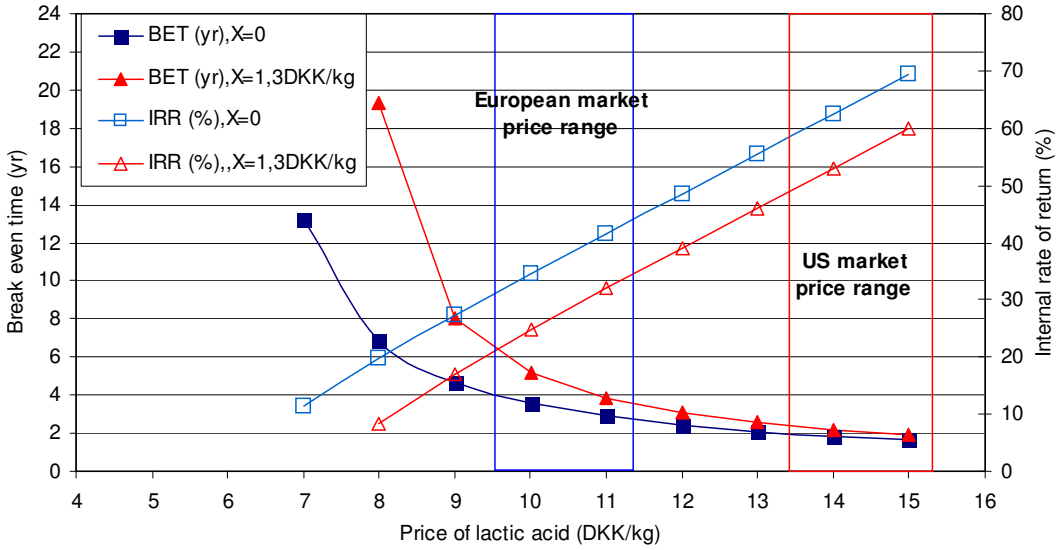

Figure 4.59 Break even time (BET) and internal rate of return (IRR) as function of lactic acid sales price. X corresponds to the cost of substrate per kg produced lactic acid. The vertical lines mark the ranges of the sales prices on the European and US markets, respectively.

In the base case the internal rate of return is 31% and the break even time is 4.0 years. If the lactic acid price improves to 11.40 DKK/kg the internal rate of return would be 44%. Alternatively, if the substrate price increases to 1.30 or 2.00 DKK per kg lactic acid produced internal rate of return will drop to 21 or 15%, respectively.

Due to a very high lactic acid price on the US market the project is seems very profitable with an internal rate of return between 50-75%, if the products can be sold here. As the factory is considered to be placed in Denmark, a more moderate, but still lucrative business on the European market can be expected. The estimates made throughout this evaluation are mainly considered to be "on the safe side". Hence, the estimated internal rate of return of 15-44%, which makes the lactic acid plant very attractive from an investor's point of view, is not unrealistic at all.

4.6 Conclusion

The purpose of this project was to establish a feasible electro-membrane process for recovering lactic acid produced by fermentation. By investigating and comparing existing suggestions for the separation, a new, unique separation process was established, the reverse electro-enhanced dialysis, which have not to the author's knowledge been previously presented. A patent application of the combination of a reverse electro-enhanced dialysis unit and an electrodialysis unit with bipolar membranes has been filed in Denmark, backed financially by the Technical University of Denmark.

A lactic acid recovery process from continuous fermentation, combining the reverse electro-enhanced dialysis with bipolar electrodialysis, desalting electrodialysis, and evaporation, has been suggested in this chapter. This process seems to be able to circumvent several of the obstacles encountered by other authors. Specifically the separation between the organic acids and the remaining bio-matter in the REED appear be a sensible solution to implement in several fermentation processes to counter product inhibition and improve cell growths.

The low energy efficiency observed during the experiments was later explained by the computer model produced. The time period between current reversals in the REED process must be sufficiently long to allow ion concentration profiles to shift. Otherwise, a membrane buffer-effect prohibits the system to take advantage of the enhanced flux.

The economical aspect of the combined processes was assessed using process parameters from experimental work or conservative estimations. The estimated investment necessary to build the designed plant depends heavily on the investment in electro-membrane process equipment. It is the fairly large area of expensive ion-exchange membrane required that is the primary reason for the relatively large investment costs. The estimated operating costs for the designed plant is low compared to the estimated sales price of the product, yielding a financially attractive prospect.

The REED process appears to be equally functional towards other organic acids and even inorganic acids and amino acids can potentially be targeted for extraction through the patented process. By replacing all the anion-exchange membranes of the REED with cation-exchange membranes and utilizing an acidic collection stream, the process is potentially functional for extraction of organic and inorganic cations as well. This potential has not yet been explored, but the changes involved are few. By utilizing ion-exchange membranes with special properties like monoselective ion-exchange membranes, other potential separations and extractions arise.
The REED process suffers from reduces energy efficiency compared to other electro-membrane processes due to the current reversal that destabilizes fouling layers. Thus, the REED process should be considered for troublesome solutions that hold fouling material, which would debilitate normal electro-membrane processes.

5

5 Commentary

5.1 Equipment design

Equipment design and construction appropriated an unexpected large amount of continued effort during the entire study. The workshop at Department of Chemical Engineering very skillfully evaluated and converted our designs into equipment. But several unexpected flaws were discovered in subsequent testing during optimization of spacer designs. To optimize the energy efficiency and mass transfer coefficient of an electro-membrane process thinner spacers are needed. But while the constructed spacers became thinner and new materials were tested, experiments demonstrated leakage between flow chambers, which rendered the experiments useless. The leakage arose for different reasons and different places. Most often leakage was due to pour sealing between ion-exchange membranes and spacers, which only the fairly thick acrylic spacers with rubber ring seals were able to accommodate. The sealing abilities of spacers made from PVC were generally bad, and the material too soft to maintain stability of the flow channels. Even at the end of this study, the spacer development was progressing toward thinner spacers with better mass transfer. But a lot of experience had to be accumulated on the way.

The general setup was very satisfying by having a flexible design, where several membrane configurations, spacers and setups could easily be utilized. The equipment was easily employed for processes like dialysis, electrodialysis, reverse electrodialysis, electrodialysis with bipolar membranes and the reversed electro-enhanced dialysis processes with minor changes in configuration.

5.2 Experimental work

The experimental work suffered somewhat by the constantly changing equipment designs. Both membrane stack and the external equipments like pumps, power supply, tube system, measurement devices and control devices were replaced and improved with time as necessary. Thus, later results were not always comparable with new results.

5.3 Applications of electro-membrane processes

Throughout the study, the possibilities of employing electro-membrane processes in combination with numerous other processes were evident. The basic electro-membrane setup transports selected ionic species across a nonporous membrane, which is by it self a complex process, but rarely enough for total production need. When an organic acid is recovered or extracted by this means from a primary stream into a secondary stream, this often accomplishes either a selective extraction or a concentration of the species. But higher concentrations of ionic species reduce selectivity of the ion-exchange membranes, and prioritizing between product purity and concentration is most often

necessary. Thus, most electro-membrane processes are successfully combined with other filtration, evaporation or other electro-membrane processes.
In both the cases of citric and lactic acid extraction, two combined electro-membrane steps were planned; first the extraction of the acid from a mixed solution through either standard electrodialysis or reverse electro-enhanced dialysis, then followed by electrodialysis with bipolar membranes for product concentration and acidification. Other well-known process combinations include electrodialysis and reverse osmosis/nanofiltration. Each membrane separation process has some advantages and disadvantages that can often be combined for a more efficient result.

5.4 Further development of the reverse electro-enhanced dialysis process

The patented reverse electro-enhanced dialysis process has been the foundation for the startup of JURAG Separation, which is going to produce electro-membrane process solutions for the biotechnology and food industry. The REED process is being further developed with support from the Technical University of Denmark and the innovation fundation, Øresund Science Park.

6

6 References list

Atkins, P. W. (1992) *Physical Chemistry*. Oxford: Oxford University Press.

Baniel, A. M., Blumberg, R. and Hajdu, K. (1981), US4275234: Recovery of acids from aqueous solutions. Imi Tami Institute Research. USA.

Bazinet,L., Lamarche,F. and Ippersiel,D. (1998) Bipolar-membrane electrodialysis: Applications of electrodialysis in the food industry. *Trends in Food Science & Technology* **9**, 107-113.

Beschkov,V., Peeva,L. and Valchanova,B. (1995), Ion-exchange separation of lactic acid from fermentation broth. *Hungarian Journal of Industrial Chemistry* **23**, 135-139.

Boniardi,N., Rota,R., Nano,G. and Mazza,B. (1996), Analysis of the sodium lactate concentration process by electrodialysis. *Separations Technology* **6**, 43-54.

Boniardi,N., Rota,R., Nano,G. and Mazza,B. (1997a), Lactic acid production by electrodialysis. Part I: Experimental tests. *Journal of Applied Electrochemistry* **27**, 125-133.

Boniardi,N., Rota,R., Nano,G. and Mazza,B. (1997b), Lactic acid production by electrodialysis. Part II: Modelling. *Journal of Applied Electrochemistry* **27**, 135-145.

Borgardts, P., Krischke, W. and Troesch, W. (1998a), US5746920: Process for purifying dairy wastewater.

Borgardts,P., Krischke,W., Trosch,W. and Brunner,H. (1998b), Integrated bioprocess for the simultaneous production of lactic acid and dairy sewage treatment. *Bioprocess Engineering* **19**, 321-329.

Bowen,W.R., Calvo,J.I. and Hernández,A. (1995), Steps of membrane blocking in flux decline during protein microfiltration. *J. Membrane Sci.* **101**, 153-165.

Boyaval,P., Lavenant,C., Gesan,G. and Daufin,G. (1996), Transient and Stationary Operating Conditions on Performance of Lactic Acid Bacteria Crossflow Microfiltration. *Biotechnology and Bioengineering* **49**, 78-86.

Bundgaard, R. and Iversen, S. L. (1992), Thesis: *Citric Acid Factory in Mexico - Extraction from Lime Juice.* Dept. of Biotech., Tech. Uni. of Den.

Böddeker, K. W., Schorm, C., Windmöller, D. and Schorm, C. G. (1997), WO9729203-A1: Organic acid production process uses Donnan-dialysis anion exchanger-membrane - overcoming limited selectivity problems in efficient, highly-selective and lower cost process. GKSS Forschunszentrum Geesthacht, GmbH.

Chiao,Y.C., Chlanda,F.P. and Mani,K.N. (1991), Bipolar Membranes for Purification of Acids and Bases. *J. Membrane Sci.* **61**, 239-252.

Cockrem, M. C. M. and Johnson Pride, D. (1993), WO9300440: Recovery of lactate esters and lactic acid from fermentation broth. DuPont Corporation, USA.

Czytko,M., Ishii,K. and Kawai,K. (1987), Continuous Glucose Fermentation for Lactic Acid Production: Recovery of Acid by Electrodialysis. *Chem. Ing. Tech.* **59 (12)**, 952-954.

Datta, R. and Glassner, D. A. (1990), EP393818: Process for production and purification of lactic acid.

Datta, R. and Tsai, S.-P. (1998), WO9823579: Esterification of fermentation-derived acids via pervaporation. Univ Chicago, USA.

de Raucourt,A., Girard,D., Prigent,Y. and Boyaval,P. (1989), Lactose continuous fermentation with cell recycled by ultrafiltration and lactate separation by electrodialysis: model identification. *Appl. Microbiol. Biotechnol.* **30**, 528-534.

Donnan,F.G. (1911), The theory of membrane equilibrium in presence of a non-dialyzable electrolyte. *Z. elektrochem* **17**, 572.

Eyal, A. M., McWilliams, P., Witzke, D. R. and Gruber, P. R. (1998a), WO9815519: A process for the recovery of lactic acid. Cargill Inc.

Eyal, A. M., McWilliams, P., Witzke, D. R. and Gruber, P. R. (1998b), WO9815519: A process for the recovery of lactic acid. Cargill Inc., USA.

Garde, A. (1997), Thesis: *Oprensning og separation af mælkesyre ved hjælp af elektrodialyse (Separation of lactic acid using electrodialysis).* Dept. Chem. Eng., Tech. Uni. Of Den.

Garde,A., Jonsson,G., Schmidt,A.S. and Ahring,B.K. (2002), Lactic acid production from wheat straw hemicellulose hydrolysate by Lactobacillus pentosus and Lactobacillus brevis. *Bioresource Technology* **81**, 217-223.

Garde, A. and Rype, J.-U. (1997), Master thesis: *Oprensning og separation ved hjælp af elektrodialyse II (Separation using electrodialysis II)*. Dept. Chem. Eng., Tech. Uni. Of Den.

Hermia,J. (1982), Constant Pressure Blocking Filtration Laws Application to Powerlaw Nonnewtonian Fluids. *Trans Inst Chem Eng* **60**, 183-187.

Hongo,M., Nomura,Y. and Iwahara,M. (1986), Novel Method of Lactic Acid Production by Electrodialysis Fermentation. *Applied and Enviromental Microbiology* **August**, 314-319.

Jeantet,R., Maubois,J.L. and Boyaval,P. (1996), Semicontinuous production of lactic acid in a bioreactor coupled with nanofiltration membranes. *Enzyme and Microbial Technology* **19**, 614-619.

Jonsson,G. and Boesen,C.E. (1977), Concentration polarization in a reverse osmosis test cell. *Desalination* **21**, 1-10.

Jonsson, G. and Boesen, C. E. (1984), Polarization phenomena in membrane processes. In *Synthetic membrane processes* pp. 101-130. Academic Press, Inc.

Jørgensen,B.B. and Kjærsgaard,L. (1987), Production of lactic, acetic and citric acid. *Department of Biotechnology*.

Kesting, R. E. (1985), *Synthetic polymeric membranes*. New York/Chichester/Brisbane/Totonto/Singapore: John Wiley & Sons.

Kleerebezem,M., Hols,P. and Hugenholtz,J. (2000), Lactic acid bacteria as a cell factory: rerouting of carbon metabolism in Lactococcus lactis by metabolic engineering. *Enzyme and Microbial Technology* **26**, 840-848.

Koros,W.J., Ma,Y.H. and Shimidzu,T. (1996), Terminology for membranes and membrane processes. *Pure & Appl. Chem.* **68**, 1479-1489.

Krishnakumar,V. (1994), Tartaric acid. Worldwide business review. *International Food Ingredients* **3**, 17-21.

Krol, J. J. (1997), Monopolar and bipolar ion exchange membranes - Mass Transport Limitations. Membrane Technology Group, University of Twente.

Kulozik,U. (1998), Physiological aspects of continuous lactic acid fermentations at high dilution rates. *Applied Microbiology and Biotechnology* **49**, 506-510.

Lee,E.G., Moon,S.-H., Chang,Y.K., Yoo,I.-K. and Chang,H.N. (1998), Lactic acid recovery using two-stage electrodialysis and its modelling. *J. Membrane Sci.* **145**, 53-66.

Lewis, C. C. (1997), Market quiet...at least for now. *Purchasing online* (www.manufacturing.net/magazine).

Liew,M.K.H., Tanaka,S. and Morita,M. (1995), Separation and purification of lactic acid: Fundamental studies on the reverse osmosis downstream process. *Desalination* **101**, 269-277.

Lindstrand,V., Jönsson,A.-S. and Sundström,G. (2000a), Organic fouling of electrodialysis membranes with and without applied voltage. *Desalination* **130**, 73-84.

Lindstrand,V., Sundström,G. and Jönsson,A.-S. (2000b), Fouling of electrodialysis membranes by organic substances. *Desalination* **128**, 91-102.

Mani, K. N. and Hadden, D. K. (1998), US5814498: Process for the recovery of organic acids and ammonia from their salts. Archer Daniels Midland Company, USA.

Miao, F. (1997), US5681728: Method and apparatus for the recovery and purificationof organic acids. Chronopol Inc., USA.

Mirasol, F. (1999), Lactic Acid Prices Falter As Competition Toughens. *Chemical Market Reporter* (March 1), 16.

Moresi,M. and Sappino,F. (1998a), Economic feasibility study of citrate recovery by electrodialysis. *Journal of Food Engineering* **35**, 75-90.

Moresi,M. and Sappino,F. (1998b), Effect of some operating variables on citrate recovery from model solutions by electrodialysis. *Biotechnology and Bioengineering* **59**, 344-350.

Mulder, M. (1991), *Basic Priciples of Membrane Technology*. Dordrecht/Boston/London: Kluwer Academic Publishers.

Muñoz de Chávez, M., Chávez Villasana, A., Roldán Amaro, J. A., Ledesma Solano, J. Á., Mendoza Martínez, E., Pérez-Gil Romo, F., Chaparro Flores, A. G. and Hernández Cordero, S. L. (1996), *Tablas de Valor Nutritivo de los Alimentos - de mayor consumo en México*. México City: Editorial Pax México, Librería Carlos Césarman.

Nomura,Y., Iwahara,M. and Hongo,M. (1987), Lactic Acid Production by Electrodialysis Fermentation Using Immobilized Growing Cells. *Biotechnology and Bioengineering* **30**, 788-793.

Nordkvist, M., Grotkjær, T. (2000), Lactic acid production. *Master Thesis*, Dept. Chem. Eng., DTU.

Novalic,S., Jagschits,F., Okwor,J. and Kulbe,K.D. (1995), Behavior of citric acid during electrodialysis. *J. Membrane Sci.* **108**, 201-205.

Novalic,S. and Kulbe,K.D. (1998), Separation and concentration of citric acid by means of electrodialytic bipolar membrane technology. *Food Technol. Biotechnol.* **36**, 193-195.

Novalic,S., Okwor,J. and Kulbe,K.D. (1996), The characteristics of citric acid separation using electrodialysis with bipolar membranes. *Desalination* **105**, 277-282.

Ohashi,R., Yamamoto,T. and Suzuki,T. (1999), Continuous Production of Lactic Acid from Molasses by Perfusion Culture of Lactococcus lactis Using a Stirred Ceramic Membrane Reactor. *Journal of Bioscience and Bioengineering* **85**, 647-654.

Portner,R. and Markl,H. (2001), Dialysis cultures. *Applied Microbiology and Biotechnology* **50**, 403-414.

Ramirez,P., Aguilella,V.M., Manzanares,J.A. and Mafé,S. (1992), Effects of Temperature and Ion Transport on Water Splitting in Bipolar Membranes. *J. Membrane Sci.* **73**, 191-201.

Rincon,J., Fuertes,J., Rodriguez,J.F., Rodriguez,L. and Monteagudo,J.M. (1997), Selection of a cation-exchange resin to produce Lactic-acid solutions from whey fermentation broths. *Solvent Extraction and Ion Exchange* **15 (2)**, 329-345.

Sappino,F., Mancini,M. and Moresi,M. (1996), Recovery of sodium citrate from aqueous solutions by electrodialysis. *Italian Journal of Food Science* **8**, 239-250.

Schmidt,J.E. and Ahring,B.K. (1996), Granular sludge formation in upflow anaerobic sludge blanket (UASB) reactors. *Biotechnology and Bioengineering* **49**, 229-246.

Scholler,C., Chaudhuri,J.B. and Pyle,D.L. (1993), Emulsion liquid membrane extraction of lactic acid from aqueous solutions and fermentation broth. *Biotechnology and Bioengineering* **42**, 50-58.

Sélégny,E. (1976), *Charged gels and membranes – Part I*. Dordrecht: D. Riedel Publishing Company.

Siebold,M., Frieling,P.v., Joppien,R., Rindfleisch,D., Schügerl,K. and Röper,H. (1995), Comparison of the Production of Lactic Acid by Three Different Lactobacilli and its Recovery by Extraction and Electrodialysis. *Process Biochemistry* **30 (1)**, 81-95.

Sinnott, R. K. (1993), *Chemical engineering*. Oxford: Pergamon Press.

Soine, S. (1998), DE19718608: Continual process to make lactic acid. Germany.

Strathmann,H. (1985), Electrodialysis and its application in the chemical process industry. *Separation and Purification Methods* **14**, 41-66.

Strathmann, H. (1992), Electrodialysis. *Membrane Handbook*. Winston Ho,W.S. and Sirkar,K.K. pp. 217-262. New York: Van Nostrand Reinhold.

Tejayadi,S. and Cheryan,M. (1995), Lactic acid from cheese whey permeate. Productivity and economics of a continuous membrane bioreactor. *Applied Microbiology and Biotechnology* **43**, 242-248.

Timmer,J.M.K., Kromkamp,J. and Robbertsen,T. (1994), Lactic acid separation from fermentation broths by reverse osmosis and nanofiltration. *J. Membrane Sci.* **92**, 185-197.

Timmer,J.M.K., van der Horst,H.C. and Robbertsen,T. (1993), Transport of lactic acid through reverse osmosis and nanofiltration membranes. *J. Membrane Sci.* **85**, 205-216.

Tokoyama (1997), Neosepta Ion-exchange membranes. Tokuyama Corp. Catalog.

Tronc,J.-S., Lamarche,F. and Makhlouf,J. (1997), Enzymatic browning inhibition in cloudy apple juice by electrodialysis. *Journal of Food Science* **62**, 75-78.

Tronc,J.-S., Lamarche,F. and Makhlouf,J. (1998), Effect of pH Variation by Electrodialysis on the Inhibition of Enzymatic Browning in Cloudy Apple Juice. *J. Agric. Food Chem.* **46**, 829-833.

Van Nispen et al. (1991), US5002881: Process for the fermentative preperation of organic acids. Cooperatieve Vereniging Suiker, USA.

Vonktaveesuk,P., Tonokawa,M. and Ishizaki,A. (1994), Stimulation of the rate of L-lactate fermentation using *Lactococcus lactis* IO-1 by periodic electrodialysis. *Journal of Fermentation and Bioengineering* **77**, 508-512.

Zayed,G. and Winter,J. (1995) Batch and continuous production of lactic acid from salt whey using free and immobilized cultures of lactobacilli. *Applied Microbiology and Biotechnology* **44**, 362-366.

Zemel,G.P., Sims,C.A., Marshall,M.R. and Balaban,M. (1990), Low pH inactivation of polyphenol oxidase in apple. *Journal of Food Science* **55**, 562-565.

Zheleznov,A., Windmöller,D., Körner,S. and Böddeker,K.W. (1998), Dialytic transport of carboxylic acids through an anion exchange membrane. *J. Membrane Sci.* **139**, 137-143.

7

7 Appendices

7.1 Citric acid experiments

7.1.1 Model experiments performed at IPN

Results of model experiments on 4% sodium citrate solution as function of initial pH and flow velocity (Q).

Current Efficiency (%)	Q = 1 ml/s	Q = 5 ml/s	Q = 10 ml/s
pH =1.2		133	41
pH = 3.8	36	16	106
pH = 8.3	101		73

Table 7.1 Current efficiency (%).

Flux (mol/m^2/s)	Q = 1 ml/s	Q = 5 ml/s	Q = 10 ml/s
pH =1.2		$3.40 \cdot 10^{-4}$	$9.94 \cdot 10^{-5}$
pH = 3.8	$2.50 \cdot 10^{-4}$	$1.17 \cdot 10^{-4}$	$2.53 \cdot 10^{-4}$
pH = 8.3	$6.25 \cdot 10^{-4}$		$4.22 \cdot 10^{-4}$

Table 7.2 Sodium citrate flux.

Energy Consumption (kWh/kg)	Q = 1 ml/s	Q = 5 ml/s	Q = 10 ml/s
pH =1.2		0.55	1.78
pH = 3.8	1.97	4.45	2.01
pH = 8.3	2.03		2.73

Table 7.3 Energy consumption.

7.1.2 Nanofiltration experiments – calculation of true retention

7.1.2.1 Calculation of boundary layer thickness

The dimensions of the crossflow cell is:
Height: 0.1 cm
Width: 4.0 cm
Length: 10 cm
Hydraulic diameter, d_h: $(4 * S/L_p) = 0.20$ cm

Feed flow, Q_{Feed}: 6.5 dm^3/min (0.11 dm^3/s)

ρ_{Water}: 1.000 g/cm^3
$\rho_{Citric\ acid}$: 1.660 g/cm^3
x_{Citric}: 0.04
ρ_{Feed}: $(1/\Sigma(x_i/\rho_i) = 1.016$ g/cm^3
mFeed : 1 cP (0.001 kg/ms)
$D_{Citrate}$: 1.869 cm^2/s

Feed flow velocity, v_{Feed}: $(Q_{Feed}/S) = 270.83$ cm/s
Reynolds number, Re_{Feed}: $(d_h v\rho/\mu) = 5370$ (Turbulent flow)
Schmidt number, Sc_{Feed}: $(\mu/\rho D_{Citrate}) = 0.0053$
Sherwood number, Sh: $0.023 \cdot Re^{0.8} Sc^{0.33} = 3.9$
δ : (d_h/Sh) **= 0.05 cm**
Mass transfer coefficient, k: $(D_{Citrate}/\delta) = 37.6$ cm/s

7.1.2.2 Graphical deduction of true retention

Values of solvent flux, J_w, feed flow velocity, *v*, and observed retention, S, are used to calculate:

$J_w/v^{0.8}$	ln[(1-S)/S]
$2{,}72955 \cdot 10^{-5}$	-2,7
$2{,}12594 \cdot 10^{-5}$	-2,5
$1{,}74545 \cdot 10^{-5}$	-2,4
$1{,}03454 \cdot 10^{-5}$	-2,0
$6{,}26655 \cdot 10^{-6}$	-1,6

Table 7.4 Calculated values for calculation of true retention, R.

The values are depicted in Figure 7.1 with a trendline showing slope and ordinate axis crossing value.

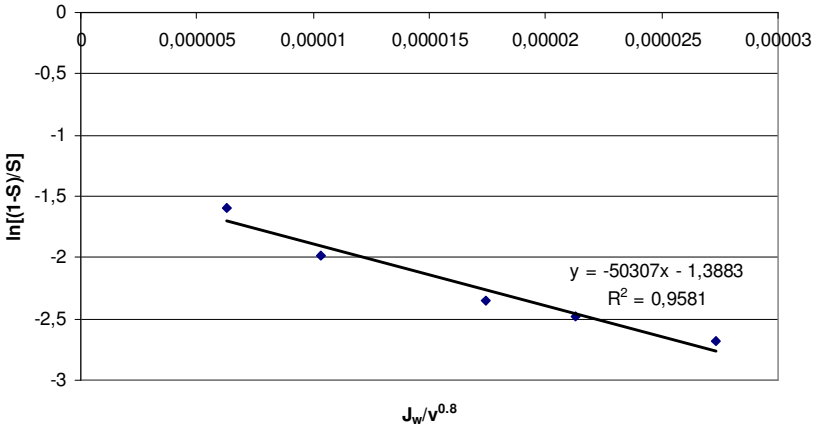

Figure 7.1 Graphical presentation of the data in Table 7.4.

The value of the ordinate axis crossing, a, is equal to ln[(1-R)/R], meaning that the true retention can be found by:

$$R = \frac{1}{e^{a}+1} = \frac{1}{e^{-1.3883}+1} = 0.80$$

The true retention is found to be 80% in this experiment, when the citrate feed pH was 1.9.

7.2 Modeling appendix

7.2.1 Watersplitting modeling

The purpose of modeling the polarization at the membrane surface is to establish the border conditions, necessary for solving the membrane profile. Since polarization in extreme cases leads to watersplitting and limiting lactate flux, Donnan equilibrium is not valid in these cases. A special approach has to be employed in finding the membrane's border-concentration of lactate at x = 0.

Since it is desired that the simulation is programmed to be more versatile, and able to handle a larger range of different inputs, some simple routines have been included in the program to handle watersplitting. This early version of the program only handles equilibrium polarization. After assuming that watersplitting does not take place, initial values of wall concentrations of lactate and hydroxide are found. If either of these values is below zero, a special situation arises. If both values are below zero, definite watersplitting takes place.

If only lactate or hydroxide concentration falls below zero, the actual physical situation arises that the flux of one ion is reduced, while the flux of the other ion increases. Thus, the linear boundary layer model cannot be employed in calculating the wall concentrations. The membrane border-concentration is calculated from a steady-state assumption:

- At steady state, the migration flux in the first membrane "slice" is equal to the collective diffusion and migration flux across the boundary layer. This assumption is illustrated for lactate in Figure 7.2.

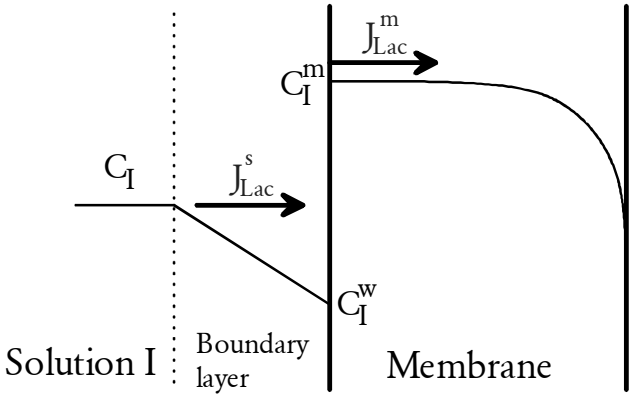

Figure 7.2 Illustration of the assumed steady-state condition that J^s must equal J^m when lactate concentration C^w reaches 0 at the membrane surface because of polarization.

$C^w_{Lac} < 0$:

The case illustrated in Figure 7.2 shows the special case, when lactate concentration reaches zero at the membrane surface as a result of polarization. Even if current density is increased, the lactate flux cannot increase. The surplus of electrical current is then carried by hydroxide ions into the membrane and hydrogen ions away from the surface. These ions arise from watersplitting as explained earlier in the theory chapter.

The lactate flux across the boundary layer, which is the basis for determining the membrane concentration, can then be calculated as:

Equation 7.1 $$J_{Lac}^{BoundaryLayer} = \frac{i_d}{z_{Lac}F} t_{Lac}^{s} + k_{Lac} C_{Lac}^{s}$$

i_d is the current density, z the ionic charge, F the Faraday number, t^s the transport number, k the mass transfer coefficient, and C^s the concentration in the bulk solution just outside the boundary layer. This flux can be readily calculated with knowledge of the bulk solution composition, the current density, and the mass transfer coefficient.
The steady-state membrane-flux included in the assumption is calculated as a pure migration flux:

Equation 7.2 $$J_{Lac}^{Inside\ \ Membrane\ \ Surface} = \frac{i_d}{z_{Lac}F} t_{Lac}^{m}$$

By setting Equation 7.1 equal to Equation 7.2, t^m can be determined, and from the transport number, the membrane concentration of lactate can be determined by combining the definition of t^m with the assumption made in Chapter 4.3 that lactate and hydroxide are the only mobile ions inside the membrane.

Equation 7.3 $$C_{Lac}^{m} + C_{OH}^{m} = C_R$$

C_R is the ion-exchange capacity of the membrane. Rearranging the simplified expression of t^m in Equation 4.9 yields:

Equation 7.4 $$C_{Lac}^{m} = \frac{\mu C_R t_{Lac}^{m}}{1-(1-\mu)t_{Lac}^{m}}, \qquad \mu = \frac{\mu_{OH}^{m}}{\mu_{Lac}^{m}}$$

$C_{Lac}^{w} > 0, \;\; C_{OH}^{w} < 0:$

In this special case, no watersplitting takes place, but the low concentration of hydroxide ions at the membrane surface stills increases the removal of lactate, and again, a different approach has to be taken, to calculate the lactate membrane border-concentration.

The problem is solved analogous to the previous, but this time, the hydroxide flux is considered. The two flux equations (Equation 7.1 and Equation 7.2) written for hydroxide are:

Equation 7.5 $$J_{OH}^{BoundaryLayer} = \frac{i_d}{z_{OH}F} t_{OH}^{s} + k_{OH} C_{OH}^{s}$$

and

Equation 7.6 $$J_{OH}^{Inside\ \ Membrane\ \ Surface} = \frac{i_d}{z_{OH}F} t_{OH}^m$$

Since

$$t_{Lac}^m = 1 - t_{OH}^m$$

the membrane's border-concentration of lactate can now be determined by Equation 7.4. However, it is necessary to check the validation of this solution, since the solution is based on the assumption that the wall concentration of lactate is still above zero. Although the initial estimate found a positive wall concentration, one has to take into account that the increase of lactate flux due to decrease of hydroxide flux, increases the lactate polarization.

The steady-state flux of lactate just inside the membrane surface is estimated as Equation 7.2, and the steady-state assumption that the lactate flux across the boundary layer must equal the membrane's border-flux yields the following expression:

Equation 7.7 $$J_{Lac}^{Inside\ \ Membrane\ \ Surface} = J_{Lac}^{BoundaryLayer} = \frac{i_d}{z_{Lac}F} t_{Lac}^s + k_{Lac}\left(C_{Lac}^s - C_{Lac}^w\right)$$

From Equation 7.7 the lactate wall concentration can be found:

Equation 7.8 $$C_{Lac}^w = C_{Lac}^s + \frac{\frac{i_d}{z_{Lac}F} t_{Lac}^s - J_{Lac}^{Inside\ \ Membrane\ \ Surface}}{k_{Lac}}$$

If the wall concentration of lactate is still positive, the assumption of increased polarization without watersplitting is correct, and the border-concentration as well as the wall concentration of lactate is ratified. If new estimation of the wall concentration on the other hand is negative, then the assumption must be discarded, since watersplitting occurs. The border-value for lactate's membrane concentration must then be found as described in the previous special case.

7.2.2 Simulation program

This simulation program was written in FORTRAN using Plato 2 compilation software from Salford Software Ltd., United Kingdom.

```
      Program Profile

      Integer I,J,K,N,IREV,NUMX,Round,TID,QANSOL
      Double Precision U(0:100,0:100),C(0:100,0:100)
      Double Precision CLW(2,0:100),COHW(2,0:100)
      Double Precision DT,DX,CLIN,CLOUT,PH(2),INISLOPE,DL,DOH
      Double Precision DIFF(0:100),ERROR,UITER(0:100)
      Double Precision CURDENS,FARADAY,ML,MOH,MNA,MH,DIFLAYER(2)
      Double Precision MASSTL(2),MASSTOH(2),MASSTNA(2)
      Double Precision IFL,IFOH,MOBL,MOBOH,ALFA,MY,COHIN,COHOUT
      Double Precision L,DML,DMOH,MEMCAP,SWELLING,IDF,CNAW,TM,TS
      Double Precision DNA,FLUXL(4,0:100),FLUXOH(2,0:100)
      Double Precision A0,A1,A2,DISC,FLUXDIF,CUREFF(4,100)
      Double Precision QACOEF(0:4),QASOL(1:4),QASOLI(1:4)
      Character Answer
      Logical LSPLIT,OHSPLIT

C ALFA is a composit constant, MEMCAP is the membrane's ion-capacity
C MY is the relationship between the mobility of OH and Lactate ions
C DML and DMOH are diffusion coefficients of Lactate and OH inside the membrane
C CLIN/CLOUT are the lactate concentration of the two extrenal solution on both sides
C PH is a vector containing the pH-values of IN (=1) and OUT (=2)
C INISLOPE is the initial diffusion-determined concentration slope through the mem
C MASSTL and MASSTOH are the mass transfer coefficients respectively of LACTATE and
C       OH in the external filmlayer
C IFOH and IFL are composit constants: Id/F times mobility of either OH or Lactate
C ERROR and DIFF are iteration error constants
C MOBOH and MOBL are the sum of the mobility of the cation and either OH or Lactate
C UITER is a vektor to calculate the iteration error
C CLW and COHW are membrane wall concentration vectors for Lactate and OH; IN (=1) and OUT
(=2)
C FLUX is a flux vector [mol/m2s] of the changing flux of Lactate or OH; IN (=1) and OUT (=2)
C ACF is the accumulated flux used for calculating the current efficiency CUREFF, which is
C calculated for each step (=1) and accumulated from 0 to index (=2)
C MIGIN is the constant electrical migration of lactate into the external boundary layer
C CNAW is the cation concentration at the membrane wall
C ML, MOH, and MNA are mobilities, and DL, DOH, and DNA are diffusion coefficients of either
C       Lactate, OH, or the cation

C Clearing matrices
      DO 30 I=0,100
        DO 20 J=0,100
        C(I,J)=0.D0
        U(I,J)=0.D0
        CLW(1,J)=0.D0
        CLW(2,J)=0.D0
        COHW(1,J)=0.D0
        COHW(2,J)=0.D0
        FLUXL(1,J)=0.D0
```

```
        FLUXL(2,J)=0.D0
        FLUXL(3,J)=0.D0
        FLUXL(4,J)=0.D0
        FLUXOH(1,J)=0.D0
        FLUXOH(2,J)=0.D0
 20     Continue
 30    Continue

C Setting physical constants
       TID=100
       CURDENS = 250.D0
       FARADAY = 96487.D0

       IDF=CURDENS/FARADAY

C       Solution constants
       ML = 0.00000004023D0
       MOH = 0.0000002064D0
       MNA = 0.0000000519D0
       MH = 0.0000003623D0
       DIFLAYER(1) = 0.000059D0
       DIFLAYER(2) = 0.000059D0
       DL = ML*0.0256907054836D0
       DOH = MOH*0.0256907054836D0
       DNA = MNA*0.0256907054836D0
       Do 5 I=1,2
         MASSTL(I) = DL/DIFLAYER(I)
         MASSTOH(I) = DOH/DIFLAYER(I)
         MASSTNA(I) = DNA/DIFLAYER(I)
    5  Continue
       IFL = CURDENS/FARADAY*ML
       IFOH = CURDENS/FARADAY*MOH
       MOBL = ML+MNA
       MOBOH = MOH+MNA

C       Membrane constants
       SWELLING = 0.30D0
       L = 200.D0/1000000.D0
       MEMCAP = 2.D0*1000.D0
       MY = MOH/ML
       ALFA = IDF*MY*MEMCAP
       DMOH = DOH*(SWELLING/(2.D0-SWELLING))**2
       DML = DL*(SWELLING/(2.D0-SWELLING))**2

C       INPUT of physical problem
       Write (*,*) 'Current density = ',CURDENS,'A/m2'
       Write (*,*) 'Membrane capacity = ',MEMCAP,'mol/m3'
       Write (*,*) 'Membrane thickness = ',(L*1000000.D0),'micrometer'
       Write (*,*) 'Diffusion layer´s Mass Trasfer Coefficient = ',
     1    MASSTL(1),' m/s'
       Write (*,*) 'Lactate diffusion coefficient :',DL,'m2/s'
       Write (*,*) 'Lactate diffusion coefficient in Membrane :',DML,
     1  'm2/s'
       Write (*,*) 'ALFA = ',ALFA
       Write (*,*) 'Input timestep size (sec.) :'
       Read (*,*) DT

       NUMX = 100
```

```
      DX = L/(NUMX)

      Write (*,*) 'Steplength :',(DX*1000000.D0),'micrometer'
      Write (*,*) 'Input Lactate concentration FEED (M) :'
      Read (*,*) CLIN
      CLIN=CLIN*1000.D0
      Write (*,*) 'Input Lactate concentration BASE (M) :'
      Read (*,*) CLOUT
      CLOUT=CLOUT*1000.D0
      Write (*,*) 'Input pH FEED :'
      Read (*,*) PH(1)
      COHIN=1000.D0*10**(PH(1)-14.D0)
      Write (*,*) 'Input pH BASE :'
      Read (*,*) PH(2)
      COHOUT=1000.D0*10**(PH(2)-14.D0)

C SETTING INITIAL VALUES
      C(0,0)=Donnan(CLIN,COHIN,MEMCAP)
      U(0,0)=(1.D0-MY)*C(0,0)+MY*MEMCAP
      C(NUMX,0)=Donnan(CLOUT,COHOUT,MEMCAP)
      U(NUMX,0)=(1.D0-MY)*C(NUMX,0)+MY*MEMCAP
      INISLOPE=(C(NUMX,0)-C(0,0))/L
      Round=1
C Initial Values for t = 0:
      DO 90 I=1,NUMX-1
        C(I,0)=C(0,0)+1.D0*I*DX*INISLOPE
        U(I,0)=(1.D0-MY)*C(I,0)+MY*MEMCAP
   90   Continue

C Resetting values
  100   CLW(1,0)=CLIN
      CLW(2,0)=CLOUT
      COHW(1,0)=COHIN
      COHW(2,0)=COHOUT
      CNAW=CLIN+COHIN
      CNAW=CNAW-IDF*(MNA*CNAW/(MOBL*CLIN+MOBOH*COHIN))/MASSTNA(1)
      LSPLIT=.FALSE.
      OHSPLIT=.FALSE.

C CALCULATION OF PROFILES
      TS=ML*CLIN/(MOBL*CLIN+MOBOH*COHIN)
C Calculation of Wall Concentration (IN)
  105    If (LSPLIT) Then
          Goto 130
        Elseif (OHSPLIT) Then
          Goto 120
        Else
          Goto 110
        Endif
C No Watersplitting
  110    A0=1.D0-MY
        A1=MY*CNAW-(1.D0-MY)*CLIN+IDF/MASSTL(1)*(1.D0-TS*(1.D0-MY))
        A2=-IDF*TS*MY*CNAW-MY*CNAW*CLIN
        DISC=A1**2-4.D0*A0*A2
        CLW(1,0)=(-A1-SQRT(DISC))/(2.D0*A0)
        COHW(1,0)=CNAW-CLW(1,0)
        If ((COHW(1,0) .LT. 0.D0) .AND. (CLIN .GT. MY*COHIN)) Then
          OHSPLIT=.TRUE.
```

```
          If (CLW(1,0) .LT. 0.D0) Then
            LSPLIT=.TRUE.
          Endif
          Goto 105
        Endif
        If (CLW(1,0) .LT. 0.D0) Then
          LSPLIT=.TRUE.
          Goto 105
        Endif
        If (CLW(1,0) .GT. CLIN) Then
          Write (*,*) 'C-Wall too large (wrong root selection) : '
     1      ,CLW(1,0)
          CLW(1,0)=(-A1+SQRT(DISC))/(2.D0*A0)
          Write (*,*) 'New C-Wall: ',CLW(1,0)
          COHW(1,0)=CNAW-CLW(1,0)
          Write (*,*) 'New COH-Wall: ',COHW(1,0)

        Endif
        If (COHW(1,0) .LT. 0.D0) Then
          OHSPLIT=.TRUE.
          If (CLW(1,0) .LT. 0.D0) Then
            LSPLIT=.TRUE.
            Write (*,*) 'Watersplitting!'
          Endif
          Goto 105
        Endif
        If (CLW(1,0) .LT. 0.D0) Then
          LSPLIT=.TRUE.
          Write (*,*) 'C-Wall = 0!'
          Goto 105
        Endif
        FLUXL(4,0)=IDF*TS-MASSTL(1)*(CLW(1,0)-CLIN)
        FLUXOH(1,0)=IDF*MOH*COHIN*TS/(ML*CLIN)-MASSTOH(1)*
     1    (COHW(1,0)-COHIN)
        C(0,0)=Donnan(CLW(1,0),COHW(1,0),MEMCAP)
        Goto 140
C OH-level too low
  120   If (CNAW .LT. 0.D0) Then
          LSPLIT=.TRUE.
          Goto 105
        Endif
        COHW(1,0)=0.D0
        FLUXDIF=IDF*MOH*COHIN/(MOBOH*COHIN+MOBL*CLIN)
     1    +MASSTOH(1)*COHIN
        TM=1.D0-FLUXDIF/IDF
        FLUXDIF=IDF*TM
        CLW(1,0)=CLIN+(IDF*TS-FLUXDIF)/MASSTL(1)
        If (CLW(1,0) .LT. 0.D0) Then
          LSPLIT=.TRUE.
          Goto 105
        Endif
        C(0,0)=TM*MY*MEMCAP/(1.D0-TM*(1.D0-MY))
        FLUXL(4,0)=IDF*TS+MASSTL(1)*(CLIN-CLW(1,0))
        FLUXOH(1,0)=IDF*MOH*COHIN*TS/(ML*CLIN)+MASSTOH(1)*COHIN
        Goto 140
C Watersplitting
  130   FLUXDIF=IDF*TS+MASSTL(1)*CLIN
        CLW(1,0)=0.D0
```

```
      If (CNAW .GT. 0.D0) Then
        COHW(1,0)=CNAW
      Else
        COHW(1,0)=0.D0
      Endif
      TM=FLUXDIF/IDF
      C(0,0)=TM*MY*MEMCAP/(1.D0-TM*(1.D0-MY))
      FLUXL(4,0)=FLUXDIF
      FLUXOH(1,0)=IDF*MOH*COHIN/(MOBL*CLIN+MOBOH*COHIN)
     1   +MASSTOH(1)*(COHIN-COHW(1,0))
  140   U(0,0)=(1.D0-MY)*C(0,0)+MY*MEMCAP

C Guessing first line and starting iterations
      Do 1000 J=1,TID
        CLW(1,J)=CLW(1,J-1)
        COHW(1,J)=COHW(1,J-1)
        Do 200 I=0,NUMX
          U(I,J)=U(I,J-1)
          C(I,J)=C(I,J-1)
          UITER(I)=U(I,J)
  200   Continue
        Do 990 N=1,49
        Do 210 I=0,NUMX
          DIFF(I)=C(I,J)
  210   Continue
C Finding Profile
        Do 320 K=1,49
          ERROR=0.D0
          Do 300 IREV=1,NUMX-1
            I=NUMX-IREV
            Call CalcU(U,IREV,J,DX,DT,DML,ALFA,MY,MEMCAP)
            Call CalcU(U,I,J,DX,DT,DML,ALFA,MY,MEMCAP)
  300       Continue
          Do 310 I=1,NUMX-1
            C(I,J)=(U(I,J)-MY*MEMCAP)/(1.D0-MY)
            ERROR=ERROR+(((U(I,J)-UITER(I))/U(I,J))**2)/NUMX
            UITER(I)=U(I,J)
  310       Continue
          If (K .LT. 4) Then
            Goto 320
          Endif
          If (ERROR .LT. 0.0000001D0) Then
            Goto 350
          Endif
  320   Continue
C Calculation of Wall Concentration (OUT)
  350   CLW(2,J)=CLW(2,J-1)
        COHW(2,J)=COHW(2,J-1)
        Do 370 I=1,4
          QASOL(I)=0.D0
          QASOLI(I)=0.D0
Continue
        Do 400 K=1,499
         ERROR=CLW(2,J)
         QACOEF(4)=MASSTOH(2)*MY*MOBOH
         QACOEF(3)=MASSTOH(2)*(MY*MOBL+(1.d0+MY)*MOBOH)*CLW(2,J)
     1            +MY*MOBOH*(DMOH/DX*C(NUMX-1,J)-MASSTOH(2)*COHOUT)
     2            -MY*MNA*IDF
```

```
      QACOEF(2)=(MASSTOH(2)*((1.d0+MY)*MOBL+MOBOH)*CLW(2,J)
     1          +((1.d0+MY)*MOBOH+MY*MOBL)*(DMOH/DX*C(NUMX-1,J)
     2          -MASSTOH(2)*COHOUT)-DMOH/DX*MY*MOBOH*MEMCAP
     3          -2.d0*MY*MNA*IDF)*CLW(2,J)
      QACOEF(1)=(MASSTOH(2)*MOBL*CLW(2,J)-DMOH/DX*(MY*MOBL+MOBOH)
     1          *MEMCAP+((1.d0+MY)*MOBL+MOBOH)
     2          *(DMOH/DX*C(NUMX-1,J)-MASSTOH(2)*COHOUT)
     3          -MY*MNA*IDF)*(CLW(2,J)**2)
      QACOEF(0)=MOBL*(DMOH/DX*(C(NUMX-1,J)-MEMCAP)-MASSTOH(2)
     1          *COHOUT)*(CLW(2,J)**3)
      Call quartic(QACOEF,QASOL,QASOLI,QANSOL)
      Do 375 I=1,QANSOL
       COHW(2,J)=QASOL(I)
       If ((COHW(2,J) .GT. 0.d0) .AND. (COHW(2,J) .LT. MEMCAP))
     1   Then
        Goto 380
       Endif
  375  Continue
  380  QACOEF(4)=MASSTL(2)*MOBL
      QACOEF(3)=MASSTL(2)*(((1.d0+MY)*MOBL+MOBOH)*COHW(2,J)
     1          -MOBL*CLOUT)+DML/DX*MOBL*(MEMCAP-C(NUMX-1,J))
     2          -MNA*IDF
      QACOEF(2)=(MASSTL(2)*(MY*(MOBL+MOBOH)*COHW(2,J)
     1          -(1.d0+MY)*MOBL*CLOUT)+DML/DX*((MY*MOBL
     2          +MOBOH)*MEMCAP-((1.d0+MY)*MOBL+MOBOH)
     3          *C(NUMX-1,J))-2.d0*MNA*IDF)*COHW(2,J)
      QACOEF(1)=(MY*MOBOH*(MASSTL(2)*COHW(2,J)+DML/DX*MEMCAP)
     1          -(MY*MOBL+(1.d0+MY)*MOBOH)
     2          *(MASSTL(2)*CLOUT+DML/DX*C(NUMX-1,J))
     3          +(ML-MOBOH)*IDF)*(COHW(2,J)**2)
      QACOEF(0)=-(MASSTL(2)*CLOUT+DML/DX*C(NUMX-1,J))*MY*MOBOH
     1          *(COHW(2,J)**3)
      Call quartic(QACOEF,QASOL,QASOLI,QANSOL)
      Do 385 I=1,QANSOL
       CLW(2,J)=QASOL(I)
       If ((CLW(2,J) .GT. 0.d0) .AND. (CLW(2,J) .LT. MEMCAP))
     1   Then
        Goto 390
       Endif
  385  Continue
  390  If ((ERROR-CLW(2,J))**2 .LT. 0.01) Then
       Goto 450
      Endif
  400  Continue
  450  C(NUMX,J)=Donnan(CLW(2,J),COHW(2,J),MEMCAP)
      U(NUMX,J)=(1.D0-MY)*C(NUMX,J)+MY*MEMCAP
      UITER(NUMX)=U(NUMX,J)

      ERROR=0.D0
      Do 550 I=0,NUMX
       ERROR=ERROR+(DIFF(I)-C(I,J))**2
  550  Continue
      If (ERROR .LT. 10.D0) Then
       Goto 990
      Endif
  990  Continue
     ERROR=0.D0
     Do 995 I=0,NUMX
```

```
        ERROR=ERROR+(U(I,J)-U(I,J-1))**2
 995    Continue
       ERROR=DT*ERROR/(NUMX+1)
       Write (*,*) 'Error = ',ERROR
       If (ERROR .LT. 5.D0) Then
        Call CalcFlux(J,NUMX,C,FLUXL,FLUXOH,CLW,COHW,MASSTL,DML,
     1  DMOH,DX,IDF,MEMCAP,MY,ML,MOH,MNA,CLIN,CLOUT,CUREFF)
        Write (*,996) DT*(J)
 996     Format ('Steady-state reached after ',F8.2,' seconds.')
        Write (*,*) 'FLUX (IN-mem) = ',FLUXL(1,J)
        Write (*,*) 'FLUX (IN-dif) = ',FLUXL(4,J)
        Write (*,*) 'FLUX (OUT-mem) = ',FLUXL(2,J)
        Write (*,*) 'FLUX (OUT-dif) = ',FLUXL(3,J)
        Write (*,*) 'Current efficiency = ',CUREFF(2,J)*100.d0,' %'
        Goto 1100
       Endif
 1000  Continue
 1010   Format ('No Steady-state reached after ',F8.2,' seconds.')
       Call CalcFlux(TID,NUMX,C,FLUXL,FLUXOH,CLW,COHW,MASSTL,DML,
     1  DMOH,DX,IDF,MEMCAP,MY,ML,MOH,MNA,CLIN,CLOUT,CUREFF)
       Write (*,1010) DT*(TID)
       Write (*,*) 'FLUX (IN-mem) = ',FLUXL(1,TID)
       Write (*,*) 'FLUX (IN-dif) = ',FLUXL(4,TID)
       Write (*,*) 'FLUX (OUT-mem) = ',FLUXL(2,TID)
       Write (*,*) 'FLUX (OUT-dif) = ',FLUXL(3,TID)
       Write (*,*) 'Current efficiency = ',CUREFF(2,TID)*100.d0,' %'
 1100  Write (*,*)'Do you wish to save results in data-file (y/n)'
      Read (*,*) Answer
      If (Answer .EQ. 'y' .or. Answer .EQ. 'Y') Then
       If (Round .LT. 0) Then
        Call Reverse(C,NUMX)
        Do 1200 J=0,TID
         Call SWITCH(CLW(1,J),CLW(2,J))
         Call SWITCH(FLUXL(1,J),FLUXL(2,J))
         Call SWITCH(FLUXL(3,J),FLUXL(4,J))
         Call SWITCH(FLUXOH(1,J),FLUXOH(2,J))
 1200     Continue
        Call Datafile(C,CLW,FLUXL,FLUXOH,CUREFF)
        Call Reverse(C,NUMX)
        Do 1300 J=0,TID
         Call SWITCH(CLW(1,J),CLW(2,J))
         Call SWITCH(FLUXL(1,J),FLUXL(2,J))
         Call SWITCH(FLUXL(3,J),FLUXL(4,J))
         Call SWITCH(FLUXOH(1,J),FLUXOH(2,J))
 1300     Continue
       Else
        Call Datafile(C,CLW,FLUXL,FLUXOH,CUREFF)
       Endif
      Endif
C Reverse Current Direction
      Write (*,*) 'Do you wish to reverse the current (y/n) ?'
      Read (*,*) Answer
      If (Answer .NE. 'y' .AND. Answer .NE. 'Y') Then
       Goto 5000
      Endif
      If (Round .GT. 0) Then
       Round=-1
       Else
```

```
        Round=1
      Endif
      Call Clear(C,NUMX)
      Do 2010 J=0,100
        Do 2000 I=0,NUMX
          U(I,J)=(1.D0-MY)*C(I,J)+MY*MEMCAP
 2000     Continue
        FLUXL(1,J)=0.D0
        FLUXL(2,J)=0.D0
        FLUXL(3,J)=0.D0
        FLUXL(4,J)=0.D0
        FLUXOH(1,J)=0.D0
        FLUXOH(2,J)=0.D0
        CLW(1,J)=0.D0
        CLW(2,J)=0.D0
        COHW(1,J)=0.D0
        COHW(2,J)=0.D0
 2010   Continue
      Call SWITCH(CLIN,CLOUT)
      Call SWITCH(COHIN,COHOUT)
      Call SWITCH(MASSTL(1),MASSTL(2))
      Call SWITCH(MASSTOH(1),MASSTOH(2))
      Call SWITCH(MASSTNA(1),MASSTNA(2))
      Call SWITCH(DIFLAYER(1),DIFLAYER(2))
      Call SWITCH(PH(1),PH(2))
      Goto 100
 5000   End


CCCCCCCCCCCCCCCCCCCCCCCCCCCCCCCCCCCCCCCCCCCCCCCCCCCCCCCCCCCCCCCCCC
C Subroutines

      Subroutine CalcU(U,I,J,DX,DT,DML,ALFA,MY,MEMCAP)
      Integer I,J
      Double Precision U(0:100,0:100),DX,DT,DML,ALFA,MY,MEMCAP
      Double Precision A1,A2,A3,Q,R,S,T,DIS,PHI,MYM,C(0:100,0:100)
      data pi2 / 1.5707963267 9489661923e0/
      MYM = MY*MEMCAP
      A1=-(DX**2*U(I,J-1)+DML*DT*(U(I+1,J)+U(I-1,J)))
      A1=A1/(2.D0*DML*DT+DX**2)
      A2 = ALFA*DX*DT/(2.D0*DML*DT+DX**2)
      A3 = -ALFA*DX*DT*U(I-1,J)/(2.D0*DML*DT+DX**2)
      Q = (3*A2-A1**2)/9.D0
      R = (9*A1*A2-27*A3-2*A1**3)/54.D0
      DIS = Q**3 + R**2
      If (DIS .LT. 0.D0) Then
        Goto 50
      Endif
C       D > 0
      S = (R+(Q**3+R**2)**0.5D0)
      T = (R-(Q**3+R**2)**0.5D0)
      If (S .LT. 0.D0) Then
        S = -1.D0*(-S)**(1/3.D0)
      Else
        S = S**(1/3.D0)
      Endif
      If (T .LT. 0.D0) Then
        T = -1.D0*(-T)**(1/3.D0)
```

```
      Else
        T = T**(1/3.D0)
      Endif
      U(I,J)=S+T-A1/3.D0
      If ((U(I,J) .GT. MYM) .or. (U(I,J) .LT. MEMCAP)) Then
        Write (*,*) '! Illegal values - Iteration continues !'
C         U(I,J)=-(S+T)/2.D0-A1/3.D0
      Endif
      Goto 100
C     D < 0
   50 PHI = acos(R/((-(Q**3))**(1/2.D0)))
      U(I,J)=2.D0*(-Q)**(1/2.D0)*cos(PHI/3.D0)-A1/3.D0
      If ((U(I,J) .GT. MYM) .or. (U(I,J) .LT. MEMCAP)) Then
        U(I,J)=2.D0*(-Q)**(1/2.D0)*cos((PHI+pi2*2/3.D0)/3.D0)-A1/3.D0
      Elseif ((U(I,J) .GT. MYM) .or. (U(I,J) .LT. MEMCAP)) Then
        U(I,J)=2.D0*(-Q)**(1/2.D0)*cos((PHI+pi2*4/3.D0)/3.D0)
     1    -A1/3.D0
      Endif
      Continue
  100 C(I,J)=(U(I,J)-MYM)/(1.D0-MY)
      End

      Subroutine CalcFlux(MAXJ,NUMX,C,FLUXL,FLUXOH,CLW,COHW,KL,DML,
     1   DMOH,DX,IDF,MEMCAP,MY,ML,MOH,MNA,CLIN,CLOUT,EFF)
      Integer J,MAXJ,NUMX
      Double Precision C(0:100,0:100),FLUXL(4,0:100),FLUXOH(2,0:100)
      Double Precision CLW(2,0:100),COHW(2,0:100),KL(2)
      Double Precision DML,DMOH,DX,IDF,MEMCAP,MY,ML,MOH,MNA
      Double Precision CLIN,CLOUT,ACF,EFF(4,100)
      Double Precision MOBL,MOBOH
      MOBL=ML+MNA
      MOBOH=MOH+MNA
      ACF=0.d0
      Do 100 J=1,MAXJ
        FLUXL(1,J)=IDF/(1.d0+MY*(MEMCAP/C(0,J)-1.d0))
     1    +DML/DX*(C(0,J)-C(1,J))
        FLUXL(2,J)=IDF/(1.d0+MY*(MEMCAP/C(NUMX,J)-1.d0))
     1    +DML/DX*(C(NUMX-1,J)-C(NUMX,J))
        FLUXL(3,J)=IDF*ML*CLW(2,J)/(MOBL*CLW(2,J)+MOBOH*COHW(2,J))
     1    +KL(2)*(CLW(2,J)-CLOUT)
        FLUXL(4,J)=IDF*ML*CLW(1,J)/(MOBL*CLW(1,J)+MOBOH*COHW(1,J))
     1    +KL(1)*(CLIN-CLW(1,J))
        FLUXOH(1,J)=IDF*(1.d0-1.d0/(1.d0+MY*(MEMCAP/C(0,J)-1.d0)))
     1    +DMOH/DX*(C(1,J)-C(0,J))
        FLUXOH(2,J)=IDF*(1.d0-1.d0/(1.d0+MY*(MEMCAP/C(NUMX,J)-1.d0)))
     1    +DMOH/DX*(C(NUMX,J)-C(NUMX-1,J))
  100 Continue
      Do 200 J=MAXJ+1,NUMX
        FLUXL(1,J)=FLUXL(1,J-1)
        FLUXL(2,J)=FLUXL(2,J-1)
        FLUXL(3,J)=FLUXL(3,J-1)
        FLUXL(4,J)=FLUXL(4,J-1)
        FLUXOH(1,J)=FLUXOH(1,J-1)
        FLUXOH(2,J)=FLUXOH(2,J-1)
  200 Continue
      Do 300 J=1,NUMX
        ACF=ACF+FLUXL(2,J)
        If (CLIN .lt. CLOUT) Then
```

```
        ACF=ACF+FLUXL(2,J)
        EFF(4,J)=ACF
       Else
        ACF=ACF+FLUXL(1,J)
        EFF(3,J)=ACF
       Endif
       If (J .gt. 1) Then
        EFF(1,J)=((EFF(3,J)-EFF(3,J-1))-(EFF(4,J)-EFF(4,J-1)))/IDF
       Else
        EFF(1,J)=(EFF(3,J)-EFF(4,J))/IDF/(J)
       Endif
       EFF(2,J)=(EFF(3,J)-EFF(4,J))/IDF/(J)
300    Continue
      End

      Subroutine Datafile(C,CLW,FLUXL,FLUXOH,EFF)
      Double precision C(0:100,0:100),CLW(2,0:100),FLUXL(4,0:100)
      Double Precision FLUXOH(2,0:100),EFF(4,100)
      Integer J
      Character*12 FILENAME
      Write (*,*) 'File-name :'
      Read (*,*) FILENAME
      Open (Unit=11,File=FILENAME)
100    Format (I3,101(';',F9.4))
      Do 200 J=0,100
        Write (11,100) J,(C(K,J),K=0,100)
200    Continue
      Write (11,*) 'Wall concentrations/Lactate fluxes/Hydroxide ',
     1  'fluxes/Current Efficiency (stepwise and accumulated)'
210    Format (I3,';Wall-C;',F9.2,';',F9.2,';L-Flux;',F8.6,';',F8.6,
     1  ';OH-Flux;',F8.6,';',F8.6,';Efficiency;',F8.6,';',F8.6,';'
     2  ,F8.6,';',F8.6)
      Do 300 J=0,100
        Write (11,210) J,CLW(1,J),CLW(2,J),FLUXL(1,J),FLUXL(2,J),
     1    FLUXOH(1,J),FLUXOH(2,J),EFF(1,J),EFF(2,J),EFF(3,J),EFF(4,J)
300    Continue
      Close (11)
      End


      Subroutine Reverse(M,NUMX)
      Double Precision M(0:100,0:100),MNEW(0:100,0:100)
      Integer I,J,NUMX
      Do 110 J=0,100
        Do 100 I=0,NUMX
          MNEW(I,J)=M(NUMX-I,J)
100     Continue
110    Continue
      Do 210 J=0,100
        Do 200 I=0,NUMX
          M(I,J)=MNEW(I,J)
200     Continue
210    Continue
      End


      Subroutine SWITCH(A,B)
      Double Precision A,B,C
```

```
      C=A
      A=B
      B=C
      End


      Subroutine Clear(M,NUMX)
      Double Precision M(0:100,0:100),INIT(0:100)
      Integer I,J,NUMX,LAST
      Logical Stability
      Stability=.FALSE.
      Do 110 J=0,100
        Do 100 I=0,NUMX
          If (M(I,100-J) .GT. 0.0001) Then
            Stability=.TRUE.
          Endif
  100     Continue
        If (Stability) Then
          LAST=100-J
          Goto 150
        Endif
  110   Continue
  150   Do 200 I=0,NUMX
        INIT(I)=M(I,LAST)
  200   Continue
      Do 310 J=1,100
        Do 300 I=0,NUMX
          M(I,0)=INIT(NUMX-I)
          M(I,J)=0.D0
  300     Continue
  310   Continue
      End

C     ***QUARTIC*************************************************25.03.98
C     Solution of a quartic equation
C     ref.: J. E. Hacke, Amer. Math. Monthly, Vol. 48, 327-328, (1941)
C     NO WARRANTY, ALWAYS TEST THIS SUBROUTINE AFTER DOWNLOADING
C     ************************************************************
C     dd(0:4)     (i)  vector containing the polynomial coefficients
C     sol(1:4)    (o)  results, real part
C     soli(1:4)   (o)  results, imaginary part
C     Nsol        (o)  number of real solutions
C     ============================================================
      subroutine quartic(dd,sol,soli,Nsol)
      implicit double precision (a-h,o-z)
      dimension dd(0:4),sol(4),soli(4)
      dimension AA(0:3),z(3)
C
      Nsol = 0
      a = dd(4)
      b = dd(3)
      c = dd(2)
      d = dd(1)
      e = dd(0)
C
      if (dd(4).eq.0.d+0) then
        write(6,*)'ERROR: NOT A QUARTIC EQUATION'
        return
```

```
      endif
C
      p = (-3.d+0*b**2 + 8.d+0*a*c)/(8.d+0*a**2)
      q = (b**3 - 4.d+0*a*b*c + 8.d+0*d*a**2)/(8.d+0*a**3)
      r = (-3.d+0*b**4 + 16.d+0*a*b**2*c - 64.d+0*a**2*b*d +
     1     256.d+0*a**3*e)/(256.d+0*a**4)
C
C     solve cubic resolvent
      AA(3) =  8.d+0
      AA(2) = -4.d+0*p
      AA(1) = -8.d+0*r
      AA(0) =  4.d+0*p*r - q**2
      call cubic(AA,z,ncube)
C
      zsol = -1.d+99
      do 5 i=1,ncube
 5      zsol = max(zsol,z(i))
      z(1) = zsol
      xK2 = 2.d+0 * z(1) - p
      xK  = sqrt(xK2)
C-------------------------------------------------
      if (xK.eq.0.d+0) then
        xL2 = z(1)**2 - r
        if (xL2.lt.0.d+0) then
          write(6,*)'Sorry, no solution'
          return
        endif
        xL  = sqrt(xL2)
      else
        xL = q/(2.d+0 * xK)
      endif
C-------------------------------------------------
      sqp = xK2 - 4.d+0*(z(1) + xL)
      sqm = xK2 - 4.d+0*(z(1) - xL)
C
      do 10 i=1,4
 10     soli(i) = 0.d+0
      if       (sqp.ge.0.d+0 .and. sqm.ge.0.d+0) then
        sol(1) = 0.5d+0*( xK + sqrt(sqp))
        sol(2) = 0.5d+0*( xK - sqrt(sqp))
        sol(3) = 0.5d+0*(-xK + sqrt(sqm))
        sol(4) = 0.5d+0*(-xK - sqrt(sqm))
        Nsol = 4
      else if  (sqp.ge.0.d+0 .and. sqm.lt.0.d+0) then
        sol(1) =  0.5d+0*(xK + sqrt(sqp))
        sol(2) =  0.5d+0*(xK - sqrt(sqp))
        sol(3) = -0.5d+0*xK
        sol(4) = -0.5d+0*xK
        soli(3) =  sqrt(-0.25d+0 * sqm)
        soli(4) = -sqrt(-0.25d+0 * sqm)
        Nsol = 2
      else if  (sqp.lt.0.d+0 .and. sqm.ge.0.d+0) then
        sol(1) = 0.5d+0*(-xK + sqrt(sqm))
        sol(2) = 0.5d+0*(-xK - sqrt(sqm))
        sol(3) =  0.5d+0*xK
        sol(4) =  0.5d+0*xK
        soli(3) =  sqrt(-0.25d+0 * sqp)
        soli(4) = -sqrt(-0.25d+0 * sqp)
```

```
      Nsol = 2
     else if  (sqp.lt.0.d+0 .and. sqm.lt.0.d+0) then
      sol(1) = -0.5d+0*xK
      sol(2) = -0.5d+0*xK
      soli(1) =  sqrt(-0.25d+0 * sqm)
      soli(2) = -sqrt(-0.25d+0 * sqm)
      sol(3) =  0.5d+0*xK
      sol(4) =  0.5d+0*xK
      soli(3) =  sqrt(-0.25d+0 * sqp)
      soli(4) = -sqrt(-0.25d+0 * sqp)
      Nsol = 0
     endif
     do 20 i=1,4
 20    sol(i) = sol(i) - b/(4.d+0*a)
C
     return
     END

C    ***CUBIC**************************************************08.11.1986
C    Solution of a cubic equation
C    Equations of lesser degree are solved by the appropriate formulas.
C    The solutions are arranged in ascending order.
C    NO WARRANTY, ALWAYS TEST THIS SUBROUTINE AFTER DOWNLOADING
C    ***********************************************************************
C    A(0:3)      (i)  vector containing the polynomial coefficients
C    X(1:L)      (o)  results
C    L           (o)  number of valid solutions (beginning with X(1))
C    =======================================================
     SUBROUTINE CUBIC(A,X,L)
     IMPLICIT DOUBLE PRECISION(A-H,O-Z)
     DIMENSION A(0:3),X(3),U(3)
     PARAMETER(PI=3.1415926535897932D+0,THIRD=1.D+0/3.D+0)
     INTRINSIC MIN,MAX,ACOS
C
C    define cubic root as statement function
     CBRT(Z)=SIGN(ABS(Z)**THIRD,Z)
C
C    ==== determine the degree of the polynomial ====
C
     IF (A(3).NE.0.D+0) THEN
C
C      cubic problem
       W=A(2)/A(3)*THIRD
       P=(A(1)/A(3)*THIRD-W**2)**3
       Q=-.5D+0*(2.D+0*W**3-(A(1)*W-A(0))/A(3))
       DIS=Q**2+P
       IF (DIS.LT.0.D+0) THEN
C        three real solutions!
C        Confine the argument of ACOS to the interval [-1;1]!
         PHI=ACOS(MIN(1.D+0,MAX(-1.D+0,Q/SQRT(-P))))
         P=2.D+0*(-P)**(5.D-1*THIRD)
         DO 100 I=1,3
  100      U(I)=P*COS((PHI+DBLE(2*I)*PI)*THIRD)-W
         X(1)=MIN(U(1),U(2),U(3))
         X(2)=MAX(MIN(U(1),U(2)),MIN(U(1),U(3)),MIN(U(2),U(3)))
         X(3)=MAX(U(1),U(2),U(3))
         L=3
       ELSE
```

```
C         only one real solution!
          DIS=SQRT(DIS)
          X(1)=CBRT(Q+DIS)+CBRT(Q-DIS)-W
          L=1
        END IF
C
      ELSE IF (A(2).NE.0.D+0) THEN
C
C       quadratic problem
        P=5.D-1*A(1)/A(2)
        DIS=P**2-A(0)/A(2)
        IF (DIS.GE.0.D+0) THEN
C         two real solutions!
          X(1)=-P-SQRT(DIS)
          X(2)=-P+SQRT(DIS)
          L=2
        ELSE
C         no real solution!
          L=0
        END IF
C
      ELSE IF (A(1).NE.0.D+0) THEN
C
C       linear equation
        X(1)=-A(0)/A(1)
        L=1
C
      ELSE
C       no equation
        L=0
      END IF
C
C     ==== perform one step of a newton iteration in order to minimize
C          round-off errors ====
      DO 110 I=1,L
        X(I)=X(I)-(A(0)+X(I)*(A(1)+X(I)*(A(2)+X(I)*A(3))))
     1  /(A(1)+X(I)*(2.D+0*A(2)+X(I)*3.D+0*A(3)))
  110 CONTINUE
      RETURN
      END

        Function Donnan(CL,COH,CAP)
        Double Precision CL,CAP,COH
        Donnan=CL*CAP/(COH+CL)
        End
```

7.2.3 Experimental plan and results

Exp No	Exp Name	Run Order	Incl/Excl	Current rev	Current den	Feed conc	Feed pH	Base pH	Base Concentration	Current efficien	Energy consump	Membrane area	Watersplitti
1	N1	13	Incl	60	250	50	4	12,89	22,5	23,47	2,52	5537	
2	N2	2	Incl	330	250	50	4	12,89	22,5	53,54	1,54	2428	
3	N3	10	Incl	600	250	50	4	12,89	22,5	62,04	1,46	2095	
4	N4	50	Incl	60	625	50	4	12,89	22,5	15,03	9,83	3458	
5	N5	1	Incl	330	625	50	4	12,89	22,5	42,52	4,85	1223	
6	N6	28	Incl	600	625	50,00	4	12,89	22,5	46,98	4,83	1107,00	
7	N7	59	Incl	60	1000	50,00	4	12,89	22,5	17,43	13,56	1864,00	x
8	N8	83	Incl	330	1000	50,00	4	12,89	22,5	37,71	8,76	862,00	x
9	N9	30	Incl	600	1000	50,00	4	12,89	22,5	40,20	9,03	808,00	x
10	N10	46	Incl	60	250	125,00	4	12,64	56,25	24,85	2,1	5231,00	
11	N11	19	Incl	330	250	125,00	4	12,64	56,25	68,04	1,11	1911,00	
12	N12	63	Incl	600	250	125,00	4	12,64	56,25	76,03	1,1	1710,00	
13	N13	33	Incl	60	625	125,00	4	12,64	56,25	26,65	4,89	1951,00	
14	N14	41	Incl	330	625	125,00	4	12,64	56,25	57,23	3,3	909,00	
15	N15	72	Incl	600	625	125,00	4	12,64	56,25	61,40	3,41	847,00	
16	N16	52	Incl	60	1000	125,00	4	12,64	56,25	22,34	9,34	1454,00	x
17	N17	27	Incl	330	1000	125,00	4	12,64	56,25	36,27	8,34	896,00	x
18	N18	42	Incl	600	1000	125,00	4	12,64	56,25	37,69	8,9	862,00	x
19	N19	49	Incl	60	250	200,00	4	12,00	90	16,84	3,09	7717,00	
20	N20	18	Incl	330	250	200,00	4	12,00	90	44,09	1,71	2948,00	
21	N21	9	Incl	600	250	200,00	4	12,00	90	47,35	1,77	2745,00	
22	N22	48	Incl	60	625	200,00	4	12,00	90	26,53	24,91	1960,00	
23	N23	65	Incl	330	625	200,00	4	12,00	90	35,70	5,29	1456,00	
24	N24	67	Incl	600	625	200,00	4	12,00	90	36,62	5,72	1420,00	
25	N25	66	Incl	60	1000	200,00	4	12,00	90	19,25	10,82	1688,00	
26	N26	8	Incl	330	1000	200,00	4	12,00	90	24,95	12,11	1303,00	
27	N27	7	Incl	600	1000	200,00	4	12,00	90	25,52	13,13	1273,00	
28	N28	77	Incl	60	250	50,00	8	12,89	22,5	23,47	2,52	5539,00	
29	N29	6	Incl	330	250	50,00	8	12,89	22,5	53,54	1,54	2428,00	
30	N30	5	Incl	600	250	50	8	12,89	22,5	62,04	1,46	2095	
31	N31	78	Incl	60	625	50	8	12,89	22,5	15,03	9,82	3458	
32	N32	82	Incl	330	625	50	8	12,89	22,5	42,52	4,85	1223	
33	N33	55	Incl	600	625	50	8	12,89	22,5	46,98	4,83	1107	
34	N34	36	Incl	60	1000	50	8	12,89	22,5	17,43	13,56	1864	x
35	N35	57	Incl	330	1000	50	8	12,89	22,5	37,71	8,76	862,00	x
36	N36	40	Incl	600	1000	50	8	12,89	22,5	40,20	9,03	808,00	x
37	N37	26	Incl	60	250	125	8	12,64	56,25	24,85	2,1	5232	
38	N38	4	Incl	330	250	125	8	12,64	56,25	68,03	1,11	1911	
39	N39	44	Incl	600	250	125	8	12,64	56,25	76,03	1,1	1710	
40	N40	17	Incl	60	625	125	8	12,64	56,25	26,65	4,89	1951	
41	N41	62	Incl	330	625	125	8	12,64	56,25	57,22	3,3	909	
42	N42	69	Incl	600	625	125	8	12,64	56,25	61,4	3,41	847	
43	N43	15	Incl	60	1000	125	8	12,64	56,25	22,34	9,34	1454,00	x
44	N44	14	Incl	330	1000	125	8	12,64	56,25	36,27	8,34	896,00	x
45	N45	25	Incl	600	1000	125	8	12,64	56,25	37,69	8,9	862,00	x
46	N46	56	Incl	60	250	200	8	12,00	90	16,84	3,09	7719	
47	N47	64	Incl	330	250	200	8	12,00	90	44,09	1,71	2948	
48	N48	20	Incl	600	250	200	8	12,00	90	48,35	1,77	2745	
49	N49	21	Incl	60	625	200	8	12,00	90	26,53	4,91	1960	
50	N50	60	Incl	330	625	200	8	12,00	90	35,7	5,29	1456	
51	N51	76	Incl	600	625	200	8	12,00	90	36,62	5,72	1420	
52	N52	34	Incl	60	1000	200	8	12,00	90	19,25	10,82	1688,00	
53	N53	22	Incl	330	1000	200	8	12,00	90	24,95	12,11	1303,00	
54	N54	29	Incl	600	1000	200	8	12,00	90	25,52	13,13	1273,00	
55	N55	79	Incl	60	250	50	12	12,89	22,5	6,41	8,49	20295	
56	N56	16	Incl	330	250	50	12	12,89	22,5	7,53	10,33	17254	
57	N57	51	Incl	600	250	50	12	12,89	22,5	8,5	10,12	15291	
58	N58	35	Incl	60	625	50	12	12,89	22,5	9,19	14,8	5661	x
59	N59	37	Incl	330	625	50	12	12,89	22,5	28,52	6,82	1823	x
60	N60	45	Incl	600	625	50	12	12,89	22,5	32,27	6,67	1611	x
61	N61	84	Incl	60	1000	50	12	12,89	22,5	7,99	27,22	4066	x
62	N62	39	Incl	330	1000	50	12	12,89	22,5	23,29	13,37	1395	x
63	N63	47	Incl	600	1000	50	12	12,89	22,5	25,26	13,63	1286	x
64	N64	61	Incl	60	250	125	12	12,64	56,25	10,46	4,89	12423	
65	N65	68	Incl	330	250	125	12	12,64	56,25	25,65	2,91	5067	
66	N66	81	Incl	600	250	125	12	12,64	56,25	30,67	2,7	4238	
67	N67	58	Incl	60	625	125	12	12,64	56,25	21,7	5,9	2397	
68	N68	23	Incl	330	625	125	12	12,64	56,25	49,97	3,73	1041	
69	N69	38	Incl	600	625	125	12	12,64	56,25	53,9	3,84	965	
70	N70	24	Incl	60	1000	125	12	12,64	56,25	16,91	12,11	1922	x
71	N71	71	Incl	330	1000	125	12	12,64	56,25	29	10,29	1121	x
72	N72	70	Incl	600	1000	125	12	12,64	56,25	30,24	10,96	1075	x
73	N73	32	Incl	60	250	200	12	12,00	90	0,8	64,75	162864	

7.3 Patent application

The patent was applied for on December 12, 2000.

A METHOD AND APPARATUS FOR ISOLATION OF IONIC SPECIES FROM A LIQUID
Patent Number: WO0248044
Publication date: 2002-06-20
Inventor(s): GARDE ARVID (DK); JONSSON GUNNAR (DK); RYPE JENS-ULRIK (DK)
Applicant(s): GARDE ARVID (DK); JONSSON GUNNAR (DK); RYPE JENS-ULRIK (DK); JURAG SEPARATION APS (DK)
Requested Patent: WO0248044
Application Number: WO2001DK00810 20011206
Priority Number(s): DK20000001862 20001212
IPC Classification: C02F1/00
EC Classification:
Equivalents:
Cited Documents:

Abstract

The present invention relates to a method for isolation of ionic species from a liquid and an apparatus for isolation of ionic species from a liquid. Moreover the invention relates to an electro enhanced dialysis cell and the use of the cell in the method and the apparatus.

A method and apparatus for isolation of ionic species from a liquid

The present invention relates to a method for isolation of ionic species from a liquid and an apparatus for isolation of ionic species from a liquid. Moreover the invention relates to an electro enhanced dialysis cell and the use of the cell in the method and the apparatus.

Isolation of ionic species from liquids is a very important industrial process used within such a broad technical field, as from refining metals to purification of lactic acid from a fermented liquid.

A large number of processes and apparatuses have been investigated and introduced in order to improve the processes of isolation of ionic species from liquids.

Among those processes and apparatuses are filtration with ultra- and nano-filters, exchanging ions with ion-exchangers and electrodialysis with electrodialysis cells.

Japanese patent application no. 63335032 discloses a desalting apparatus. The apparatus consists of a donnan dialysis apparatus to desalt a solution and an electric dialysis apparatus for reproducing and re-using an acidic or alkaline solution in the desalting process. The apparatus is not suitable for desalting liquid-containing particles.

US patent no. 5746920 discloses a process for purifying dairy wastewater. The process comprises first treating the wastewater with base. The treated wastewater is then introduced into a fermenting

tank, where the lactose present in the wastewater is fermented to form a broth and lactic acid. The broth is subjected to purification by ion-exchanging and nano-filtration and the purified broth is subjected to bipolar electrodialysis to yield concentrated acid and base solutions from the purified broth. The process according to the US patent is complex and costly to carry out and there is a substantial loss of product during the filtration. Furthermore the process is designed to isolate specific ionic species.

Japanese patent application JP7232038 discloses a method of recovering high concentration alkali from liquid containing alkali utilizing a combination of diffusion dialysis using cation-exchange membranes and bipolar electrodialysis. No counter-measures are taken to prevent fouling of ion exchange membranes in the diffusion cell from liquids containing proteinuous material, e.g. fermentation broth. Due to the very low driving force across the cation exchange membrane in the diffusion dialysis cell only a very limited flux can be obtained.

Japanese patent application JP63291608 discloses a system for regenerating acidic waste liquid utilizing a combination of diffusion dialysis using anion exchange membranes and bipolar electrodialysis. The flux in the diffusion cell is low. Moreover impurities such as calcium and magnesium ions would prevent the use of bipolar electrodialysis due to the fact that bipolar membranes are damaged or destroyed by presence of even very small amounts of calcium or magnesium ions.

German patent no. DE 19700044 Cl discloses a method for production of acid and alkaline products by monopolar electrodialysis followed by bipolar electrodialysis. The monopolar electrodialysis cannot selectively remove either cations or anions from a liquid, thus lactic acid cannot be removed without removing e.g. calcium, which would cause problems in the bipolar electrodialysis. The conventional monopolar electrodialysis is susceptible to fouling by biological material, proteins, etc.

Due to the drawbacks of the prior art technology there is a need for a method and an apparatus for isolation of ionic species, which is able to isolate ionic species from different kinds of liquids and furthermore is costeffective and results in a high output.

The object of the present invention is to provide an alternative method and an alternative apparatus for isolation of ionic species from a liquid.

Another object of the invention is to provide a method and an apparatus for isolation of ionic species, which method and apparatus are simple and cost-effective and provide a high output.

A further object of the invention is to provide a method and an apparatus for isolation of ionic species which method and apparatus can be used for isolation of ionic species in liquids containing solids and particles. The invention is in particular useful for separating ionic species from liquids containing particles of organic material and multivalent inorganic metal ions.

Moreover it is an object of the invention to provide a method and an apparatus for isolation of ionic species which method and appratus are useful for isolation of ionic species in a liquid containing organic material.

These objects are achieved by the present invention as defined in the claims.

By the term ionic species is meant that the species are in an ionic state. For example when sodiumchloride NaCl is dissolved in water it dissociates into the ions Na^+ (cation) and Cl^- (anion). As the ions have a small electric charge, it is possible to move the ions in an electric field.

The invention provides a method and an apparatus for separating ionic species from a liquid. By using the invention it is possible to separate ionic species from liquids, which are highly contaminated, e.g. with particles. The separation can be performed without any need for a filtration step and it is possible to obtain a high output.

The method according to the invention for isolation of ionic species from a first liquid comprises the steps of: treating the first liquid in an electro enhanced dialysis cell to transfer the ionic species from the first liquid into a second liquid, and - optionally treating the second liquid in a bipolar electrodialysis cell to transfer the ionic species from the second liquid into a third liquid, - optionally separating the ionic species from the second or third liquid.

The first liquid may be provided to the electro enhanced dialysis cell from a storage tank. In a dialysis cell the ionic species are transferred into a second liquid, which has a pH value differing form the pH value of the first liquid. The difference in pH causes a difference in concentration of H^+ and OH^- in the first and the second liquid. The concentration difference between the first and the second liquid will be the driving forces in the electro enhanced dialysis cell. The difference in concentration will cause a flow of either H^+ or OH^- ions from the second liquid into the first liquid thereby building up an electric potential difference or a diffusion potential which will cause either cat-ions (M^+) or an-ions (X^-) of the ionic species to be transported from the first liquid into the second liquid through cation exchange membranes or an-ion membranes, respectively.

If the ionic species are cations, the second liquid will be acidic compared to the first liquid, and visa versa, if the ionic species are anions. This process has been enhanced by the electro enhanced dialysis cell according to the invention, in which the driving forces have been enhanced by use of an electric field. The electro enhanced dialysis cell will be described in more details in the following.

After treatment in the electro enhanced dialysis cell the second liquid may be treated in a bipolar electrodialysis cell. In the bipolar electrodialysis cell the ionic species will be concentrated. If the ionic species are cations, the third liquid will be basic compared to the second liquid, and visa versa, if the ionic species are an-ions. The driving force in the bipolar electrodialysis cell is a difference in electric potential caused by a constant direct current through the cell.

The membranes, acid, bases, and pH can of course be selected depending on the ionic species to be separated.

This selection can be done by the skilled person.

When the ionic species are separated and concentrated into the third liquid, it can of course be separated from the third liquid, e.g. to obtain a dry or a substantially dry product.

The method according to the invention comprises the feature of applying an electric field of direct current through the electro enhanced dialysis cell during the treatment of the first liquid. In this way

the electric potential difference or diffusion potential is enhanced and thereby increases the number of ionic species which are transferred into the second liquid from the first liquid.

In order to improve the results from the cell it is preferred to change the direction of the electric field during the treatment of the first liquid. The direction of the electric field is preferably changed by changing the direction of the direct current. By changing the direction of the electric field it is possible to give a "self-cleaning"effect to the membranes used in the electro enhanced dialysis cell and prevent fouling of the membranes during treatment of the first liquid. When an electric field of direct current is applied to the cell electrically loaded particles are driven from the first liquid onto the membrane surfaces of the cell. Here the particles will build up a layer and after a time cause fouling which will make the membranes useless. If the electric field is reversed before the particles have caused fouling, the particles will be driven back from the membranes into the first liquid and the membranes will be cleaned.

In an embodiment according to the invention the electric field can be changed at predetermined substantially regular intervals, said intervals preferably being within the range from 5 seconds to 6000 seconds, more preferably within the range from 8 to 1000 seconds and even more preferably within the range from 10 seconds to 360 seconds. More specificly the intervals are determined by the nature of the first liquid and the amount and nature of particles present herein.

In a preferred embodiment of the method according to the invention for isolation of ionic species stored in a first tank, the method comprises the steps of: - treating the first liquid in an electro enhanced dialysis cell to transfer the ionic species from the first liquid into a second liquid and optionally storing said second liquid in a second tank; - treating the second liquid in a bipolar electrodialysis cell to transfer the ionic species from the second liquid into a third liquid and optionally storing the third liquid in a third tank
By using a first, a second and a third tank for storing the first liquid, the second liquid and the third liquid, respectively, it is possible to obtain better control over the processes and optimise the treatment of the liquids in the electro enhanced dialysis cell and the bipolar electrodialysis cell. During the treatment the tanks serve as storage and/or buffers for the treated liquid or the liquid to be treated.

It is preferred that at least a part of the first liquid is recycled to the first tank after treatment in the electro enhanced dialysis cell. The liquid can be recycled via pipelines e. g. supplied with a pump and optionally a purge by which a part of the treated first liquid can be removed and/or replaced by untreated first liquid.

Moreover it is preferred that at least a part of the second liquid is recycled to the electro enhanced dialysis cell after being treated in the bipolar electrodialysis cell. The liquid can be recycled via pipelines, e.g. provided with a pump and optionally a purge by which a part of the treated second liquid can be removed and/or replaced.

Furthermore it is preferred that at least a part of the third liquid is recycled from the third tank to the bipolar electrodialysis cell. The third liquid may be recycled directly from the bipolar electrodialysis cell or from the third tank. By recycling the third liquid the ionic species will be concentrated in the liquid. It is possible to achieve very high concentrations in the third liquid. The concentration may be a factor 5 to 10 higher than in the know methods for separating ionic species

from a liquid. Like in the previously mentioned recycling circuits pipelines, pumps, and a purge may be used.

In one preferred embodiment of the method according to the invention, the method further comprises the step of treating the third liquid in an electrodialysis cell to remove undesired ions, e. g. the presence of inorganic ions may be undesired, when you are separating ion of organic species from a liquid.

In a preferred embodiment of the method according to the invention the method further comprises the step of evaporating and/or crystallising and/or chromatographic treatment of the third liquid to separate the ionic species from the third liquid. By use of this embodiment of the method it is possible to achieve a very pure final product.

In a preferred embodiment of the method, the ionic species comprises anions from inorganic acids, organic acids, enzymes, peptides, hormones, antibiotics or amino acids. Moreover the ionic species comprises cat-ions from inorganic bases, organic bases, enzymes, peptides, hormones, antibiotics or amino acids. Thereby the method is useful for a wide range from of liquids containing ionic species. The method may e. g. be used for separating ionic species from streams from metal etching and food processing, including fermentation broth from fermentation of grass juice using strains of Lactobacillus bacteria, waste stream from lactic acid metal etching and waste streams from citrus oil production.

Preferably the ionic species separated according to the invention has a molar weight up to about 1000 g/mol.
The invention also relates to the use of the method according to the invention for isolating ionic species from a liquid.

Moreover the invention relates to isolated ionic species obtained by the method.

The invention also comprises an apparatus for isolation of ionic species from a first liquid which apparatus comprises - an electro enhanced dialysis cell to transfer the ionic species from the first liquid into a second liguid, - a bipolar electrodialysis cell to transfer the ionic species from the second liquid into a third liquid, - optionally means for separating the ionic species from the third liquid.

The apparatus according to the invention has excellent properties with regard to separating ionic species from a liquid. Very high output can be achieved compared to known apparatuses. The function of the electro enhanced dialysis cell and the bipolar electrodialysis cell is as explained previously in the application.

In a preferred embodiment of the apparatus the electro enhanced dialysis cell comprises means for applying an electric field of direct current. The electric field enhances the electric potential difference in the cell and thereby increases the number of ionic species that can be transferred from the first liquid to the second liquid.

In a more preferred embodiment of the apparatus according to the invention the electro enhanced dialysis cell comprises means for changing the direction of the electric field. Preferably means for changing the direction of the direct current. The means may be in the form of electric switches,

rectifiers, relays and the like. By changing the direction of the direct current a "self-cleaning"effect of the membranes is established.

In order to obtain the best possible"self-cleaning" effect the electric field can be changed at predetermined substantially regular intervals, said intervals preferably being within the range from 5 seconds to 6000 seconds, more preferably within the range from 8 to 1000 seconds and even more preferably within the range from 10 seconds to 360 seconds. The specific interval is dependent on the liquid from which it is wanted to separate the ionic species. The specific interval, which is useful for a specific liquid, can be determined by the skilled person as a matter of routine.

In a preferred embodiment the apparatus according to the invention comprises a first tank for the first liquid.

The first tank is preferably placed before the electro enhanced dialysis cell. Furthermore the apparatus preferably comprises a second tank for the second liquid.

This second tank is preferably placed after the electro enhanced dialysis cell.

Moreover the apparatus preferably comprises a third tank for the third liquid. The third tank is preferably placed after the bipolar electrodialysis cell.

In this specificly preferred embodiment of the invention the first, the second, and the third tank serve as storage and/or buffer for the first liquid, the second liquid, and the third liquid, respectively.

In another preferred embodiment of the apparatus according to the invention the apparatus comprises means for re-circulating at least a part of the first liquid from the electro enhanced dialysis cell to the first tank.

Furthermore the apparatus preferably comprises means for re-circulating at least a part of the second liquid to the electro enhanced dialysis cell after treatment in the bipolar electrodialysis cell.

Moreover the apparatus preferably comprises means for recirculating at least a part of the third liquid from the third tank to the bipolar electrodialysis cell.

The means for re-circulating the liquids are normally pipelines, which may be supplied with pumps and optionally with purges for removing/replacing liquid.

In a preferred embodiment of the apparatus according to the invention the means for applying an electric field of direct current is in the form of electrodes placed at two opposing ends in the electro enhanced dialysis cell. The electrodes may be of any known type and have any desired shape for the purpose.

In a particularly preferred embodiment of the apparatus according to the invention the electro enhanced dialysis cell is constituted by two or more electrodes placed at two opposing ends with cation-exchange membranes (CEM) and/or anion-exchange membranes (AEM) placed there between.

The electro enhanced dialysis cell is normally box-shaped with a parallel bottom and top element, two parallel side elements and two end-elements. The membranes are placed in the cell with the membrane surface parallel to the end elements of the cell.

In a more preferred embodiment of the apparatus the electro enhanced dialysis cell is constituted by two electrodes placed at two opposing ends and with two endmembranes being placed next to each of the two electrodes, the end-membranes facing each other and having cation-exchange membranes (CEM) and/or anion-exchange membranes (AEM) placed in between. The endmembranes and cation-exchange membranes (CEM) and/or anion-exchange membranes (AEM) form adjacent chambers throughout the electro enhanced dialysis cell.

Preferably the end-membranes are neutral membranes and/or cation-exchange membranes and/or anion-exchange membranes. The purpose of the end-membranes is substantially to prevent contact between the electrodes and contaminated liquid e.g. a first liquid.

When the apparatus is used for separating cat-ionic species from a liquid it is preferred to use cat-ion exchange membranes in the electro enhanced dialysis cell.
When the apparatus is used for separating an-ionic species from a liquid it is preferred to use an-ion exchange membranes in the electro enhanced dialysis cell.

The membranes form adjacent chambers throughout the cell in a direction parallel with surfaces of the sideelements of the cell. The surfaces of the membranes are perpendicular to this direction. The adjacent chambers are preferably adapted alternately to receive the first and the second liquid. The liquids are introduced in the cell in the known way by use of tubes, pipelines, valves, etc.

In one of the most simple embodiments of the apparatus according to the invention the electro enhanced dialysis cell is constituted of at least two an-ion exchange membranes or at least two cat-ion exchange membranes which, with the end-membranes, form a central chamber for the first liquid and a chamber on each side of the central chamber for the second liquid.

In a preferred embodiment of the apparatus according to the invention an even number of an-ion exchange membranes or an even number of cat-ion exchange membranes form an uneven number of chambers between and with the two endmembranes, said chambers being adapted alternately to receive the first and the second liquid in such a way that the two chambers constituted by an end-membrane and an an-ion exchange membrane or a cat-ion exchange membrane are adapted for receiving the second liquid. By organizing the membranes in such a way, it is possible to optimise the output of the cell. The number of membranes in the cell may be several hundreds, all placed parallel to each other and optionally with spacer gaskets in between, and which constitutes the adjacent chambers.

When the apparatus according to the invention is prepared for separating cat-ionic species, preferably the electro enhanced dialysis cell for separating cat-ionic species has cat-ion exchange membranes placed between the endmembranes
When the apparatus according to the invention is prepared for separating an-ionic species, preferably the electro enhanced dialysis cell for separating an-ionic species has an-ion exchange membranes placed between the endmembranes

In a preferred embodiment the apparatus further comprises an electrodialysis cell adapted to remove undesired ions from the third liquid, preferably the electrodialysis cell is placed after the bipolar electrodialysis cell.

In another preferred embodiment of the apparatus according to the invention the apparatus further comprises means for evaporating and/or crystallising and/or chromatographic treatment of the third liquid.

Thereby, it is possible to obtain a dry and/or pure final product by use of the apparatus.

The invention also relates to use of an apparatus according to the invention in the method according to the invention.

Furthermore the invention relates to use of the apparatus according to the invention for isolating ionic species from a liquid.

The invention also comprises an electro enhanced dialysis cell wherein the dialysis cell is enhanced with an electric field.

Preferably the electro enhanced dialysis cell is enhanced with an electric field of direct current.

In a preferred embodiment of the electro enhanced dialysis cell according to the invention the electro enhanced dialysis cell comprises means for changing the direction of the electric field, and preferably means for changing the direction of the direct current. The means for changing direction of the electric field may be electric switches, rectifiers, relays, and the like. By changing the direction of the electric field a "selfcleaning" effect of the cell can be achieved as explained previously.

Preferably the electric field can be changed at predetermined substantially regular intervals, preferably said intervals are within the range from 5 seconds to 6000 seconds, more preferably within the range from 8 to 1000 seconds and even more preferably within the range from 10 seconds to 360 seconds. Hereby it is possible to adjust the cell to have the optimal"self-cleaning" effect.

In a preferred embodiment the electro enhanced dialysis cell the electric field is applied by electrodes, which are placed at two opposing ends, in the electro enhanced dialysis cell.

Preferably the electro enhanced dialysis cell is constituted by electrodes placed at two opposing ends with cation-exchange membranes (CEM) and/or anion-exchange membranes (AEM) placed there between. When the cell is used for separation of cat-ionic species, it is preferred to use cat-ion exchange membranes. When the cell is used for separation of an-ionic species, it is preferred to use an-ion exchange membranes.

In a preferred embodiment of the electro enhanced dialysis cell the electro enhanced dialysis cell is constituted by electrodes placed at two opposing ends with two end-membranes being placed next to each of the two electrodes, said end-membranes facing each other and having cation-exchange membranes (CEM) and/or anion-exchange membranes (AEM) placed in between.

It is preferred that the end-membranes are neutral membranes and/or cat-ion exchange membranes and/or an-ion exchange membranes. The purpose of the end-membranes is to prevent contact between the electrodes and contaminated liquid.

Moreover it is preferred that in the electro enhanced dialysis cell according to the invention the end-membranes and cation-exchange membranes (CEM) and/or anion exchange membranes are forming adjacent chambers, and the adjacent chambers are adapted to receive a first and a second liquid, preferably alternately.

When the electro enhanced dialysis cell is prepared for separating cat-ionic species, it is preferred that the electro enhanced dialysis cell has a first and a second electrode where the first electrode is placed at a first end-element in the electro enhanced dialysis cell and the second electrode is placed at a second end-element of the electro enhanced dialysis cell. The first and second endelement is opposite to each other. The electro enhanced dialysis cell further has a first and a second an-ion exchange membrane where the first an-ion exchange membrane is placed next to the first electrode and the second an-ion exchange membrane is placed next to the second electrode. The first and the second an-ion exchange membrane are facing each other and at least two cat-ion exchange membranes are placed between the first and the second anion-exchange membrane with a distance from the anion-exchange membranes and each other to provide adjacent chambers between adjacent membranes.

When the cell is used for separating anionic species the placing of the cat-ion exchange membrane and the an-ion exchange membrane is reversed.

The invention relates to use of the electro enhanced dialysis cell according to the invention in the method according to the invention.

Moreover the invention relates to use of the electro enhanced dialysis cell according to the invention in the apparatus according to the invention.

The invention will now be described in further details with examples and reference to a drawing where:

Fig. 1 shows an electro enhanced dialysis cell according to the invention, adapted to separate an-ionic species.

Fig. 2 shows a bipolar electrodialysis cell according to the invention adapted to separate an-ionic species.

Fig. 3 shows a diagram of the apparatus and method according to the invention.

Fig. 4 shows a configuration of an electro enhanced dialysis cell according to the invention.

Fig. 5 shows the concentration of lactic acid in a feed stream and alkaline solution.

Fig. 6 shows the potential drop across an electro enhanced dialysis cell pair.

Fig. 7 shows the potential drop across an electro enhanced dialysis cell pair.

Fig. 8 shows a configuration of a bipolar electrodialysis cell according to the invention.

Fig. 9 shows the transport of lactate from a feed stream to a combined acid and base stream.

Fig. 10 shows the pH and conductivity as well as current efficiency and energy consumption in a feed stream.

Fig. 11 shows the concentration profiles of citric and malic acid.

Fig. 12 shows the conductivity, pH and cell resistance in a cell.

Fig. 13 shows the concentration of glycine.

Fig. 14 shows the current through the stack.

Fig. 15 shows the concentration of lysine.

Example 1

Figure 1 shows a schematic drawing of an electro enhanced dialysis cell according to the invention. The cell has two electrodes E1 and E2, placed in electrode chambers EC1 and EC2, which are placed at opposite ends in the cell. The electrode chambers are separated from the central part of the cell by two end-membranes, which in this case are two cation-exchange membranes CEM. The two end-membranes have four anion-exchange membranes AEM placed in between. Thereby the two end-membranes and the four anion-exchange membranes form five adjacent chambers Cl, C2, C3, C4 and C5.

With this configuration the cell is adapted for separating anions X^- from a liquid L1. Liquid L1 is led to the chambers C2 and C4 of the cell. The second liquid L2, which is a base when anions are separated, is led to the chambers Cl, C3 and C5 of the cell. The difference in electrical potential between the two liquids is enhanced by a direct current applied by the electrodes E1 and E2.

When the situation is as illustrated in figure 1, where E1 is the positive electrode, the anions X^- move in the direction of E1 and pass through the anion-exchange membranes from the liquid L1 in chambers C2 and C3 to liquid L2 in chambers Cl and C3 as indicated by arrows.

The anions X^- from L1 are replaced by hydroxide ions OH from L2.

When the direction of the direct current is reversed, the anions X^- move in the direction of E2 from the liquid L1 in chambers C2 and C4 through the anion-exchange membranes into the liquid L2 in chambers C3 and C5.

Furthermore, if the anion-exchange membranes have been covered with particles, the anion-exchange membranes will be cleaned as the particles are caused to move away from the membrane and as hydroxide ions penetrate the membrane and dissolve the fouling layer.

As it is evident from figure 1, when the second liquid L2 is running in chambers on both sides of the chambers, where the first liquid LI is running, the second liquid L2 will always receive anions X^- from the first liquid L1 independently of the direction of the electric field.

Figure 2 shows a schematic drawing of the bipolar electrodialysis cell according to the invention which is used for further treatment of the second liquid L2 from the electro enhanced dialysis cell. The bipolar electrodialysis cell has an electrode in each end: a positive electrode E+ in the first end and a negative electrode E- in the second end of the cell. Between the electrodes from E+ to E- are placed repeatingly first a bipolar membrane BM, an anion-exchange membrane AEM and a cation-exchange membrane CEM. The stack of membranes forms adjacent chambers C11, C12, C13, C14, C15 and C16 and is finished with a bipolar membrane before the electrode E-.
In the case where the bipolar electrodialysis cell is used for separating anions the second liquid L2, which is basic compared to the third liquid L3, is first sent through the chambers C12 and C15 between an anion-exchange membrane AEM and a cation-exchange membrane CEM. According to the invention the second liquid L2 is further sent through the chambers C13 and C16 between a cation-exchange membrane and a bipolar membrane.

Hereafter the second liquid is recycled to the electro enhanced dialysis cell.

The third liquid L3, which is acidic compared to the second liquid L2, is sent through chambers C11 and C14 between a bipolar membrane and anion-exchange membrane.

Due to the constant electric direct current through the cell, the ions (X^-, M^+, OH^- and H^+) are drawn in directions transversely to the membrane stack as indicated with arrows. The anions X^- are together with hydrogen ions H^+ concentrated in the third liquid L3 in chambers Cll and C14.

It is clear that in case the bipolar electrodialysis cell is used for separating cations from the second liquid L2, the second liquid will be sent through the chambers C12 and C15 between an anion-exchange membrane and a cation-exchange membrane and further through chambers C11 and C14 between an anion-exchange membrane and a bipolar membrane.

Figure 3a shows a flow sheet of the method according to the invention. The first tank T1 contains the first liquid L1, which is fed to the electro enhanced dialysis cell EEC and treated herein. Hereafter the first liquid is recycled to the tank T1. In the electro enhanced dialysis cell EEC the ionic species are transferred from the first liquid L1 into the second liquid L2. After treatment in the electro enhanced dialysis cell EEC, the second liquid L2 is first stored in a tank T2, before it is treated in the bipolar electrodialysis cell EDBM.

After the treatment in the bipolar electrodialysis cell EDBM, the second liquid L2 is recycled to the electro enhanced dialysis cell EEC. The third liquid L3 is treated in the bipolar electrodialysis cell EDBM where the third liquid L3 receives the ionic species from the second liquid L2. After treatment in the bipolar electrodialysis cell EDBM the third liquid L3 is stored in a tank T3 and recycled trough the bipolar electrodialysis cell until a satisfactory concentration of the ionic species is obtained in the third liquid L3.

In the process it is preferred that e.g. three tanks are used parallel for storing the third liquid L3 from the bipolar electrodialysis cell EDBM. During the process one tank T3 is open for receiving

the third liquid L3 and recycle it to the bipolar electrodialysis cell EDBM. The third liquid L3 in the two other tanks is optionally submitted to the processes shown in figures 3b and 3c.

Figure 3b is a flow sheet showing the process of treating the third liquid L3 in an electrodialysis cell ED to remove undesired ions which are transferred to a fifth liquid L5 and stored in a fifth tank T5.

Figure 3c is a flow sheet showing the process of evaporating the third liquid L3 in an evaporater EV to obtain a concentrated liquid, which is stored in the tank T6.

Example 2. Description of experimental extraction through an Electro enhanced Dialysis cell according to the invention

In the electro enhanced dialysis cell, the cell stack was configured with four anion-exchange membranes 1 (Neosepta AMX, Tokuyama Corp., Japan) and two cation-exchange membranes 2 (Neosepta CMH, Tokuyama Corp., Japan) as shown in figure 4. The effective membrane area was 40 cm^2.

In the two end-chambers 3 between the platinum electrodes 6 and 7 (each 31.5 cm^2) and each cation-exchange membrane, a flow of electrode-rinsing solution was maintained in the end-chambers. The solution was an aqueous solution of 0.1M K_2SO_4.

Through the chambers 4, 250 ml of an aqueous alkaline solution of 0.5M KOH (pH 12.5) was pumped from a storage container, to which the solution was returned after each passage. The volume flow was 10 g/s. The thickness of the chambers 4 between the membranes was 6 mm. Net spacers were introduced to promote turbulent flow.

Through the chambers 5, 250 ml of the feed solution, which was fermented brown juice from grass pellet production with around 16 g/1 lactic acid, was passed from a storage container. The treated feed solution was returned to the container after each pass. The fermented solution had initially been adjusted to a pH-value of 5.5 by adding KOH pellets. Nothing else had been done to the broth. The volume flow was 10 g/s. The thickness of the chambers 5 was 12 mm. No spacers were introduced in these chambers.

Each chamber 4 and 5 had a 10 cm long flow-path that was 4 cm wide.

The temperature of the electrode-rinse, the alkaline and the fermented solutions was held constant at 40 degrees Celsius during the experiment.

During the experiment, the pH was continuously measured in the fermented solution and held constant at pH 5.5 by titration of more fermented solution (pH 2) with a high lactic acid concentration (70 g/1).

In the middle of each of the chambers 5, a silver/silver chloride electrode was placed, so the voltage drop across a cell pair could be continuously measured by data collection (Fluke 123-Industrial Scopemeter, Fluke Corporation, USA).

When the experiment was started, the electrode-rinse, the fermented broth and the alkaline solution was pumped through the cell. Direct current across the cell was added by a power supply (EA-PS 3032-10 (0..32V/0..10A), EA-Elektro-Automatik, Germany) that regulates the power to uphold a

constant current of 1.0 A. An IBM personal computer controlled a relay, shifting the direction of the electrical current every 10 seconds.

Samples from the fermentation broth and the alkaline solution were taken every 30 minutes. pH and conductivity were noted, and lactic content was measured by HPLC using an AMINEX HPX-87H column (Biorad, USA) at 35 degrees Celsius using 4 mM sulfuric acid as eluent.

After 4 hours, the alkaline solution was replaced by a fresh solution, and the experiment was continued.

Figure 5 shows the concentration profile of lactic acid in the feed and alkaline solutions during an eight-hour experiment. In the fermented brown juice, the initial lactic acid concentration of 16 g/1 goes up during the experiment, because pH is regulated by titration of fermentation solution having higher lactic acid content.

The alkaline solution was replaced after four hours to simulate the regeneration process in the EDBM process.

The lactate flux was found to be 1.2-10-4 mol/mrs during the first four hours, and 1.7-10"* mol/nrs during the next four hours. Some of this increase might originate from the rising lactate concentration in the feed.

Figures 6 and 7 show the potential drop across a cell pair at the beginning and at the end of the first fourhour run, respectively. The 10 second intervals were evident as the direction of current changes between positive and negative potential drops. At the beginning of each interval, both figures show an almost constant initial drop that in figure 3 increases slightly and in figure 4 increases significantly during the 10 seconds.

These increments relate to the increase of electrical resistance partly from ionic polarization, but also from a build-up of organic matter on the membrane surface in the feed chamber.

Especially figure 8 shows that the organic fouling can be removed by changing the direction of the electric current. The reversal does not remove the organic matter completely, as an increase in initial cell-resistance from about 1.5 Ohm to 2 Ohm was evident during the experiment.

The divergence between the form of the positive and negative potential drop in figure 8 must derive from different flow conditions in the two feed chambers in the laboratory equipment.

Example 3

The electro enhanced dialysis cell was configured as in example 1 but the AMX anion-exchange membrane was replaced with a monoselective anion-exchange membrane (Neosepta ACS, Tokuyama Corp., Japan).

500 ml brown juice was circulated in the feed chambers and the pH was held constant at 5.5 by titration of lactic acid. In the base chambers 500 ml of 0.5 M KOH was passed and 500 ml 0.1 M K_2SO_4 was used as electrode rinsing solution.

Samples were taken at 0, 60, and 120 min. from the feed and base streams and the contents of calcium and magnesium were determined by Atom Absorption Spectroscopy (AAS).

Time (min)	$[Ca^{2+}]_{Feed}$ (mg/l)	$[Ca^{2+}]_{Base}$ (mg/l)	$[Mg^{2+}]_{Feed}$ (mg/l)	$[Mg^{2+}]_{Base}$ (mg/l)
0	667	0.15	394	0.01
60	737	0.09	425	0.01
120	705	0.13	403	0.02

From these results, it is evident that divalent cations are retained sufficiently to be non-damaging in the following EDBM process, which usually requires such concentrations to be lower than 2 ppm.

Using a mono-selective anion-exchange membrane in this experiment does not affect retention of cations significantly, but does improve retention of divalent anions such as sulfate and phosphate.

Example 4

In the experiments with the bipolar electrodialysis cell, the cell was equipped with three bipolar membranes 8 in figure 8 (Neosepta BP-1, Tokuyama Corp., Japan), two anion-exchange membranes 1 (Neosepta AMX, Tokuyama Corp., Japan) and two cation-exchange membranes 2 (Neosepta CMH, Tokuyama Corp., Japan) as shown on figure 8.

In the two end-chambers 3 between the platinum electrodes 6 and 7 (each 31.5 cm^2) and a set of bipolar membranes, a flow of electrode-rinsing solution was established. The electrode-rinsing solution was an aqueous solution of 0.1M K_2SO_4. Through the feed chambers 9 between the anion-exchange membrane and the cation exchange membrane 500 ml of a mixture of 0.5 M KOH and 0.4 M lactic acid was circulated to a container. 1000 ml of an alkaline 0.1M KOH solution was circulated in both the acid chamber 10 between the bipolar membrane and the anion-exchange membrane and in the base chamber 11 between the bipolar membrane and the cation-exchange membrane. The streams from the acid and base chambers 10 and 11 were mixed in a container after each pass. The thickness of the chambers 9, 10, and 11 between the membranes was 6 mm. Net spacers were introduced to promote turbulent flow.

The temperature of the electrode-rinse, the feed and the base solutions was held constant at 40 degrees Celsius during the experiment.

In the feed chambers 9, silver/silver chloride electrodes were placed so the voltage drop across a cell pair could be continuously measured and data collected (Fluke 123 Industrial Scopemeter, Fluke Corporation, USA). Samples from the feed and the alkaline solution were taken every 30 minutes. pH and conductivity were noted, and lactic content was measured by HPLC using an AMINEX HPX-87H column (Biorad, USA) at 35 degrees Celsius using 4 mM sulfuric acid as eluent.

Figure 9 shows the transport of lactate from the feed stream to the combined acid and base stream, reaching a lactate concentration of 0.8 g/1 in the feed stream after 180 min., corresponding to more than 97% acid recovery.

Figure 10 shows the pH and conductivity in the feed solution during the experiment as well as the current efficiency, and corresponding effect on energy consumption. It is clear that the significant decrease in conductivity near the end of the experiment was causing a rise in cell resistance and thus energy consumption.

The current efficiency was above 80% during most of the experiment, except for the beginning and final part. The low efficiency in the final phase probably originates from polarization, leading to ineffective water-splitting at the mono-polar membranes.

Example 5

Another experiment with a bipolar electrodialysis cell was carried out exactly as example 4, except the 500 ml feed mixture was composed of 0.5M KOH, 0.1M (0.3N) citric acid, and 0.05M (0.1N) malic acid.

The acid content of the samples was measured by HPLC as before.

Figure 11 shows the concentration profiles of the citric and malic acid in the feed solution and the mixed acid/base solution.

From figure 11 it is evident that most of the citric and malic acid is extracted from the feed solution. The recovery of both citric and malic acid was higher than 97%.

However, the recovery of the last 5-10% of the organic acids is very costly, as can be seen in figure 12. As pH and conductivity in the feed decrease, cell resistance and thus energy consumption increase drastically.

Example 6

The electro enhanced dialysis cell stack was configured as in example 1, but with 4 cation-exchange membranes (Neosepta CMB, Tokuyama Corp., Japan) replacing the anion-exchange membranes and (Neosepta AMX, Tokuyama Corp., Japan) membranes replacing the cation-exchange membranes.

250 ml aqueous solution of 0.2M glycine, which is an amino acid with pKr~oH = 2.34, pH3+= 9.60 and pI = 5.97, was circulated in the feed chambers. In the dialysate chambers 1750 ml of 0.1M H_2SO_4 was circulated and 500 ml 0.1M Na_2SO_4 was used as electrode rinsing solution. The concentration of glycine was determined using HPLC. The liquids were circulated for 5 min. before the experiment was started. Current reversal was omitted, as the feed stream did not contain material that could cause fouling of the membranes.

Figure 13 shows the concentration of glycine in the feed and dialysate during the experiment. At the beginning of the experiment glycine is transported from the feed stream to the dialysate stream at a relatively low rate because the starting pH is close to the isoelectric point of the amino acid. The voltage drop across a cell pair was not allowed to exceed 14 V, which resulted in a current starting very low and slowly increasing as pH went down and conductivity increased in the feed, see figure 14. Within 180 min. 84% of the glycine is removed from the feed at a current efficiency of 580.

Example 7

The electro enhanced dialysis cell stack was configured as in example 5.

250 ml aqueous solution consisting of 50 g/1 bakers yeast and 0.2M lysine, which at the experimental conditions was a positively charged amino acid, was circulated in the feed chambers. In the dialysate chambers 1750 ml of 0.1M H_2SO_4 was circulated and 500 ml 0.1M Na_2S0_4 was

used as electrode rinsing solution. The liquids were circulated for 5 min. before the experiment was started.

Direct current across the cell was added by a power supply (EA-PS 9072-040 (0.. 72V/0.. 40A), EA-Elektro Automatik, Germany) regulating the power to keep a constant current of 1.0 A. The concentration of lysine is determined using HPLC.

Without current reversal the experiment had to be terminated as the voltage drop across a single cell pair increased from 10V to 30 V during the first 8 minutes in order to keep a current of 1 A (25 mA/cm^2).
When the experiment was repeated with a current reversal time of 300 sec., it was possible to keep the average voltage drop across a cell pair at approx. 15 V. Figure 15 shows the concentration of lysine in the feed and dialysate during the experiment. During the first 60 min. of the experiment the lysine concentration in the feed decreased 30% at a current efficiency of 24%.

Claims

1. A method for isolation of ionic species from a first liquid comprising the steps of: - treating the first liquid in an electro enhanced dialysis cell to transfer the ionic species from the first liquid into a second liquid, and - optionally treating the second liquid in a bipolar electrodialysis cell to transfer the ionic species from the second liquid into a third liquid, - optionally separating the ionic species from the second or third liquid.

2. A method according to claim 1 wherein the electro enhanced dialysis cell is enhanced by applying an electric field of direct current through said electro enhanced dialysis cell during the treatment of the first liquid, the direction of said electric field preferably being changed during the treatment of the first liquid, preferably by changing the direction of the direct current.

3. A method according to claim 2 wherein the electric field is changed at predetermined substantially regular intervals, said intervals preferably being within the range from 5 seconds to 6000 seconds, more preferably within the range from 8 to 1000 seconds and even more preferably within the range from 10 seconds to 360 seconds.

4. A method according to claims 1-3 for isolation of ionic species stored in a first tank comprising the steps of: - treating the first liquid in an electro enhanced dialysis cell to transfer the ionic species from the first liquid into a second liquid and optionally storing said second liquid in a second tank - treating the second liquid in a bipolar electrodialysis cell to transfer the ionic species from the second liquid into a third liquid and storing said third liquid in a third tank 5. A method according to claim 4 wherein at least a part of the first liquid is recycled to the first tank after treatment in the electro enhanced dialysis cell.

6. A method according to any one of claims 4-5 wherein at least a part of the second liquid is recycled to the electro enhanced dialysis cell after being treated in the bipolar electrodialysis cell.

7. A method according to any one of claims 4-6 wherein at least a part of the third liquid is recycled from the third tank to the bipolar electrodialysis cell.

8. A method according to any of the preceding claims wherein the method further comprises the step of treating the third liquid in an electrodialysis cell to remove undesired ions.

9. A method according to any one of the preceding claims wherein the method further comprises the step of evaporating and/or crystallising and/or chromatographic treatment of the third liquid to separate the ionic species from the third liquid.

10. A method according to any one of claims 1-9 wherein the ionic species comprises anions or anions from inorganic acids, organic acids, enzymes, peptides, hormones, antibiotics, or amino acids.

11. A method according to any one claims 1-10 wherein the ionic species has a molar weight up to about 1000 g/mol.

12. Use of the method according to claims 1-11 for isolating ionic species from a liquid.

13. Isolated ionic species obtained by the method according to claims 1-11 14. An apparatus for isolation of ionic species from a first liquid comprising - an electro enhanced dialysis cell to transfer the ionic species from the first liquid into a second liquid, - a bipolar electrodialysis cell to transfer the ionic species from the second liquid into a third liquid, - optionally means for separating the ionic species from the third liquid.

15. An apparatus according to claim 14 wherein said electro enhanced dialysis cell comprises means for applying an electric field of direct current.

16. An apparatus according to claim 15 wherein the electro enhanced dialysis cell comprises means for changing the direction of said electric field, preferably by changing the direction of the direct current.

17. An apparatus according to claim 16 wherein the electric field can be changed at predetermined substantially regular intervals, preferably said intervals are within the range from 5 seconds to 6000 seconds, more preferably within the range from 8 to 1000 seconds and even more preferably within the range from 10 seconds to 360 seconds.

18. An apparatus according to claims 14-17, which further comprises means for storing and recirculating said liquids, said means preferably being tanks and pumps.

19. An apparatus according to any one of claims 14-18 wherein said means for applying an electric field of direct current are in the form of electrodes placed at two opposing ends in the electro enhanced dialysis cell.

20. An apparatus according to any one of claims 14-19 wherein the electro enhanced dialysis cell is constituted by two or more electrodes placed at two opposing ends with cation-exchange membranes (CEM) and/or anion-exchange membranes (AEM) placed there between.

21. An apparatus according to any one of claims 14-19 wherein the electro enhanced dialysis cell is constituted by two electrodes placed at two opposing ends and with two end-membranes being placed next to each of the two electrodes, said end-membranes facing each other and having cation-exchange membranes (CEM) and/or anion-exchange membranes (AEM) placed in between, and said endmembranes and cation-exchange membranes (CEM) and/or anion-exchange membranes (AEM) forming adjacent chambers throughout the electro enhanced dialysis cell.

22. An apparatus according to claim 20 wherein said end-membranes are neutral membranes and/or cation-exchange membranes and/or anion-exchange membranes.

23. An apparatus according to claims 14-22 wherein the electro enhanced dialysis cell is prepared for separating cat-ionic species, said electro enhanced dialysis cell for separating cationic species having cation-exchange membranes placed between the end-membranes 24. An apparatus according to claims 14-22 wherein the electro enhanced dialysis cell is prepared for separating an-ionic species, said electro enhanced dialysis cell for separating an-ionic species having anion-exchange membranes placed between the end-membranes 25. An apparatus according to any of the preceding claims 14-24 wherein the apparatus further comprises an electrodialysis cell adapted to remove undesired ions from the third liquid, the electrodialysis cell preferably being placed after the bipolar electrodialysis cell.

26. An apparatus according to any one of claims 14-25 wherein the apparatus further comprises means for evaporating and/or crystallising and/or chromatographic treatment of the third liquid.

27 Use of an apparatus according to any one of claims 1426 in the method according to claims 1-11.

28. Use of the apparatus according to any one of claims 14-26 for isolating ionic species from a liquid.

29. An electro enhanced dialysis cell wherein the dialysis cell is enhanced with an electric field, preferablythe electro enhanced dialysis cell is enhanced with an electric field of direct current.

30. An electro enhanced dialysis cell according to claim 29 comprising means for changing the direction of said electric field, preferably means for changing the direction of the direct current.

31. An electro enhanced dialysis cell according to claim 30 wherein the electric field can be changed at predetermined substantially regular intervals, said intervals preferably being within the range from 5 seconds to 6000 seconds, more preferably within the range from 8 to 1000 seconds and even more preferably within the range from 10 seconds to 360 seconds.

32. An electro enhanced dialysis cell according to any one of claims 29-31 wherein said electric field is applied by electrodes placed at two opposing ends in the electro enhanced dialysis cell.

33. An electro enhanced dialysis cell according to any one of claims 29-32 wherein the electro enhanced dialysis cell is constituted by electrodes placed at two opposing ends with cation-exchange membranes (CEM) and/or anion-exchange membranes (AEM) placed there between.

34. An electro enhanced dialysis cell according to any one of claims 29-33 wherein the electro enhanced dialysis cell is constituted by electrodes placed at two opposing ends with two end-membranes being placed next to each of the two electrodes, said end-membranes facing each other and having cation-exchange membranes (CEM) and/or anion-exchange membranes placed in between.

35. An electro enhanced dialysis cell according to claim 34 wherein said end-membranes are neutral membranes and/or cation-exchange membranes and/or anion-exchange membranes.

36. An electro enhanced dialysis cell according to any one of claims 33-35 wherein said end-membranes and cation-exchange membranes (CEM) and/or anion-exchange membranes are forming adjacent chambers, said adjacent chambers being adapted to receive a first and a second liquid, preferably alternately.

37. Use of an electro enhanced dialysis cell according to any one of claims 29-36 in the method according to claims 1-11.

38. Use of an electro enhanced dialysis cell according to any one of claims 29-36 in the apparatus according to claims 14-26.

Drawings:

Fig.1

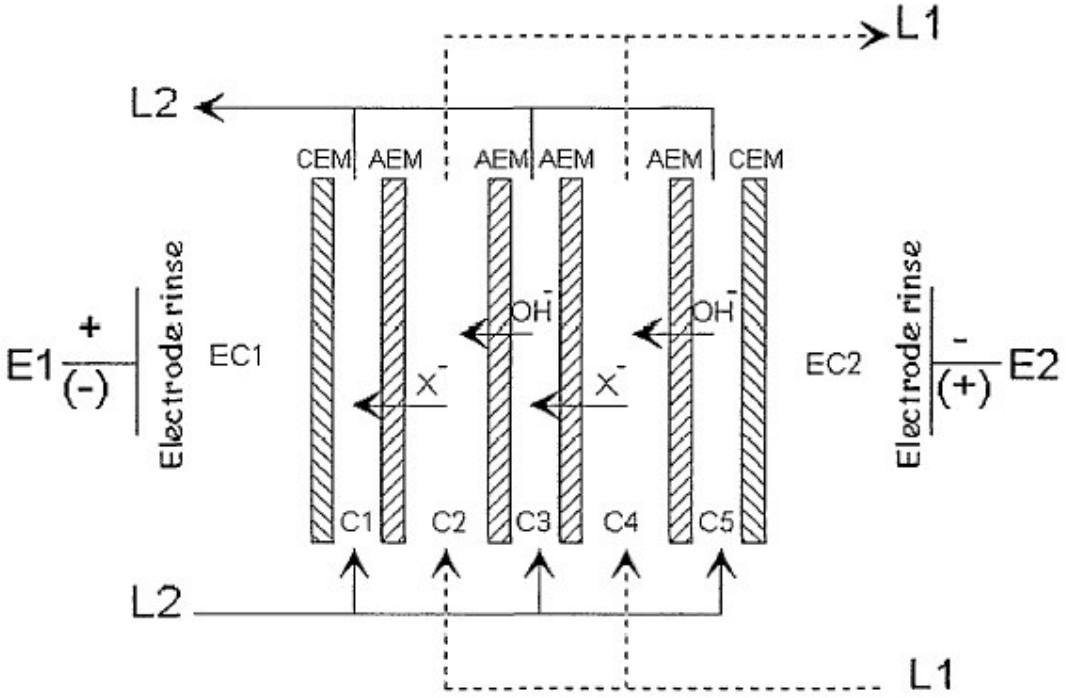

Fig. 2

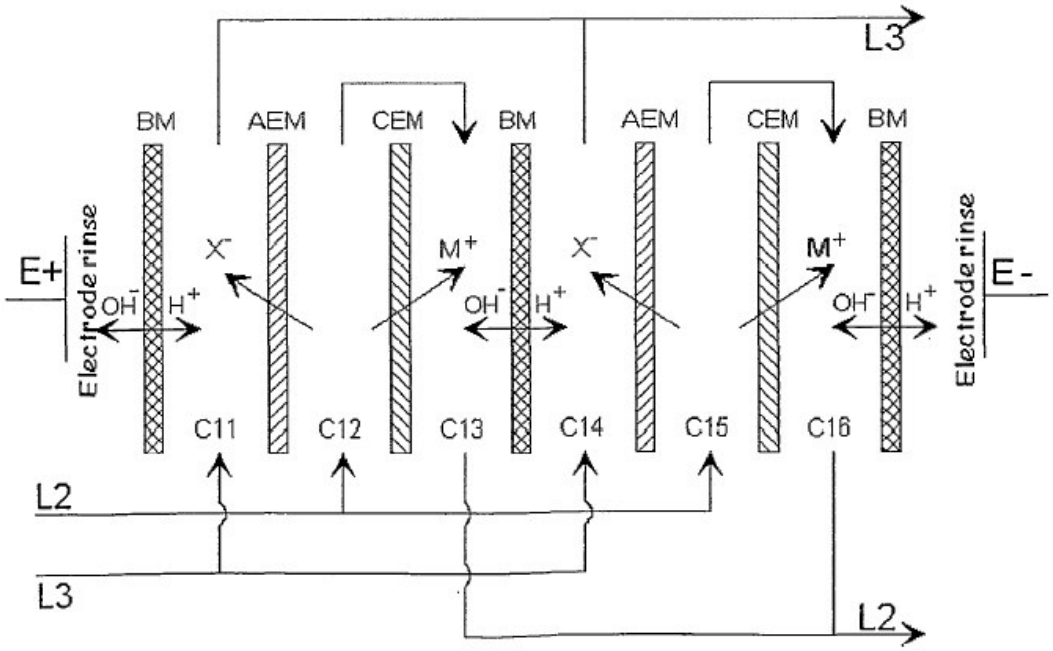

Fig. 3A

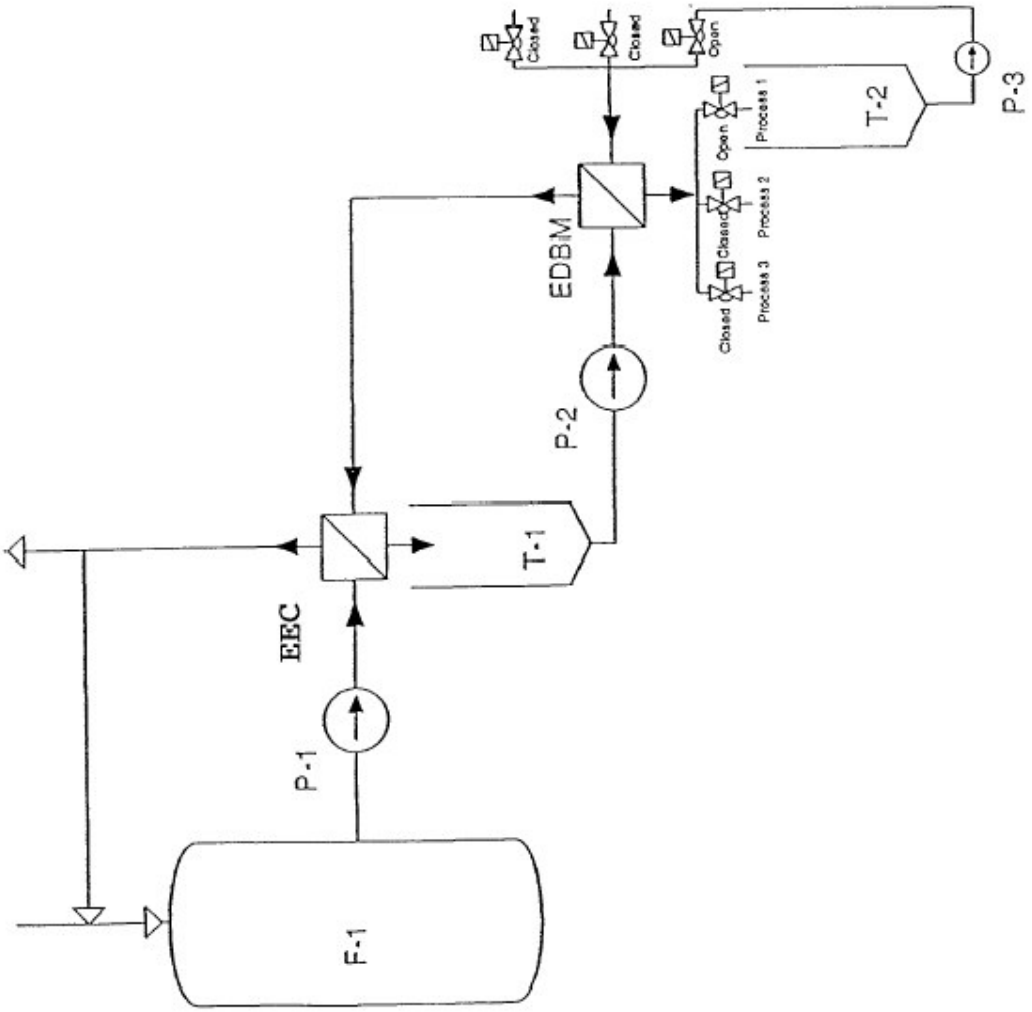
Closed
Closed
Open
T-2
P-3
Process 1
Open
Process 2
Closed
Process 3
Closed
EDBM
P-2
T-1
EEC
P-1
F-1

Fig. 3B

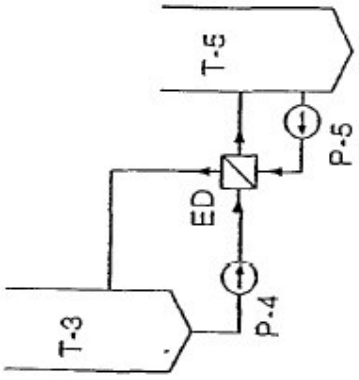
T-5
P-5
ED
P-4
T-3

Fig. 3C

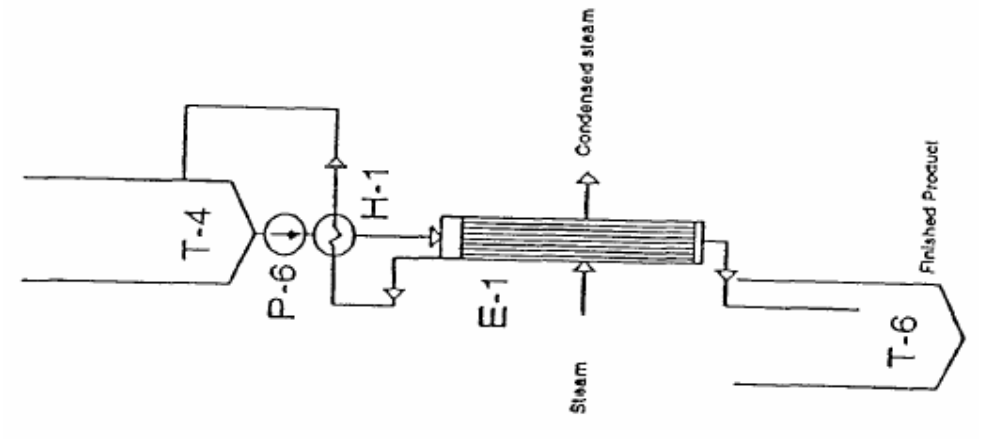
T-4
P-6
H-1
E-1
Condensed steam
Steam
Finished Product
T-6

Fig. 4

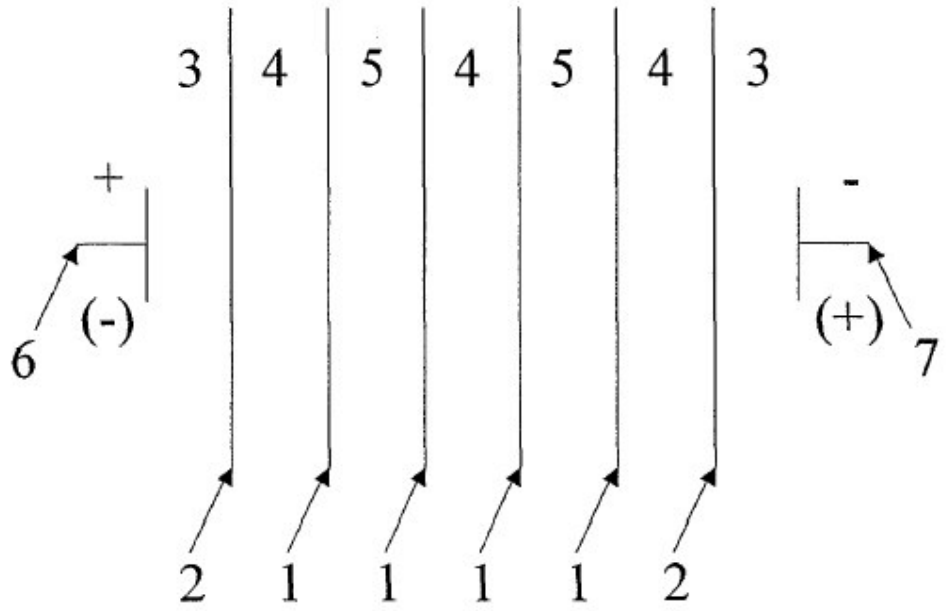
3
4
5
4
5
4
3
+
(-)
6
-
(+)
7
2
1
1
1
1
2

Fig. 5

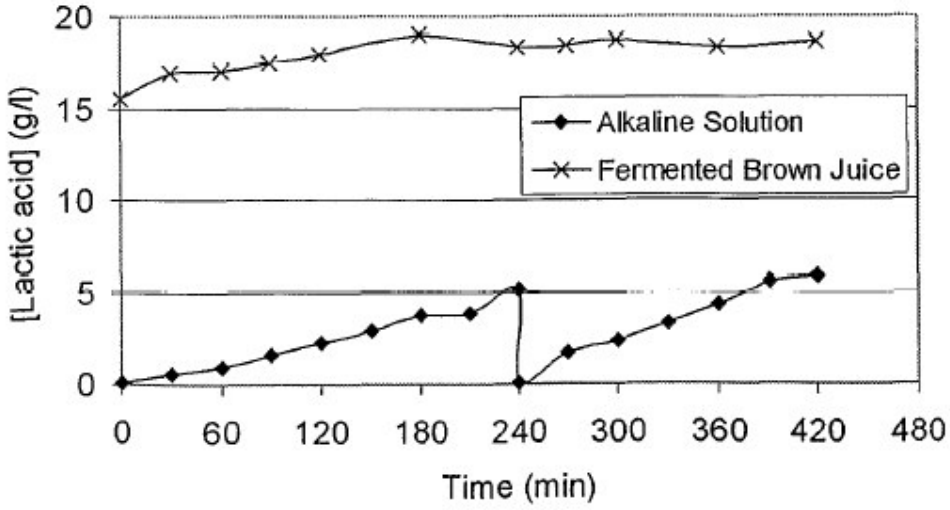

Fig. 6

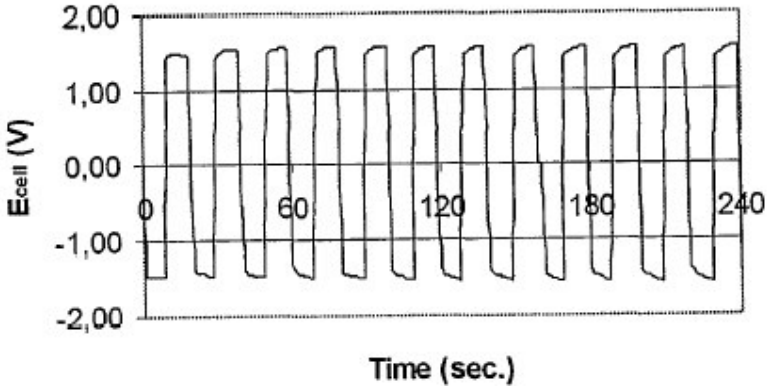

Fig. 7

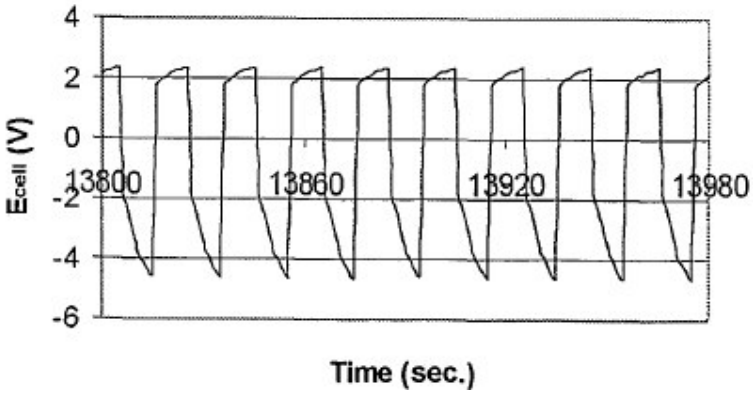

Fig. 8

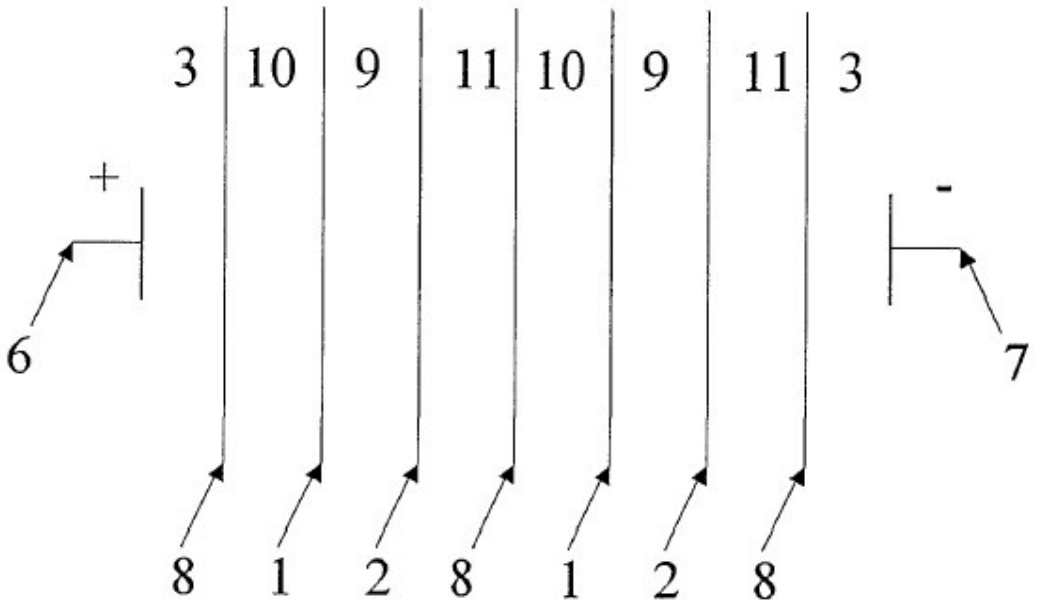
3
10
9
11
10
9
11
3
+
-
6
7
8
1
2
8
1
2
8

Fig. 9

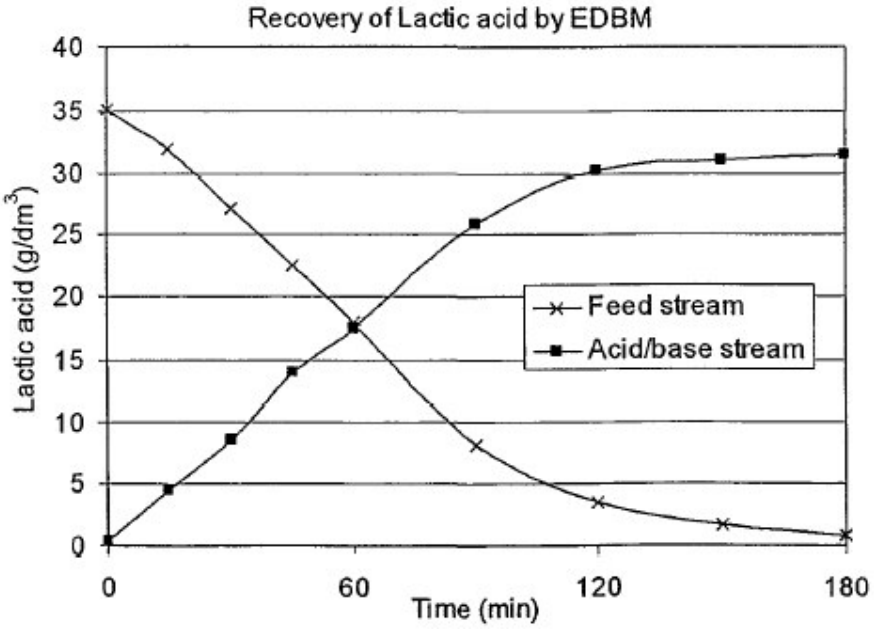
Recovery of Lactic acid by EDBM
Lactic acid (g/dm3)
40
35
30
25
20
15
10
5
0
0
60
120
180
Time (min)
Feed stream
Acid/base stream

Fig. 10

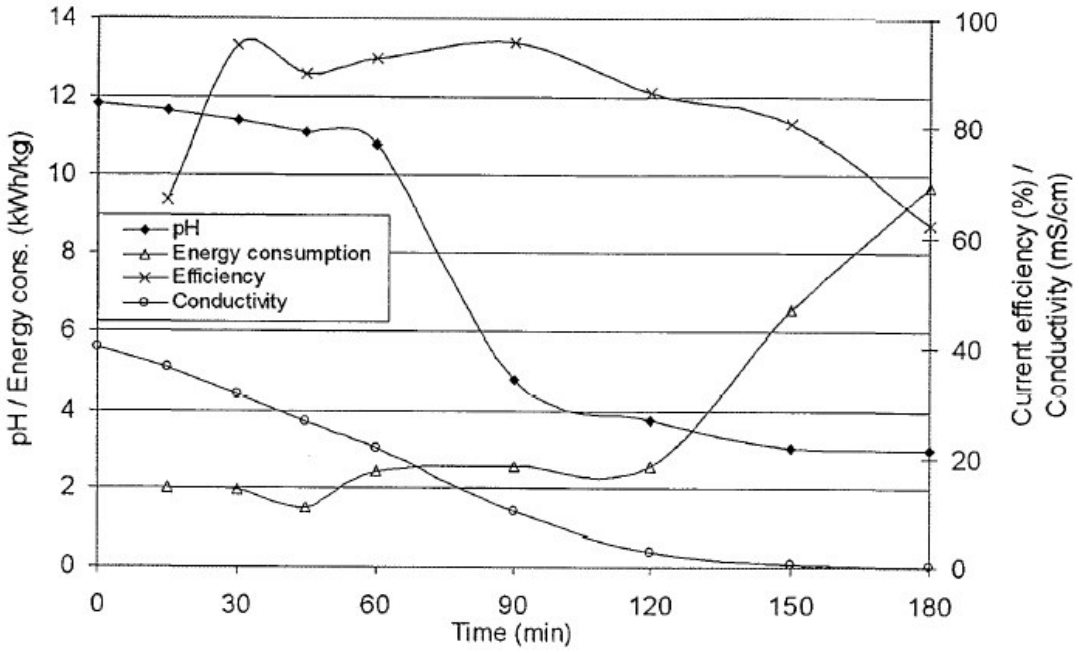
pH / Energy cons. (kWh/kg)
Current efficiency (%) / Conductivity (mS/cm)
Time (min)
pH
Energy consumption
Efficiency
Conductivity
0
2
4
6
8
10
12
14
0
20
40
60
80
100
0
30
60
90
120
150
180

Fig. 11

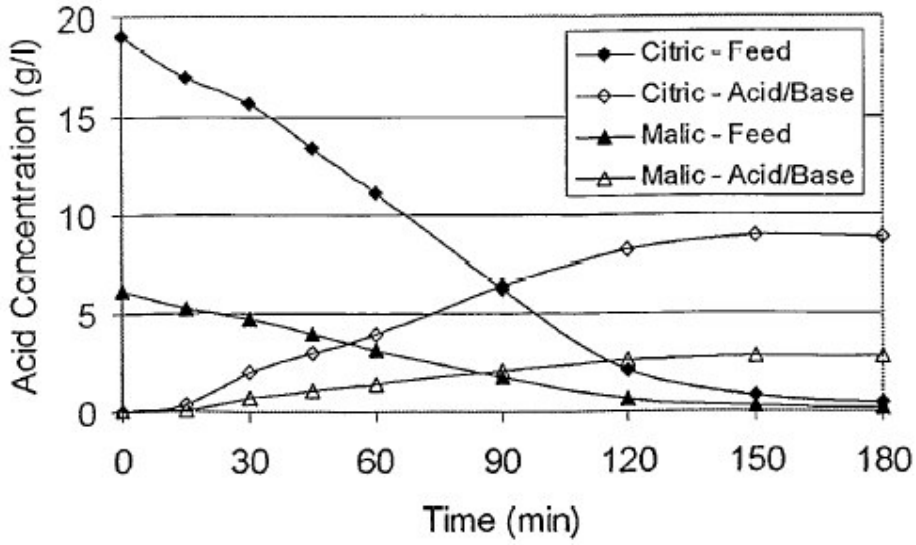
Acid Concentration (g/l)
Time (min)
Citric - Feed
Citric - Acid/Base
Malic - Feed
Malic - Acid/Base
0
5
10
15
20
0
30
60
90
120
150
180

Fig. 12

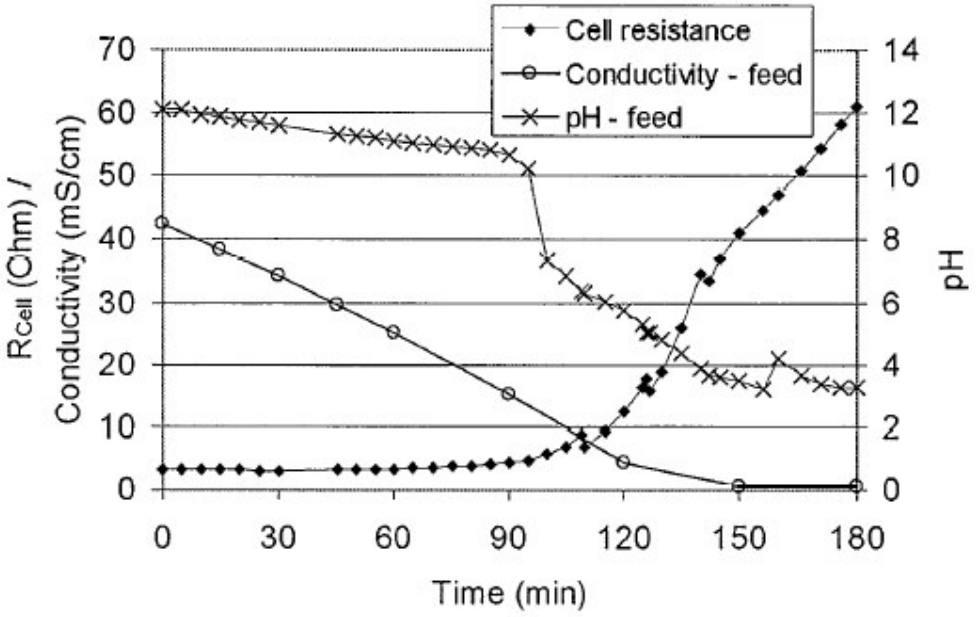
Cell resistance
Conductivity - feed
pH - feed
Rcell (Chm) /
Conductivity (mS/cm)
pH
Time (min)
0
10
20
30
40
50
60
70
0
2
4
6
8
10
12
14
0
30
60
90
120
150
180

Fig. 13

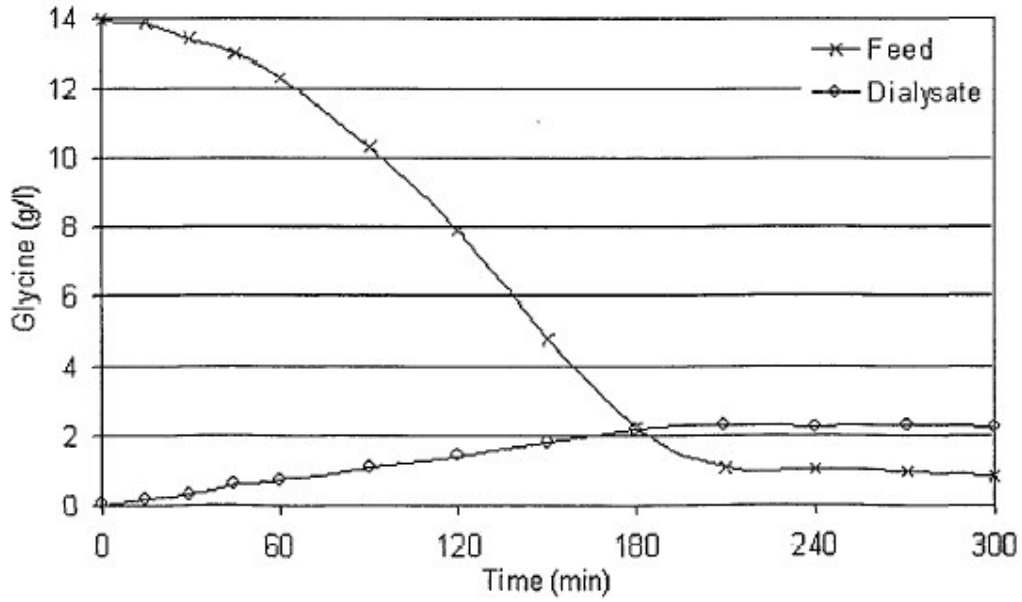
Feed
Dialysate
Glycine (g/l)
Time (min)
0
2
4
6
8
10
12
14
0
60
120
180
240
300

Fig. 14

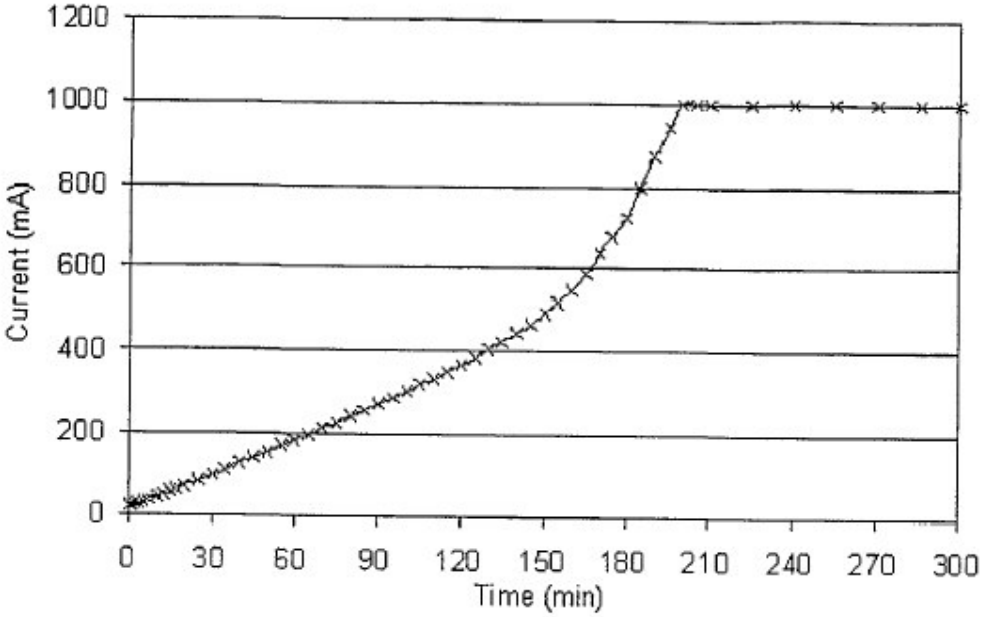
1200
1000
800
600
400
200
0
Current (mA)
0
30
60
90
120
150
180
210
240
270
300
Time (min)

Fig. 15

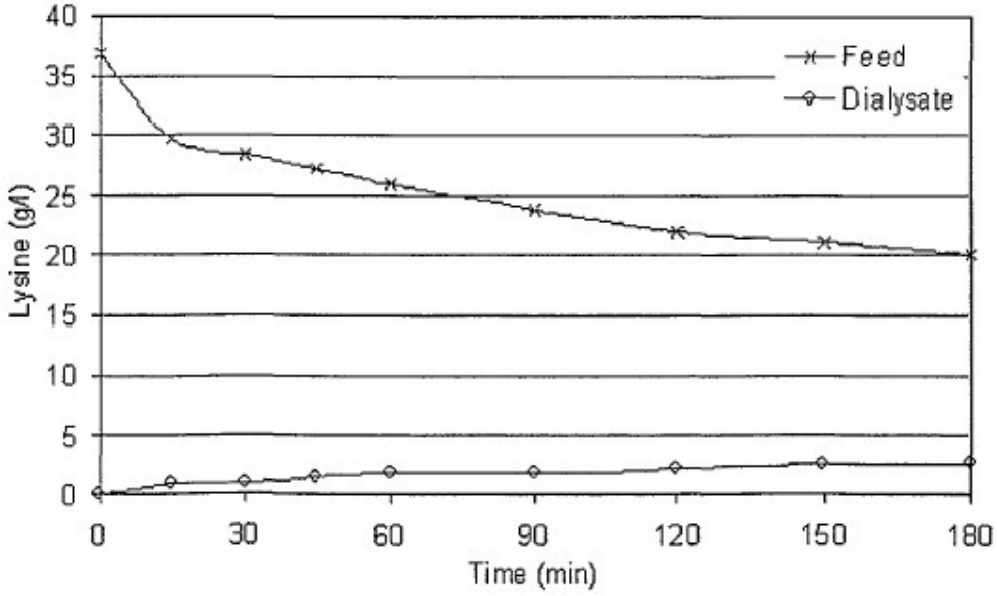
40
35
30
25
20
15
10
5
0
Lysine (g/l)
Feed
Dialysate
0
30
60
90
120
150
180
Time (min)